

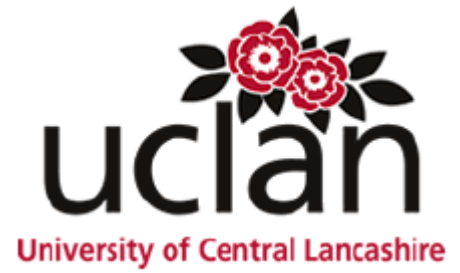
**MATHEMATICAL AND COMPUTATIONAL MODELLING  
OF SOFT AND ACTIVE MATTER**

**by**

**ISRAR AHMED**

A thesis submitted in partial fulfilment for the requirements for the degree of  
Doctor of Philosophy at the University of Central Lancashire

SEPTEMBER, 2016



## **Student Declaration Form**

I declare that while registered as a candidate for the research degree, I have not been a registered candidate or enrolled student for another award of the University or at another academic or professional institution. I declare that no material contained in the thesis has been used in any other submission for an academic award and is solely my own work.

**Signature of Candidate**

**Type of Award**

Doctor of Philosophy (PhD)

**School**

Physical sciences and computing

## **ACKNOWLEDGEMENTS**

Firstly, I would like to thank my supervisors, Dr. Dung Ly and Prof Waqar Ahmed for their help and encouragement throughout this research. The work presented in this thesis could not have been done without their inspirational ideas and valuable insights.

I should most like to thank my family, for their support and trust. Without their unfailing love and encouragement, it would have proved much more difficult to get through my research.

## List of publications

- **Ahmed I, Ly D and Ahmed W**, “*Collective behaviour of self-propelled particles in homogeneous and heterogeneous medium*” , International Journal of Modelling, Simulation, and Scientific Computing (submitted).
- **Ahmed I, Ly D and Ahmed W** “Collective behaviour of self-propelled particles in the presence of moving obstacles” Physical Review Letter (under process of submission)

## Abstract

The collective motion of organisms such as flights of birds, swimming of school of fish, migration of bacteria and movement of herds across long distances is a fascinating phenomenon that has intrigued man for centuries. Long and details observations have resulted in numerous abstract hypothesis and theories regarding the collective motion animals and organisms. In recent years the developments in supercomputers and general computational power along with highly refined mathematical theories and equations have enabled the collective motion of particles to be investigated in a logical and systematic manner. Hence, this study is focused mathematical principles are harnessed along with computational programmes in order to obtain a better understanding of collective behaviour of particles.

Two types of systems have been considered namely homogeneous and heterogeneous systems, which represent collective motion with and without obstacles respectively. The Vicsek model has been used to investigate the collective behaviour of the particles in 2D and 3D systems. Based on this, a new model was developed: the obstacle avoidance model. This showed the interaction of particles with fixed and moving obstacles. It was established using this model that the collective motion of the particles was very low when higher noise was involved in the system and the collective motion of the particles was higher when lower noise and interaction radius existed. Very little is known about the collective motion of self-propelled particles in heterogeneous mediums, especially when noise is added to the system, and when the interaction radius between particles and obstacles is changed. In the presence of moving obstacles, particles exhibited a greater collective motion than with the fixed obstacles. Collective motion showed non-monotonic behaviour and the existence of optimal noise maximised the collective motion. In the presence of moving obstacles there were fluctuations in the value of the order parameter.

Collective systems studies are highly useful in order to produce artificial swarms of autonomous vehicles, to develop effective fishing strategies and to understand human interactions in crowds for devising and implementing efficient and safe crowd control policies. These will help to avoid fatalities in highly crowded situations such as music concerts and sports and entertainment events with large audiences, as well as crowded shopping centres.

In this study, a new model termed the obstacle avoidance model is presented which investigates the collective motion of self-propelled particles in the heterogeneous medium. In future work this model can be extended to include a combination of a number of motionless and moving obstacles hence bringing the modelling closer to reality.

# Contents

CHAPTER 1 .....	1
Introduction and Background .....	1
1.1 Introduction .....	1
1.2 Collective behaviour .....	2
1.3 Self-propelled particles (SPP) .....	3
1.4 Phase transition .....	4
1.5 Aim .....	10
1.6 Objectives.....	10
1.7 Outline of the thesis.....	11
CHAPTER 2 .....	14
Collective behaviour of self-propelled particles - a literature review .....	14
2.1 Introduction .....	14
2.2 Collective Behaviour in Homogeneous Medium .....	15
2.3 Statistical physics of self-propelled particles .....	19
2.4 Collective Behaviour in Heterogeneous Medium .....	23
2.4.1 Fixed obstacles.....	24
2.4.2 Moving Obstacles.....	26
CHAPTER 3.....	28
Models for Collective Behaviour of Self-Propelled Particles .....	28
for Homogeneous and Heterogeneous Systems .....	28
3.1 Introduction .....	28
3.2 Methods for the collective behaviour of self-propelled particles in homogeneous and heterogeneous medium.....	29
3.2.1 Vicsek model in 2D.....	29
3.2.2 Vicsek model in 3D.....	32
3.2.3 Chepizkho model .....	33
3.2.4 Order of phase transitions .....	36
3.2.5 Limitations of the existing models.....	37
3.3 Development of a new improved model for understanding the collective behaviour of self-propelled particles .....	38
3.3.1 Obstacle avoidance model (OAM) .....	38
(i) Moving obstacles.....	41
3.4 Comparison of OAM and the Chepizkho model .....	42
3.7 Conclusions .....	45
CHAPTER 4.....	46

Simulations Studies using the 2D Vicsek Model .....	46
for Self-Propelled Particles .....	46
4.1 Introduction .....	46
4.2 Parameter table .....	47
4.3 Comparison of calculated results and the simulation results.....	47
4.4 Simulation results .....	49
4.4.1 Larger number of particles.....	54
4.4.2 Phase transitions.....	58
(i) Variation in noise.....	58
(ii) Variation in the density .....	62
4.4.3 Effect of the interaction radius .....	64
4.4.4 Effect of the Speed.....	66
4.4.5 Collective motion as a function time .....	68
4.4.6 Order of the phase transition .....	71
4.5 Conclusions .....	75
CHAPTER 5.....	77
Simulations Studies using the Vicsek 3D Model .....	77
5.1 Introduction .....	77
5.2 Results obtained from the simulation studies .....	78
5.2.1 Effect of speed .....	88
5.2.2 Effect of noise .....	90
5.2.3 Effect of particle densities .....	92
5.2.4 Effect of the interaction radius .....	94
5.2.5 Order of phase transitions .....	96
5.2.6 Collective motion as a function of time .....	100
5.3 Conclusions .....	104
CHAPTER 6.....	106
Simulations using new Obstacle Avoidance Model .....	106
6.1 Introduction .....	106
6.2 Parameter table .....	107
6.3 Comparison of simulation results and manual calculation results.....	108
6.4 Simulation results .....	110
6.4.2 Simulation results for 19600 particles .....	124
6.4.3 Comparison of 1000 and 10000 particles .....	130
6.4.4 Collective motion as a function of time .....	131

6.4.5 Effect of the interaction radius .....	136
6.4.6 Effect of noise .....	139
6.4.7. Effect of the speed .....	140
6.4.8 Order of phase transition.....	142
6.5 Conclusions .....	147
CHAPTER 7.....	149
Collective Behaviour of Self-Propelled Particles.....	149
7.1 Introduction .....	149
7.2 Simulation results .....	150
7.2.1. Effect of avoidance radius.....	158
7.2.2. Effect of obstacle density.....	159
7.2.3 Collective motion as a function of time .....	161
7.2.4. Order of phase transition.....	168
7.3. Comparison between obstacle avoidance model and the physical system from the literature .....	170
7.4. Conclusions .....	175
CHAPTER 8 .....	176
Conclusions and Future work .....	176
8.1 Summary .....	176
8.2 Findings and main contributions.....	178
8.3 How objects were met? .....	180
8.4 Future work.....	181
References .....	182
Appendix .....	192

## List of Figures

Figure 1.1 Collective motion of a flock of starlings .....	2
Figure 2.1 Particles show behaviour of attraction, alignment, and repulsion .....	17
Figure 2.2 Predator and prey behaviour is shown. Preys tried to escape from the predators .....	27
Figure 3.1 Interaction of self-propelled particles in the original Vicsek model .....	31
Figure 3.2 Collective behaviour of particles in three-dimensional space .....	33
Figure 3.3 Collective motion of self-propelled particles in the presence of obstacles ...	35
Figure 3.4 Free body diagram represents the behaviour of the particle.....	40
Figure 4.1 Random motion of the particles at $L = 7, \eta = 2, N = 300, t = 0, r = 1, v = 0.03$ .....	50
Figure 4.2 Group formation by the particles at $L = 25, \eta = 0.1, N = 300, v = 0.03, t = 20, r = 1$ . .....	51
Figure 4.3 Movement of the particles with some correlation at $L = 7, \eta = 2, t = 20, r = 1, v = 0.03, N = 300$ . .....	52
Figure 4.4 Alignment in the direction of the particles at $L = 5, \eta = 0.1, r = 1, t = 20, v = 0.03, N = 300$ . .....	53
Figure 4.5 Random motion for at $N = 2000 \eta = 0.1, r = 1, t = 20, v = 0.03$ , .....	54
Figure 4.6 Group formation by the particles at $N = 2000, L = 25, \eta = 0.1, t = 20, v = 0.03, r = 1$ . .....	55
Figure 4.7 Correlation in the system at $N = 2000, L = 7, \eta = 2, t = 20, r = 1, v = 0.03$ , .	56
Figure 4.8 Alignment in the system at $L = 7, \eta = 2, t = 20, r = 1, v = 0.03, N = 2000$ .	57
Figure 4.9 Phase transition for 40 particles at $L = 5$ .....	59
Figure 4.10 Phase transition for 100 particles at $L = 5$ .....	60
Figure 4.11 Phase transition for 400 particles at $L = 10$ .....	60
Figure 4.12 Phase transition for 4000 particles at $L = 31.6$ .....	61
Figure 4.13 Phase transitions for 10000 particles at $L = 50$ . .....	61
Figure 4.14 Evolution of collective motion for different densities at $t = 500$ .....	63
Figure 4.15 Evolution of the collective motion for different particle densities at $t = 2500$ . .....	63
Figure 4.16 Collective motion as a function of interaction radius for smaller number of time steps.....	64

Figure 4.17 Collective motion as a function of interaction radius for 1000 and 3000 time steps.....	65
Figure 4.18 Collective motion as a function of speed for small number of time steps...	66
Figure 4.19 Collective motion as a function of speed for large 1000 and 3000 time steps .....	67
Figure 4.20 Collective motion as a function of time for 56 and 112 particles.....	68
Figure 4.21 Collective motion as a function of time for 336 and 504 particles.....	69
Figure 4.22 Collective motion as a function of time for 560 and 720 particles.....	70
Figure 4.23 Evolution of collective motion for 2800 and 4000 particles .....	70
Figure 4.24 First order phase transition at noise level .....	72
Figure 4.25 First order phase transition at $\eta = 0.193$ .....	73
Figure 4.26 Second order phase transitions at $\eta = 0.196$ .....	74
Figure 4.27 Second order phase transitions at $\eta = 2.0$ .....	74
Figure 5.1 Random motion of the particles at $L = 7, \eta = 2, N = 300, t = 0, r = 1, v = 0.03$ .....	78
Figure 5.2 Disordered motion of the particles at $L = 25, \eta = 0.1, N = 300, t = 20, v = 0.03$ . .....	79
Figure 5.3 Disordered motion of the particles at $L = 7, \eta = 2, N = 300, t = 20, r = 1, v = 0.03$ . .....	80
Figure 5.4 Group formation by the particles at $L = 5, \eta = 0.1, N = 300, t = 20, r = 1, v = 0.03$ . .....	81
Figure 5.5 Initial movement of the particles at $L = 7, \eta = 2, N = 2000, t = 0, r = 1, v = 0.03$ . .....	82
Figure 5.6 Disordered motion at $L = 25, \eta = 0.1, N = 2000, v = 0.03, t = 20, r = 1$ . .....	83
Figure 5.7 Loss of cohesion in the system at $L = 7, \eta = 2, N = 2000, t = 20, r = 1, v = 0.03$ . .....	84
Figure 5.8 Ordered motion at $L = 5, \eta = 0.1, N = 2000, t = 20, r = 1, v = 0.03$ .....	85
Figure 5.9 Alignment in particles at $L = 20, N = 3800, t = 3001, \eta = 0.1, r = 1, v = 1.0$ ...	86
Figure 5.10 Group formation by the particles at $L = 20, N = 3000, t = 3000, \eta = 0.0, r = 0.5, v = 1.0$ . .....	87
Figure 5.11 Collective motion as a function of speed for 500 and 1000 time steps .....	89
Figure 5.12 Collective motion as a function of speed for 2000 and 3000 time steps ....	89
Figure 5.14 Collective motion as a function of noise for 2000 and 3000 time steps.....	91

Figure 5.15 Collective motion as a function of particle density for 500 and 1000 time steps.....	93
Figure 5.16 Collective motion as a function of particle density for 2000 and 3000 time steps.....	93
Figure 5.17 Collective motion as a function of interaction radius for 100 and 500 time steps.....	95
Figure 5.18 Collective motion as a function of interaction radius for a large number of time steps.....	95
Figure 5.19 Second order phase transitions at $L=20$ , $\nu=1$ , $N=3000$ , $t=3000$ , $\eta=1.0$ , $r=1.0$ .....	97
Figure 5.20 Second order phase transitions at $L=20$ , $\nu=1$ , $N=3000$ , $t=3000$ , $\eta=1.5$ , $r=1.0$ .....	97
Figure 5.21 Second order phase transitions at $L=100$ , $\nu=0.5$ , $N=3000$ , $t=3000$ , $\eta=0.1$ , $r=1.0$ .....	98
Figure 5.22 First order phase transitions at $L=100$ , $\nu=1$ , $N=3000$ , $t=3000$ , $\eta=0.1$ , $r=1.0$ .....	99
Figure 5.23 First order phase transitions at $L=100$ , $\nu=1$ , $N=3000$ , $t=3000$ , $\eta=0.1$ , $r=1.5$ .....	99
Figure 5.24 First order phase transitions at $L=100$ , $\nu=1.5$ , $N=3000$ , $t=3001$ , $\eta=0.1$ , $r=1.0$ .....	100
Figure 5.25 Collective motion as a function of time at different noise values .....	101
Figure 5.26 Collective motion as a function of time for strong noise values .....	101
Figure 5.27 Collective motion as a function of time for 200 and 4000 particles.....	103
Figure 6.1 Avoidance of particles from the obstacles is displayed in the sequence of snapshots from the video from (a) to (f) .....	112
Figure 6.2 Static images from (a) to (f) for the same time steps at which snapshots of the video were taken which are shown in figure 6.1 .....	114
Figure 6.3 Random distribution of particles at initial time step ( $\eta = 0.01$ ).....	116
Figure 6.4 Collective motion of the particles in groups at the 10000th time step for..	117
Figure 6.5 Small rectangular boxes in (a) and (c) show particles and obstacles viewed from close range; these can be seen in (b) and (d). These are taken from Figure 6.4...	118
Figure 6.6 Group formation in the system at noise $\eta = 0.03$ .....	119
Figure 6.7 Collective motion of the particles at noise $\eta = 0.06$ .....	120

Figure 6.8 Collective motion of the particles at noise $\eta = 0.1$ .....	121
Figure 6.9 Decline in the collective motion of the particles at noise $\eta = 0.3$ .....	122
Figure 6.10 Randomness in the direction of the particles at noise $\eta = 0.6$ .....	123
Figure 6.11 Collective motion of the particles in groups at noise amplitude $\eta = 0.01$	124
Figure 6.12 Group for motion in the system by the particles at $\eta = 0.03$ .....	125
Figure 6.13 Collective motion of the particles at $\eta = 0.06$ .....	126
Figure 6.14 Higher alignment in the direction of the particles at $\eta = 0.1$ .....	127
Figure 6.15 Decline in the collective motion of the particles at $\eta = 0.3$ .....	128
Figure 6.16 Disordered motion of the particles at $\eta = 0.6$ .....	129
Figure 6.17 Collective motion as a function of time at $\eta = 0.01$ .....	131
Figure 6.18 Collective motion as a function of time at $\eta = 0.03$ .....	132
Figure 6.19 Collective motion as a function of time at $\eta = 0.06$ .....	132
Figure 6.20 Collective motion as a function of time at $\eta = 0.1$ .....	134
Figure 6.21 Collective motion as a function of time at $\eta = 0.3$ .....	135
Figure 6.22 Collective motion as a function of time at $\eta = 0.6$ .....	135
Figure 6.23 Collective motion as a function of the interaction radius $r$ for $N_b = 1000$ .....	137
Figure 6.24 Collective motion as function of $r$ for $N_b = 10000$ .....	138
Figure 6.25 Collective motion as a function of the noise for two values of obstacle density, and .....	139
Figure 6.26 Collective motion as a function of the speed for obstacle density, for $\rho_o = 0$ and $\rho_o = 0.0125$ (20 obstacles) .....	141
Figure 6.27 Second order phase transition at $\eta = 0.01$ .....	143
Figure 6.28 First order phase transition at $\eta = 0.03$ .....	144
Figure 6.29 First order phase transition at $\eta = 0.06$ . .....	144
Figure 6.30 First order phase transition at $\eta = 0.1$ . .....	145
Figure 6.31 Second order phase transition at $\eta = 0.3$ .....	146
Figure 6.32 Second order phase transition at $\eta = 0.6$ .....	146
Figure 7.1 Randomness in the motion of the particles at initial time $t = 0$ for $\eta = 0.01$ .....	151

Figure 7.2 Cluster formation by particles in presence of moving obstacles at $t = 4000$ for $\eta = 0.01$ .....	152
Figure 7.3 Group formation by the particles at $t = 7000$ for $\eta = 0.01$ .....	152
Figure 7.4 Cohesive behaviour of the particles at $t = 10000$ for $\eta = 0.01$ .....	153
Figure 7.5 Decline in the collective motion of the particles at $t = 10000$ and $\eta = 0.3$	154
Figure 7.6 Randomness in the direction of the particles due to $\eta = 0.6$ at $t = 10000$ ..	155
Figure 7.7 Loss of cohesion in the system at $t = 10000$ for $\eta = 1.0$ .....	156
Figure 7.8 System in state of disorder for noise $\eta = 1.5, t = 10000$ .....	157
Figure 7.9 Collective motion as a function of the avoidance radius .....	159
Figure 7.10 Collective motion as a function of the obstacle density .....	160
Figure 7.11 Collective motion as a function of time at $\eta = 0.01$ .....	161
Figure 7.12 Collective motion as a function of the time at $\eta = 0.3$ .....	162
Figure 6.13 Collective motion as a function of time at $\eta = 0.6$ .....	163
Figure 6.14 Collective motion as a function of time at $\eta = 1.0$ .....	163
Figure 7.15 Collective motion as a function of time at $\eta = 1.5$ .....	164
Figure 7.16 Comparison of collective motion for fixed and moving obstacles at different noise values .....	166
Figure 7.17 First order phase transition at $\eta = 0.01$ .....	168
Figure 7.18 Second order phase transition at $\eta = 0.3$ .....	170
Figure 7.19 Second order phase transition at $\eta = 0.6$ .....	170
Figure 7.20 Flock formation in starlings [120].....	173
Figure 7.21 Group formation in particles.....	173

## List of tables

Table 4.1 – Symbols used in captions of figures .....	47
Table 4.2 Initial positions and the velocities of the two particles.....	48
Table 4.3 Calculations of two particles at first time step.....	48
Table 4.4 Calculations of two particles at second time step .....	48
Table 4.5 Simulation result of two particles at first time step .....	49
Table 4.6 Simulation result of two particles at second time step.....	49
Table 5.1 Symbols used in captions of figures .....	78
Table 6.1 Parameters used in the simulation.....	107
Table 6.2 Initial positions and velocity directions of three particles .....	108
Table 6.3 Initial positions and velocity directions for one obstacle.....	108
Table 6.4 Manual calculation of three particles at first time steps.....	109
Table 6.5 Manual calculation of three particles at second time step .....	109
Table 6.6 Program values of three particles at first time steps .....	109
Table 6.7 Program values of three particles at second time step .....	110
Table 6.8 Distance between 3 particles and 1 obstacle.....	115
Table 7.1 – Symbols are defined which are used in figure captions.....	150

# CHAPTER 1

## Introduction and Background

### 1.1 Introduction

Active matter is a new branch of soft matter physics that includes systems of collectively moving entities in nature, for example: flocks of birds, migrating bacteria, swimming schools of fish, herds of quadrupeds in motion, ants, molds or pedestrians [1]. It is of prime importance to understand the universal features and behaviours of these entities when many organisms are included, and when their parameters, such as the level of perturbation or the mean distance between the individuals, are varied. An understanding of the collective motion of such entities can be helpful in many areas which are useful in our daily life; for example, an artificial swarm of autonomous vehicles can be produced leading to highly developed fishing strategies, or human interactions in crowds which may be helpful in devising and implementing efficient and safe crowd control policies, thus avoiding casualties in crowded situations [2].

Collective motion takes place when individuals interact with one another. Eye-catching displays of collectively moving animals are fascinating. Schools of fish can move in order or they can change direction abruptly. When a predator is near, the same fish can swirl like a vehemently stirred fluid. Flocks of starlings fly together to fields in groups moving uniformly. When these starlings return to their roosting site they create turbulent and fascinating displays. Numerous examples from the living and non-living world include the rich behaviour of the systems in which permanently interacting moving units exist [3]. There needs to be better understanding of collective behaviour.

## 1.2 Collective behaviour

In a system containing similar entities (for example molecules or flocks of birds) the interaction between the entities can be simple such as attraction and repulsion or more intricate, and can take place between neighbouring entities in space or in a fundamental network. Under certain conditions transitions can happen during which the entities implement a pattern of behaviour almost fully determined by the collective effects due to other entities in the system. The main property of collective behaviour is that the action of an individual unit is dominated by the influence of others; the behaviour of a unit is totally different from the way it would behave on its own. Such systems exhibit fascinating ordering phenomena as the entities simultaneously change their behaviour to a common pattern. For example, a group of randomly oriented pigeons on the ground looking for food will order themselves into an orderly flying flock when leaving the scene after a large disturbance. Understanding new phenomena is usually obtained by linking them to known ones: a more complex system is understood by investigating its simpler modifications.



**Figure 1.1** Collective motion of a flock of starlings [4]

In recent years researchers have modelled the collective behaviour of self-propelled particles. Self-propelled particles play an important role in understanding the key features of biological systems, such as the collective motion of a flock of birds [5]. Self-propelled

particles are present everywhere in nature, for example, non-animated matter such as running droplets [6-9] and crawling cells [10-14]. Systems become non-equilibrium due to the self-propulsion of the particles. These are fascinating complex behaviours which depend upon the interaction of the particles, for example, the energy consumption involved in propulsion mechanisms and the amount of energy used for these active particles to move without fluctuation dissipation theorem [15-19].

Interacting self-propelled particles have extensive applications such as autonomous robots, traffic, human crowds and biological systems [20-23]. These include birds [24] and bacteria [25, 26]. Interacting active particles show behaviours not included in the equilibrium systems. There is the possibility of a long-range orientation order in a two-dimensional coordinate system with continuum symmetry [27].

### **1.3 Self-propelled particles (SPP)**

Self-propelled particles (SPP) or the Vicsek model is basically a concept which is used for the purpose of modelling the collective motion of large groups of organisms. In SPP the motion of flocking organisms is modelled by the collection of particles that assume a constant speed but respond to random noise by assuming at each time increment the average direction of motion of the other particles in their neighbourhood [28]. Interaction between SPPs can produce dynamic behaviours that are more complex than those in which particles move independently. The Vicsek model defines many features of the dynamics of particles with high collective motion in which particles align with their neighbours and make groups [29].

The Vicsek model [28] produces motion of macroscopic and microscopic groups. The macroscopic groups include schools of fish and flocks of birds [30]; and microscopic

groups include bacterial swarms and cancerous tumors [31]. In the Vicsek model, particles aligned with their neighbours when they were in the range of the interaction radius. It shows a phase transition in one-directional motion as a function of particle density and noise amplitude. Modifications of the Vicsek model involve the addition of steric interactions [32] and cohesion [33]; however very little work has been done to understand the interaction of flocking particles with obstacles [29].

In the 1970s, researchers introduced an important concept in statistical physics in the form of the renormalization group method which provided a detailed theoretical understanding of the general phase transition. The theory demonstrated that the key features of transitions in equilibrium systems are insensitive to the details of the interactions between the individuals in a system [3].

## **1.4 Phase transition**

Phase transition takes place in a system consisting of a large number of interacting particles undergoing a transition from one phase to another as a function of one or more external parameters [3]. Physical systems can be solids, liquids and gaseous phases. A well-known example of phase transition is the freezing of a substance when it is cooled. Phase transitions occur when particular system variables, known as order parameters, are changed.

The term ‘order parameter’ has been given because of the observation that phase transitions usually include due to an abrupt change in a symmetry property of the system. When matter is in a solid state the atoms are arranged in an ordered crystal lattice. In liquids and gases, the positions of the atoms are disordered and random. Order parameter can be considered as the degree of the symmetry which characterises the phase. Order

parameter will have a value equal to zero when the system is disordered, and it will equal 1 when highly ordered. i.e. if  $\psi = 0$  then the system is disordered and if  $\psi = 1$  then the system is in perfect order.

In the case of collective motion, the order parameter is the average normalized velocity

$$\psi(t) = \frac{1}{Nv_o} \left| \sum_{i=1}^N V_i(t) \right| \quad (1.1)$$

where  $N$  represents the total number of particles, and  $v_o$  is the absolute velocity of the particles in the system. If the motion is in a disordered state then the velocities of the particles will be in random directions and will average out to give a small magnitude vector, whereas for ordered motion the velocities add up to a vector of absolute velocity close to  $Nv_o$ .

Order parameter can change from 0 to 1 for large values of  $N$ . Firstly, order transition takes place when the order parameter changes discontinuously. For example, the volume of water changes discontinuously when it forms ice. However, the second order (or continuous) phase transition takes place when the order parameter changes continuously, whereas its derivative with respect to the control parameter is discontinuous. Large fluctuations occur when the second order phase transition takes place. A spontaneous symmetry breaking takes place during phase transition. For example, if the critical value of the control parameter is exceeded, such as temperature or pressure, the symmetry of the system will change. A control parameter is basically a parameter which brings changes to the phase transition; for example, a system undergoes a transition from one phase to another as a function of the control parameter. In the self-propelled particle model, the control parameter is considered to be the noise because the scale of noise can disturb the

system: if the noise is very much smaller, the particles will show a higher collective motion, and if the noise is much higher, the particles will not demonstrate collective motion and there will be a state of disorder in the system. The symmetry of the system changes if we pass the critical value of the control parameter (for example, temperature or pressure).

The collective motion exhibited by schools of fish and flocks of bird is a fascinating example. They move together in the same direction and have a highly cohesive shape. They change their direction in a very short time. When they face any obstacle they change their direction from the beginning to the end of the group at the same time in order to avoid collision. When humans move in crowded spaces they often form a mass and bump against each other. What is the particular characteristic of these animal flocks which makes a difference between humans and animals? How can they receive, send and integrate information from each individual to show movement in their dynamical patterns? These questions have been studied in various ways with different approaches. Individual-based collective motion modelling by computer simulation is one of the important types of study to investigate the collective motion of the flocks [34].

From a functional perspective, the movement of animals in groups is beneficial in numerous different ways concerning moving cohesively and staying together. This involves an increased ability to detect and avoid predators [35] and reach a target destination [36, 37]. As a group, individuals have to balance their own preferences against the benefit of staying in a group, for example when negotiating a common direction of movement or a common activity [38]. A large body of biological literature exists on how such direction consensus is obtained. The main focus is, either on the mechanism by which consensus is reached, involving nonlinear, quorum-sensing type responses [39], or on individual differences which affect the weight of an animal in a group decision [40-

43]. There are many features of collective decision-making which do not demand heterogeneity in the behaviour of the individual; consistency in individual differences in leadership have been found in various species, for instance pigeons [44,45], mosquitos, fish [46], zebras [40] and several species of primates [41].

Leadership means some individuals have a greater influence on the group, inferred from the fact that choice of the group follows those individuals' information or preferences. A group decision can show leadership without the active participation of group members in choosing a leader. Simulations by Conradt *et al.* [47] show examples in which heterogeneity becomes the source of self-organized leadership without the demand of global communication or recognition of the individual. These are divided into two categories 'leading by need' and 'leading by social indifference'. In 'leading by need', stronger attraction to a target stimulus happens, whereas in 'leading by social indifference', weaker responses to specifics take place. The basis of the two categories involves the contrasting functional priorities of the individual: the importance given to reaching the target versus the importance of remaining with the rest of group. It is difficult to understand the group decision-making without an understanding of the core interaction amongst individuals. The interaction rules that are developed by a particular species will reveal a trade-off between the numerous features of collective behaviour, for example group cohesion, the accuracy and speed of the group decisions and an ability of an individual to avoid predators within the selfish herd' [46,48,49].

Due to these competing pressures, it is unclear that the interaction rules will maximise collective behaviour. Providing mechanistic links between measured interaction rules and group results will help to determine the functional significance of interaction rules, for instance whether they enhance the tracking gradient [50] or avoid predators [49]. If the positioning of individuals within the group in the context of their interactions can be

described, then it is possible to form a link between the interaction rules and the information processing at the group level. Consider a group which includes only two individuals. Assuming that there is the existence of blind visual angle, the transfer of information will be unidirectional if the individuals move one behind the other, whereas travelling side by side they can see each other supporting bidirectional information transfer [51].

The study of active particle systems has emerged in a promising new direction: the design and manufacture of biometric and artificial active particles. The directed driving is frequently achieved by making asymmetric particles that keep two distinct friction coefficients [52-54], light absorption coefficients [55-58], or catalytic properties [59-62], subject to whether energy injection is done through vibration, light emission or chemical reaction respectively. Artificial active particles are characterised by their diffusion coefficient  $>1$  achieved using symmetric particles [59]. Theoretical and experimental studies have been undertaken on the statistical description of the motion of the particle in idealized, homogeneous mediums. However, the most natural active particle systems exist in the wild in the heterogeneous media. For example, active transport inside a cell takes place in a space containing organelles and vesicles [63]; the motion of bacteria in highly heterogeneous environments such as soil or complex tissues, such as in the gastrointestinal tract [64] and diffusion in random media [65, 66]. The impact of the heterogeneous medium on the locomotion patterns of active particles is not well understood. A simple model is used in which the active particles move at a constant speed in a heterogeneous two-dimensional space, where the heterogeneity is specified by the obstacles randomly distributed in the system. An obstacle can represent the source of a repellent chemical, a burning spot in a forest, a light gradient, or whatever threat makes our self-propelled particles turn away upon sensing danger: the avoidance of the obstacle is described by a (maximum) turning speed  $\gamma$ . The analysis shows that the similar

evolution equations, behaviour rules become the source of various locomotion patterns at lower and higher density of the obstacles. Here, the meaning of analysis is a detailed examination of the model undertaken by the authors of the articles. They varied different parameters for this purpose. These parameters are the particle's turning speed and the obstacle density.

For weaker obstacle densities there is no conflicting information and particles can easily turn away from the unwanted area in their way. Alternatively, where environmental conditions, for example organisms, sense numerous repellent sources at the same time, the process of information is not simple. Particles compute the local obstacle density gradient and utilize this information to turn away from higher obstacle densities. Since the obstacles are randomly distributed, as the number of obstacles increase, this task becomes increasingly challenging. No strategy guarantees how to turn away from obstacles and the particles behave more and more if there were no obstacles exist.

For smaller values of  $\gamma$  the change in behaviour is reflected by the minimum shown by the diffusion coefficient at intermediate obstacle densities. For higher values of  $\gamma$ , particle motion is diffusive at smaller obstacle densities  $\rho_o$ , whereas for large obstacle densities a new phenomenon appears: the spontaneous trapping of particles. These traps are closed orbits found by the particles in a landscape of obstacles. The results open a new way to control the systems of the active particle. For example, the emergence of spontaneous trapping as a dynamical phenomenon that depends on the basic properties of the particles permits us to form a generic filter of active particles.

The physics of interacting and non-interacting self-propelled particles can be helpful in understanding non-equilibrium statistical physics, ecology and developmental biology [27].

## **1.5 Aim**

The aim of this study is to obtain a better understanding of the collective motion of self-propelled particles and how these can be applied more widely in important applications such as crowd control policies, fishing strategies, and in designing migration and navigation strategies.

## **1.6 Objectives**

The collective behaviour of self-propelled particles will be investigated in the homogeneous medium with a focus on the effects of various parameters on the system of 2D self-propelled particles. Furthermore, the order of phase transition will be also investigated. The collective motion of self-propelled particles will be investigated in three-dimensional spaces to investigate how particles behave when there is a change in parameters. Different values of noise parameter will be used to study the changes in the order parameter. Furthermore, there will be variation in the interaction radius and speed for the purpose of checking their effect on the collective behaviour of particles. Different particle densities will be applied to investigate the patterns formed by the particles.

To investigate the collective motion of the self-propelled particles in the heterogeneous medium, the motion of the particles will be studied in the presence of fixed obstacles. Collective motion in homogeneous and heterogeneous media will be compared. The order of phase transition will be also investigated. Collective motion will be plotted against each time step. Obstacle density and its effect on the collective motion of the particles will also be investigated.

To investigate the collective motion of self-propelled particles in the presence of moving obstacles at different parameters to check their effect on the motion of particles, comparison will be made for collective motion in the presence of static and moving obstacles. Motion will be plotted against each time step.

## **1.7 Outline of the thesis**

This thesis is divided into seven chapters. The first is the introductory chapter which presents the contents, highlights the aims and objectives and gives a brief outline of the chapters.

In chapter 2 literature review is discussed. Main focus is on heterogeneous and homogeneous mediums of self-propelled particles.

The chapter 3 gives details about the methods that are used in the project. First of all, the method of the Vicsek model is defined in 2D and then in 3D. Movement of the particles is given in three-dimensional space. Collective behaviour of self-propelled particles is investigated in the heterogeneous medium. A new model is proposed, termed the obstacle avoidance model, where the particles move in the heterogeneous medium involving fixed obstacles and moving obstacles. This model is compared with the Chepizkho model [69]. The obstacle avoidance model proposed in this study is simpler and easier to simulate.

The chapter 4 presents and discusses the simulation results. The collective behaviour of self-propelled particles is presented in two-dimensional space. The effects of various parameters such as noise, interaction radius, speed of the particles, and particle density on the collective behaviour of self-propelled particles are investigated. The collective motion is plotted against time. The order of phase transition is also investigated. It was

observed that for weaker noise systems there was a state of order, and stronger noise particles showed random directions.

In chapter 5 the Vicsek model in 3D is discussed. The positions and the directions of the particles are defined in the x, y and z coordinate system. The effects of different parameters including noise, interaction radius of the particles, speed and particle density on the collective motion of self-propelled particles is investigated. It was observed that, in the case of the higher particles such as  $N=3800$  along with smaller noise  $\eta = 0.1$ , particles showed alignment in their directions.

Results obtained from the obstacle avoidance model are discussed in chapter 6. The effects of fixed obstacles on the collective motion of self-propelled particles are investigated. Various parameters used in this model such as noise, interaction radius of the particles, particle density, avoidance radius, and obstacle density are investigated and their effects described. The collective motion of the particles is plotted against time. The order of phase transition is also investigated. Collective motion is compared in homogeneous and heterogeneous mediums. It was observed that the value of the order parameter was more consistent in homogeneous systems while there were fluctuations in the heterogeneous mediums.

In chapter 7 simulation results in the presence of moving obstacles are discussed. The collective behaviour of self-propelled particles is investigated in the presence of moving obstacles. Values of avoidance radius and the obstacle density were varied to investigate their effects on the collective motion of the particles. The other parameters that were involved in the model were noise, interaction radius, speed, particle density, obstacle density, speed of the obstacles, and avoidance radius. Order parameter was plotted as a function of time. Moreover, the order of phase transition was also investigated. Compared

to fixed obstacles, particles showed fewer fluctuations in the case of moving obstacles for lower noise levels.

In chapter 8 a summary of results obtained and conclusions are presented. The future work is also highlighted.

## CHAPTER 2

### Collective behaviour of self-propelled particles - a literature review

#### 2.1 Introduction

The study of self-propelled particles is a fascinating area of interdisciplinary research which is at the frontier between biology and physics. Current research on self-propelled particles focuses on three major directions:

- i) The motion and transport of individual self-propelled particles;
- ii) The motion of self-propelled particles in external and self-produced fields;
- iii) The collective motion of particles that are in contact with one another through binary interactions.

Systems of self-propelled particles are connected with each other through binary interactions that produce fascinating patterns of group dynamics, for example, flocks of birds, schools of fish, or herds of sheep. The collective motion in nature may give enormous advantages for members of the group as well as being of great scientific interest [67]. Even though collective motion is a fascinating occurrence in nature, little scientific work has been carried out using numerical and mathematical simulations. In this review, some of the work carried out using mathematical simulations is presented.

## 2.2 Collective Behaviour in Homogeneous Medium

The collective behaviour of self-propelled particles in homogeneous systems, where the particles are identical, has been investigated by several groups [28, 68, 69]. Examples in nature include: bacteria swarming on surfaces [70], the movement of locusts [71], and the movement of microtubules on a carpet of fixed molecular motors [72].

The first computational model for the behaviour of organisms in flocks was developed by Reynolds in 1987 [73]. This model paid attention to the individual behaviour of each organism in the system. Almost a decade later, in the year 1995, the concept of self-propelled particles was modelled by Vicsek *et al.* [28]. This model focused on the collective behaviour of all organisms or particles rather than individual particles. In the Vicsek *et al.* [28] model the only rule was that at each time step the particle followed the average direction of the movement of particles which were within its interaction radius, with some random noise added. This model enabled larger system sizes to be simulated. The results of the model showed that the interaction between the individuals could display complex behaviour. Moreover, phase transitions were introduced from disordered to ordered systems showing variations in noise and density. This model can be treated in terms of moving spins, with the velocity of the particles given by the spinvector. This similarity with a spin system allows the alignment mechanism to be denoted as ferromagnetic (F-alignment). The temperature associated with spin-systems enters the Vicsek model as noise in the alignment mechanism [74]. Self-propelling particles fall into two categories:

- i) the first, in which the particles interact with the background, and
- ii) the second, in which the particles interact with each other via kinematic constraints [73].

The Vicsek model belongs to the second type, as the only interactions in the system are through the particles aligning with the velocities.

Since Vicsek *et al.* introduced self-propelling particles to investigate collective behaviour, other models based on self-propelling particles have been developed. Such models include Lagrangian [75-77], Newtonian mechanics [78, 79] and the mean field theory [74]. A simpler model for interaction was given by Couzin *et al.* [80] who used specific behavioural rules. This model updated the positions in the same way as the Vicsek model [28], but the velocities were updated according to the behavioural rules. The model consisted of three zones and a perception region. The three zones were:

- i) a repulsion zone,
- ii) an orientation zone, and
- iii) an attraction zone.

The top priority rule in this model was that each particle must have a minimal separation distance in order to avoid collision. If all the particles were greater than the minimal separation, then the second rule would be implemented, which required individuals to attract and orient themselves to avoid isolation.

Ballerini *et al.* [81] conducted a study using stereo metric and computer techniques. They measured in 3D the positions of individuals within flocks involving up to 2600 starlings. They showed that, rather than the individual starling interaction through a metric radius of interaction, they interacted with just 6-7 of their nearest neighbours. With the help of simple predator models, one using metric interaction and the other topological, the topological results provided a lower number of groups than in the metric case, which was more of a resemblance to the known survival mechanisms of starlings. In Ref. [82] it is revealed that experiments on flocks of birds indicated that interactions are topological.

This paper showed that a significantly better stability was achieved when the neighbours were selected according to a spatially balanced topological rule.

The dynamics of systems of SPP with kinematic constraints on the velocities has also been studied [83]. A continuum model was proposed that considered the stability of ordered motion with respect to noise.

An important consideration is in the way in which individuals perceive their neighbours and the criteria used to decide which neighbours are influential. A simple but effective approach to this problem was given in the Couzin model, where individuals responded to their neighbours according to the neighbour's distance [80]. Researchers gave topological based rules through which individuals followed a fixed number of neighbours without knowing their distances [84].

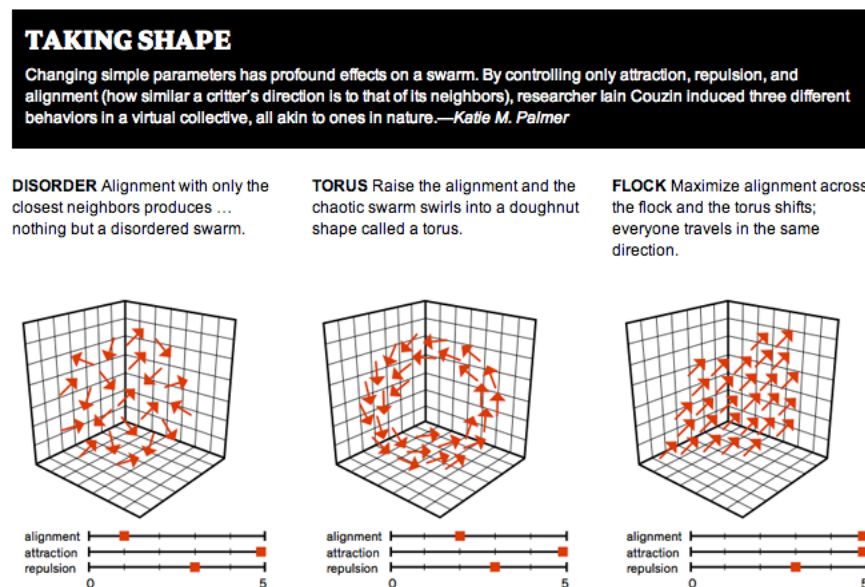


**Figure 2.1** Particles show behaviour of attraction, alignment, and repulsion [85]

The hydrodynamic interactions encouraged the rise in the collective motion, which could take the shape of a macroscopic flock at small densities, or it could be in a homogeneous polar phase when there were greater densities [86]. When large density variations took

place, the hydrodynamics safeguarded the polar-liquid state. It can be observed here that physical interactions at the individual level were enough to set the particles into an unchanging focused motion.

A variant of the Vicsek model that involved pairwise repulsive interactions was also used [87]. They observed that there could be changes in the appearance of the system if it was confined between two parallel lines; there would be the emergence of a laning state. There was the same direction of particles in all lanes and there was a finite separation distance between the lanes. In some parameter ranges collectively, the moving clusters arranged themselves in an almost hexagonal way. It has been suggested that the reason for such a structure is an overreaction in the alignment mechanism.

The interaction between a pair of pigeons was studied using a high resolution global positioning system [51]. Small changes in the velocity showed alignment with the direction of the nearest particle, and also there was an attraction or avoidance that depended on the distance. When a neighbour was in front, the responses were stronger. From the flocking behaviour, the model predicted that this feature was how groups found their direction. It was shown that the interactions between pigeons made a stable side-by-side alignment, helping bidirectional information transfer and decreasing the risk of separation. If any bird came in forward-facing, it would lead to directional choices. The model discussed in this paper [51] predicted that when a faster bird came in front, it determined the direction of the route. Results showed how the group decision arose from individual single differences in determining direction behaviour.

The physical behaviour of the scalar noise model was studied in the smaller velocity regimes from different angles. It was proposed that there was an ordering of the particles as the noise was reduced below a critical value of the particle density or velocity dependent [5].

There is some debate on the nature of the order disorder transition in the Vicsek model. Simulations done by the Vicsek group supported consistent second order transitions [28]; this contradicts work done by Chate *et al.* [88], who claimed that the transition was discontinuous, i.e. first order. Further controversy arose when subsequent papers of Vicsek *et al.* [5, 89], Aldana *et al.* [90, 91], Dosetti *et al.* [92], and Baglietto *et al.* [93, 94], supported the critical nature of the phase transition. These papers are in conflict with the results given by the Chate group [95-97]. A careful review of the existing literature showed that various researchers introduced complex changes to the Vicsek model; for example, changes in the velocity update process and changes in noise evolution. In Ref. [89], the nature of the phase transition is discussed in the scalar noise model. The results of the paper verified the findings of the Vicsek *et al.* model [28] where for small velocities ( $v \leq 0.1$ ), the nature of the order-disorder transition was continuous second order phase transition. For larger velocities ( $v \geq 0.3$ ), strong anisotropy was found in particle diffusion in comparison with the isotropic diffusion for smaller velocities. The artificial symmetry breaking and the first order transitions were due to the interplay between the anisotropic diffusion and the periodic boundary conditions. It is impossible to draw a conclusion regarding physical behaviour in a higher particle velocity regime based on the scalar noise model.

### **2.3 Statistical physics of self-propelled particles**

Recently, there has been an increase in the number of scientific studies on self-propelled particles in the context of statistical properties of the motion where the particles freely move without any obstacles or gradients acting on them. One of the main purposes of such studies is to understand the role of the fluctuations in the motion of the self-propelled particles. The statistics of such free movement may give useful information on the efficiency of the different kinds of motion.

Statistical physics and its theoretical methods and models have provided a unifying viewpoint for kinetic modelling of the single and multiple particle systems. The modelling of spatio-temporal behaviour as non-equilibrium processes needs new tools in the theory of non-linear stochastic dynamics and new experimental techniques for *in vivo* observations [67]. The solution to new situations in living matters requires an interdisciplinary focus.

The first study was undertaken by Vestergaad *et al.* [98], where they investigated the estimation of motility parameters of self-propelled particles from experimental data, especially in situations where the empirical data analysis was challenging, i.e. when the trajectories were shorter and with a smaller number of them. Brownian motion with a linear time-dependent of the mean squared displacement was considered, along with different causes of errors, and provided the best estimator for diffusion coefficients.

Gotz *et al.* [99], applying similar methods, studied the impact of the intracellular architecture and cytoskeleton dynamics on the intracellular transport. The mean square displacement of the silica particles was investigated. These particles were engulfed by the slime mould *Dictyostelium discoideum*. In this paper, the authors reported the roles of active transport, subdiffusive, diffusive, and super-diffusive particle motion.

Raatz *et al.* [100] studied the swimming patterns of the bacterium *Pseudomonas putida* particles in confined atmospheres. They defined a systematic approach by means of proven experimental (microfluidic) technologies. They also used a data analysis algorithm to describe the swimming motility of the *P. putida*. Furthermore, they discussed the hydrodynamic effect of obstacles and interfaces on the swimming patterns and showed how growing confinement brought about changes to the turning angle statistics and the mean run lengths of bacteria.

Rodiek and Hauser [101] studied experimentally the motility of amoeboid cells of the slime mould *Physarum polycephalum*. An investigation of their trajectories and mean square displacements showed two characteristic behaviours that depended upon the time interval considered. The free migration of the cells showed persistent random motion. The motility was due to changes in the cell shape encouraged by the peristaltic pumping of protoplasm through the cell. Superdiffusive motion was observed during free migration. An asymptotic component was shown by the typical velocity distributions from the freely migrating cells. The higher propagation velocities correlated with straight motion and an elongated cell shape. The mean square displacement of the trajectories was compared for cells, avoiding their own slime trails, to freely migrating cells.

Romanczuk *et al.* [102] investigated the velocity distributions of swimming algae *Euglena gracilis* into a microfluidic channel and interpreted the data. The observed velocity distributions were consistent with the theory based on the Brownian motion with active fluctuations. The applied theory of active fluctuations involved forced fluctuations heading in the direction of the propulsions. Fluctuations took place due to the random internal performance of the propulsive motors; hence noise originated in the propulsive mechanism.

Solon *et al.* [103] provided a theoretical comparison of “active” and “run and tumble movements”. For these two cases, the analysis was done on the basis of kinetic description by means of master equations and equations for the moments of the probability density functions. They also investigated the behaviour of individual particles in external fields and in confinement, as well as the interaction of the particles. There is a great deal of material given, which also comprises a broad description of the technical details of the applied approach. The crossover from a particle-oriented description to a field description with density dependent velocity is explained.

Hernandez-Navarro *et al.* [104] studied the driven motion of colloids in anisotropic matrices such as nematic liquid crystals. The colloids' driving mechanism was based on the principle of nonlinear electrophoresis which was brought about by the asymmetry in the structure of the defects created by the inclusions in the host's elastic matrix. They discussed numerous kinds of individual and collective motion of charged colloids, which were brought about by the electric fields.

Kaiser *et al.* [105] studied the motion of two wedge shaped objects in a bath of self-propelled rods. The wedges were moved when pushed by the self-propelled rods, whereas their orientation remained constant. In experiments, this situation was controlled by the influence of the magnetic field.

The hydrodynamic limit for collective motion in the Vicsek model was discussed by Ihle [106], who established an exact equation for the N-particle distribution function. The hydrodynamic equation explained two cases by means of a mean-field approximation and by a dimensional reduction through eliminating fast variables.

Grobmann *et al.* [107] undertook an amendment to the Vicsek model and showed that the particles added provided additional alignment rules. Apart from repulsion-like behaviour at very small distances, the particles displayed parallel alignment interactions at short separation distances; whereas at a greater separation, the particles showed antiparallel alignments. Lastly, the extremely separated particles did not interact. These types of competing effects brought about a wide range of structures and patterns collectively; for instance, grouped structures and turbulent regimes.

Slomaka and Dunkel [108] used a Navier-Stokes-like equation to describe a fluid involving SPPs or bacteria. They derived two equations for the fluid velocity and for the

active component. They gave priority to the effective one-component description, but provided the addition of higher-order terms into the stress tensor.

The incompressible Navier-Stokes equation for Newtonian fluids is given as:

$$\partial_t V + (V \cdot \nabla)V - \nabla \cdot (2\nu DV) + \nabla p = f \quad (1.1)$$

$$\nabla \cdot V = 0 \quad (1.2)$$

where  $V$  represents the velocity of the flow,  $DV = \frac{1}{2}(\nabla v + \nabla v^t)$  its deformation tensor, and  $p$  represents its pressure. The equation (1.1) is obtained from Newton's law, while equation (1.2) represents the mass conservation equation.

In the actual Navier stock equation for incompressible fluid there is no stress tensor given up to the sixth order partial differential equation, but in [108] the authors have given a minimal generalized Navier stock equation which has a stress tensor up to the sixth order. This appears to be the main difference between the actual Navier stock equation and the equation discussed in [108]. Furthermore, the authors provided the analytical and numerical solution of the Navier stock equation. It was assumed that complex fluid-swimmer interactions can be captured by the generalised form of stress energy tensor, which can be expanded in the context of higher order differential equations that creates turbulent flow features.

## 2.4 Collective Behaviour in Heterogeneous Medium

The collective behaviour of self-propelled particles for identical particles has been widely studied [28, 68, 69, 109]; however little work has been done to introduce a second component to the system, such as an obstacle which could be moving or fixed [110].

### **2.4.1 Fixed obstacles**

Movement in dynamic and complex environments is an integral part of our daily activities such as involving driving on busy roads, walking in crowded spaces and playing sports. Many of these tasks that humans perform in such environments involve interactions with static or fixed obstacles. There is a need to coordinate ways in which to deal with the obstacles [111]. This theory can also be applied to other living things, such as flocks of birds, which also face obstacles while moving collectively. It is also very important to understand the detection and avoidance of the obstacles wherewith existing noise.

The interaction of individual particles with obstacles from different angles has been investigated [112-114]. There is still an urgent need to investigate natural systems involving fixed obstacles because the collective motion of the natural system sometimes takes place in a heterogeneous media. Many examples are available in the natural environment: bacteria show complex collective behaviours, for example swarming in a heterogeneous environment such as soil or highly complex tissues in the gastrointestinal tract; in addition, herds of mammals travelling long distances crossing rivers and forests [115]. There has been little work done on experimenting and theorising regarding the impact of a heterogeneous medium on collective motion [3].

An individual based modelling approach was discussed which defined group interactions with obstacles [116]. The particles' avoidance behaviour was simulated. The effect was also measured by group size where there was the probability of a single particle colliding with a fixed obstacle and the degree of efficiency in navigation and cohesion; when larger model suppositions and larger values of parameters occurred, the social interactions had a higher chance of colliding with the obstacles. The risk of colliding was a non-linear function of the group sizing. It was shown that the motion created due to social interaction had an impact on the metrics, which could be useful in managing and policy deciding.

A continuum model was involved which involved flocks [49] where the linearized interaction of a flock to an obstacle was studied. The flock behaviour, after interacting with obstacles, was shown by the density disturbances. This disturbance is like Mach cones, in which order is expressed by an anisotropic spread of waves of flocking. It was shown through a simple model that the existence of obstacles, either static or moving, could change the dynamics of collective motion [115]. The optimal noise amplitude maximized the collective motion, while in a homogeneous medium this type of optimal did not exist. When there were small obstacle densities, with a weak heterogeneous media in the system, the collective motion showed a unique critical point below which the system showed a long range order similar to that of the homogeneous media. Furthermore, when there were high obstacle densities and a strong heterogeneous media, it was found that there were two critical points which made the system disordered at both low and large noise amplitudes, and showing only a quasi-long range order in between these critical points. The optimal noise that increased the collective motion was helpful in developing and understanding migration and navigation strategies in a moveable or non-moveable heterogeneous media, which should help to understand the evolution and adaptation of stochastic components in natural systems which show collective motion.

The movement of self-propelled particles was studied in a heterogeneous environment. Here obstacles were randomly placed into a 2-dimensional space [64]. In this model, the particles were avoiding obstacles and the particles' avoidance was determined by the turning speed  $\gamma$ . It was shown in this model that the mean square displacement of individuals was giving two regimes as a function of the obstacle density  $\rho_o$ , and  $\gamma$ . It was also found that when there was a smaller value of  $\gamma$ , the movement of the particles was diffusive and was defined by the diffusion coefficient, which showed a least at intermediate densities of obstacles  $\rho_o$ .

The model proposed by the authors showed the dynamics of the particles in the presence of obstacles [115]. This model involved too many terms in the final equation of the model. Incorporating the noise parameter, it created a high degree of randomness in the system. This model showed a lower collective behaviour of particles with little cluster formation. There was a need to develop a more simple and easily applicable model.

### **2.4.2 Moving Obstacles**

An example of moving obstacle is a predator. Such models involving the presence of a predator or predators are the Inada model for the order and flexibility in schools of fish [117], and Lee's model which investigated the escaping behaviour of a prey-flock in response to a predator's attack [118]. The Zheng model involved collective evasion from predation in fish schools and Nishimura's model showed a prey-predator game model [119]. In Inada's model there was a reaction field for fish such as that in the Couzin model [80]. The model was modified for the inclusion of a predator by causing the fish to align its velocity in the direction to repulse the predator if it was within the reaction field. The predator in this model aligned its velocity to attract the prey within the reaction field, and if no prey was found then it moved in random directions to search for prey.

Lee's model made use of molecular dynamics simulations in a 2D continuum model. In this model, the behaviour of individuals in a school without a predator involved regions of repulsion, orientation and attraction. The predator's behaviour aligned its velocity to the centre of the prey. Zheng's model also included zones, but in this case the prey behaved in a manner to confuse the predator as it made a strike. Individual prey components focused on the behavioural rules depending on the three zones: a selfish zone where the prey orients to repulse the predator; a zone of decision to behave selfishly; and a no detection zone, where schooling motion takes place. In this model the predator

selects its prey at random at every time step. Carere *et al.* [120] studied the movement of starlings with different predation pressures and found that small groups formed roosts with lower predation pressures in comparison to that of a roost in which the predator's pressure was high.

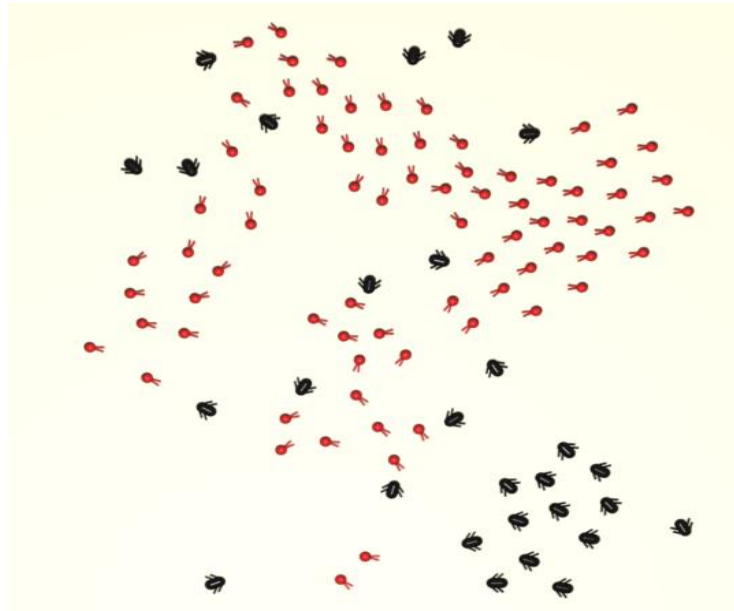


**Figure 2.2** Predator and prey behaviour is shown. Preys tried to escape from the predators [121].

Two groups of self-propelled organisms have been simulated using a Vicsek-like model involving steric intragroup repulsion. Chase and escape are described by intergroup interactions, attraction for predators and repulsion for preys from the nearest particles of the interactions [121]. The risk-related selection for collective motion by allowing real predators to hunt mobile virtual prey has also been investigated [49]. They isolated predator effect while controlling for confounding factors. They found that prey with tendency to be attracted toward and to align direction of travel with, near neighbours tended to form mobile coordinated groups and were rarely attacked.

## CHAPTER 3

### **Models for Collective Behaviour of Self-Propelled Particles for Homogeneous and Heterogeneous Systems**

#### **3.1 Introduction**

To investigate the collective motion of self-propelled particles in the heterogeneous medium (presence of obstacles) and to see the effect of various parameters on the collective motion of the particles, it is necessary to model the motion in the homogeneous medium (without obstacles); hence the Vicsek model is reproduced. This model is done in two-dimensional and three-dimensional spaces. Particles move without obstacles. The effects of various parameters were investigated including noise, interaction radius, speed and particle density. Following on from the homogeneous medium, the heterogeneous medium, where motion of the particles was modelled in the presence of obstacles, was discussed. For this purpose, the Chepizkho model was explained in detail. Subsequently a new model was developed and named the ‘obstacle avoidance model’. The effects of fixed obstacles and moving obstacles were studied. Different parameters were investigated, such as noise, interaction radius, speed of the particles, particle density, obstacle density and avoidance radius. An order parameter was used to characterise the macroscopic collective motion of the self-propelled particles.

## 3.2 Methods for the collective behaviour of self-propelled particles in homogeneous and heterogeneous medium

In this section existing methods are discussed for the collective behaviour of self-propelled particles in homogenous and heterogeneous mediums. Homogeneous systems contain particles alone, whereas heterogeneous systems contain both particles and obstacles. The latter is a better representation of behaviour in nature, such as in a school of fish or a flock of birds, where obstacles are frequently encountered.

### 3.2.1 Vicsek model in 2D

This model was employed to simulate collective motion in homogeneous systems in which no obstacles were included. The Vicsek model [28] is basically a concept which is used to model the collective motion of large groups of organisms. The motion of flocking organisms is modelled by a collection of particles that assume a constant speed but respond to a random noise by assuming at each time increment the average direction of motion of the other particles in their local neighbourhood. This model is used to simulate  $N$  identical particles, each with an absolute velocity  $v$ . Simulation is undertaken in a square-shaped box which has size  $L$  and periodic boundary conditions. Particles are expressed through points that move inside the box. Interaction radius  $r$  is used to measure the distance between the particles. At a time step equal to zero, particles move randomly; each particle has a random direction which is defined by  $\theta$ . Equations used in this model are taken from [28]. The position of the particle is updated at every time-step according to the following equation:

$$\mathbf{x}_i(t + \Delta t) = \mathbf{x}_i(t) + \mathbf{v}_i(t)\Delta t, \quad (3.1)$$

where  $\mathbf{x}_i$  represents the position vector of the  $i$ th particle,  $\Delta t$  is the time unit, and  $\mathbf{v}_i(t)$  represents the velocity of the particle with an absolute velocity  $v$ .

The direction of the particles within the interaction radius is defined as:

$$\langle \theta(t) \rangle_r = \arctan \left\{ \langle \sin(\theta) \rangle_r / \langle \cos(\theta) \rangle_r \right\}, \quad (3.2)$$

and the direction of the particles after adding random noise can be given as:

$$\theta(t+1) = \langle \theta(t) \rangle_r + \Delta \theta. \quad (3.3)$$

Here  $\langle \theta(t) \rangle_r$  is the average direction of the particles. Unit of angle  $\langle \theta(t) \rangle$  is in the radian measure between the velocity vector and x-axis.  $\Delta \theta$  represents random noise, which can be chosen by using uniform probability distribution from the interval  $[-\eta/2, \eta/2]$ .

The amount of order at any time in the system is given by an instantaneous order parameter that is determined as the absolute value of the sum of all the particle velocities in the system, divided by the total number of particles multiplied by the speed:

$$\psi(t) = \frac{1}{Nv_o} \left| \sum_{i=1}^N V_i(t) \right|. \quad (3.4)$$

In the case of collective motion, the order parameter is the average normalized velocity where  $N$  represents the total number of the particles and  $v_o$  is the absolute velocity of the particles in the system. If the motion is in a disordered state, the velocities of the particles will be in random directions and will average out to give a small magnitude vector, whereas in the case of ordered motion, the velocities will add up to a vector of absolute of velocity close to  $Nv_o$ .

There are two main parameters of the Vicsek model:  $\rho$  the surface density of the particle which is defined as  $\rho = N/L^2$ , and  $\eta$ , the noise strength. At zero noise, perfect alignment takes place in the system. At maximum noise value, particles have random direction and they have non-interacting behaviour.

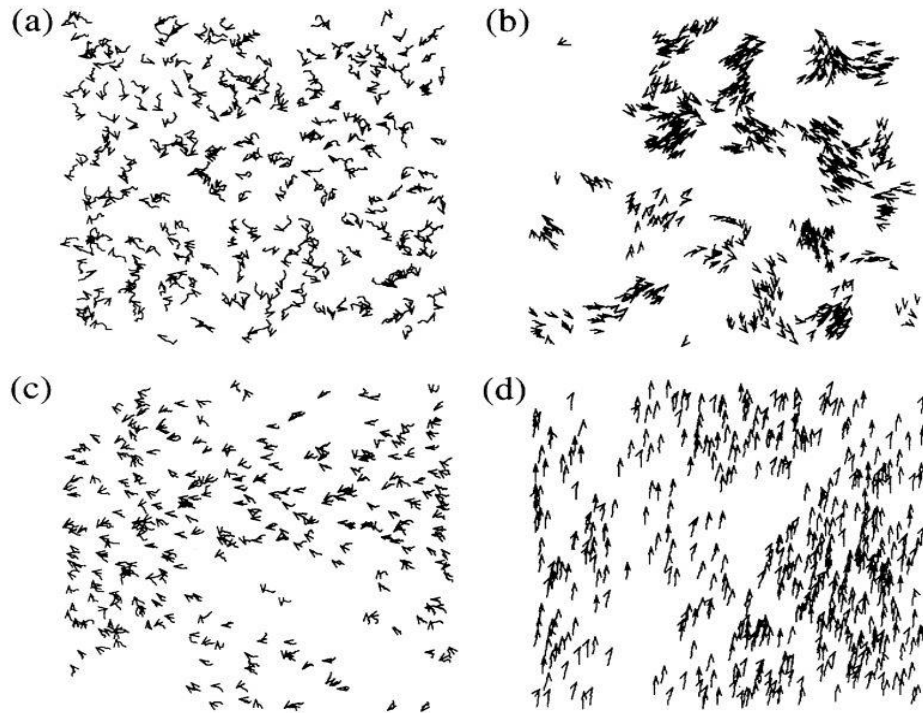


**Figure 3.1.** Interaction of self-propelled particles in the original Vicsek model [28]

In Figure 3.1 the velocities of the particles are shown for varying values of the density and noise. The number of particles is  $N = 300$  in each case. (a) For initial time step particles have random motion, here  $t = 0$ ,  $\eta = 2.0$ . (b) For smaller densities and the noise particles make groups move coherently in the random directions, here,  $L = 25$ ,  $\eta = 0.1$ . (c) For larger densities and higher noise ( $L = 7$ ,  $\eta = 2.0$ ) the particles move randomly with some correlation. (d) For higher densities and smaller noise ( $L = 5$ ,  $\eta = 0.1$ ) the motion of the particles show order and it is at a larger scale.

### 3.2.2 Vicsek model in 3D

The model has also been used for homogeneous systems and, as for 2D models, no obstacles were included. In this model the particles move in the three-dimensional space with periodic boundary conditions. At each time-step a particle follows the average direction of the motion of the neighbouring particles with some noise [122]. At the start time the particles are randomly distributed. Each particle has an interaction radius and speed. In this model, spherical coordinates are utilized. The positions and the directions of the particles are defined in the three-dimensional coordinate system. Czirik *et al* [122] defined the equation of the direction of the particle as follows:

$$\vec{v}_i(t + \Delta t) = N(N(\langle \vec{v}(t) \rangle_{s(i)})) + \vec{\xi}, \quad (3.5)$$

where  $N(\vec{u}) = \vec{u}/|\vec{u}|$  and the noise  $\vec{\xi}$  has uniform distribution in a sphere of radius  $\eta$ . Here  $s(i)$  represents the local neighbourhood. It is at radius  $r$  where particles start an interaction with each other.

The positions of the particles are defined as follows:

$$\vec{x}_i(t + \Delta t) = \vec{x}_i(t) + v_o \vec{v}_i(t) \Delta t, \quad (3.6)$$

For statistical characterisation of the system, an order parameter is defined as:

$$\phi = \frac{1}{N} \left| \sum_{i=1}^N \vec{v}_i \right|. \quad (3.7)$$

The value of  $\phi$  is between 0 and 1. If the value of  $\phi$  reaches near to 1, we say there is direction consensus in the system.

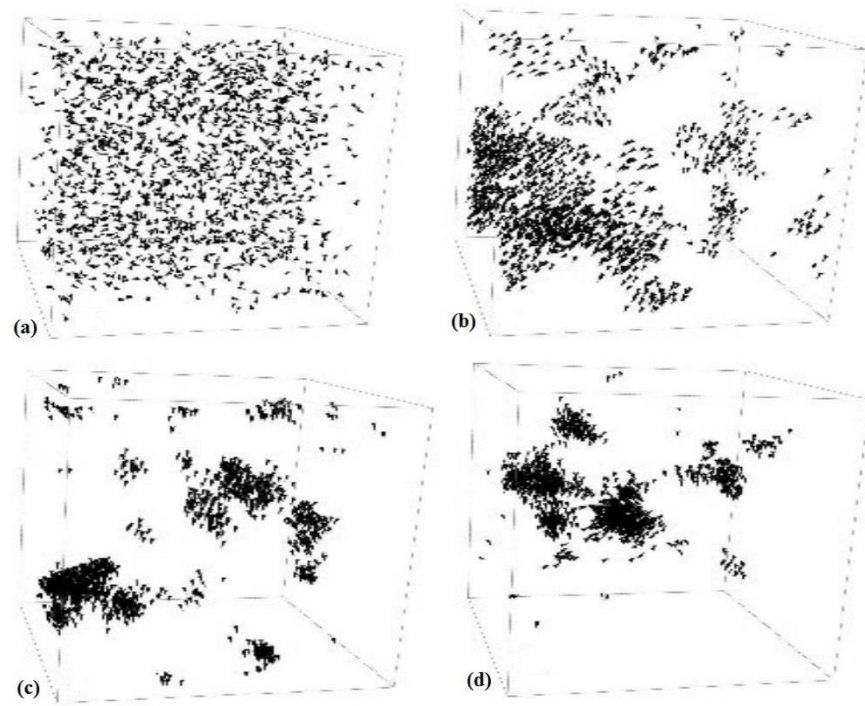


**Figure 3.2** Collective behaviour of particles in three-dimensional space [123]

This figure displays the distribution of particles for different values of the  $v_o$  : (a) the initial distribution of the particles. The final distribution of the particles for (b)  $v_o = 0.02$ ; (c)  $v_o = 0.3$ ; (d)  $v_o = 0.5$ , respectively.

### 3.2.3 Chepizkho model

This model has been applied to heterogeneous systems in which obstacles have been included. It involves a more realistic modelling of real systems in which schools of fish or flocks of birds often encounter obstacles during their collective motion and thus have to respond to these to maintain collective motion in as ordered manner as possible. This model represents an advance on the previous two models described previously since it includes obstacles.

Chepizkho *et al.* [115] studied the effect of spatial heterogeneity on the collective motion of the self-propelled particles. They considered a continuum time model for  $N_b$  self-

propelled particles which move in two dimensions with periodic boundary conditions of size  $L$ . The movement of particles is modelled in the presence of fixed obstacles. The introduction of a new element in the equation of motion for self-propelled particles is expressed by the obstacle avoidance interaction function. Equations of motion of an  $i$ th particle are given as:

$$\dot{\mathbf{x}}_i = v_o \mathbf{V}(\theta_i) \quad (3.8)$$

Here  $v_o$  is absolute velocity of the particle,  $\mathbf{V}(\theta)$  is a two dimensional vector and it can be defined as  $\mathbf{V}(\theta) \equiv (\cos(\theta), \sin(\theta))^T$ . The direction of the particle is given by the following equation:

$$\dot{\theta}_i = g(\mathbf{x}_i) \left[ \frac{\gamma_b}{n_b(\mathbf{x}_i)} \sum_{|\mathbf{x}_i - \mathbf{x}_j| < R_b} \sin(\theta_j - \theta_i) \right] + h(\mathbf{x}_i) + \eta \xi_i(t), \quad (3.9)$$

where the dot represents the temporal derivative,  $\mathbf{x}_i$  denotes the position of the  $i$ th particle and  $\theta_i$  represents the direction of the  $i$ th particle. The function  $h(\mathbf{x}_i)$  denotes the particle's interaction with obstacles and is defined as:

$$h(\mathbf{x}_i) = \begin{cases} \frac{\gamma_o}{n_o(\mathbf{x}_i)} \sum_{|\mathbf{x}_i - \mathbf{y}_k| < R_o} \sin(\alpha_{k,i} - \theta_i) & \text{if } n_o(\mathbf{x}_i) > 0 \\ 0 & \text{if } n_o(\mathbf{x}_i) = 0 \end{cases}, \quad (3.10)$$

In Equation (3.10),  $\mathbf{y}_k$  represents the position of the  $k$ th obstacle.  $R_o$  is the interaction radius between particle and obstacle, and  $n_o(\mathbf{x}_i)$  represents the number of obstacles which are located at a distance less than  $R_o$  from particle  $\mathbf{x}_i$ . In the above Equation

(3.10), two conditions are given. In the first, if  $n_o(\mathbf{x}_i) > 0$ , then  $h(\mathbf{x}_i)$  will show an interaction with obstacles; in the second condition, if  $n_o(\mathbf{x}_i) = 0$ , then  $h(\mathbf{x}_i)$  will be zero.

In Equation (3.10) there is the term  $|\mathbf{x}_i - \mathbf{y}_k| < R_o$ . This means that if the distance between the obstacle and the particle is less than the interaction radius  $R_o$ , then the values of sine will be summed; the term  $\sum \sin(\alpha_{k,i} - \theta_i)$ , is the sum of sine values. The number of sine values that will be summed will depend on the number of obstacles ( $n_o(\mathbf{x}_i)$ ) that are located in the interaction radius range of the particle  $\mathbf{x}_i$ . The term  $\alpha_{k,i}$  represents the angle in polar coordinates of the vector  $\mathbf{x}_i - \mathbf{y}_k$  and it is also known as polar angle. In the above equation there is the parameter  $\gamma_o$ , which is for the interaction with obstacles and particles; it is known as the particle's turning speed during interaction with the obstacle.

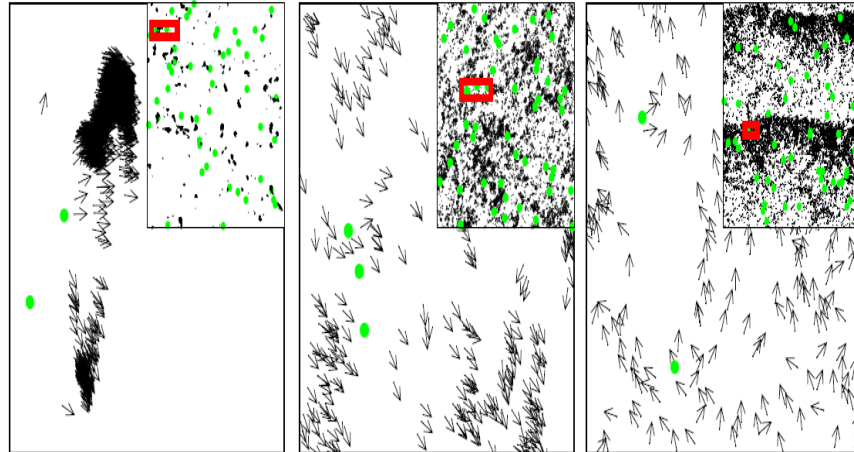


**Figure 3.3.** Collective motion of self-propelled particles in the presence of obstacles [115]

Snapshots of different phases are shown by the system with an obstacle density  $\rho = 2.55 \times 10^{-3}$ : (left) clustered phase, (centre) homogeneous phase, and (right) band phase.

The insets show snapshots of the entire system, where the red box displays the area that is shown in the main panel.

The band phase takes place in the case of polar alignment in self-propelled particles. Polar alignment is where particles lead to parallel alignment. Huge group formation occurs in the case of band phase, where large numbers of particles are very close to each other. In the band phase there is the presence of large scale, higher density structures. By increasing noise value, there appears large scale, elongated, high density, high ordered, solitary structures.

### **3.2.4 Order of phase transitions**

The order of phase transition can be investigated by plotting the probability density function (PDF) of the order parameter. This technique of finding the order of phase transition is introduced in the [5]. If the curve is one-humped, we will say that phase transition is of the second order; if the curve has more than one hump, then phase transition will be of the first order.

The process of finding a smooth curve is undertaken by finding the frequency of the values of the order parameter for each interval at the last time step. After that, this frequency is divided by the value which is obtained after multiplication of the width of the interval by the total sum of the frequency values. After doing this, values are connected with the smooth curves. Hence the area under the curve is equal to 1.

### 3.2.5 Limitations of the existing models

The Vicsek model consists of three major components: the interaction radius, the velocities of birds, and the noise. Particles make their decisions on the basis of these components. The limitations of this model include the following:

- This model has a minimalistic approach to model complex living systems and it needs more control terms;
- It does not inform us how living entities influence the average [124];
- It does not give information when a higher interaction radius and speed are applied in the system. Not all articles have an azimuthal field of vision corresponding to their surroundings, thus particles are unaware of other particle neighbours travelling behind each other [125].

The Chepizkho model [115] is an improvement on the Vicsek models and involves three main terms interaction of particles: with each other, interaction of particle with obstacles, and noise. Here the interaction of the particles depends upon two parameters  $\gamma_b$  and  $R_b$ .

This model has the following disadvantages:

- It contains too many parameters. There is no need to introduce two parameters; interaction can be defined by introducing a single parameter  $R_b$ ;
- The effect of noise is not investigated on a larger scale;
- There is a lack of focus on moving obstacles;
- The order of phase transition is not investigated.

### **3.3 Development of a new improved model for understanding the collective behaviour of self-propelled particles**

In order to overcome the limitations of existing models from the literature in this study, a new model is introduced. This model has been termed the ‘Obstacle Avoidance Model’ (OAM). The major advantage of the OAM is that it enables the collective behaviour of self-propelled particles to be studied in the presence of fixed and moving obstacles.

#### **3.3.1 Obstacle avoidance model (OAM)**

The OAM investigates the effects of various parameters on the collective motion of self-propelled particles in the presence of obstacles. These parameters include noise, interaction radius, avoidance radius, speed, number of particles, and number of obstacles. The motion of the  $N_b$  self-propelled particles is in a two-dimensional space with periodic boundary conditions of size  $L$ . Here,  $L$  denotes the box length in which the simulations are carried out. In this model, particles move collectively in the presence of obstacles. The obstacles can be fixed or moveable. In the case of fixed obstacles there is no change in the position of the obstacles, whereas for moving obstacles their positions are changed according to Equation (3.15), which is the sum of the previous position of the obstacle and the new velocity value. Obstacles are randomly distributed in the system. Interaction of the particles among themselves is the same as in the Vicsek model [28], where the particle assumes the average direction of the neighbours that are in its interaction radius  $r$ . Noise parameter is also introduced to the system, which is randomly given and has a value in  $[-\pi, \pi]$ . At a time step equal to zero, each particle has a random position and random direction. Particles update their positions according to Equation (3.1). This equation is rewritten here:

$$\mathbf{x}_i(t + \Delta t) = \mathbf{x}_i(t) + \mathbf{v}_i(t)\Delta t, \quad (3.11)$$

The direction of the particle is defined by the following equation:

$$\theta_i(t + \Delta t) = \langle \theta(t) \rangle_r + h(\mathbf{x}_i) + \eta \Delta \theta, \quad (3.12)$$

In Equation (3.11),  $\mathbf{x}_i$  represents the position of the  $i$ th particle.  $\mathbf{v}_i(t)$  is the velocity of the particle with absolute velocity  $v_o$ , and  $\Delta t$  is the time interval that particles take to move from one point to another.

In Equation (3.12),  $\theta_i$  represents the direction of the particle.  $\Delta \theta$  is the random fluctuation in the system, which is created by noise; this is chosen randomly and has a value of  $[-\pi, \pi]$ .  $\eta$  is the noise amplitude.  $\langle \theta(t) \rangle_r$  represents the average direction of the particles which are within the interaction radius  $r$ . This  $r$  is the radius of interaction between the self-propelled particles.  $\langle \theta(t) \rangle_r$  is given in the following equation:

$$\langle \theta(t) \rangle_r = \arctan \left\{ \frac{\langle \sin(\theta) \rangle_r}{\langle \cos(\theta) \rangle_r} \right\}, \quad (3.13)$$

In Equation (3.12), the function  $h(\mathbf{x}_i)$  defines the interaction of the particle with the obstacles. Through this function, the particle avoids the obstacles that are located in its neighbourhood. The interaction of the particle with the obstacle is defined by Equation (3.14) which is taken from [115]:

$$h(\mathbf{x}_i) = \begin{cases} \frac{\gamma_0}{n_o(\mathbf{x}_i)} \sum_{|\mathbf{x}_i - \mathbf{y}_k| < R_o} \sin(\alpha_{k,i} - \theta_i) & \text{if } n_o(\mathbf{x}_i) > 0 \\ 0 & \text{if } n_o(\mathbf{x}_i) = 0 \end{cases}, \quad (3.14)$$

In Equation (3.14),  $\mathbf{x}_i$  is the position of the  $i$ th particle, and  $\mathbf{y}_k$  is the position of the  $k$ th obstacle.  $R_o$  is known as the interaction radius between the particle and the obstacle.  $n_o(\mathbf{x}_i)$  represents the number of obstacles located at a distance less than  $R_o$  from  $\mathbf{x}_i$ . In the above equation, two conditions are given; in the first, if  $n_o(\mathbf{x}_i)$  is greater than zero,  $h(\mathbf{x}_i)$  will show interaction with obstacles; in the second, if  $n_o(\mathbf{x}_i)$  is equal to zero,  $h(\mathbf{x}_i)$  will be zero, meaning that no obstacle is located near the particle.

In Equation (3.14) there is the term:  $|\mathbf{x}_i - \mathbf{y}_k| < R_o$ , which means that if the distance between the obstacle and the particle is less than the interaction radius  $R_o$ , then the summation of sine  $(\sum \sin(\alpha_{k,i} - \theta_i))$  will take place. The number of sine values that will be summed depends upon the number of obstacles ( $n_o(\mathbf{x}_i)$ ) that are located in the interaction radius range of the particle  $\mathbf{x}_i$ . The term  $\alpha_{k,i}$  represents the angle in the polar coordinates of the vector  $\mathbf{x}_i - \mathbf{y}_k$ . In the above equation there is parameter  $\gamma_o$ , which is, for interaction purposes, known as the particle's turning speed when it interacts with the obstacle. The simulation studies using this new model are presented in Chapters 6 and 7.

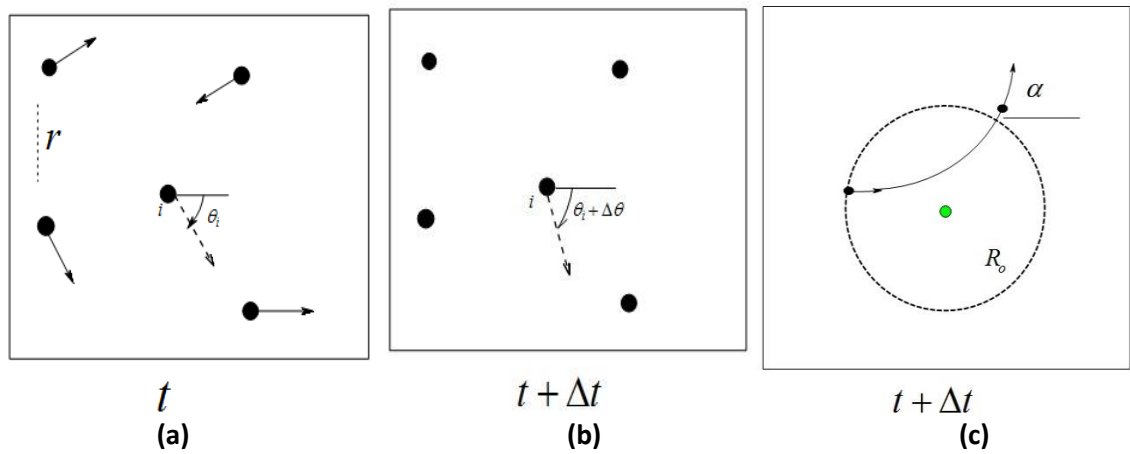


**Figure 3.4** Free body diagram represents the behaviour of the particle.

The above figure demonstrates the free body diagram of the self-propelled particles, and it can be clearly seen that there are five particles given in the domain, see figures 3.4(a) and 3.4(b).

To obtain its new orientation, particle  $i$  calculates the mean orientation  $\theta_i$  of the neighbours which are in the domain (figure 3.4(a)), and makes an error  $\Delta\theta$  (figure 3.4(b)).

The dynamics of the self-propelled particles is simulated in periodic boundary conditions.

The interaction radius  $r$  and the time step  $\Delta t$  can be set to 1. In figure 3.4(c), interaction between the self-propelled particle and the obstacle is demonstrated. The dashed circle shows the interaction area of radius  $R_o$ , the solid curve represents the trajectory of the particle, and  $\alpha$  is known as the scattered angle.

### (i) Moving obstacles

The collective behaviour of self-propelled particles in the presence of moving obstacles is investigated. These obstacles move with random directions. The position of particle  $\mathbf{x}_i$

is updated by Equation (3.11), and the direction of the particle is given by Equation (3.12).

Moving obstacle  $\mathbf{y}_k$  updates its position in the following way:

$$\mathbf{y}_k(t + \Delta t) = \mathbf{y}_k(t) + \mathbf{v}_k(t)\Delta t, \quad (3.15)$$

Here  $\mathbf{y}_k$  is the position of the  $k$ th obstacle, and  $\mathbf{v}_k(t)$  is the velocity of the obstacle with an absolute velocity  $v_y$ .  $\Delta t$  is the time taken by the obstacle to move from one point to

another. The following order parameter ( $w$ ) is used to characterise the macroscopic collective movement of the particles [115]:

$$w = \langle w(t) \rangle_t = \left\langle \left| \frac{1}{N_b} \sum_{i=1}^{N_b} e^{i\theta_i(t)} \right| \right\rangle_t, \quad (3.16)$$

Here  $\langle w(t) \rangle_t$  shows the temporal average. The term  $e^{i\theta(t)}$  represents the complex number. This complex number is a particle whose direction is determined after interaction with obstacles. In this equation, a modulus of complex numbers is determined and then divided by the total number of particles  $N_b$ . Equation (3.16) determines the average collective motion of the particles.

In developed model particles, density  $\rho_b$  can be interpreted by using the following equation:

$$\rho_b = N_b / L^2, \quad (3.17)$$

Here  $N_b$  is the number of particles, and  $L$  is the length of the box.

### 3.4 Comparison of OAM and the Chepizkho model

The obstacle avoidance model which is proposed in this thesis investigates the collective motion of self-propelled particles in the presence of obstacles. The main reason for proposing a new model was to study the effect of fixed and moving obstacles on self-propelled particles when noise values are varied in the system.

Chepizkho *et al.* [115] also studied the effect of obstacles on the collective motion of self-propelled particles; their model is discussed in Section 3.2.3 of this chapter. The main difference between the Chepizkho model and the obstacle avoidance model is in defining the direction of the particle, the control of strength of alignment ( $g(\mathbf{x}_i)$ ) of the particles, and the declaration of the noise value in the model. In their model (Eq. 3.9), the direction

of the particles includes three terms which are:  $g(\mathbf{x}_i) \left[ \frac{\gamma_b}{n_b(\mathbf{x}_i)} \sum_{|\mathbf{x}_i - \mathbf{x}_j| < R_b} \sin(\theta_j - \theta_i) \right]$ ,  $h(\mathbf{x}_i)$

, and  $\eta \xi_i(t)$ .

The term  $g(\mathbf{x}_i) \left[ \frac{\gamma_b}{n_b(\mathbf{x}_i)} \sum_{|\mathbf{x}_i - \mathbf{x}_j| < R_b} \sin(\theta_j - \theta_i) \right]$  shows the average direction of the particles

which interact with each other; here interaction of the particles depends upon two parameters  $\gamma_b$  and  $R_b$ . If the values of these parameters are larger then there will be more interaction, and if the values of the parameters are smaller, there will be less interaction in the particles. In the obstacle avoidance model (Eq. 3.12) there is no such dependence of interaction on these two parameters. Particles interact with each other only through the interaction radius  $r$ . The direction of the interacting particles is given by a very simple equation which has three terms  $\langle \theta(t) \rangle_r$ ,  $h(\mathbf{x}_i)$ , and  $\eta \Delta \theta$ , where  $\langle \theta(t) \rangle_r$  represents the average direction of the velocities of the particles within an interaction radius  $r$ ; and  $h(\mathbf{x}_i)$  is the obstacle interaction function and  $\Delta \theta$  is the random fluctuation. In the Chepizkho model (Eq. 3.9) there is the term:  $\sin(\theta_j - \theta_i)$ , which calculates the difference of directions of two neighbouring particles. In the obstacle avoidance model this sine function does not exist because when particles interact with each other their velocities are summed and as a result of this the particles move collectively. The term  $g(\mathbf{x}_i)$  in Equation (3.9) controls the strength of alignment of the particles. This term does not exist in the obstacle avoidance model (Eq. 3.12) because the motion of the particles follows the rules of the self-propelled particles, where alignment of the particles is controlled through the interaction radius and the noise value.

In the Chepizkho model equation (3.9) there is the term:  $\eta \xi_i(t)$ , which represents the noise in the system where  $\eta$  is the noise amplitude which is multiplied with the interval  $\xi_i(t) = [-\pi, \pi]$ . This noise term produces randomness, whereas in the obstacle avoidance model (Eq. (3.12) there is the term  $\eta \Delta\theta$  which is called random fluctuation. This random fluctuation is due to the noise which is chosen with a uniform probability from the interval  $[-\pi, \pi]$ , where  $\eta$  is the noise amplitude. This process of introducing noise into the system is beneficial because particles are not only able to deal with obstacles, but also face noise in the system more efficiently. A higher value of noise also generates huge randomness in the system, but particles have the ability to move collectively at smaller noise values  $\eta \leq 0.1$ . Collective motion shown by the particles at smaller noise levels ( $\eta = 0.01$ ) is greater than the results in [115] at the same noise. In Equation (3.9), obstacle interaction function  $h(\mathbf{x}_i)$  works in the same way as it does in the obstacle avoidance model in Equation (3.12). The Chepizkho model [115] works for the fixed obstacles, whereas the obstacle avoidance model not only works for the fixed obstacles but it also works for the moving obstacles. In the case of moving obstacles, the position of the obstacles is updated by a simple rule given in Equation (3.15): in the presence of moving obstacles, particles show more collective motion than fixed obstacles.

### 3.7 Conclusions

The various models for self-propelled particles are discussed in detail. Two types of media are used, firstly the homogeneous medium, and secondly the heterogeneous medium. The homogeneous medium involved the 2D Vicsek model and the 3D Vicsek model. Movement of the particles is very smooth when there are no obstacles in the system. The collective behaviour of the particles continuously decreases when noise increases in the system and collective motion increases when there is an increase in the interaction radius of the particles.

In the 3D Vicsek model, the positions and the directions of the particles are defined in the x, y, and z coordinates. In this model, different parameters are used to investigate the collective motion of the particles. These parameters are noise, interaction radius, and particle density. For the movement of the particles in the heterogeneous medium, a new model was used: the obstacle avoidance model. In this model, particles interacted with fixed and moving obstacles. This model compared with the Chepizkho model [115]. It observed that obstacle avoidance was more simple and easy to simulate. For large obstacle densities, the particles showed a different behaviour, displaying trapping. Movement of the particles was totally disturbed. Furthermore it was also observed that avoidance of the particles depended on the gamma parameter which is the particle's turning speed when it interacts with the obstacle. An order parameter was introduced which measured the collective motion of the self-propelled particles. For simulation, Fortran language was used. Plots were obtained by the GNUPLOT and the videos were obtained through OPENDX software.

## CHAPTER 4

### Simulations Studies using the 2D Vicsek Model for Self-Propelled Particles

#### 4.1 Introduction

In this chapter the simulations of the self-propelled model are presented. This is known as the Vicsek model. The effect of different parameters on the collective motion of self-propelled particles is investigated. In this model the particles interacted with each other via an interaction radius. The velocities of the particles were determined by a simple rule and the random perturbation in the system. Each particle assumed the average direction of the particles in the radius  $r$  and some random perturbation was added. The level of random perturbation is analogous with the temperature.

The Vicsek model has applications in a wide range of biological systems involving clustering and migration, for example, in flocks of birds, schools of fish, herds of quadrupeds and bacterial colony growth.

In the Vicsek model, variations take place in two main parameters: the density of the particles and the noise. Other parameters, such as the interaction radius and the speed of the particles, were also varied. The order of the phase transition is also investigated by using probability density function. The Vicsek model is characterised by Equations 3.1 and 3.2, as discussed in Chapter 3.

## 4.2 Parameter table

The parameters that were used in the Vicsek model are given in Table 4.1. Variation took place in the parameters such as noise, density of the particles, speed of the particles, and the interaction radius of the particles.

**Table 4.1** Symbols used in captions of figures

<i>Symbol</i>	<i>Description</i>
$L$	Box Length
$N$	Number of Particles
$t$	Number of time steps
$\eta$	Noise
$r$	Interaction radius
$v$	Absolute Velocity or speed

## 4.3 Comparison of calculated results and the simulation results

In this section a comparison between the manual calculation results and the simulation results of the Vicsek model is given. Two particles were chosen for two time steps. Firstly, the positions and the directions of the particles were selected randomly. The length and width of the box was equal to 6. A smaller box size was chosen because of the interaction of the two particles. Noise was kept to zero. It was observed that there was consistency in the manually calculated values and the simulation results. This can be seen in Tables 4.2-4.6. The initial positions and the velocity direction of two particles are given in Table 4.2.

**Table 4.2** Initial positions and the velocities of the two particles

Particle serial No.	Position		Velocity direction	
	X	Y	X	Y
1	0.000001	0.127402	-0.600501	0.799623
2	3.334572	4.815278	0.526714	-0.850042

**Table 4.3** Calculations of two particles at first time step

First time step				
Particle serial No.	Position		Velocity direction	
	X	Y	X	Y
1	4.975232	0.110477	-0.024769	-0.016925
2	3.309802	4.798352	-0.024769	-0.016925

**Table 4.4** Calculations of two particles at second time step

Second time step				
Particle serial No.	Position		Velocity direction	
	X	Y	X	Y
1	4.950462	0.093551	-0.024769	-0.016925
2	3.285032	4.781427	-0.024769	-0.016925

In the following tables, the simulation results of two particles are given:

**Table 4.5** Simulation result of two particles at first time step

First time step				
Particle serial No.	Position		Velocity direction	
	X	Y	X	Y
1	4.975232	0.110477	-0.024769	-0.016925
2	3.309803	4.798352	-0.024769	-0.016925

**Table 4.6** Simulation result of two particles at second time step

Second time step				
Particle serial No.	Position		Velocity direction	
	X	Y	X	Y
1	4.950462	0.093551	-0.024769	-0.016925
2	3.285032	4.781427	-0.024769	-0.016925

#### 4.4 Simulation results

The results were obtained from the simulation with the help of Fortran 90 by using the Linux operating system. The figures given below are obtained with the help of GNUPLOT. The particle density and noise were varied and the results are displayed in the figures. For smaller densities and lower noise, the particles moved in groups and showed coherence in the system. After a period and with large particle densities of particles, they tried to move with some correlation. In the case of higher particle densities and lower noise value, i.e  $L = 5$  and  $\eta = 0.1$ , the particles showed an ordered motion and a strong coordination in the system.

Figures 4.1-4.4 demonstrate the actual selection of the variation of the particle density  $\rho$  and  $\eta$ ; the actual velocity of the particle is indicated by an arrow. The trajectory of the particle is given by the short continuous curve for 20 time steps.

In the following results, the movement of the particles is given at the initial time step.

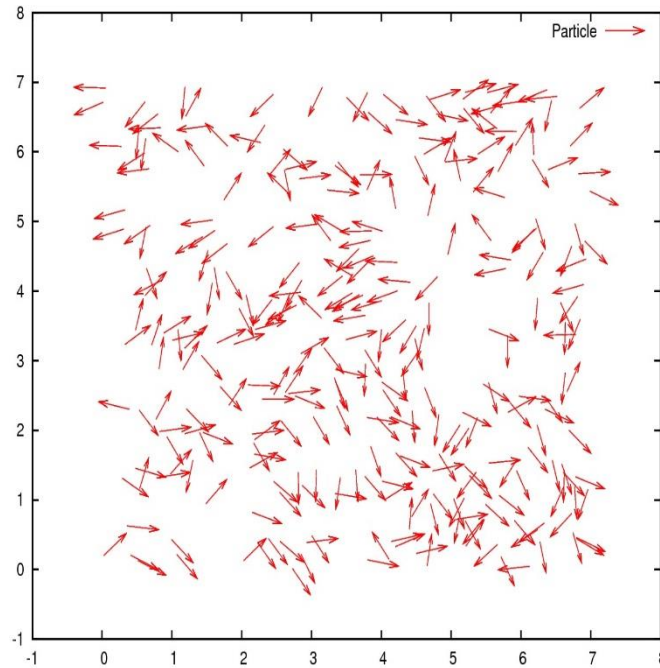


**Figure 4.1** Random motion of the particles at  $L = 7, \eta = 2, N = 300, t = 0, r = 1, v = 0.03$

This result was obtained at a time step equal to zero. Here the density was higher because the box length was  $L = 7$ . It can be clearly seen that particles took random directions and the positions of the particles were randomly distributed. At the zero time step they were not in a position to contact one another. There was higher noise in the system. In this result system was in a state of disorder;  $v = 0.03$  was the absolute velocity of the particles, which remained constant for all the particles.

The time steps were increased along with the box length for the purpose of seeing the movement of the particles.

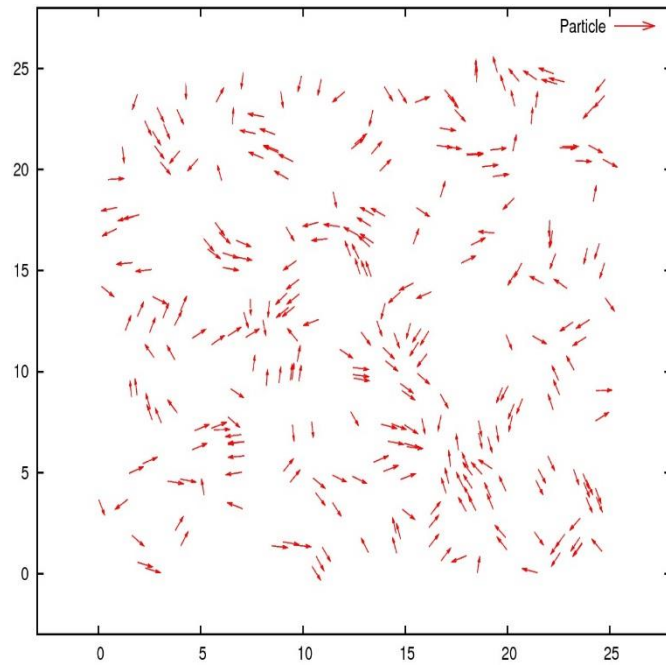


**Figure 4.2** Group formation by the particles at  $L = 25, \eta = 0.1, N = 300, \nu = 0.03, t = 20,$   
 $r = 1.$

In figure 4.2, the density and noise chosen were lower; the formula for the density was  $\rho = N / L^2$ . The value of the density was 0.48. It can be clearly seen that particles have formed groups and inside the groups, particles had coherent movement. Particles showed this behaviour because of the huge space provided to them and there was lower noise. At the initial time step, each particle moved randomly; after some time steps they contacted each other and formed groups.

In the following result, a higher density and higher noise was used.

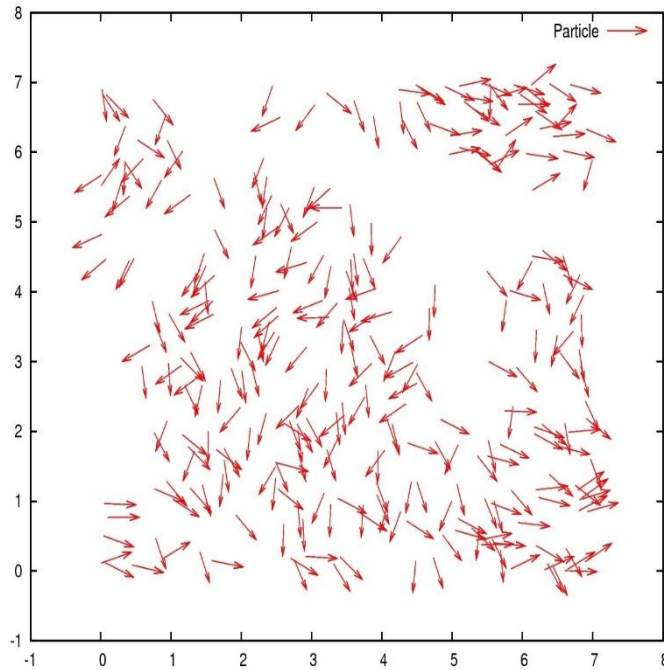


**Figure 4.3** Movement of the particles with some correlation at  $L = 7, \eta = 2, t = 20,$   
 $r = 1, \nu = 0.03, N = 300.$

The impact of higher noise and higher density on the movement of particles is shown in figure 4.3. It can be clearly seen in this figure that the particles showed random movement. Here the particles had randomness due to higher noise. After the 20<sup>th</sup> time step they exhibited some correlation which was due to a higher density and the interaction radius.

In the self-propelled particle model, collective motion is quantified through an order parameter which is defined in Section 3. If the value of the order parameter is approximately zero, it is said to be disordered motion, and if the value of the order parameter is approximately 1, we say there is ordered motion in the system.

In figure 4.4, the impact of low noise and higher density can be seen. The system displays an important behaviour of the particles.

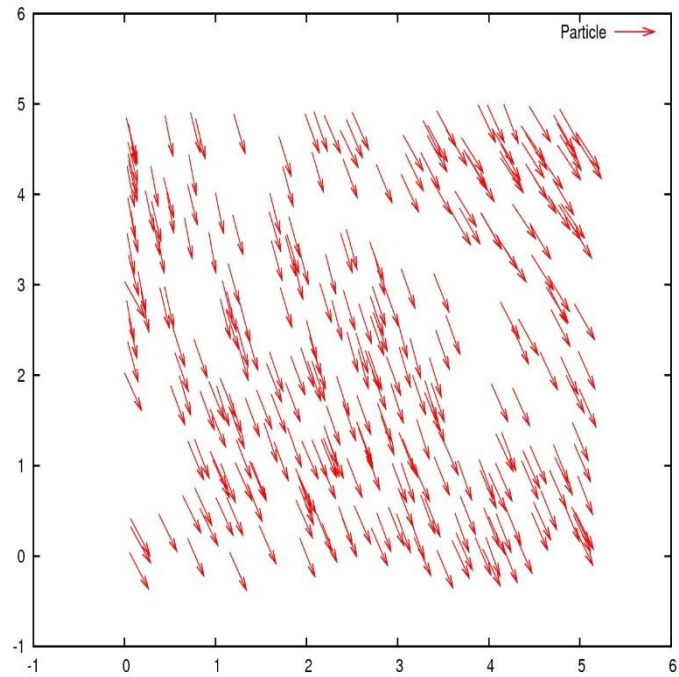


**Figure 4.4** Alignment in the direction of the particles at  $L = 5$ ,  $\eta = 0.1$ ,  $r = 1$ ,  $t = 20$ ,  $v = 0.03$ ,  $N = 300$ .

This is the most interesting result. In figure 4.4, it can be clearly seen that the system is in a state of order. Particles had the same direction. The motion of the particles appeared to be in order. This movement of particles was due to the low noise ( $\eta = 0.1$ ) and higher densities. When the box length was smaller ( $L = 7$ ), higher density in the system took place; particles came close to each other for the purpose of collective movement. Furthermore, there were fewer disturbances which were helpful in ordering them. Having 20 time steps played an important role in giving the system a state of order; the particles had more time to coordinate with each other.

### 4.4.1 Larger number of particles

The following figures were obtained by using the same parameters as were used in the results shown in figures 4.1-4.4, the only difference being in the parameters concerning the number of particles. In the results shown in figures 4.5-4.8, 2000 particles were used. The simulation results showed similar behaviour to those in Vicsek's results.

The main difference between the results for  $N=300$  and  $N=2000$  appears in the value of the collective motion. For a larger number of particles, the system showed higher collective motion because there were more particles and there were more chances of coordination in the system. Within a short time they showed alignment with each other.

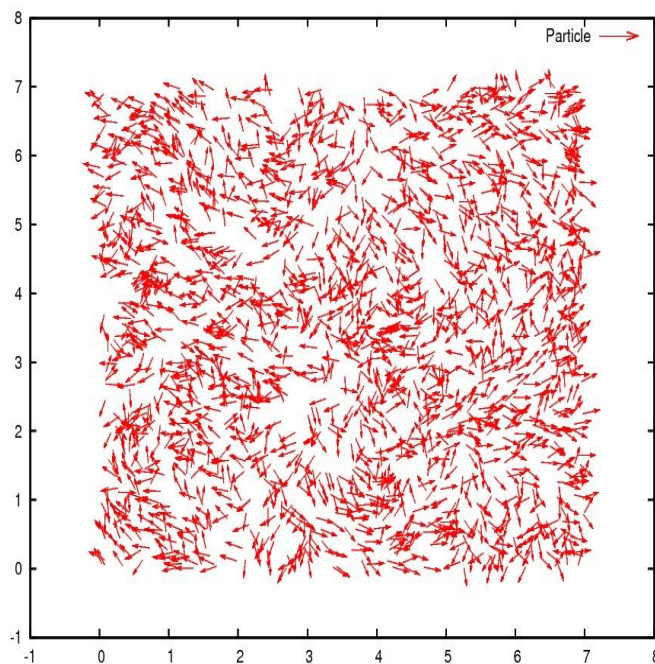


**Figure 4.5** Random motion for  $N = 2000$  at  $t = 0$ .  $L = 7, \eta = 2, r = 1, v = 0.03$ .

The above figure 4.5 demonstrates the results for the first time step. The particles exhibited random motion, with each particle moving in a different direction. The particles were scattered across the whole box. Collective motion was approximately zero,

suggesting that the system was in a state of disorder. Higher noise ( $\eta = 2$ ) was used in the system, which also provided perturbation to the orientation of the particles. The system appeared to be very dense. Each particle carried a radius of 1. Through this radius they interacted with each other. Each particle assumed the average direction of the neighbouring particles which were in its interaction range and also particles received some random perturbation.

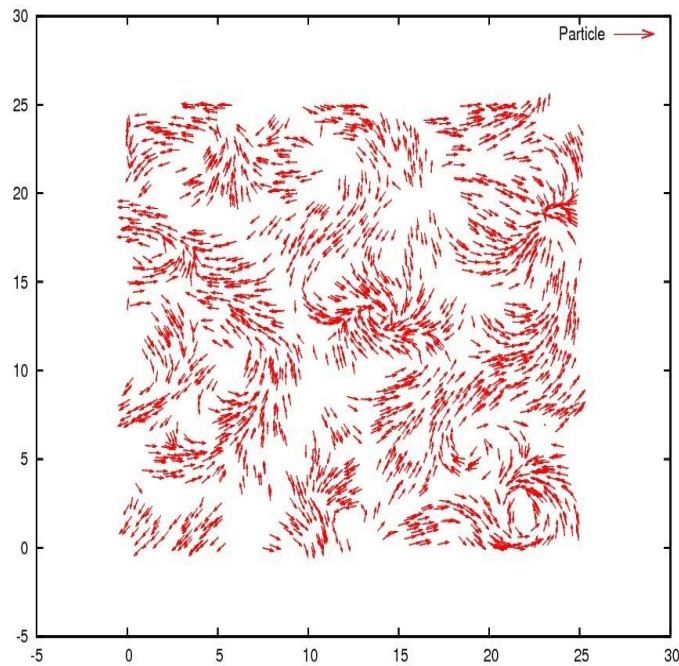


**Figure 4.6** Group formation by the particles at  $L = 25$ ,  $\eta = 0.1$ ,  $N = 2000$ ,  $t = 20$ ,  $\nu = 0.03$ ,  $r = 1$ .

The above figure demonstrates the results of simulation at the 20th time step. The length of the box was increased to 25 and noise was kept very low at  $\eta = 0.1$ . It was observed that the particles formed groups, each group having a different direction. The behaviour exhibited by the particles was similar to that shown in figure 4.2, the only difference being that here, 2000 particles were used. Due to the larger box length, particles were scattered in the form of groups. Lower noise provided much less disturbance in the system. There is another factor which helped the particles to align in groups, which was the number of the time steps, at 20, so the particles had time to interact with each other.

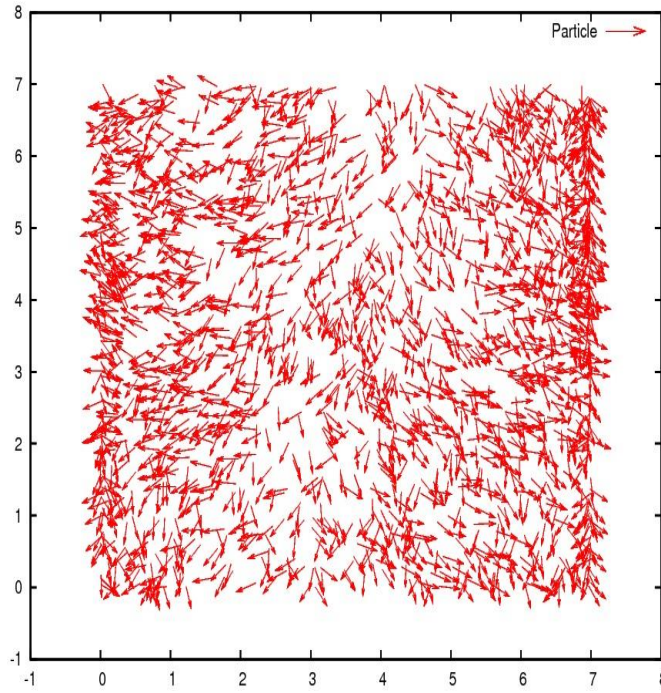


**Figure 4.7** Correlation in the system  $L = 7, \eta = 2, t = 20, r = 1, v = 0.03, N = 2000$

In the above figure 4.7, simulation is shown for a smaller box length ( $L = 7$ ) and higher noise level ( $\eta = 2$ ). It can be clearly seen that at the 20th time step, particles exhibited some correlation. Due to the noise, the randomness in the motion of the particles can be seen but this randomness was on a smaller scale even when the noise level was higher. Due to the smaller box length and large number of particles, the system becomes very dense. The value of the order parameter obtained at the last time step was equal to 0.61. This value suggests that there existed collective motion in the system.

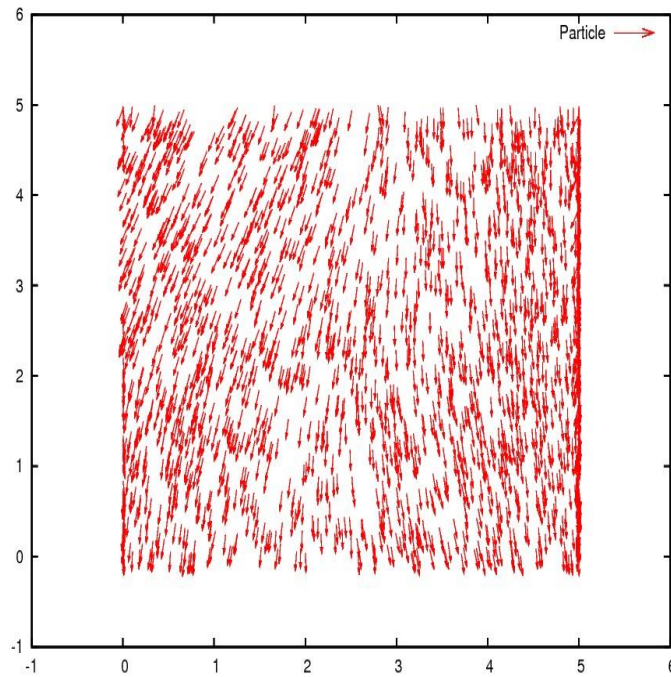


**Figure 4.8** Alignment in the system at  $L = 5, \eta = 0.1, t = 20, r = 1, v = 0.03, N = 2000$ .

Above figure (4.8) demonstrates the result for a smaller box length ( $L = 5$ ) and lower noise level ( $\eta = 0.1$ ). It was observed that at the 20<sup>th</sup> time step the particles exhibited fascinating behaviour. The particles showed ordered motion and were aligned in one direction. The collective motion was higher in the system because of the similar direction of the particles. The behaviour exhibited by the particles was due to the lower noise and higher density of the particles. In the previous figure, the results showed some randomness, whereas in this result no randomness existed. Hence, less noise and a higher density of the particles made the system more stable. It is believed that if more than 2000 particles were used, by keeping the other parameters the same, then the particles would show a similar behaviour pattern.

#### **4.4.2 Phase transitions**

A system is said to have a phase transition when there exists a large number of interacting particles undergoing from one phase to another as a function of one or more external parameters [3]. A well-known example of phase transition is the freezing of a substance when it is cooled. Phase transitions occur when particular system variables, known as order parameters, are changed. The term ‘order parameter’ is given because of the observations that phase transitions usually include to an abrupt change in the symmetry property of the system.

The nature of the phase transition was investigated by determining the absolute value of the average normalized velocity of the whole system when changes take place in the density and the noise. This average velocity carries a value approximately equal to zero when there is random direction of the particles, while for the case where particles have ordered direction, average velocity carries a value which is approximately equal to 1.

##### **(i) Variation in noise**

In the following results, trajectories are given. Noise slowly increased for various sizes for fixed density of the particles in the system. There is transition from orderly state to disorderly motion in the system. The interaction radius is  $r = 1$ , speed  $v = 0.03$  and time is  $t = 2500$ .

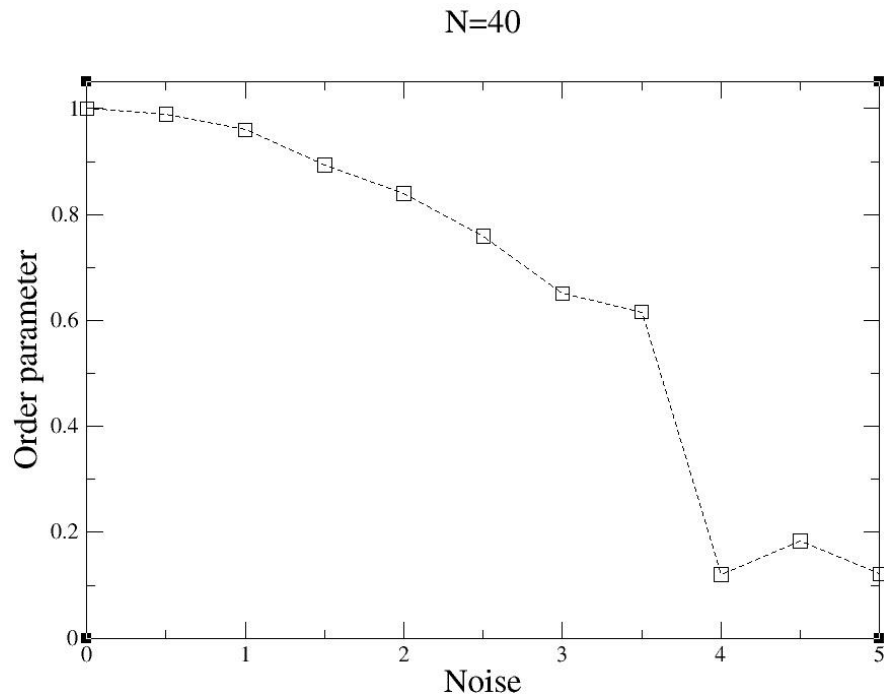


**Figure 4.9** Phase transition for 40 particles at  $L = 3.1$ .

In the system of self-propelled particles, noise is considered to be the control parameter. Noise has a huge effect on the collective motion of the particles. Phase transitions take place in the system when noise is varied. An example of phase transition can be seen in figure 4.9. At zero value of noise, we see collective motion is highly ordered; there was a decline in the collective motion of the self-propelled particles when noise was increased. At noise value equal to 5, collective motion was much lower, suggesting a disordered phase in the system; and there was a transition from a highly ordered to a disordered phase.

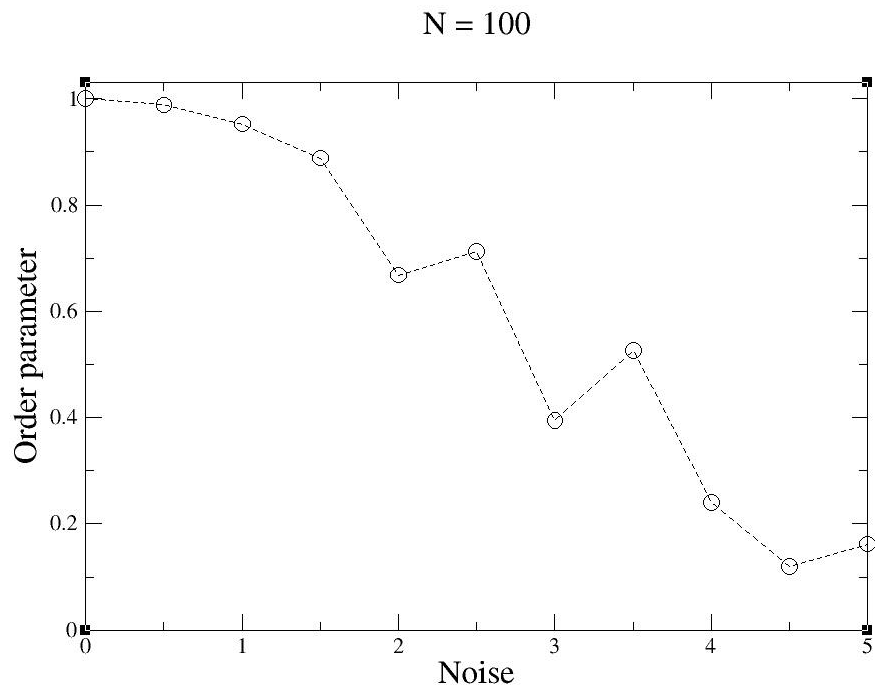


**Figure 4.10** Phase transition for 100 particles at  $L = 5$

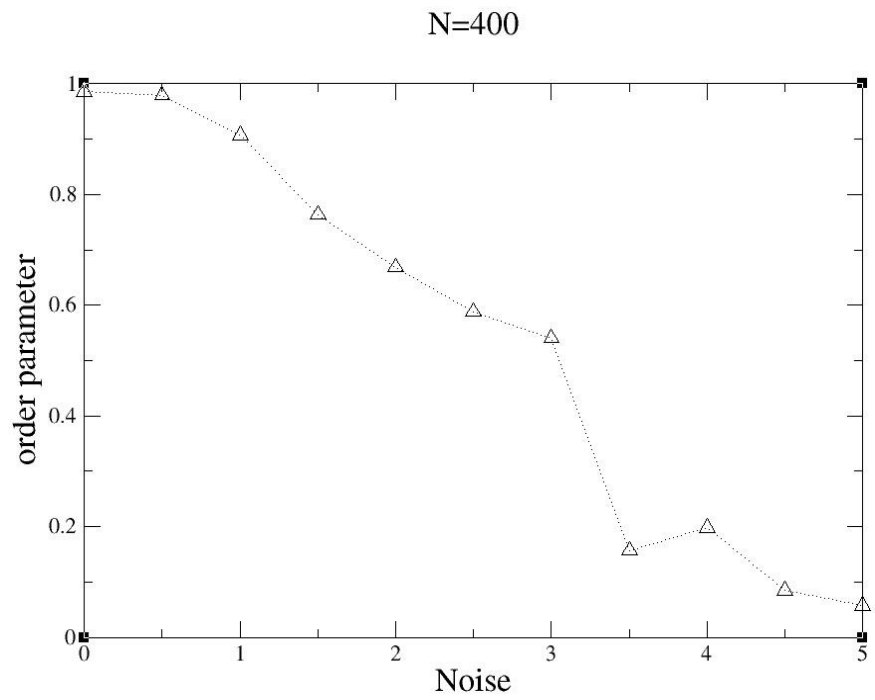


**Figure 4.11** Phase transition of 400 particles at  $L = 10$ .

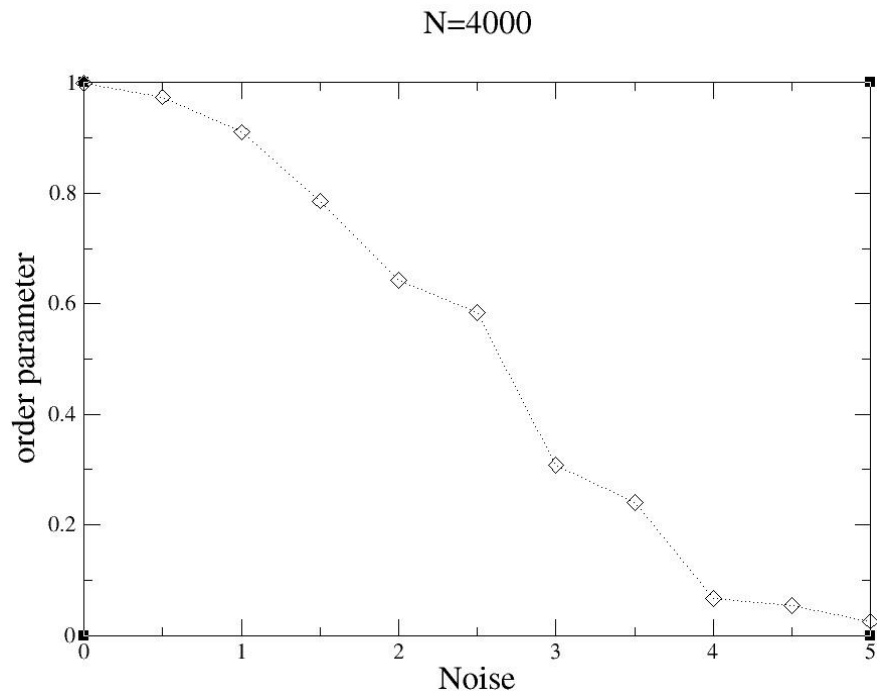


**Figure 4.12** Phase transition for 4000 particles at  $L = 31.6$ .

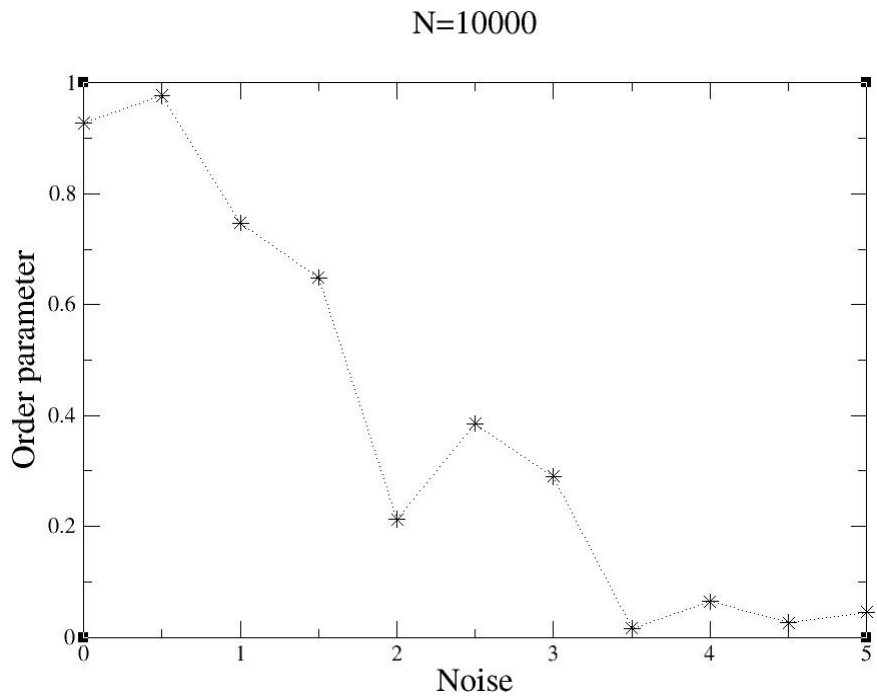


**Figure 4.13** Phase transitions for 10000 particles at  $L = 50$

In the above figures (4.9-4.13), the order parameter was plotted against noise. The noise values varied from 0 to 5 with an interval length of 0.5. It can be clearly seen that when noise slowly increased in the system, the collective motion of the particles decreased. It was also observed that fluctuations in collective motion took place. The main reason for

this was that when the number of particles was increased, the system showed larger fluctuations because noise provided random values in the system.

In figure 4.10, more fluctuations were observed and the curve showed a downward trend. At  $\eta = 5.0$ , the order parameter had a value equal to 0.1621; if a higher value of noise was applied then the order parameter would go down further. For a higher number of particles the order parameter was approximately equal to 0 at noise level  $\eta = 5.0$ . This can be clearly seen from figures 4.11-4.13. For large system sizes there was the need to use a larger number of time steps in order for the particles to coordinate with each other. It was also observed that at noise value  $\eta = 0.0$ , the order parameter was approximately equal to 1.

## **(ii) Variation in the density**

Another aspect of the phase transition was also investigated: the noise was kept constant in the system and the density of the particles was increased. The other parameter values that were constant in the system were  $L = 20$ ,  $\eta = 2.0$ , and  $r = 1$ . The collective motion of the self-propelled particles increased when noise was kept constant and only the number of particles was increased.

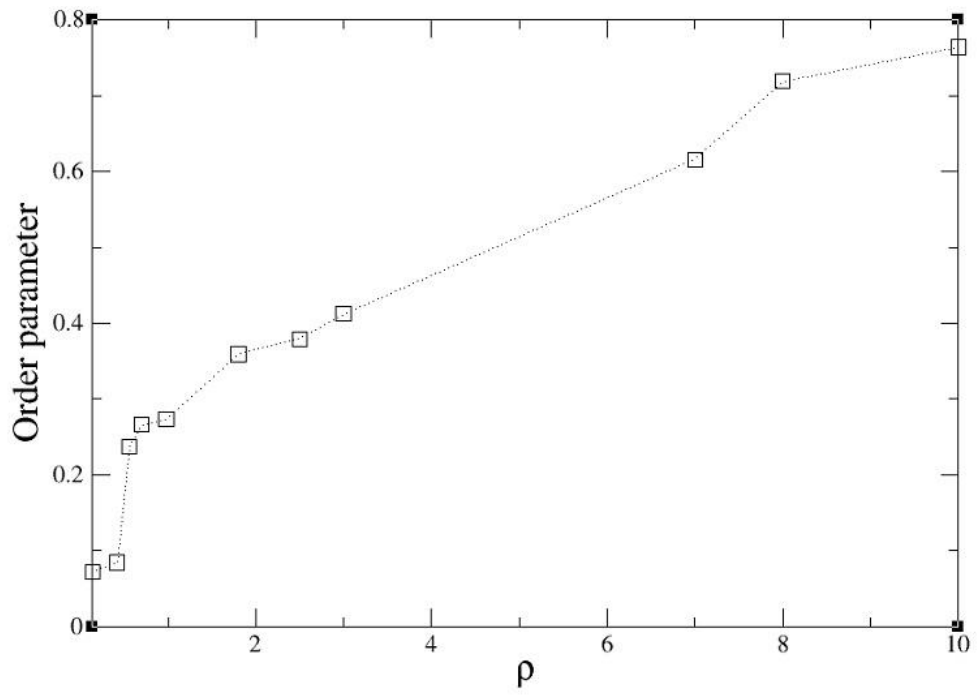


**Figure 4.14** Evolution of collective motion for different densities at  $t = 500$

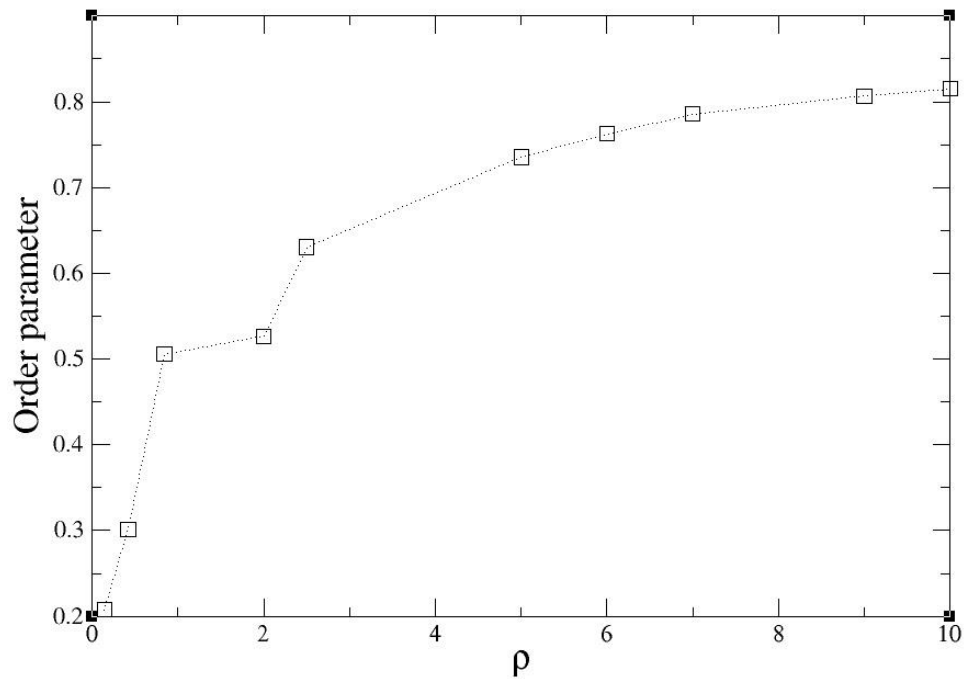


**Figure 4.15** Evolution of the collective motion for different particle densities at  $t = 2500$

In figure 4.14 it is observed that with increasing density a growth in the collective motion appears. This observation also proved that with the increasing number of particles, the collective motion rose. At a particle density of 1, the order parameter had a value equal

to 0.76. Furthermore, in figure 4.15 the same type of behaviour was observed. The collective motion of the particles increased along with a slower increase in the density of the particles. It can be clearly seen that at  $\rho = 10$ , the value for the order parameter was 0.81, which was the highest value.

#### 4.4.3 Effect of the interaction radius

The effect of the interaction radius was studied in the Vicsek model, which was not studied in the original model [28] presented in the literature. In their work, the radius was kept to 1, but the model developed here was simulated for the radius value and varied from 0 to 10 with an interval length of 0.5. The simulation results were obtained at different time steps. The noise value used here was very small at  $\eta = 0.1$ . The box length was  $L = 20$  and the number of particles was  $N = 3000$ . The following results were obtained at  $t = 200, 500, 1000$  and 3000.

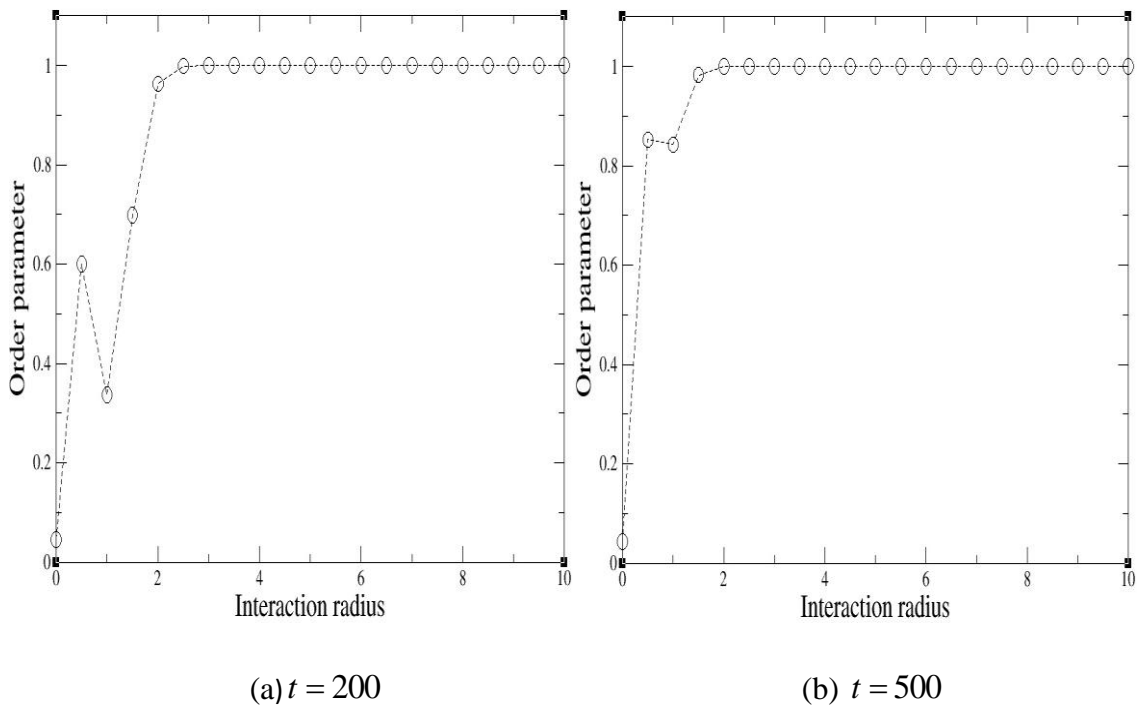


**Figure 4.16** Collective motion as a function of interaction radius for smaller number of time steps

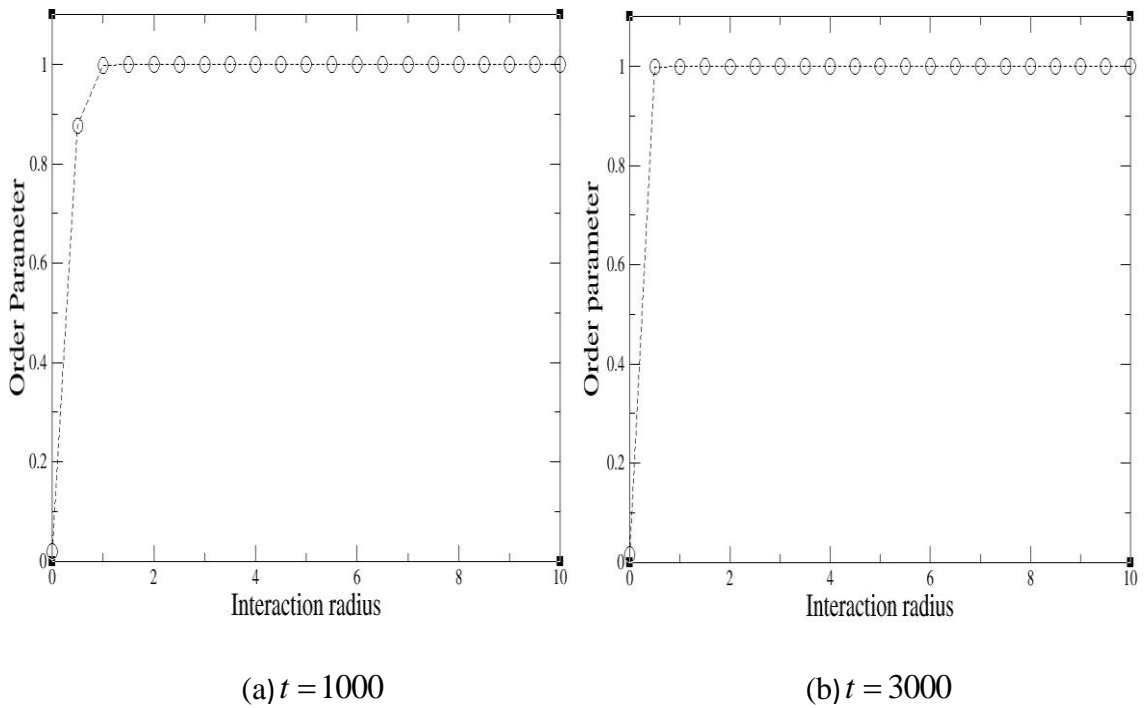


**Figure 4.17** Collective motion as a function of interaction radius for 1000 and 3000 time steps

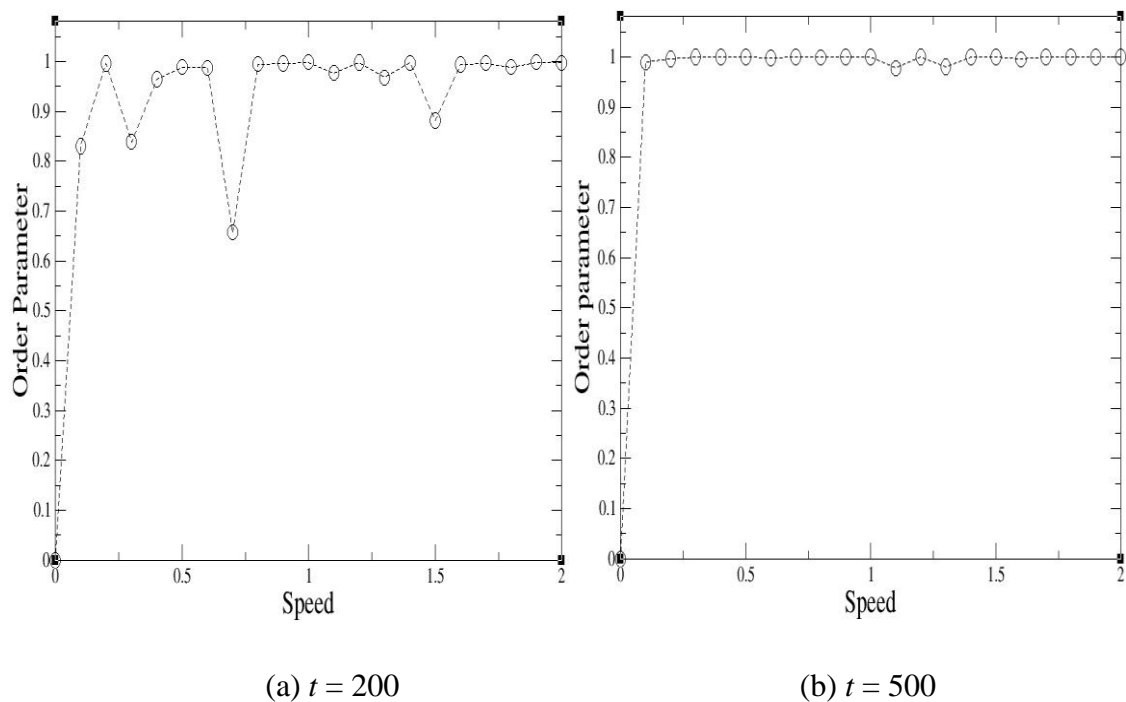
Figures 4.16-4.17 demonstrate the effect of the interaction radius on the collective motion of self-propelled particles at different time steps. It can be clearly seen that the value of the order parameter remained almost 1 for all the radius values greater than 0. At the initial value of  $r = 0$ , the order parameter carried a value near to zero. This showed there was no collective motion occurring in the system. There was ordered motion when lower noise levels and  $r > 0$  existed in the system.

Increasing the value of the radius parameter enabled more particles to interact with one another. The collective motion remained consistent when a higher number of time steps was used to simulate the system. If fewer steps were used, the system showed fluctuations. This could be seen in the case where  $t = 200$ . The results showed that the order parameter had fluctuations when  $r \leq 1$ . From  $r = 1.5$ , the system showed a higher order as the collective motion approached a value of 1. As the simulation time increased, fewer fluctuations appeared in the system. This can be seen from the result where  $t = 500$ ; the

figure showed zigzag behaviour, but it was at a smaller scale. For  $t = 1000$ , the collective motion was better than at the two previous time step results. The graph showed an upward trend. As the time steps were increased further to 3000, the results exhibited fascinating behaviour, and the particles showed a higher collective motion. The value of the order parameter was near to 1 for all values of radius except for  $r = 0$ .

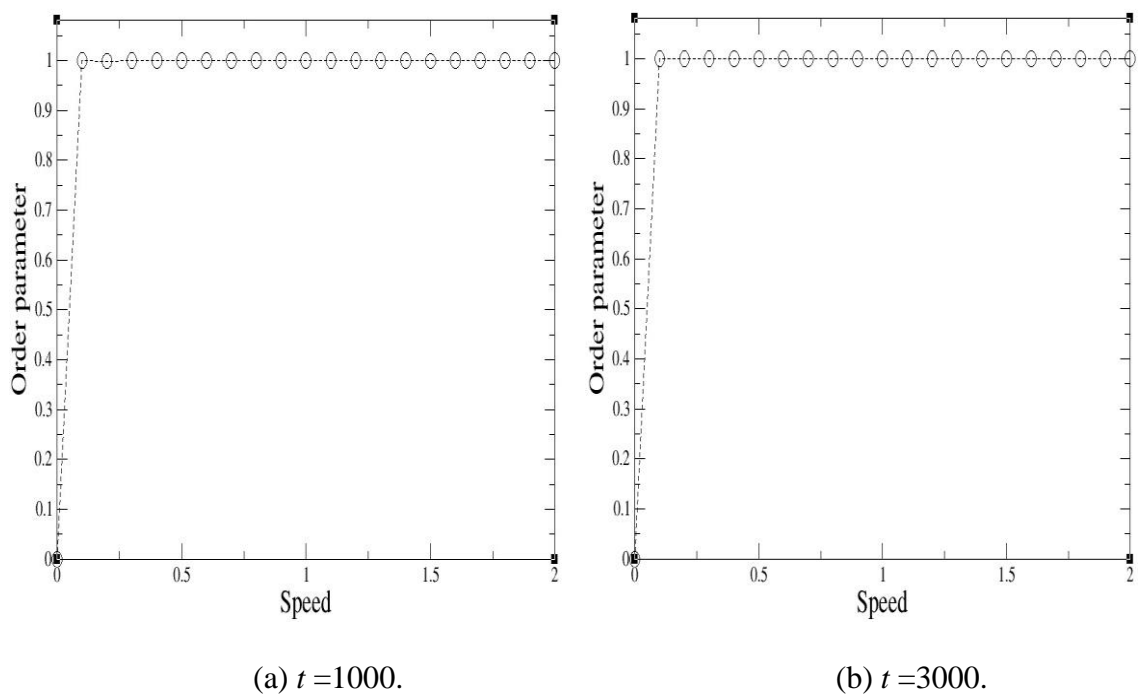
#### 4.4.4 Effect of the Speed

The effect of the speed ( $v$ ) was investigated at various time steps. The number of particles was  $N = 3000$ ; the box length was  $L = 20$ ; noise was  $\eta = 0.1$ ; the interaction radius was  $r = 1$ . The value of the speed parameter  $v$  was varied from 0.1 to 2.0 with an interval length of 0.1. The trajectories were plotted for time steps of  $t = 200, 500, 1000$  and 3000.



**Figure 4.18** Collective motion as a function of speed for small number of time steps

Figure 4.18 presents the collective motion as a function of the speed. It was observed that for  $t = 200$ , the system showed inconsistency due to the fluctuations in the order parameter; for  $t = 500$ , the system showed greater stability. The highly ordered motion in the system was evident. The results showed that time played an important role in stabilising the system. For shorter times, the particles had fewer chances of interacting with each other, whereas in the case of longer time steps, the chances of higher coordination increased.



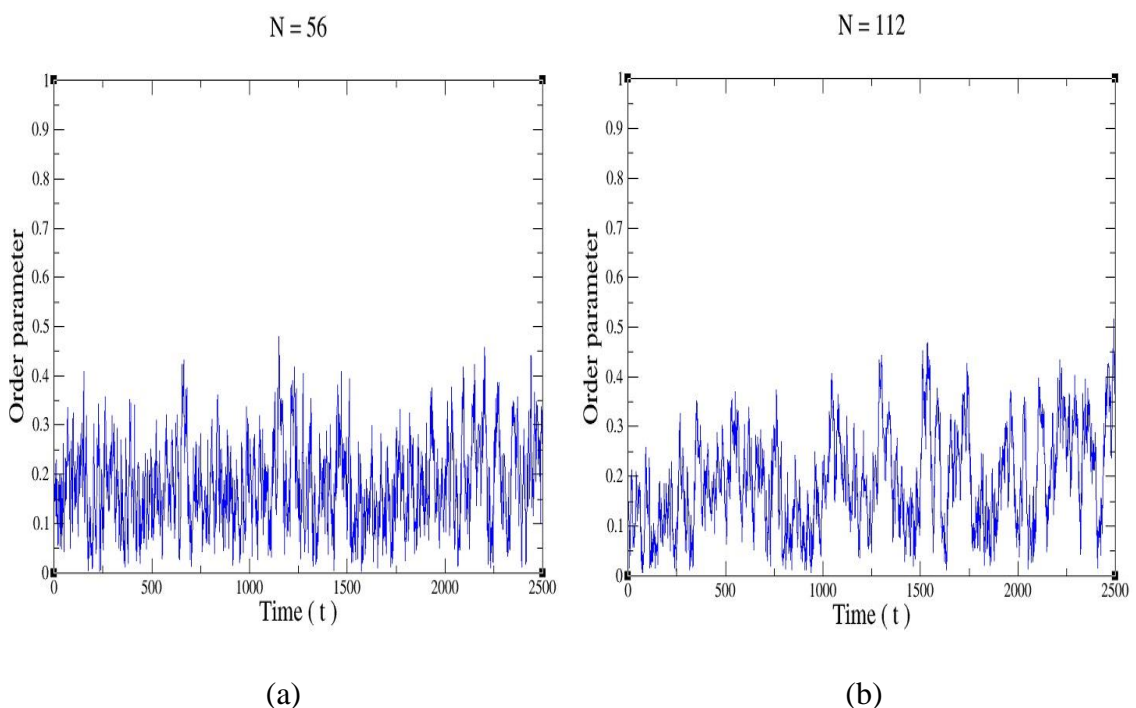
**Figure 4.19** Collective motion as a function of speed for large 1000 and 3000 time steps

Figure 4.19 shows that no fluctuations were observed. The values of the order parameter were close to 1 for all the values of the speed. At  $t = 1000$ , the system achieved a better position in terms of collective motion; similar behaviour was also observed in the case of  $t = 3000$ . It can be clearly seen that the value of the order parameter was consistent and close to 1 for all the values of speed greater than zero. From these results it was observed that time played an important role in the collective motion of the self-propelled

particles when speed variations took place. For further increases in the simulation time, the value of order parameter remained near to 1.

#### 4.4.5 Collective motion as a function time

The collective motion was plotted against time using various numbers of particles. Noise was equal to 2.0 in order to see how particles behaved at each time step in the presence of greater noise. Here  $L = 20$ ,  $t = 2500$ ,  $r = 1$ , and  $v = 0.03$ .



**Figure 4.20** Collective motion as a function of time for 56 and 112 particles

The graphs in figure 4.20 are demonstrated for the purpose of giving a comparison for the collective motion of the particles when variation in particle density takes place. There were initially 56 particles simulated and then their collective motion was plotted against each time step. After this, there were 112 particles simulated and then their collective motion was also plotted. In figure 4.20(a), particle density was  $\rho = 0.14$ , whereas in figure 4.20(b), particle density was  $\rho = 0.28$ . It was found from this comparison that when  $\rho = 0.14$ , the system showed very frequent rise and fall in the value of the order

parameter, which can be clearly seen in figure 4.20(a). In the case of  $\rho = 0.28$ , the order parameter also had fluctuations but these were less fluctuations, which can be seen in figure 4.20(b). By comparing both graphs it was found that the graph in figure 4.20(b) is better than the graph in figure 4.20(a) because fewer fluctuations are shown in figure 4.20(b).

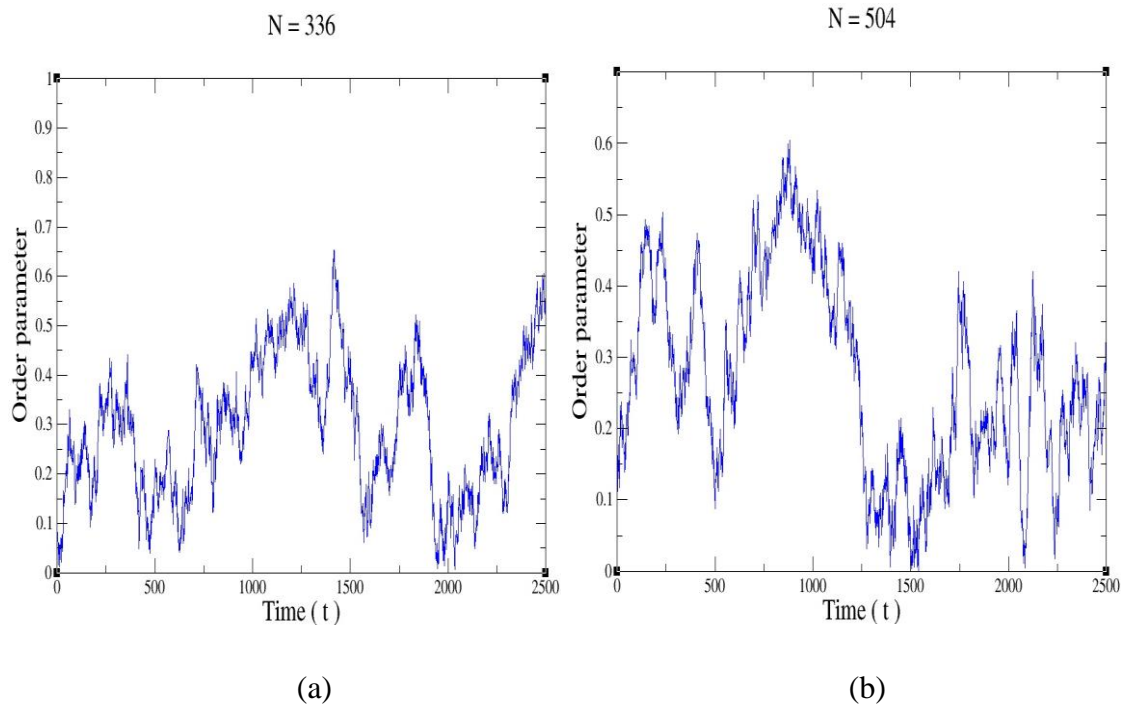


**Figure 4.21** Collective motion as a function of time for 336 and 504 particles

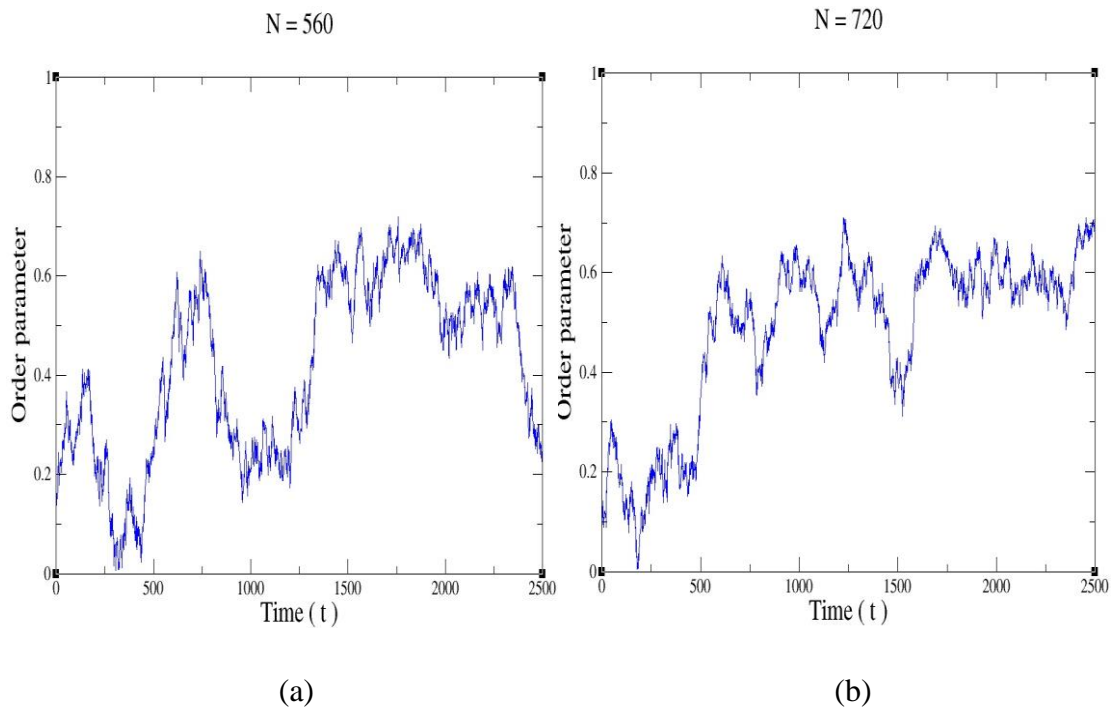


**Figure 4.22** Collective motion as a function of time for 560 and 720 particles

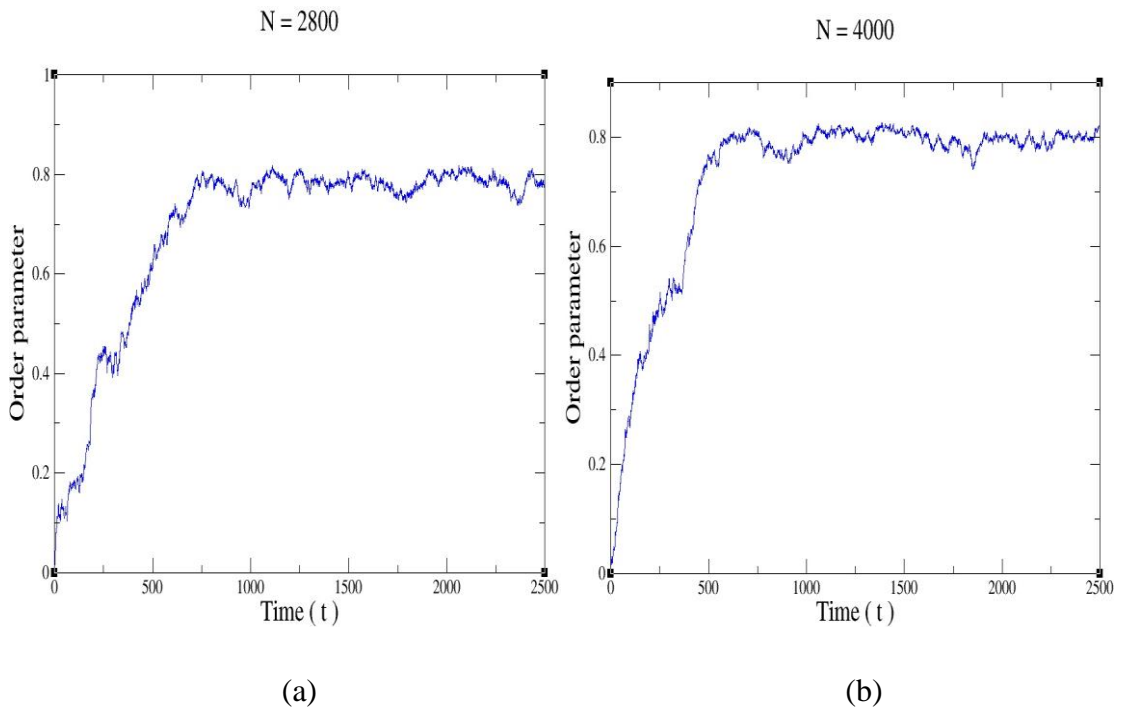


**Figure 4.23** Evolution of collective motion for 2800 and 4000 particles

In the results shown (figures 4.21-4.22), fluctuations were observed in the order parameter, but these fluctuations were lower compared with the results shown in figure 4.20. It was observed that for higher particle density, the system showed very little

fluctuation, even in the case of higher noise, i.e.  $\eta = 2.0$ . In figure 4.23(a), the result was shown for  $N = 2800$ . The order parameter had a value equal to 0.78, indicating good alignment in the direction of the particles. At the initial time step there was little order in the system, but after several time steps, the order start increasing. It can also be seen that sometimes it rises but appears to decrease suddenly due to random noise in the system. In figure 4.23(b), where  $N = 4000$ , a similar type of behaviour was shown to that in figure 4.23(a). The order parameter was equal to 0.81 at the 2500<sup>th</sup> time step.

#### **4.4.6 Order of the phase transition**

For this purpose, the probability density function (PDF) of the order parameter was plotted. The probability density function of an order parameter is the function that describes the relative likelihood of the order parameter to take on a given value. The probability density function of the order parameter is non-negative everywhere, and its integral over the entire space was equal to 1.

It is known that phase transition occurs when the value of the order parameter changes from 0 to 1. If the value of the order parameter is approximately zero, we say that there is a disordered phase. If the value of the order parameter is approximately equal to 1, we say that there is a highly ordered motion in the system, in other words, ordered phase exists in the system. In the figure 4.24 it can be clearly seen that the order parameter has values near to zero and as well as near to 1. These values suggest that phase transition exists in the system.

In order to learn the order of phase transition, there was a need to see the formation of the curve. If the curve had one hump, then the phase transition was of the second order; if the curve had more than one hump, then the phase transition was of the first order. A large number of particles was chosen, such as  $N = 32768$ . The box length was also larger, at

$L = 512$ . The speed was  $v = 0.5$ , with three noise values and 5000 time steps used in the simulation. A similar technique of finding the order of the phase transition was also used in [5].

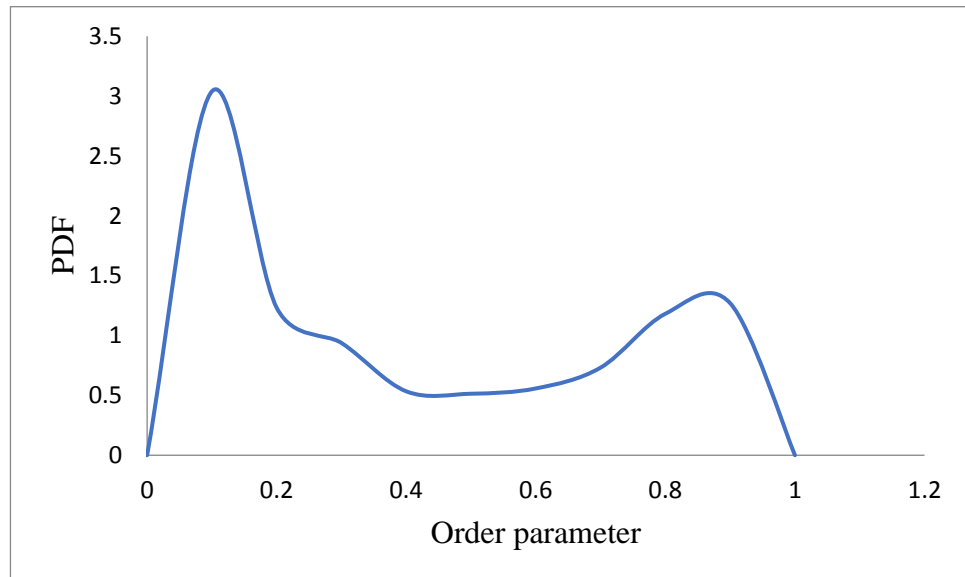


**Figure 4.24** First order phase transition at noise level  $\eta = 0.193$

The graph shown in figure 4.24 tells us only about the order of phase transitions. Noise  $\eta = 0.193$  was applied, which provided a first order phase transition. This curve shows us that there is occurrence of phase transition, but it is not continuous because the curve has shown more than one hump. This graph shows the occurrence of phase transitions and we knew this from the values of the order parameter. At the order parameter 0.1, the PDF has a higher value, which suggests that most of the time there remains a disordered phase. At 0.9, the PDF also has a value which shows an ordered phase. This variation in the values of the order parameter suggests that phase transitions exist in the system.

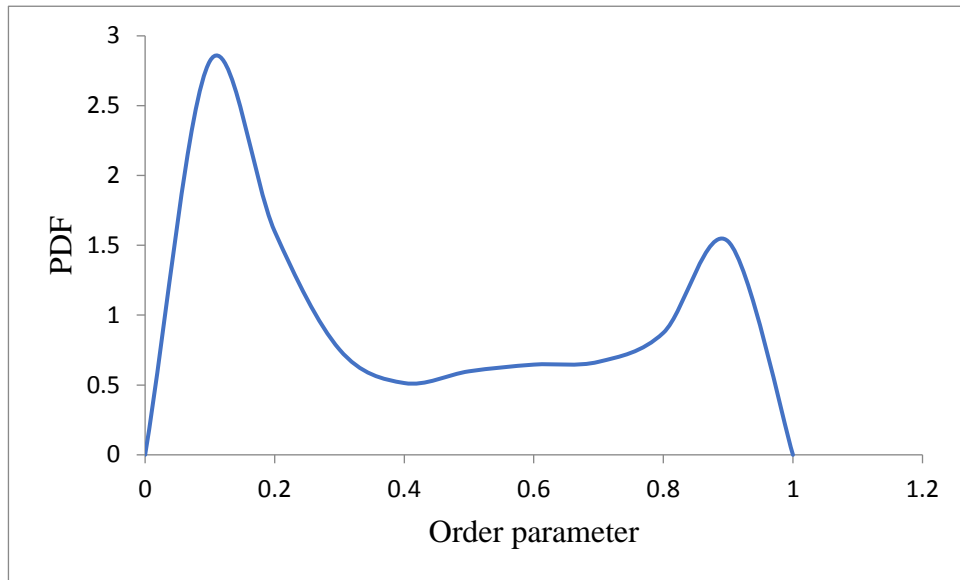


**Figure 4.25** First order phase transition at  $\eta = 0.196$ .

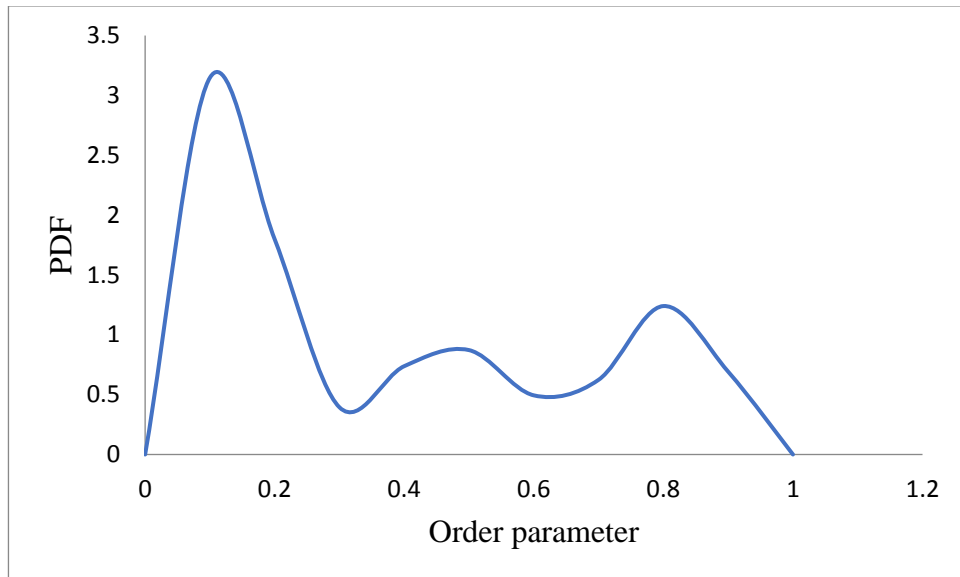


**Figure 4.26** First order phase transition at  $\eta = 0.198$

Figures 4.24-4.26 show the first order phase transition as exhibited by the system. From figure 4.24, it can be clearly seen that two bigger humps are shown. These humps suggest that the phase transition was discontinuous (first order). In figure 4.25, the same behaviour was shown where there are two humps. The phase transition was of the first order. In figure 4.26, the phase transition was also discontinuous and had the first order. These results show that for smaller noise values and larger box length, there was a loss in the cohesion. Collective motion of the particles alternates between larger scale and

Smaller scale.

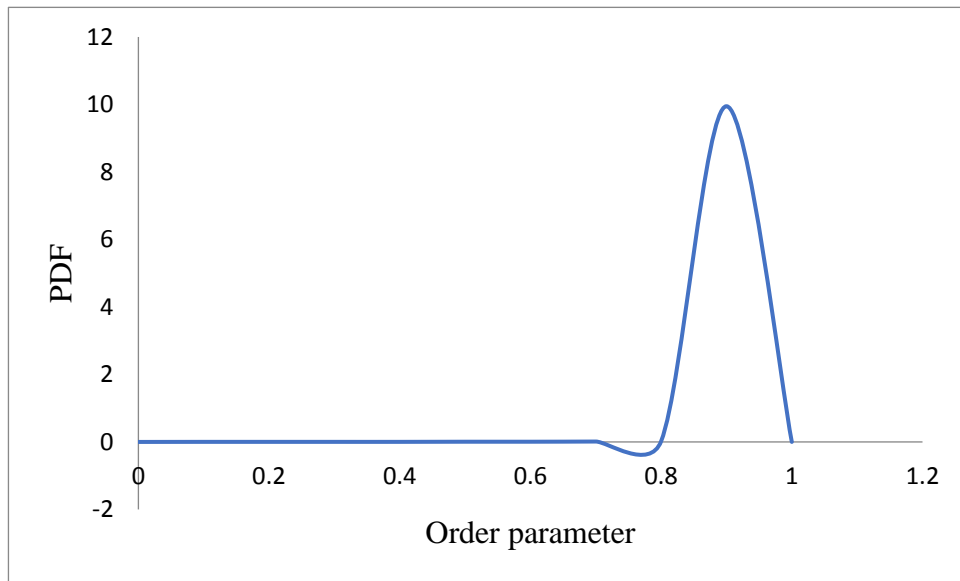


**Figure 4.27** Second order phase transitions at  $\eta = 2.0$

Higher noise and higher densities of particles were used. The results are demonstrated in figure 4.27. The curve shows one larger hump which suggests that phase transition was of the second order. The above results show that higher densities and higher noise values had a greater impact on making the phase transition the second order. Initially, collective motion of the particles remained disordered, but after some time the particles started aligning with each other due to the higher density of the particles. The system will show second order phase transition when further higher noise is applied, for example  $\eta > 2.0$ .

## 4.5 Conclusions

In this chapter, the simulation results of self-propelled particles models are presented. At the initial time step, 300 particles showed a completely disordered phase of the system. At the 20<sup>th</sup> time step and at  $L = 25$ , particles made groups which had random directions. This group formation was because of the smaller density of the particles. The system was not sufficiently dense to align all the particles with each other. At  $L = 7$  and  $\eta = 2.0$  there was correlation in the system, which was due to the higher densities and noise. For smaller noise levels ( $\eta = 0.1$ ) and smaller box lengths ( $L = 5$ ), particles showed highly ordered motion, with all particles aligned in the same direction. The self-propelled particles model was also tested with a large number of particles:  $N = 2000$ . The simulation results showed similar behaviour, as in the case of particles where  $N = 300$ . The effect of noise on the collective motion was investigated to show the different densities of the particles. It was observed that due to lower noise, the collective motion was at a larger scale and in the case of higher noise, collective motion was at a smaller scale. For large system sizes, fluctuations appeared.

The effect of particle density on collective motion was also investigated. In this case, noise was kept constant and the particle density was varied. It was observed that when the particle density was increased, the order parameter obtained a larger value which meant that the particles had a higher collective motion.

The effect of the interaction radius on the collective motion of self-propelled particles was also studied. The results showed fascinating behaviour of the particles: the order parameter obtained a very consistent value for higher time steps. In this case, the particles showed alignment in their directions.

The collective motion of the particles was also investigated for higher speed  $v \geq 0.1$  at different time steps. It observed that at  $t = 200$ , collective motion was not consistent because fluctuations appeared in the value of the order parameter. When the simulation was run for  $t = 3000$ , the collective motion remained consistent because the order parameter had a value near to 1.

The order parameter was also plotted as a function of time for different numbers of particles at noise level  $\eta = 2.0$ . It was observed that for a smaller number of particles, for example  $N = 56$ , large variations in the value of the order parameter appeared with increasing time. When the number of particles was higher, for example  $N = 4000$ , fewer fluctuations appeared in the system; the curve showed more smoothness when it compared with the curve for a smaller number of particles.

The order of phase transition was also investigated. The results showed that for lower noise levels,  $\eta \leq 0.198$ , there existed first order phase transition. For larger noise values, for example  $\eta \geq 2.0$ , there existed second order phase transition.

## CHAPTER 5

### Simulations Studies using the Vicsek 3D Model for Self-Propelled Particles

#### 5.1 Introduction

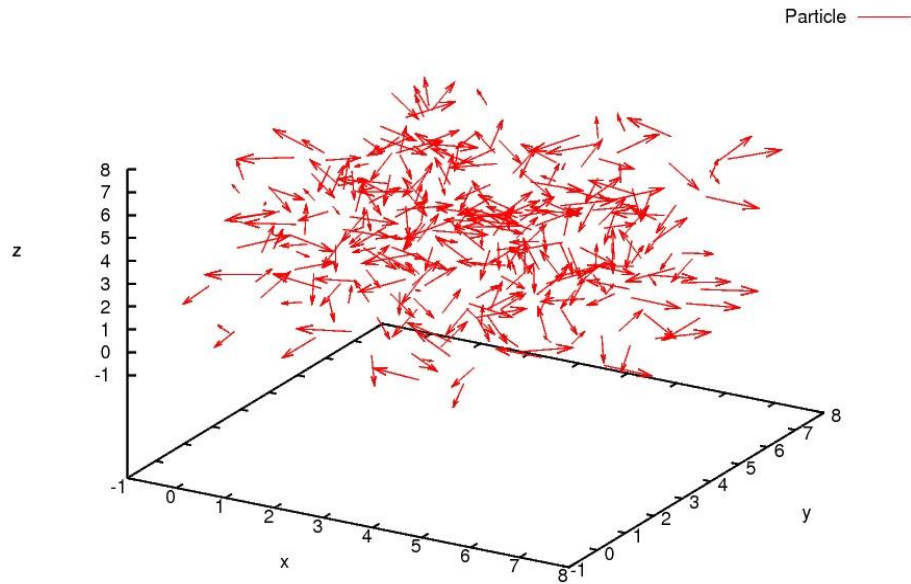
In this chapter the simulation results are presented for the Vicsek 3D model. The positions and direction of the self-propelled particles are defined by  $x$ ,  $y$  and  $z$  coordinates. Particles move in three-dimensional spaces with a linear size of  $L$  with periodic boundary conditions. Each particle has position and velocity. Initially, particles are randomly distributed with a constant absolute velocity. Velocities of the particles are updated simultaneously at every time step. A particle assumes the average direction of the motion of its neighbour along with some random perturbation. Average normalised velocity is used to characterise the collective motion of self-propelled particles and to describe the phase transition. The effects of various parameters are investigated including noise, interaction radius, speed and particle density. The order of the phase transition is also investigated. The collective motion of the particles is plotted as a function of the time. In this study the parameters given in Table 5.1 were used in the simulations.

**Table 5.1** Symbols used in captions of figures

<i>Symbol</i>	<i>Description</i>
$L$	Box length
$N$	Number of particles
$t$	Number of time steps
$\eta$	Noise
$r$	Interaction radius
$v_o$	Absolute velocity

## 5.2 Results obtained from the simulation studies

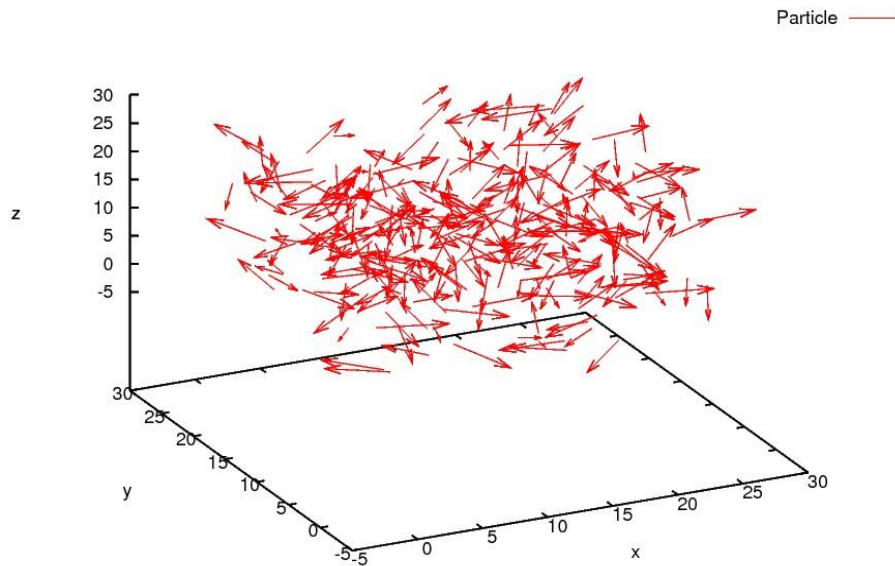
Initially, the parameter values applied were the same as they were in the Vicsek 2D model. After applying these parameters, the effects of the different parameters were investigated including speed, noise, particle density and interaction radius.



**Figure 5.1** Random motion of the particles at  $L = 7, \eta = 2, N = 300, t = 0, r = 1, v_o = 0.03$

Figure 5.1 demonstrates the initial stage of the movement of the particles. The results obtained for higher noise levels and higher density of the particles is shown by the red arrows indicating a disordered motion in the system. The order parameter was 0.06, which is approximately equal to zero. The motion of the particles was highly disturbed, and there was a loss of cohesion in the system. When more time steps are applied, there will be contact between the particles because of their self-propelled nature.

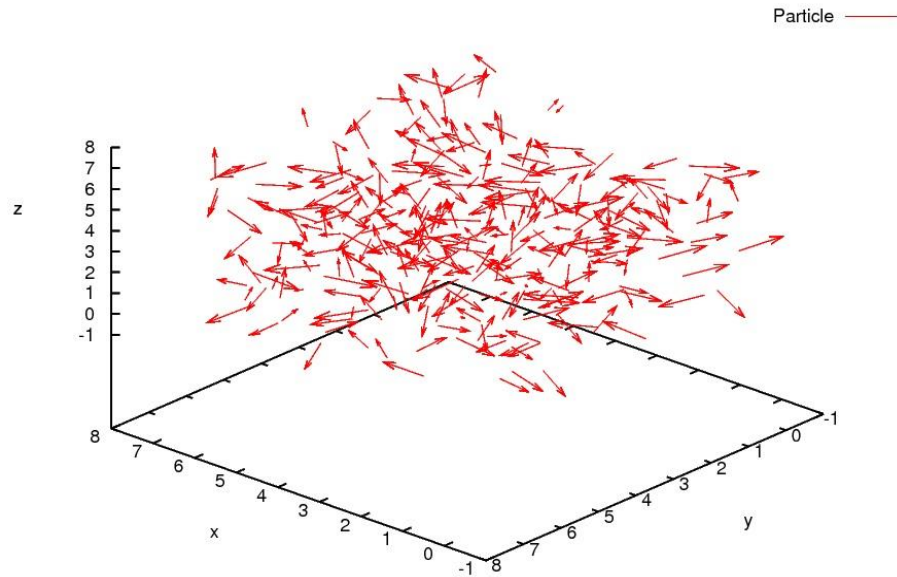
The order parameter in a three dimensional coordinate system is defined by the equation (3.7) in Section 3.2.2 of Chapter 3. It is rewritten here  $\phi = \frac{1}{N} \left| \sum_{i=1}^N \vec{v}_i \right|$ , where  $\vec{v}_i$  is the vector in a three dimensional coordinate system and whose magnitude is given as  $|\vec{v}_i| = \sqrt{x^2 + y^2 + z^2}$  and  $N$  is the number of particles.



**Figure 5.2** Disordered motion of the particles at  $L = 25, \eta = 0.1, N = 300, t = 20,$   
 $v_o = 0.03$

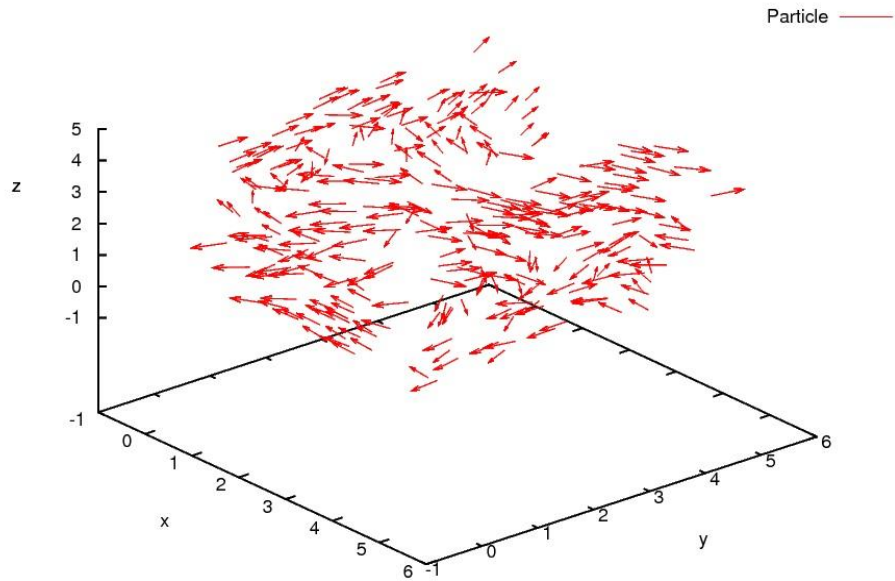
The results obtained demonstrate the movement of the particles at the 20<sup>th</sup> time steps, as shown in figure 5.2. At the smaller particle density,  $\rho = 0.0192$ , and with lower noise of  $\eta = 0.1$ , the order parameter had a value approximately equal to zero. For weaker noise

particles, alignment was expected but it can be clearly seen that there is no alignment or cohesion in the direction of the particles due to the lower particle density. The system was not too dense; therefore there was a loss of cohesion. The smaller particle density was also a source of providing the value of the order parameter equal to zero. The value of the order parameter was equal to 0.07.



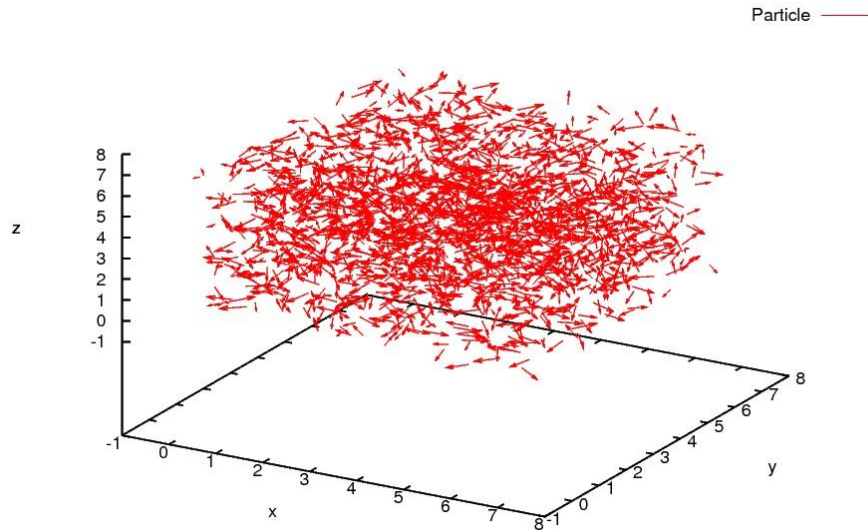
**Figure 5.3** Disordered motion of the particles at  $L = 7, \eta = 2, N = 300, t = 20, r = 1, v_o = 0.03$

Figure 5.3 shows the results of the simulation where a higher density and greater noise were applied. The higher density provided the particles with greater chances of interacting with one another. As a result, some particles moved in the same direction and the high noise value disturbed the movement of the particles. As is evident from the above figure, some particles took a random direction. The occurrence of the two behaviours at the same time: randomness and ordered motion, showed an interesting property of the 3D model. When there was higher interaction between the particles, they were not influenced by the noise; when particles were not in the interaction radius range they were highly disturbed and the value of the order parameter obtained here was equal to 0.09.



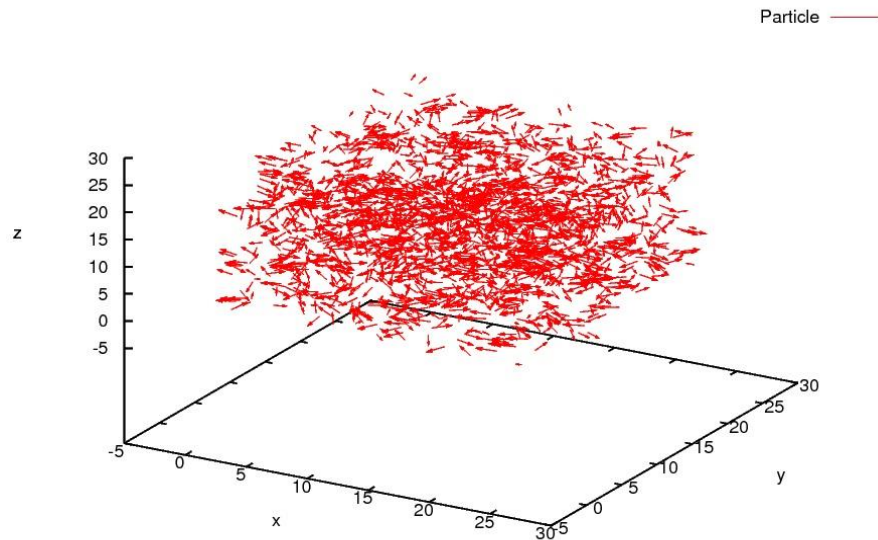
**Figure 5.4** Group formation by the particles at  $L = 5, \eta = 0.1, N = 300, t = 20, r = 1,$   
 $v_o = 0.03$

The impact of the higher density ( $\rho = 2.4$ ) along with lower noise and interaction radius, is shown in figure 5.4. The particles have formed groups, with each group having random directions. The results indicated that the particles showed a correlation. The interaction radius played an important role in the collective motion of self-propelled particles. The particles moved collectively due to the contact between the particles, this contact is in the form of interaction radius; the smaller degree of randomness can be seen which was produced by the lower noise. The order parameter obtained through the simulation was equal to 0.18.



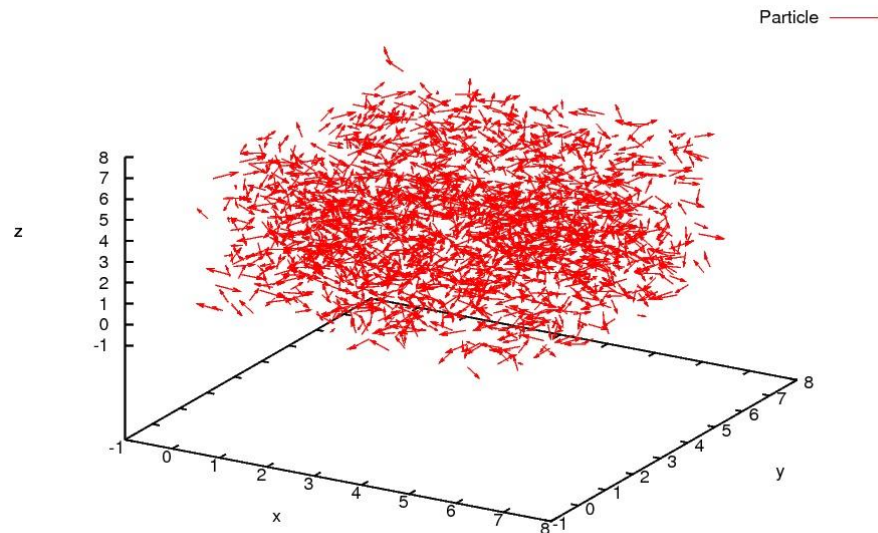
**Figure 5.5** Initial movement of the particles at  $L = 7, \eta = 2, N = 2000, t = 0, r = 1,$   
 $v_o = 0.03$

Figure 5.5 shows the result for the  $N = 2000$  particles. At  $t = 0$ , and in the presence of higher noise, the particles showed completely disordered motion; each particle had a different direction. The system was quite dense, having a particle density of  $\rho = 5.8$ . The value of the order parameter obtained after simulation was equal to 0.02, which is approximately zero. This is the initial stage where the particles start moving in the general direction of their neighbourhood. Due to the smaller box length and higher number of particles, the system was very dense and the particles were very close to each other.



**Figure 5.6** Disordered motion at  $L = 25, \eta = 0.1, N = 2000, v_o = 0.03, t = 20, r = 1$

The impact for lower noise ( $\eta = 0.1$ ) and smaller particle density ( $\rho = 0.128$ ) is demonstrated in figure 5.6. It can be clearly seen that the system was in a state of disorder and the particles showed disordered motion, having random directions. The behaviour exhibited by the particles was due to the smaller particle density. Where there was smaller particle density, there was a loss of cohesion. This density is higher than the density given in figure 5.2; however, in both cases, the results were similar because the order parameter had a value of approximately zero.



**Figure 5.7** Loss of cohesion in the system at  $L = 7, \eta = 2, N = 2000, t = 20, r = 1,$   
 $v_o = 0.03$

The impact of the higher noise and higher density of the particles is shown in figure 5.7. It can be clearly seen that the collective motion of the particles was highly disordered due to the higher noise level in the system. The value of the order parameter was equal to 0.11 at the 20<sup>th</sup> time step, which was slightly higher than the values in figures 5.5 and 5.6. This rise in the value of order parameter was due to the dense system because  $\rho = 5.8$ . Despite the higher density of the particles, their motion was highly affected due to the noise and the particles moved in different directions with a loss of cohesion and there was no alignment in the direction of the particles.

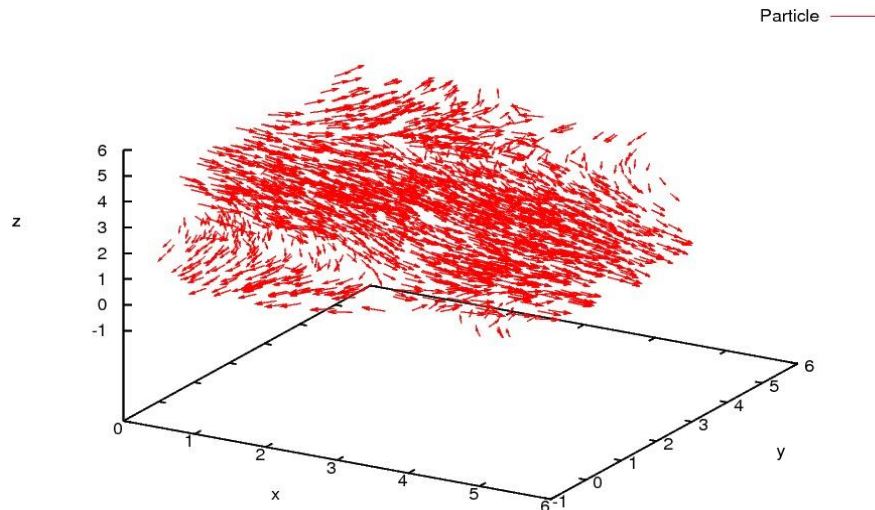


**Figure 5.8** Ordered motion at  $L = 5, \eta = 0.1, N = 2000, t = 20, r = 1, v_o = 0.03$

It can be clearly seen from figure 5.8 that the particles showed some order and group formation. Some of the particles in groups moved in different directions, but the majority of the particles took the same direction. This type of behaviour was due to the lower noise level and higher particle density and the particles became cohesive and tried to align with each other. The value of the order parameter was equal to 0.79, whereas in previous cases it was equal to zero. The interaction radius was equal to 1. If the value of the radius was higher than 1, then there would be more coordination amongst the particles. At longer time steps there would be greater chances for the particles to interact with each other; as a result, the collective motion of the particles would increase with a particle density of  $\rho = 16$ .

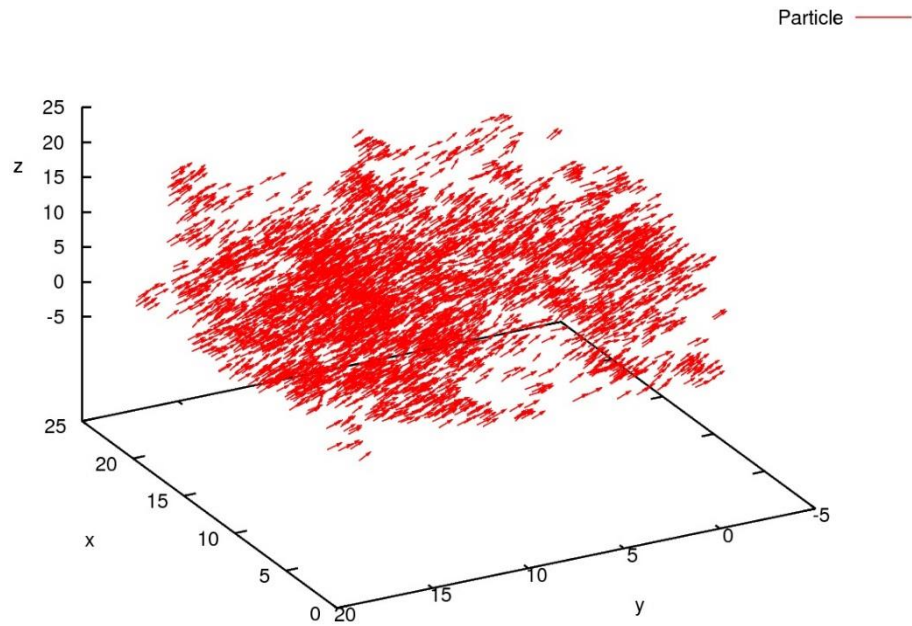


**Figure 5.9** Alignment in particles at  $L = 20, N = 3800, t = 3001, \eta = 0.1, r = 1, v_o = 1.0$

Figure 5.9 demonstrates a very fascinating collective behaviour of particles, where all the particles moved in the same direction and the system was in a state of order. There are three aspects involved that contribute to this: firstly, we see that there is a non-zero interaction radius which is 1; due to this value, the interaction of the particles with each other was very high. Secondly, the noise value was equal to 0.1; due to this the lower value particles showed little disturbance. Thirdly, the time provided for the simulation was very high and was equal to 3000 time steps. The time played an important role because at a higher value of time steps, the particles had a greater chance of coordinating with each other with more time to move and with the motion being more ordered. The particle density was equal to  $\rho = 0.475$  and the order parameter at the 3000<sup>th</sup> time step was equal to 0.98. This is a very high value that showed the system in a state of order.

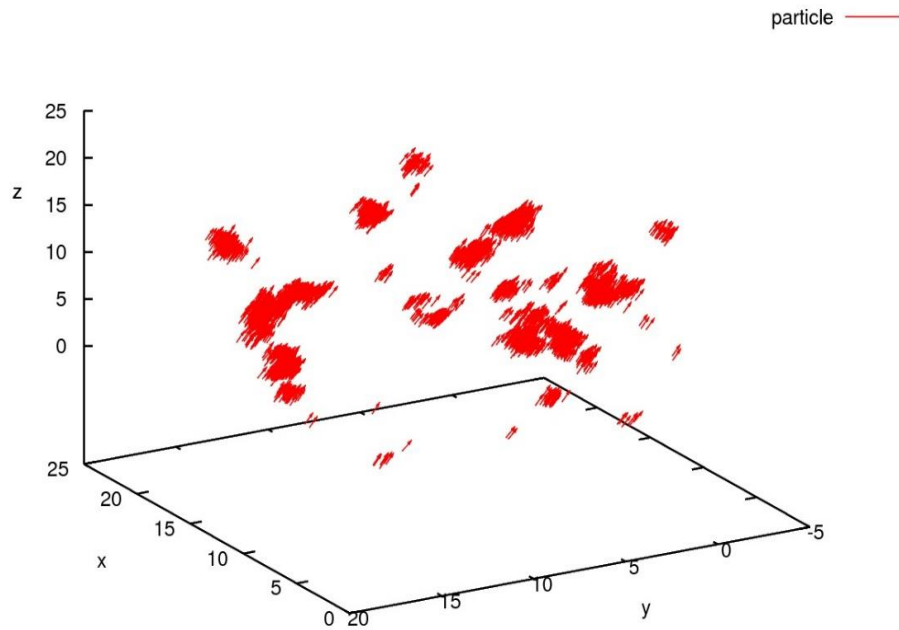


Figure 5.10 Group formation by the particles at  $L = 20$ ,  $N = 3000$ ,  $t = 3000$ ,  $\eta = 0.0$ ,  
 $r = 0.5$ ,  $v_o = 1.0$

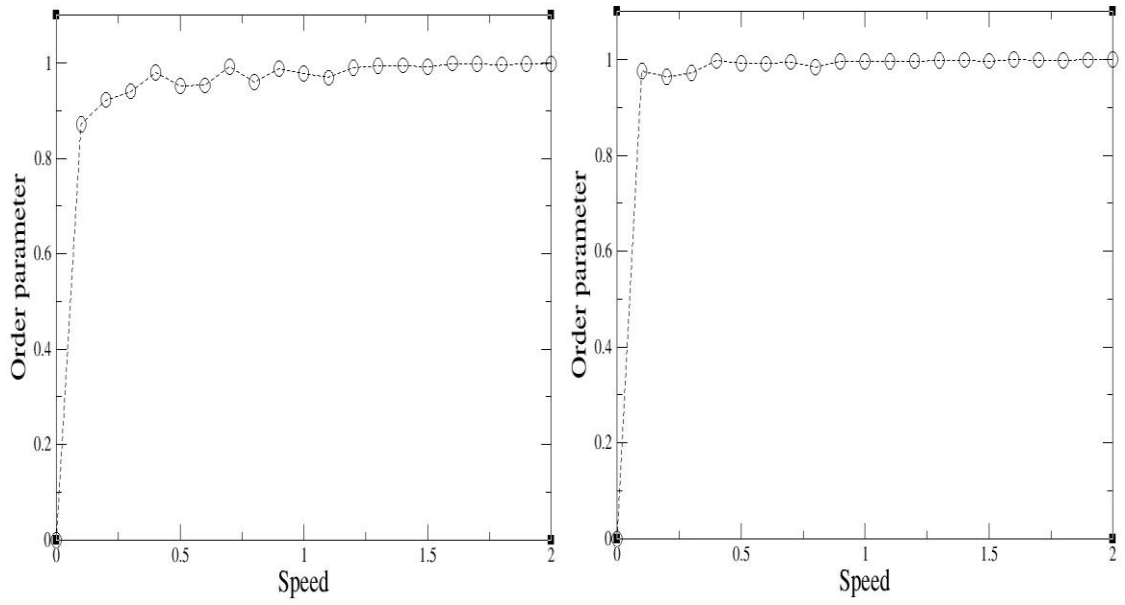
From figure 5.10, a group formation is clearly evident and the impact of the smaller interaction radius is given, which is equal to 0.5 and the noise was maintained at 0.0. Due to these parameter values, the particles formed groups. There was a very high alignment in the direction of the particles, moving in a similar direction. The value of the order parameter after the 3000<sup>th</sup> time step was equal to 0.99, indicating a state of order. This result carried a higher value of order parameter than the results as shown in the previous figure 5.9. Hence, there is always higher cohesion in the system when no noise exists in the system.

Group formation in the system occurred due to the large box size and the smaller interaction radius. The particles have plenty of space inside the box and they interacted only when they were close to each other. The system was not quite dense where each particle gets the opportunity to interact with every other particle. The absence of noise also played an important role in making a group formation because noise always provides disturbance in the direction of the particles. The interaction radius played an important

role in making the group formation. If we compare this result with the result demonstrated in figure 5.9, where the radius was 1, we see a higher alignment in that case; hence it was observed that a smaller radius will lead the self-propelled particles to a group formation.

### **5.2.1 Effect of speed**

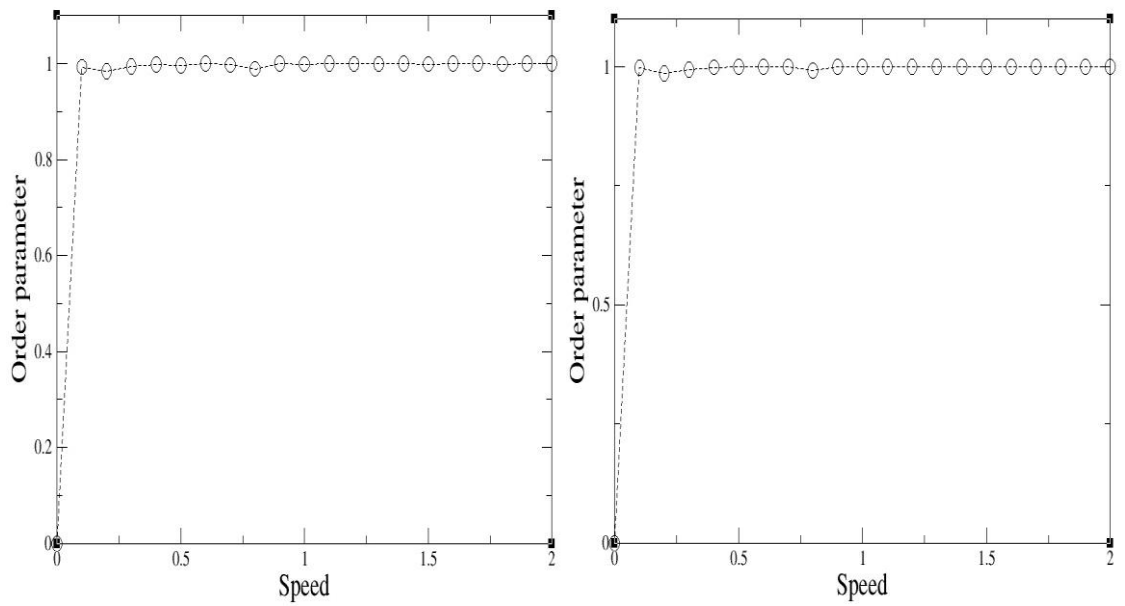
The speed parameter was varied from 0.0 to 2.0, with an interval length of 0.1. At  $v_o = 0.0$  the collective motion of the particles had a value equal to zero. There was no movement in the particles and the model became an equilibrium type. If  $v_o > 0.1$ , then the model becomes a self-propelled model and the order parameter has values. The parameter values that were used in the simulations were: box length  $L = 20$ , noise  $\eta = 0.0$ , particles  $N = 3000$  and interaction radius  $r = 1.0$ . The following figures demonstrate the effect of speed at different time steps. It was observed that at a lower speed, less collective motion took place; whereas at a higher speed, the order parameter became greater, which showed that collective motion took place on a larger scale.



(a)  $t = 500$ .

(b)  $t = 1000$ .

**Figure 5.11** Collective motion as a function of speed for 500 and 1000 time steps



(a)  $t = 2000$

(b)  $t = 3000$

**Figure 5.12** Collective motion as a function of speed for 2000 and 3000 time steps

In the above figures, the results are plotted for the order parameter as a function of the speed at different time steps, such as  $t = 500, 1000, 2000,$  and  $3000$ . Figure 5.11(a) shows that at initial values of  $v$  such as  $0.1, 0.2$  less collective motion occurred, with fluctuations at  $t = 500$ . With the value of speed equal to  $1.4$ , the system became consistent and there were no fluctuations in the system. In figure 5.11(b), the collective motion appeared to be more stable compared to in the previous case but slight fluctuations occurred. Figure 5.12(a) shows that the order parameter had a consistent value and the system was more stable than in the previous two cases. Figure 5.12(b) at  $t = 3000$  shows that the order parameter remained approximately equal to 1 with no fluctuations for  $v_o > 0$ . Collective motion of the particles occurred on a larger scale. This shows that with a higher time step, particles had more time to interact with each other and develop collective motion.

### **5.2.2 Effect of noise**

The collective motion of the particles was investigated by varying noise parameter  $\eta$ . The value of  $\eta$  was varied between 0 to 2 with an interval length of 0.1. The parameter values that were used in the simulations were box length  $L = 20$ , particles  $N = 3000$ , speed  $v_o = 1$  and interaction radius  $r = 1.0$ . The following results were obtained at  $t = 500, 1000, 2000,$  and  $3000$ . It was observed that the noise parameter had a huge impact on the collective motion of the particles.

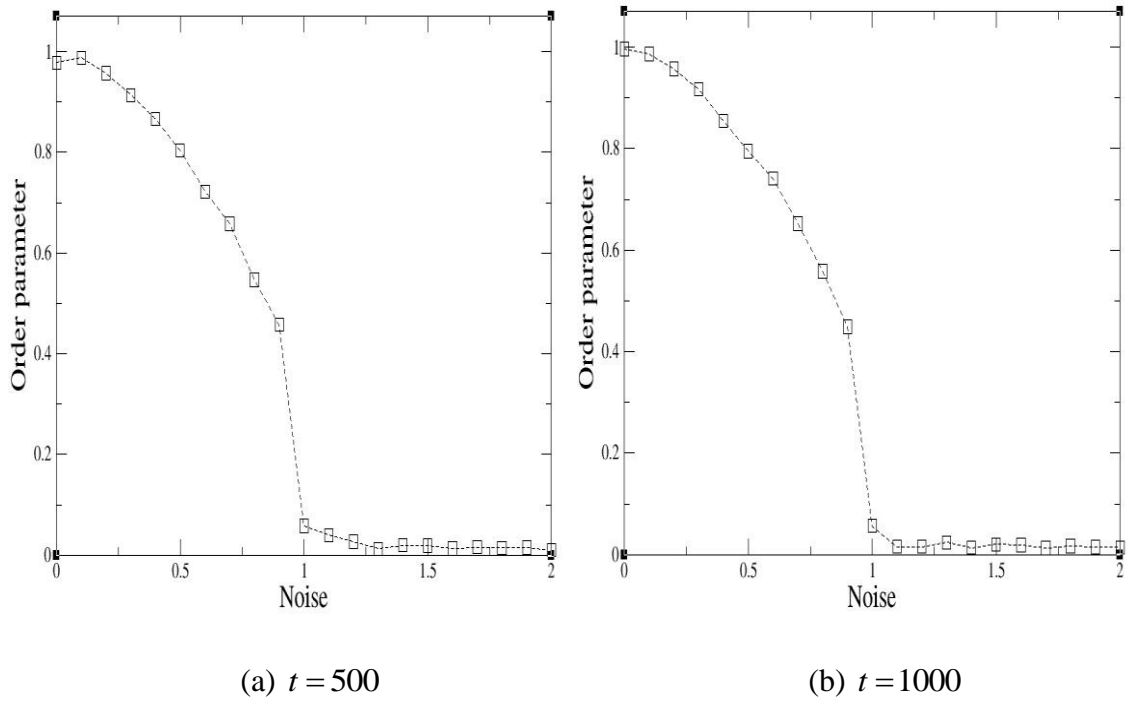


**Figure 5.13** Collective motion as a function of noise for 500 and 1000 time steps

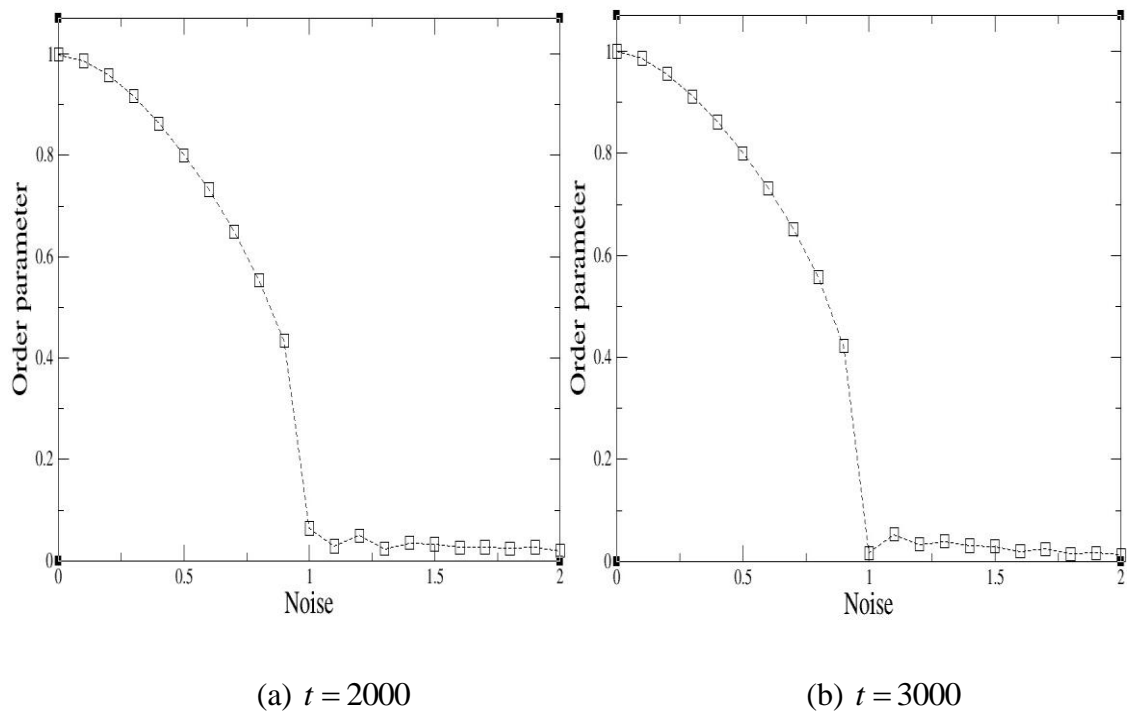


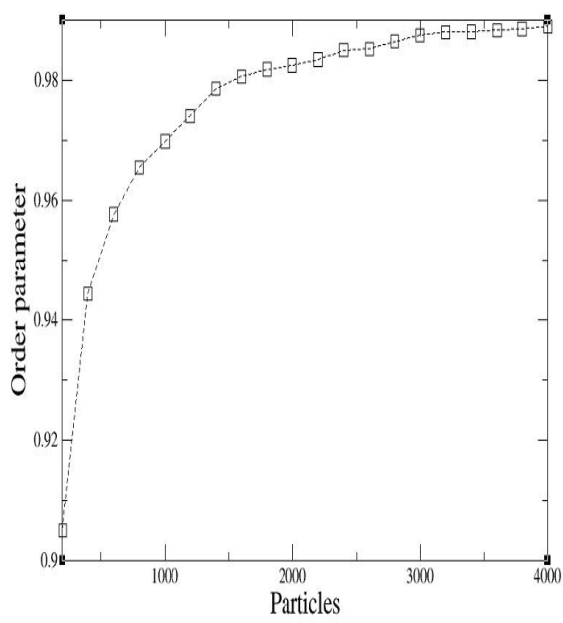
**Figure 5.14** Collective motion as a function of noise for 2000 and 3000 time steps

With increasing noise, there was a loss of cohesion in the system and the order parameter became of a smaller value. The collective motion of the particles took place on a smaller

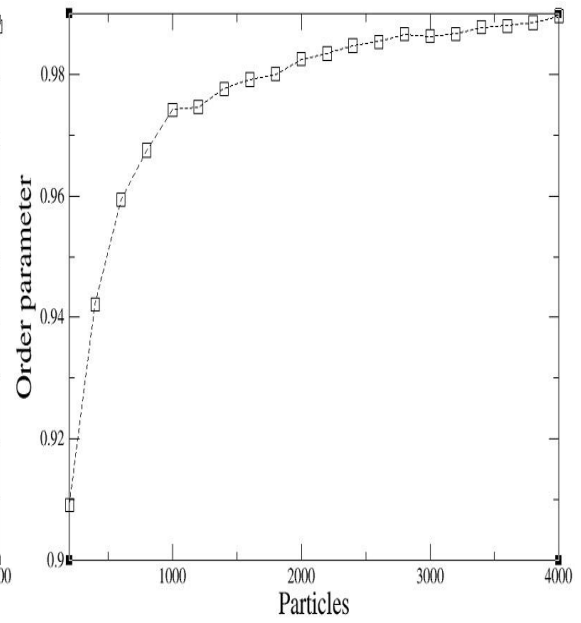
scale when greater noise was applied. Figure 5.13(a) shows results for  $t = 500$ . For a lower value of noise, the order parameter was approximately equal to 1. At noise level  $\eta = 2$ , the value of the order parameter was approximately equal to zero. Figure 5.14 shows similar behaviour at  $t = 2000$  and  $3000$ . It was observed that with the increase in time, the noise continuously put the motion of the particles in a state of disorder. This can be clearly seen as at  $\eta = 2$ , the value of the order parameter was approximately equal to zero, whereas at  $\eta = 0$  the order parameter was approximately 1.

### **5.2.3 Effect of particle densities**

The collective motion of the self-propelled particles was plotted against particle densities. Only the number of particles ( $N$ ) was varied from 200 to 4000 with an interval length of 200 and all other parameters were fixed. The noise value was fixed to  $\eta = 0.1$ , whereas the other parameter values were  $r = 1.0$ ,  $v_o = 1$ , and  $L = 20$ . The results for different time steps such as  $t = 500, 1000, 2000,$  and  $3000$  are given in figures 5.15 and 5.16.

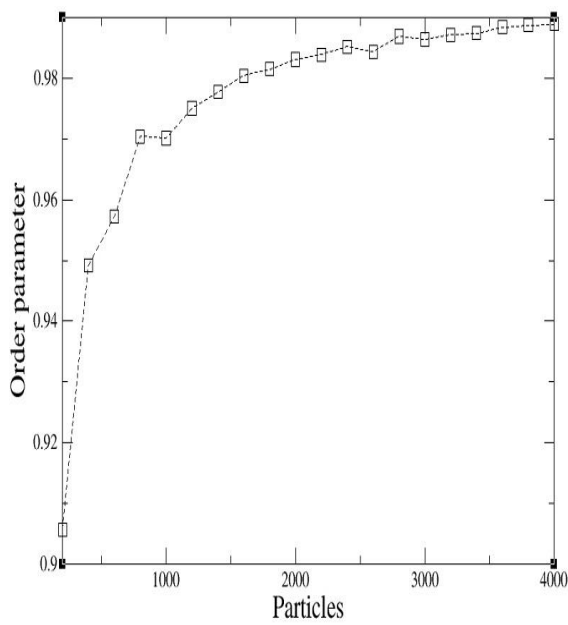


(a)  $t = 500$

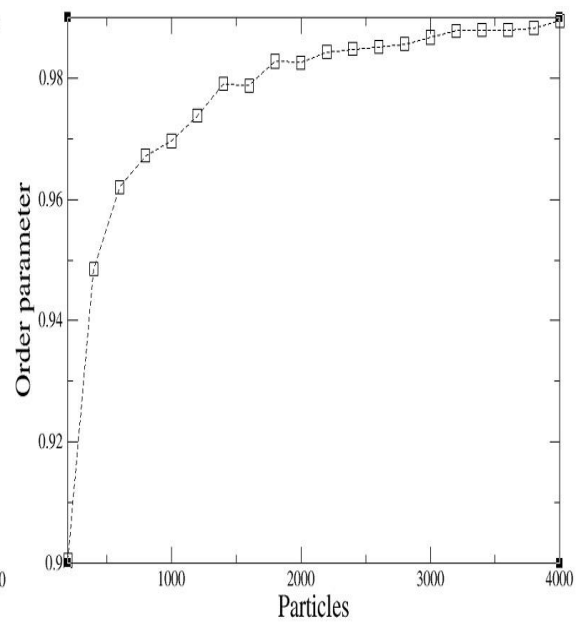


(b)  $t = 1000$

**Figure 5.15** Collective motion as a function of particle density for 500 and 1000 time steps



(a)  $t = 2000$ .



(b)  $t = 3000$

**Figure 5.16** Collective motion as a function of particle density for 2000 and 3000 time steps

The above figures demonstrate results for the order parameter as a function of the particle density. At  $t = 500$  in figure 5.15(a) it can be clearly seen that for  $N = 200$  the order parameter has a value equal to 0.90 whereas at  $N = 4000$  the value reached 0.98, which is the maximum value. As the number of particles increased, the collective motion of the particles also increased. At  $t = 1000$  in figure 5.15(b), more consistency occurred in the value of the order parameter than in the previous case. At  $t = 2000$  and  $t = 3000$ , the order parameter was stable, as shown in the curve in figures 5.16(a) and 5.16(b). It was also observed that a large number of time steps were required when there was a higher number of particles used in the system. In the above results, smaller perturbation was added, which was  $\eta = 0.1$  and the interaction radius value was kept constant, which was equal to 1.

#### **5.2.4 Effect of the interaction radius**

The effect of the interaction radius on the collective motion of the self-propelled particles is given and the interaction radius varied from 0 to 10 with an interval length of 0.5. This radius is the distance at which particles contact each other. The parameter values used in the simulation were  $N = 3000$ ,  $v_o = 1$ ,  $L = 20$ , and noise was kept equal to zero. The results are demonstrated at different time steps.

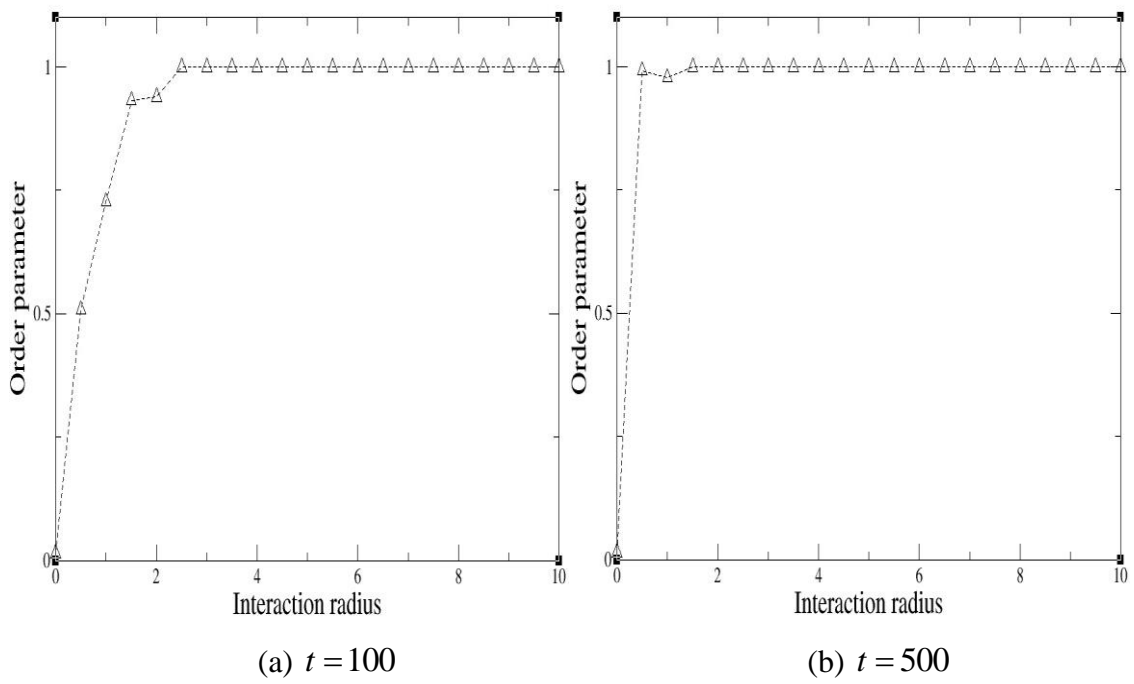


**Figure 5.17** Collective motion as a function of interaction radius for 100 and 500 time steps

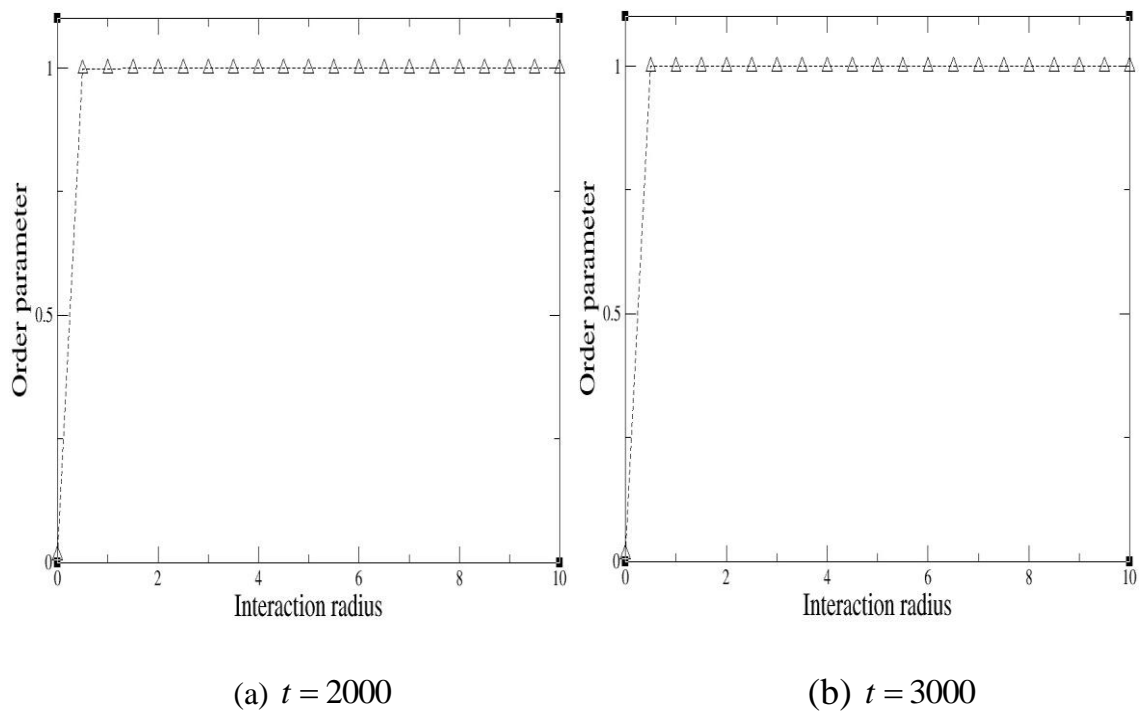


**Figure 5.18** Collective motion as a function of interaction radius for a large number of time steps

Figures 5.17 to 5.18 show that the order parameter had a consistent value. It can be seen in figure 5.17(a) that at  $t = 100$  some fluctuations were observed, but these fluctuations were not large scale and the value of the order parameter was approximately equal to 1 from  $r \geq 1$ . In the case of  $r = 0$ , the collective motion of the particles was in a disordered state with no interaction between the particles. In figure 5.17(b) the collective motion of the particles is shown at  $t = 500$ , at a radius equal to zero, the particles showed similar behaviour as in the previous case where the system showed disordered motion. At  $r = 0.5$ , the order parameter had a value equal to 0.99 which suggested that there was greater alignment in the direction of the particles. Here the value of the order parameter was more stable than in the previous case, see figure 5.17(a). In figure 5.18(a) the results are shown for the time  $t = 2000$ , at  $r = 0$ , and the system is in a state of total disorder. For  $r > 0$ , collective motion takes place on a larger scale. Similar behaviour was shown by the particles at  $t = 3000$  which is shown in figure 5.18(b). For  $r > 0$ , the order parameter was approximately equal to 1.

### **5.2.5 Order of phase transitions**

For this purpose, the probability density function of the order parameter was plotted. This technique of finding the order of phase transition is introduced in the [5]. If the curve had one hump, the phase transition was of the second order; if the curve had two humps then the phase transition was of the first order.

Following the simulation, results were obtained after variation in the noise, density, radius, and the speed parameters. Figures 5.19 to 5.21 demonstrate the second order phase transitions and the following figures 5.22 to 5.24 demonstrate the first order phase transitions.

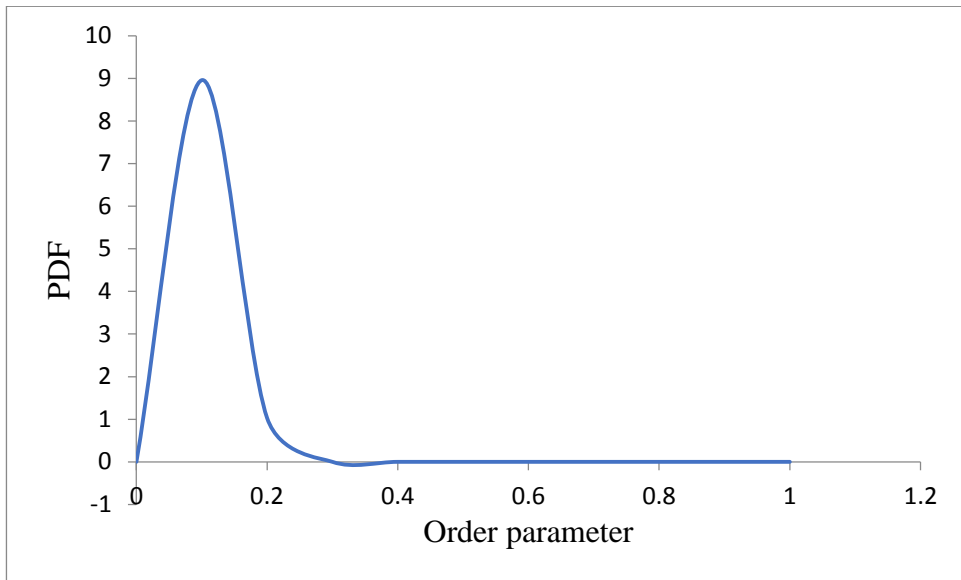


**Figure 5.19** Second order phase transitions at  $L=20$ ,  $v_o=1$ ,  $N=3000$ ,  $t=3000$ ,  $\eta=1.0$ ,  $r=1.0$

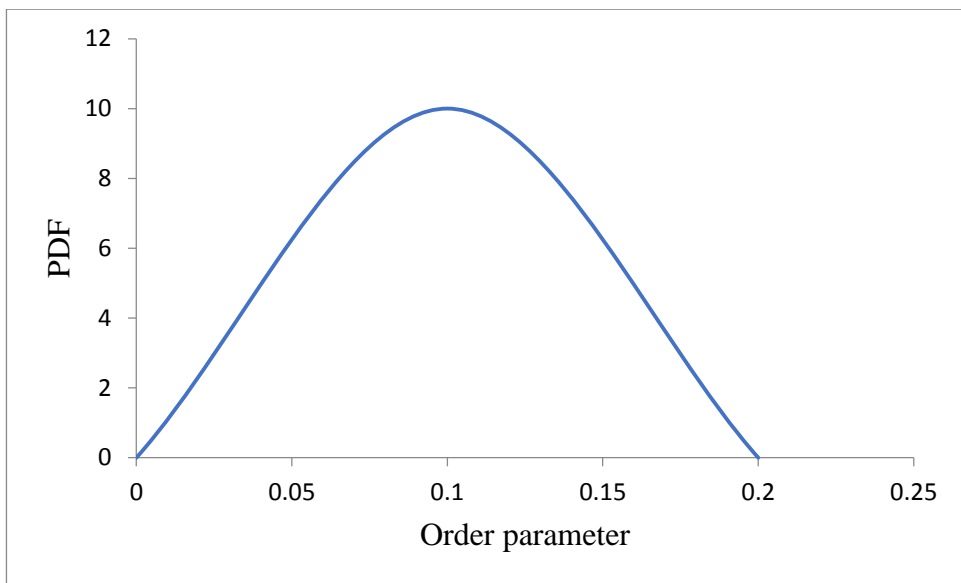


**Figure 5.20** Second order phase transitions at  $L=20$ ,  $v_o=1$ ,  $N=3000$ ,  $t=3000$ ,  $\eta=1.5$ ,  $r=1.0$

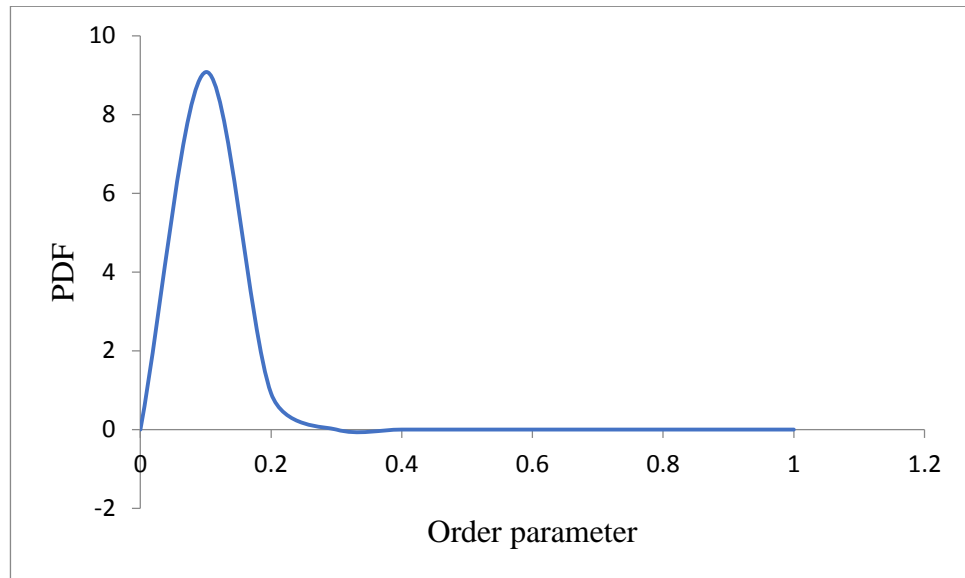


**Figure 5.21** Second order phase transitions at  $L=100$ ,  $v_o=0.5$ ,  $N=3000$ ,  $t=3000$ ,  $\eta=0.1$ ,  $r=1.0$

The second order phase transition is demonstrated in figure 5.19. It shows one big hump, indicating that the phase transition was of the second order. Higher noise was considered at  $\eta = 1.0$ . Figure 5.20 demonstrates the results for a slightly higher noise value of  $\eta = 1.5$ . The curve shows one big hump, which suggests second order phase transition. The box size was increased from 20 to 100 and the noise was kept lower to  $\eta = 0.1$ ; the speed parameter was also decreased from 1 to 0.5 in this investigation of the system and the simulation results are shown in figure 5.21, demonstrating a second order phase transition.

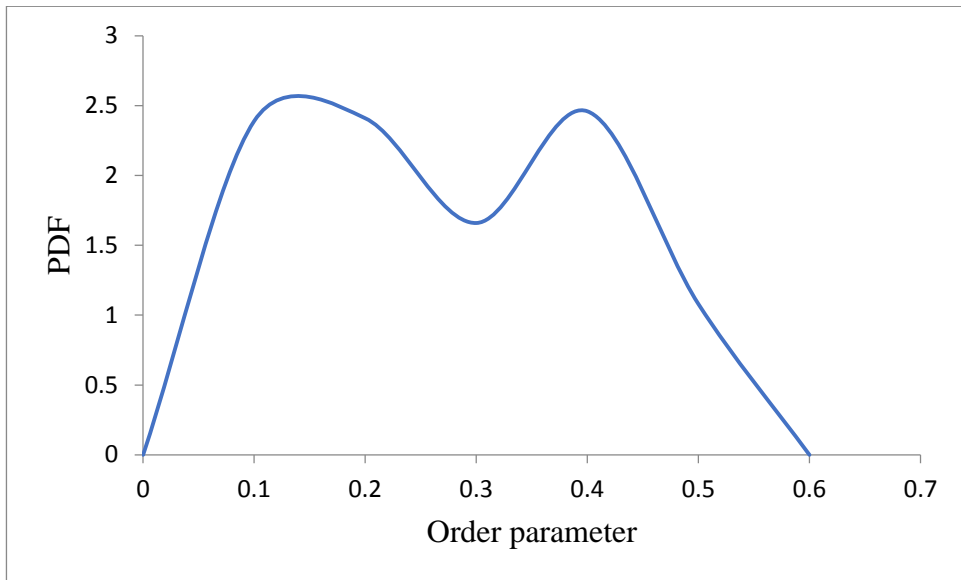


**Figure 5.22** First order phase transitions at  $L=100$ ,  $v_o=1$ ,  $N=3000$ ,  $t=3000$ ,  $\eta=0.1$ ,  $r=1.0$

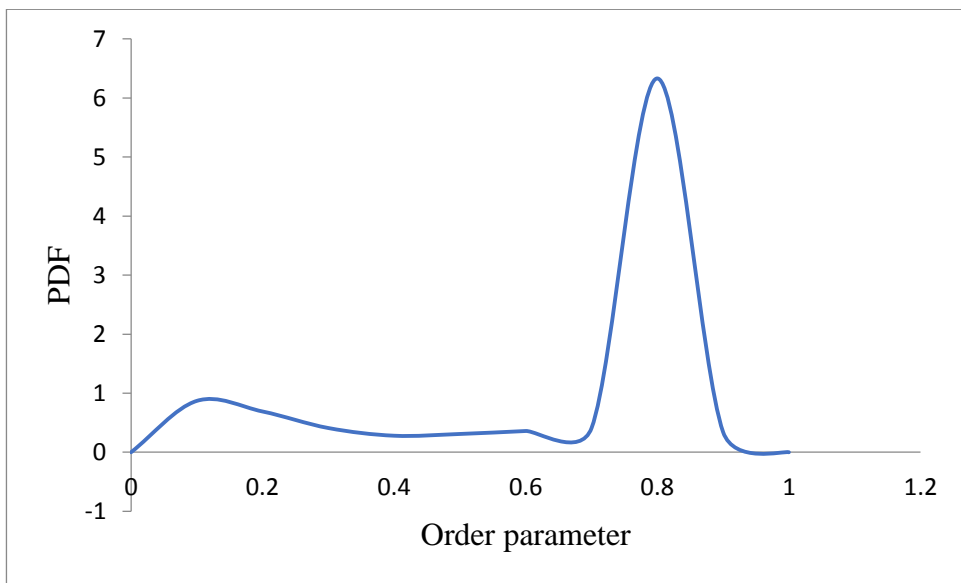


**Figure 5.23** First order phase transitions at  $L=100$ ,  $v_o=1$ ,  $N=3000$ ,  $t=3000$ ,  $\eta=0.1$ ,  $r=1.5$

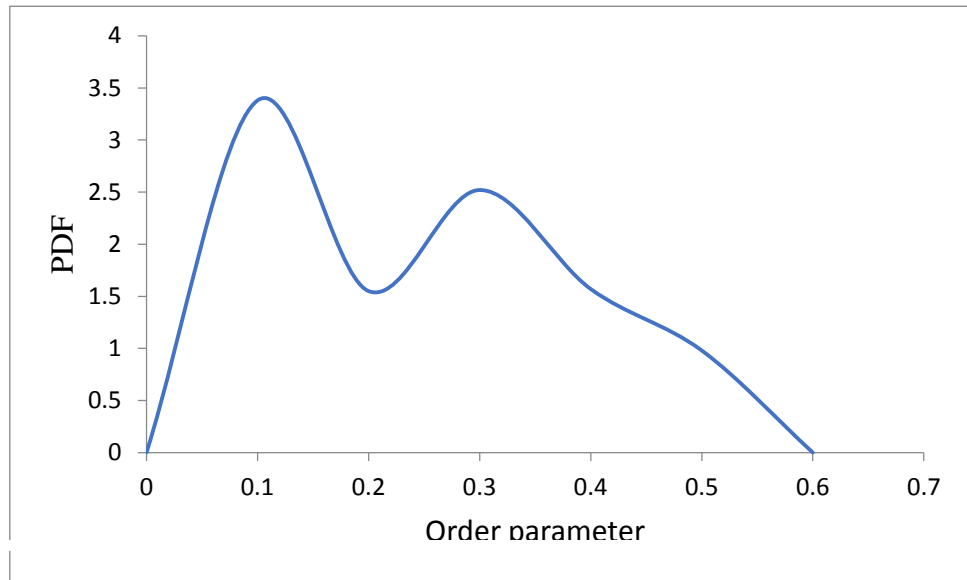


**Figure 5.24** First order phase transitions at  $L=100$ ,  $v_o=1.5$ ,  $N=3000$ ,  $t=3000$ ,  $\eta=0.1$ ,  $r=1.0$

The first order phase transition is demonstrated in figures 5.22 to 5.24 and the curve has more than one hump; due to the nature of the curve, the system is said to have first order phase transition. Figure 5.22 shows a density of  $\rho=0.003$  and it can be clearly seen that, at this smaller density of the particles, first order phase transition takes place. Here, two large humps occur in the curve. The interaction radius was changed from 1 to 1.5, the result showing first order phase transition. This result is given in figure 5.23. Moreover, by keeping the particle density fixed to  $\rho=0.003$  and the interaction radius to  $r=1$  and by changing only speed parameter from 1 to 1.5, the system exhibited first order phase transition, as shown in figure 5.24.

### 5.2.6 Collective motion as a function of time

The order parameter as a function of time was investigated. The noise level and the density of the particles were varied and the curve shows the evolution of collective motion with time. The speed of the particles was 1, time steps were 3000, and the box length was equal to 20. In the first four figures the number of particles was  $N=3000$  and in the next

two figures the density of the particles was varied to investigate the effect on the collective motion.

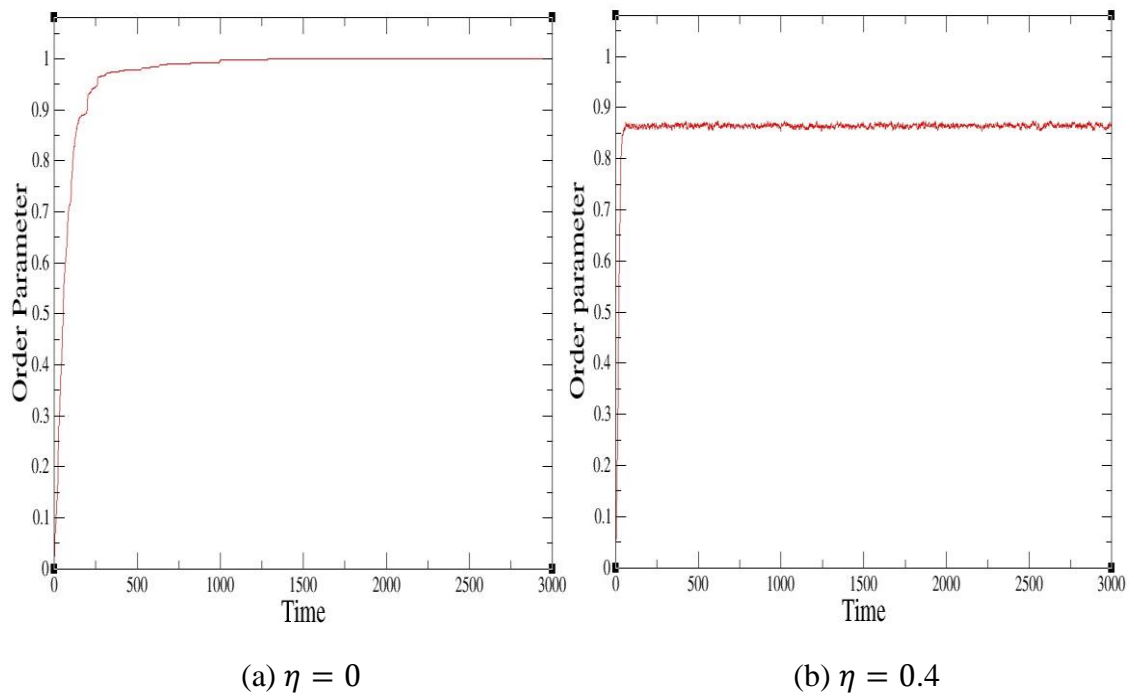


**Figure 5.25** Collective motion as a function of time at different noise values

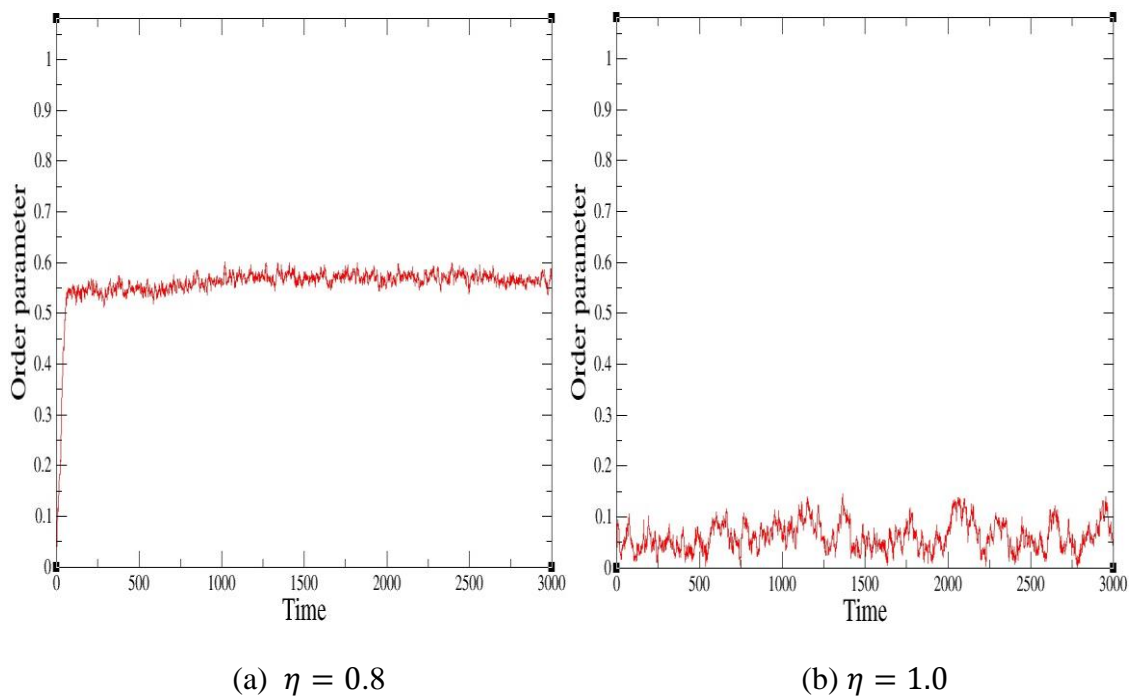


**Figure 5.26** Collective motion as a function of time for strong noise values

Collective behaviour is plotted as a function of time for different noise values at  $\eta = 0.0, 0.4, 0.8,$  and  $1.2$  (figures 5.25 to 5.26). At the initial time steps, the particles had random direction and positions but after several time steps they began to align with each other. At  $\eta = 0$ , the particles showed very smoothing behaviour, see figure 5.25(a). The value of the order parameter was consistent and remained approximately equal to 1, suggesting that there was a higher alignment in the direction of the particles. At  $\eta = 0.4$ , the value of the order parameter decreased. The curve showed smaller fluctuations, see figure 5.25(b). Most of the time, the value of the order parameter remained between 0.8 and 0.9. The noise value increased from 0.4 to 0.8. There was greater impact of this value on the collective motion of the particles. There were more fluctuations in the collective motion than in the two previous cases of noise, see figure 5.26(a). The value of the order parameter remained between 0.5 and 0.6 and this value suggested that collective motion of the particles existed but on a smaller scale. The noise was further increased to 1.0. There was a huge disturbance in the direction of the particles due to the stronger noise in the system. The impact of this noise can be seen in Figure 5.26(b). The system was in a complete state of disorder.

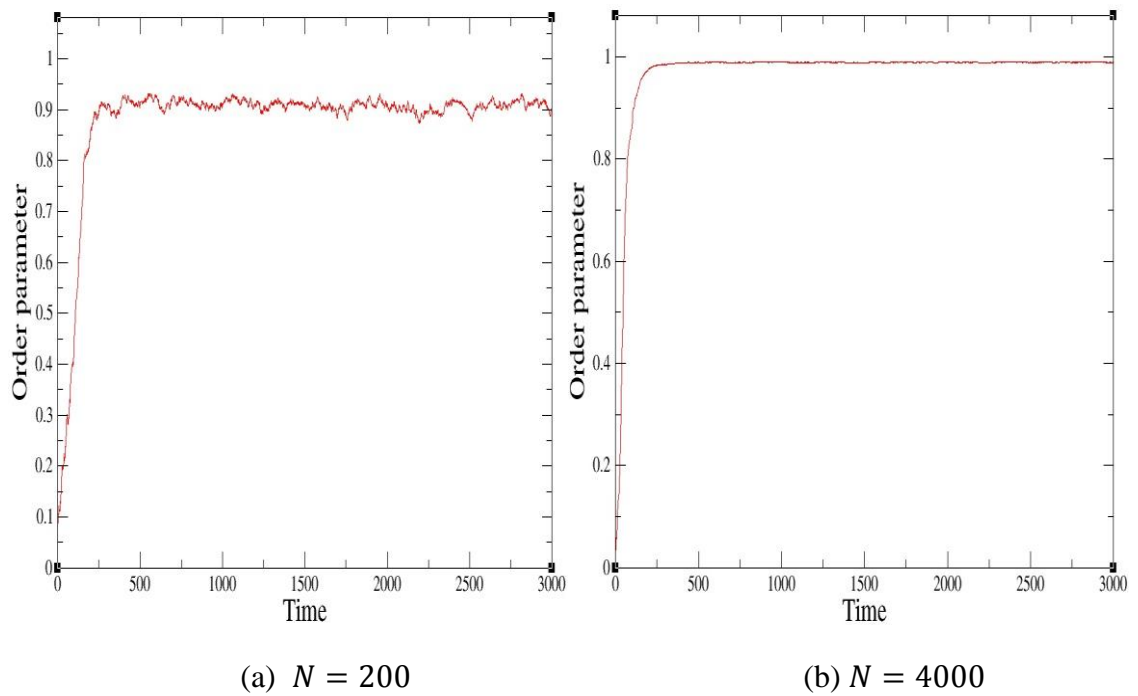


**Figure 5.27** Collective motion as a function of time for 200 and 4000 particles

Particle density was varied in the system and the results are shown in figure 5.27. Noise was fixed to 0.1 while other parameter values were the same as had been used in other results of this section. It can be clearly seen in figure 5.27(a) that the order parameter at the initial time step was smaller, but after some time steps it increased. There were also fluctuations in the system due to the smaller number of particles. The number of particles was further increased from 200 to 4000. This is a very large number and the results of this simulation are shown in Figure 5.27(b) with a smooth curve. The larger number of particles thus exhibited more collective motion than the smaller number of particles.

### 5.3 Conclusions

The three-dimensional self-propelled particles model was studied in detail and the effects of the different parameters investigated. These are: speed, interaction radius, noise, and the density of the particles, and it was observed that at the first time step the order parameter obtained a value approximately equal to zero and the particles showed randomness. Similar behaviour was also observed in the case of higher noise when the density of the particles was equal to 0.87.

Particles had a loss of cohesion with a small particle density of 0.019. At a lower noise level of 0.1 and a higher density of 2.87, the particles showed ordered motion. . For a larger number of particles such as  $N=3800$  , along with lower noise of  $\eta = 0.1$ , particles showed alignment in the direction of the particles. In the case of  $r=0.5$  and in the absence of noise, however, where there were 3000 particles simulated, the results showed group formation in the system which was due to the smaller radius.

It was observed that with an increase in speed the collective motion of the particles increased. The effect of the interaction radius was also investigated, showing that at  $r = 0$ , the system was in a complete state of disorder; the increment in the value of the radius parameter brought the collective motion to a larger scale. Variations in the noise parameter had a significant effect on the collective motion of the particles. At zero noise, collective motion was higher and with a gradual increase in the noise, collective motion started decreasing; at  $\eta = 2.0$ , collective motion did not exist. The order of phase transition was also investigated, and with noise level  $\eta \geq 1.0$ , the system showed second order phase transition.

Furthermore, for a density of  $\rho=0.003$  along with a speed of  $v_o = 0.5$ , the simulation results showed second order phase transition. For density  $\rho=0.003$  and by using  $v_o = 1.0, 1.5$  and  $r = 1.0, 1.5$ , the curve showed more than one hump which suggested that there was first order phase transition in the system. For collective motion as a function of time at various noise values and particles it was observed that for zero noise and a large number of particles, collective motion was higher; whereas for higher noise levels, collective motion was decreased.

The main difference seen in 3D compared to 2D is that in 3D there is a better view of the particle. 2D is flat and has only two dimensions, while 3D has depth and rotation. The 3D model exhibits a more realistic collective dynamic. In 3D more time steps are required for the particles to interact with each other; particles show less collective motion than in 2D. In 3D, more smoothness appears in the noise graphs compared to 2D. In 3D there is less collective motion observed than in the 2D, which can be seen in Figures 5.1-5.4.

At the initial time step in both cases the particles showed random motion. In the 2D for  $L = 25$ , and  $N = 300$ , there was group formation, but in 3D for the same parameter values, no group formation occurred; an example can be seen in figures 4.2 and 5.2. At  $L = 5$ ,  $\eta = 0.1$ , and  $N = 300$ , there was perfect alignment in the particles in the 2D system, whereas in 3D there was alignment but it was not as high as it was in 2D.

There was another difference which appeared in the 3D compared to 2D, that in the 3D second order phase, transitions existed for noise  $\eta \leq 1.0$ , whereas in the case of 2D, first order phase transition existed in the system for  $\eta \leq 1.0$ .

## CHAPTER 6

### Simulations using new Obstacle Avoidance Model

#### 6.1 Introduction

This chapter focuses on the model that has been developed in this study. As mentioned earlier, this model is termed the obstacle avoidance model (OAM). Even though the collective behaviour of particles has been investigated using previous models, no work has been carried out on investigating collective motion with the presence of a variety of obstacles along with various parameters. There are many examples available in the environment where the dynamics of particles is given in the presence of obstacles. Bacteria show complex collective behaviours, for example, swarming in a heterogeneous environment such as soil, or highly complex tissues in a gastrointestinal tract; herds of mammals travel long distances crossing rivers and forests [115].

The results obtained from the obstacle avoidance model are discussed in this chapter. Particles move in the presence of static obstacles. First of all, the simulation results are presented for various system sizes. Collective motion was plotted as a function of time. The effects of interaction radius, noise and speed on the collective motion of the particles was also investigated in both homogeneous and heterogeneous media. The order of phase transition was also investigated for large numbers of particles.

## 6.2 Parameter table

The key parameters used in this model for simulation studies are summarised in Table 6.1. These were discussed in Chapter 3 (see the equations developed for the obstacle avoidance model).

**Table 6.1** Parameters used in the simulation

<i>Symbol</i>	<i>Description</i>
$L$	Length of box
$N_b$	Number of particles
$N_o$	Number of obstacles
$t$	Time step
$\eta$	Noise amplitude
$R_o$	Interaction radius between the particle and the obstacles
$r$	Interaction radius between the particles
$v_o$	Absolute velocity
$\gamma_o$	Particle's turning speed when it interacts with obstacle
$\Delta t$	Time interval
$w$	Collective motion parameter (order parameter)

### 6.3 Comparison of simulation results and manual calculation results

The tables below describe the simulation results and manual calculation results for three particles and one obstacle. Initially, the positions and the velocity directions of three particles and one obstacle were selected. These values were then put in the obstacle avoidance model. For this calculation, the length of the box was  $L = 5$ , the interaction radius between the particle and the obstacle was  $R_o = 3.8$ , the radius between the particles was  $r = 2$ , the absolute velocity was  $v_o = 1$ , and the noise was  $\eta = 0.01$ . The calculation was undertaken for two time steps.

**Table 6.2** Initial positions and velocity directions of three particles

Particle serial No.	Position		Velocity direction	
	x	Y	X	Y
1	0.000001	0.127402	-0.060050	0.079962
2	3.334572	4.815278	0.052671	-0.085004
3	1.676775	4.576636	0.028419	-0.095876

**Table 6.3** Initial positions and velocity directions for one obstacle

Obstacle serial No.	Position		Velocity direction	
	x	Y	X	Y
1	4.163465	1.725213	0.689950	-0.723856

**Table 6.4** Manual calculation of three particles at first time steps

First time step				
Particle serial No.	Position		Velocity direction	
	x	Y	X	Y
1	4.942032	0.208885	-0.579701	0.814829
2	3.434565	4.816496	0.999925	0.012183
3	1.697530	4.674459	0.207544	0.978225

**Table 6.5** Manual calculation of three particles at second time step

Second time step				
Particle serial No.	Position		Velocity direction	
	x	Y	X	Y
1	4.914804	0.305107	-0.272275	0.962219
2	3.362638	4.885970	-0.719264	0.694736
3	1.776611	4.735665	0.7908094	0.612062

**Table 6.6** Program values of three particles at first time steps

First time step				
Particle serial No.	Position		Velocity direction	
	x	Y	X	Y
1	4.942032	0.208885	-0.579701	0.814829
2	3.434565	4.816496	0.999925	0.012183
3	1.697530	4.674459	0.207544	0.978225

**Table 6.7** Program values of three particles at second time step

Second time step				
Particle serial No.	Position		Velocity direction	
	x	Y	X	Y
1	4.914804	0.305107	-0.272275	0.962219
2	3.362638	4.885970	-0.719264	0.694736
3	1.776611	4.735665	0.7908094	0.612062

Tables 6.4-6.7 demonstrate manual calculations and the simulation results of the obstacle avoidance model. It was observed that there was consistency in the values of the positions and directions of the particles.

Tables 6.4 and 6.6 have consistency up to 6 decimal places. These two tables are given for the first time step. There is also a consistency up to 6 decimal places between Tables 6.5 and Table 6.7. These two tables show results for the second time step.

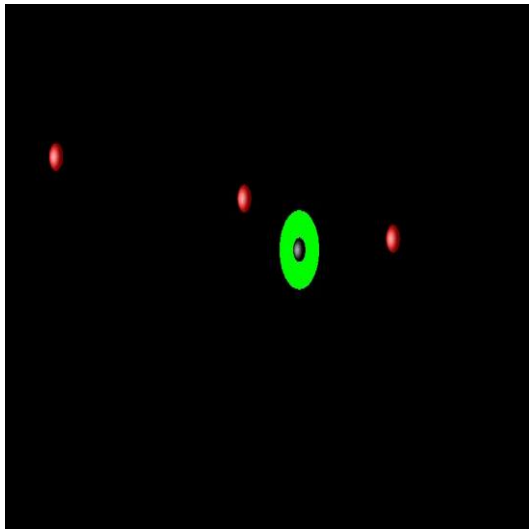
## 6.4 Simulation results

The motion of the  $N_b$  self-propelled particles was in two-dimensional space with periodic boundary conditions of size  $L$ , where  $L$  denotes the box length in which the simulations were carried out. In this model, the particles moved collectively in the presence of fixed obstacles. These obstacles were randomly distributed in the system. The interaction of the particles among themselves was same as in the Vicsek model [28] where the particle assumes the average direction of the neighbours in its interaction radius  $r$ .

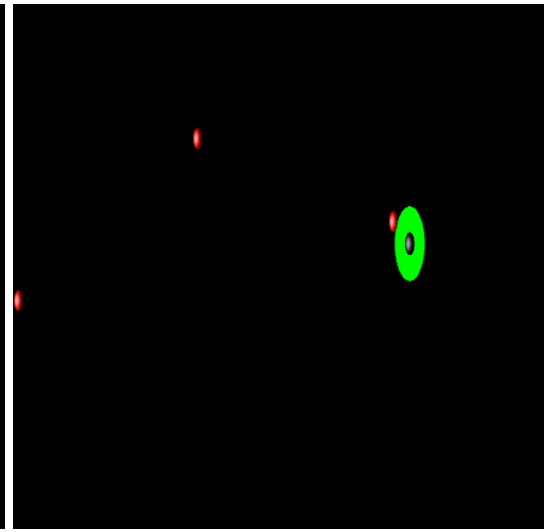
Following a sequence of snapshot displays, the interaction of the three particles and one obstacle was observed at different time steps. These snapshots were taken from the video

simulation of obstacle avoidance model through Opendx. Here, parameter values were

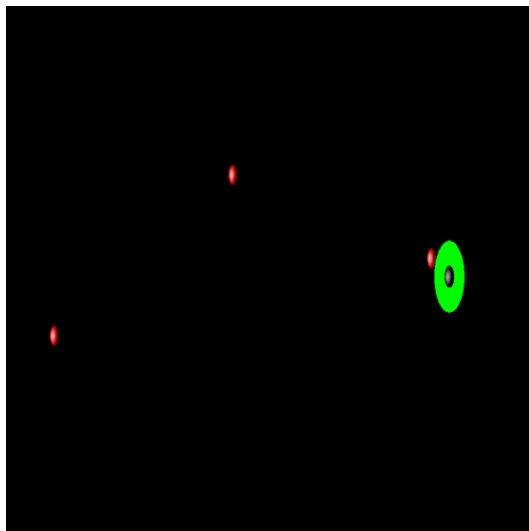
$L = 50, N_b = 3, N_o = 1, R_o = 2, r = 1, \eta = 0.01, t = 1000, v_o = 1, \gamma_o = 5, \Delta t = 0.1.$



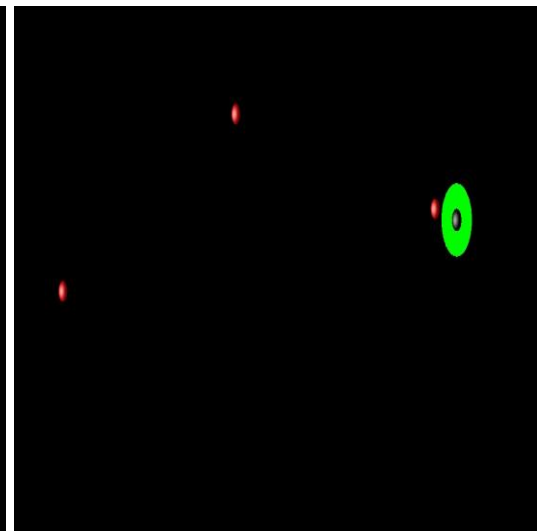
(a)  $t = 348$



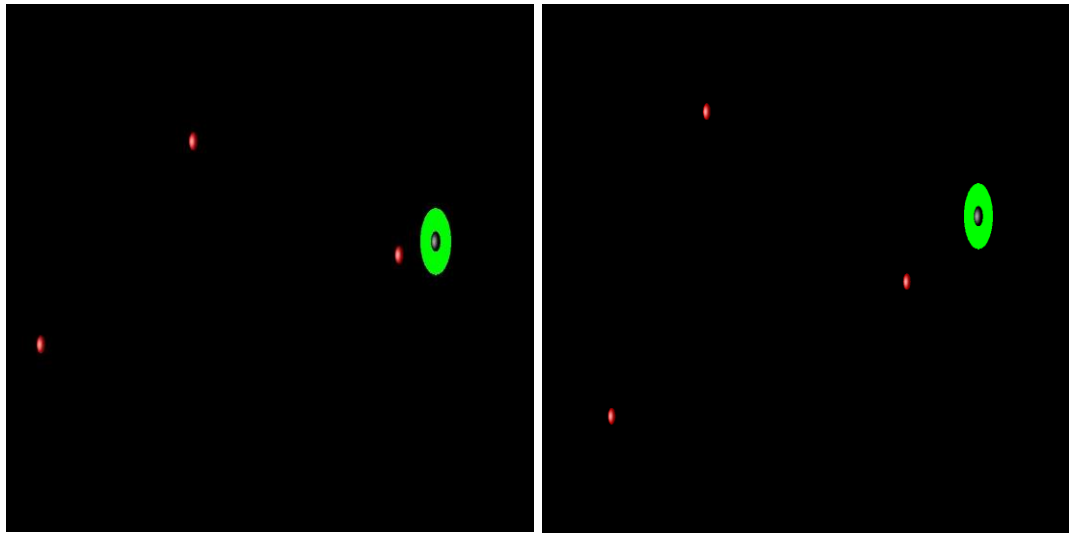
(b)  $t = 378$



(c)  $t = 380$



(d)  $t = 385$



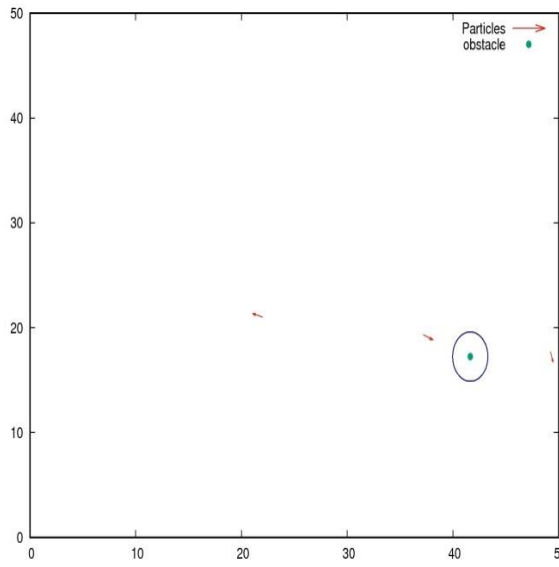
(e)  $t = 404$

(f)  $t = 452$

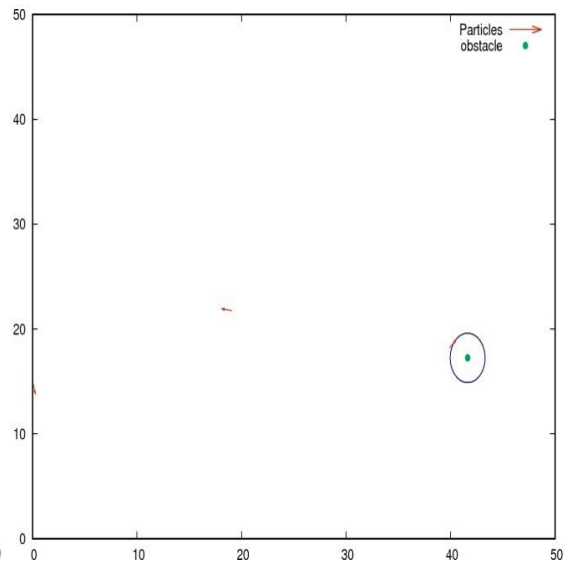
**Figure 6.1** Avoidance of particles from the obstacles is displayed in the sequence of snapshots from the video from (a) to (f)

In Figure 6.1 from (a) to (f), the sequence of snapshots displayed the avoidance of the particles from the obstacle. The particles are shown in red and the obstacle is represented in blue. The green circle shows the interaction radius between the particles and the obstacle. When a particle reached the green circle, it attempted to turn away from the obstacle. In snapshot (a) at the 348<sup>th</sup> time step, one particle moved towards the obstacle and the other was going away from the obstacle; in (b) at the 378<sup>th</sup> time step the particle touched the interaction radius range. Subsequently, it started to move away from the obstacle. This avoidance can be seen in the snapshots from (c) to (f). In (c) at the 380<sup>th</sup> time step it started to turn away from the obstacle and in (f) at the 452<sup>th</sup> time step the particles were distant from the obstacle.

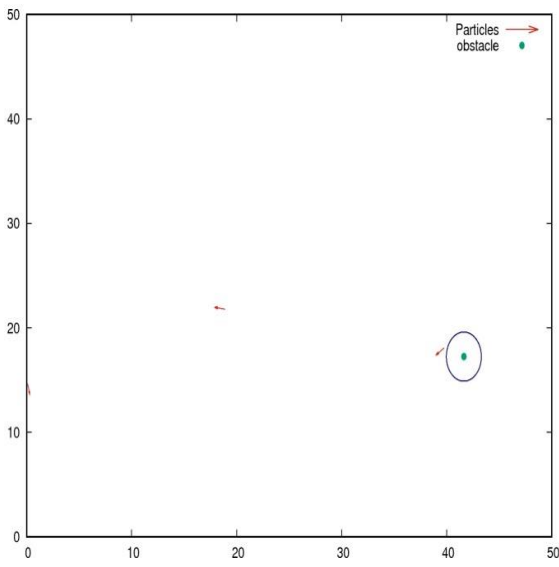
Figure 6.2 displays static images for the same time steps at which snapshots were taken (figure 6.1). These static images were obtained through the GNUPLOT. All parameters were kept constant.



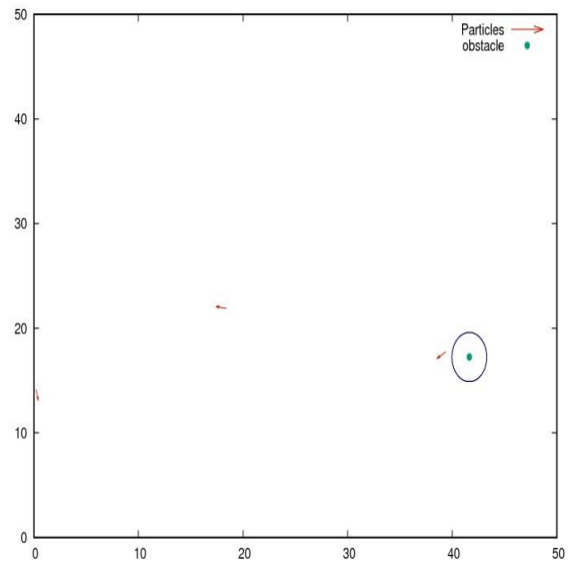
(a)  $t = 348$



(b)  $t = 378$



(c)  $t = 380$



(d)  $t = 385$

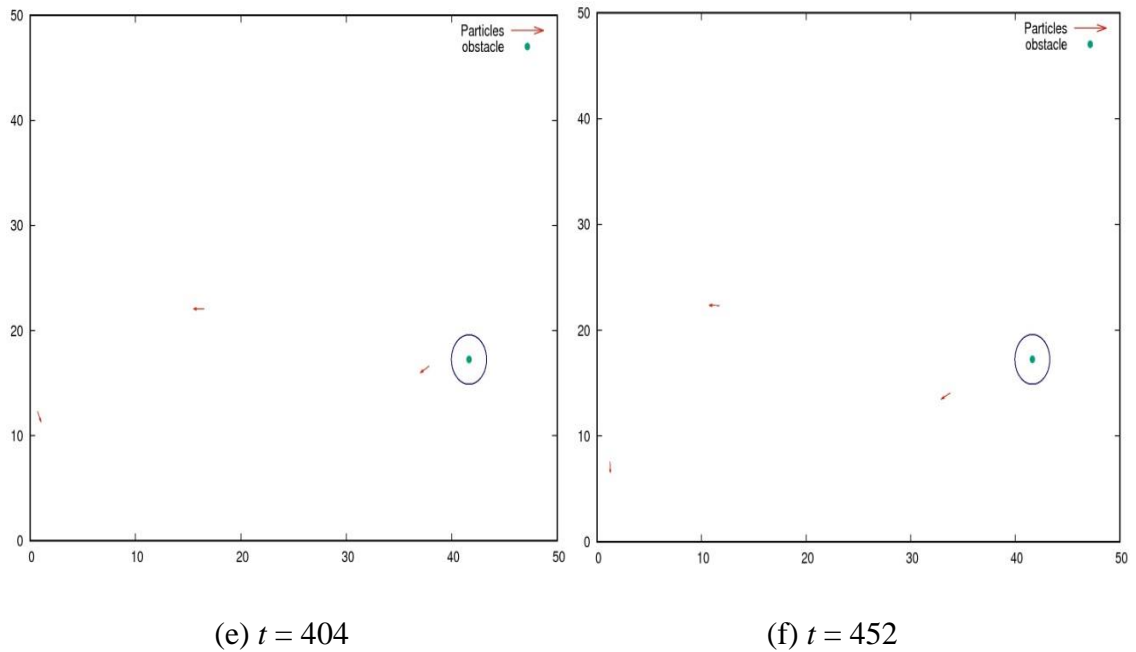


**Figure 6.2** Static images from (a) to (f) for the same time steps at which snapshots of the video were taken which are shown in figure 6.1

In figure 6.2 the particles are represented by arrows and the obstacle is represented by a point and it is in green. The blue circle represents the interaction radius range of the obstacle at which the particles interacted with the obstacles. The particles started avoiding the obstacle when they touched the circle. In (a) at the 348<sup>th</sup> time step, one particle moved towards the obstacle because at this time step the particle was not in the interaction radius range of the obstacle; in (b) at the 378<sup>th</sup> time step, one particle touched the circle, whereas the other two particles were away from the obstacle; in (c) at the 380<sup>th</sup> time step, the particle changed its direction and moved away from the obstacle; in (d) at the 385<sup>th</sup> time step, it can be clearly seen that the particle travelled in the opposite direction to the obstacle, which showed the avoidance of the particles from the obstacle; in (e) and (f) the particle showed avoidance behaviour.

**Table 6.8** Distance between 3 particles and 1 obstacle

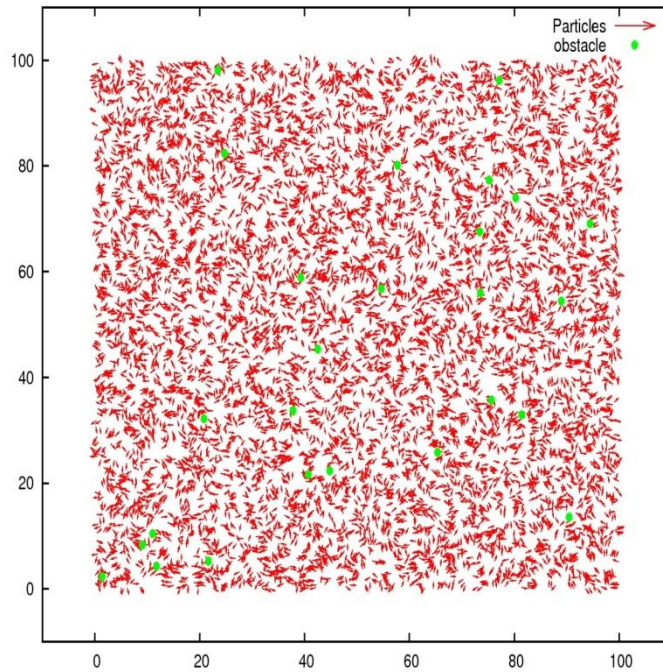
Time steps ( $t$ )	$t = 348$	$t = 378$	$t = 380$	$t = 385$	$t = 404$	$t = 452$
Distance between particles and obstacle	19.907123	22.895081	23.095054	23.594984	25.483352	30.242180
	7.572995	41.666076	41.636233	41.555266	41.227371	41.505400
	4.997251	1.999359	2.015389	2.259693	3.756319	8.382383

Table 6.8 shows the distance between the particles and the obstacle at the same time steps as were used for snapshots in figure 6.2.

#### 6.4.1 Simulation results for 10000 particles

Simulations of 10000 particles in the presence of 26 obstacles were carried out. Only the noise value was varied in each result of this section, while all the other parameters were the same. The density of the particles was set to 1 and the density of the obstacles was 0.0026. The time steps start from zero and run to 10000. The following figure shows the movement of the particles at the initial time step.

The parameter values were as follows: box length  $L = 100$ , time  $t = 10000$ , particles  $N_b = 10000$ , obstacles  $N_o = 26$ , interaction radius  $r = 1$ , avoidance radius  $R_o = 1$ , speed  $v_o = 1$ , particle's turning speed  $\gamma_o = 1$ , time interval  $\Delta t = 0.1$ .



**Figure 6.3** Random distribution of particles at initial time step ( $\eta = 0.01$ )

In the above figure 6.3, circles represent the obstacles and arrows represent the particles. This figure demonstrates the initial movement of the particles. The particles and the obstacles were randomly distributed and scattered in the box with random directions. During the initial stage, the particles had no contact with each other and did not have the ability to give a response to noise. They were in a complete state of disorder since the value of the order parameter obtained at the first time step was approximately equal to zero. The particles did not recognise the obstacles. However, as the time steps increased, the particles' ability to respond to obstacles, noise and interaction with neighbouring particles also increased (figure 6.4)

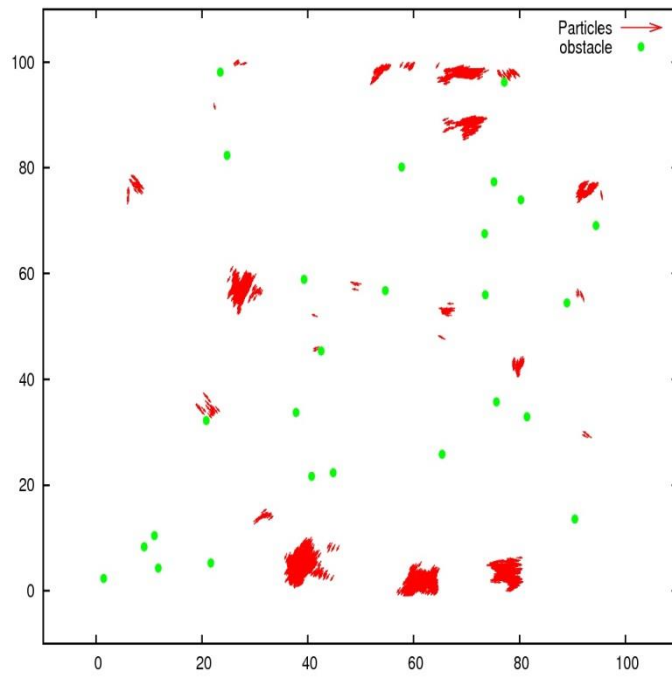
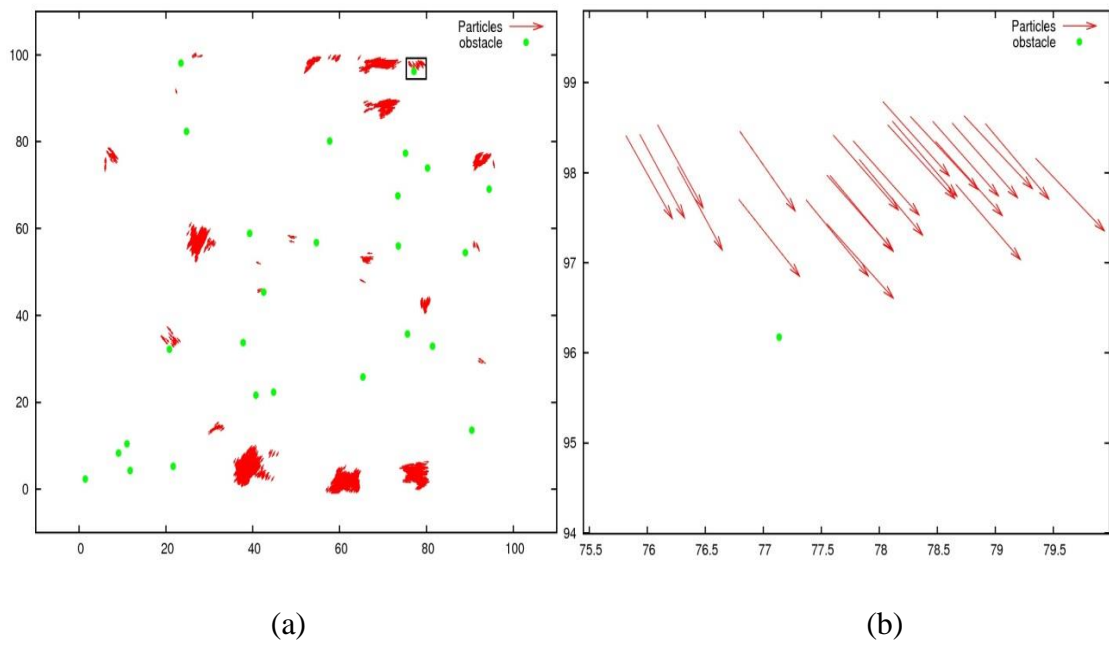
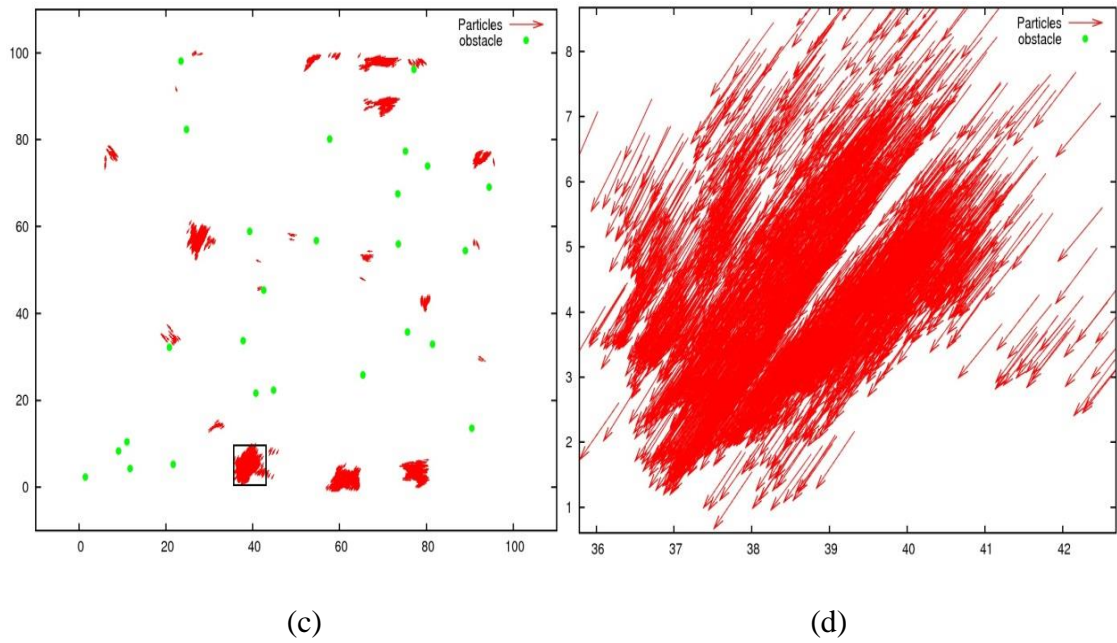


**Figure 6.4** Collective motion of the particles in groups at the 10000<sup>th</sup> time step for  $\eta = 0.01$



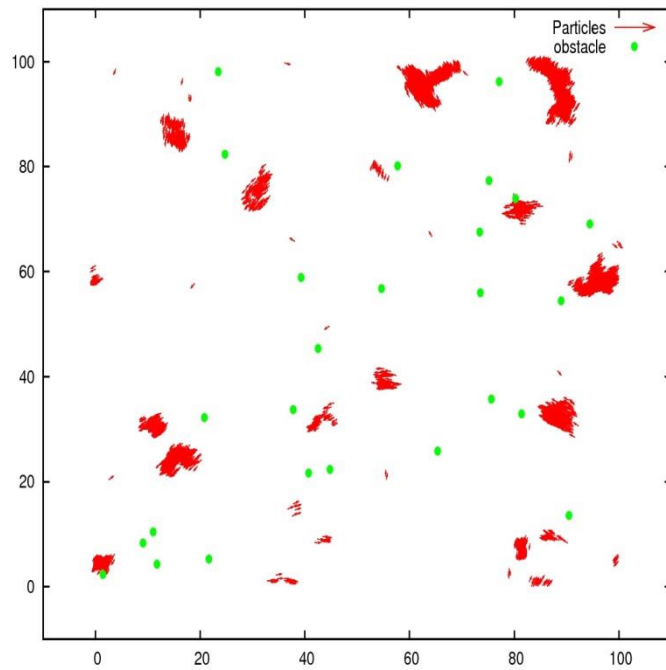
(a)

(b)



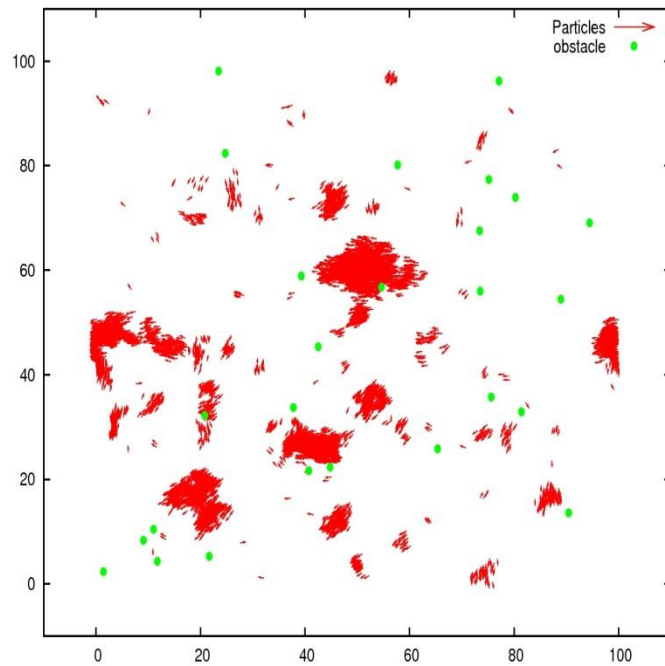
**Figure 6.5** Small rectangular boxes in (a) and (c) show particles and obstacles viewed from close range; these can be seen in (b) and (d). These are taken from Figure 6.4

Initially every particle moved randomly, but after some time they started to move collectively. The above result is for the 10000<sup>th</sup> time-step (figure 6.4). It can be clearly seen that the particles were grouped together and each group moved randomly. When these got closer to the obstacle they turned away from the obstacle as there was a very small noise value ( $\eta = 0.01$ ) used and as a result the particles became clusters. In these clusters the particles were very close to each other. The particles had a greater ability to come in contact with each other and align with each other due to the interaction radius. The particles followed the average direction of their neighbours and the value of the order parameter at the 10000<sup>th</sup> time step was equal to 0.63.



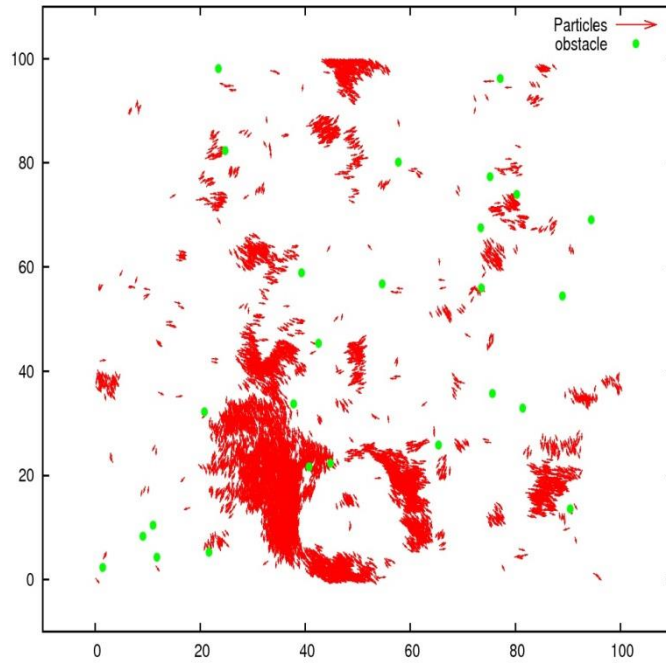
**Figure 6.6** Group formation in the system at noise  $\eta = 0.03$

The noise was increased from 0.01 to 0.03 and its effect is shown in figure 6.6. It can be clearly seen that bands were formed and some individual movement appeared in the particles. Most of the time they remained connected with each other in the form of groups. Band formation occurred when the particles were distant from the obstacles. The particles scattered when they came near to the obstacles. The value of the order parameter was equal to 0.45, which is smaller than in the previous case of noise. This value of the order parameter suggested that with increasing noise there was a decline in the value of the order parameter. It was also observed that at the last time step each group moved a different direction.



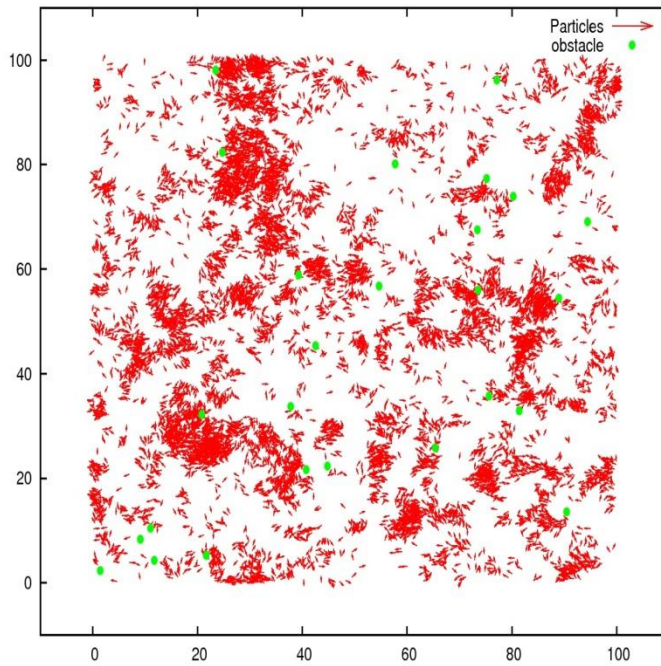
**Figure 6.7** Collective motion of the particles at noise  $\eta = 0.06$

Noise was further increased to 0.06 and the effect is shown in figure 6.7. Due to this noise value, the particles exhibited a fascinating behaviour. The value of the order parameter at the last time step was equal to 0.82. This value of the order parameter suggested that there was higher collective motion than in the previous two cases. With increasing noise there was increasing collective motion in the system. This did not happen in the homogeneous systems because there was a continuous decline in the value of the order parameter with increasing noise. The behaviour shown by the particles was due to the random distribution of the obstacles.



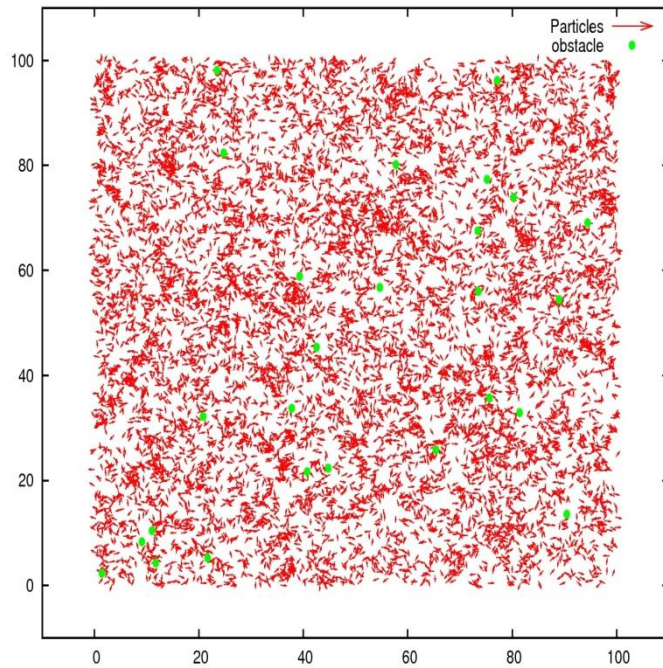
**Figure 6.8** Collective motion of the particles at noise  $\eta = 0.1$

Figure 6.8 shows that the particles have formed a big group with some particles moving individually. At some initial time steps, the particles had very low collective motion and at a higher time their collective motion was increased. At the last time step the order parameter value was equal to 0.79, which is higher than the results shown in figures 6.5 and 6.6. This value is less than the result given in figure 6.7. From the above four results it was observed that at  $\eta = 0.06$  the collective motion was higher. Hence, there was an optimal noise which maximised the collective motion of the self-propelled particles.



**Figure 6.9** Decline in the collective motion of the particles at noise  $\eta = 0.3$

The impact of higher noise  $\eta = 0.3$  is demonstrated in figure 6.9 and it can be seen that the particles are scattered. The system showed little collective motion and little alignment and group formation. The order parameter value was equal to 0.2. This order parameter value suggested that there was less collective motion. This value was less than the previous values of the order parameters obtained in figures 6.4 to 6.8. Due to this noise value ( $\eta = 0.3$ ), their interaction was also distributed between the obstacles. The particles faced greater disturbance from the noise in the system.



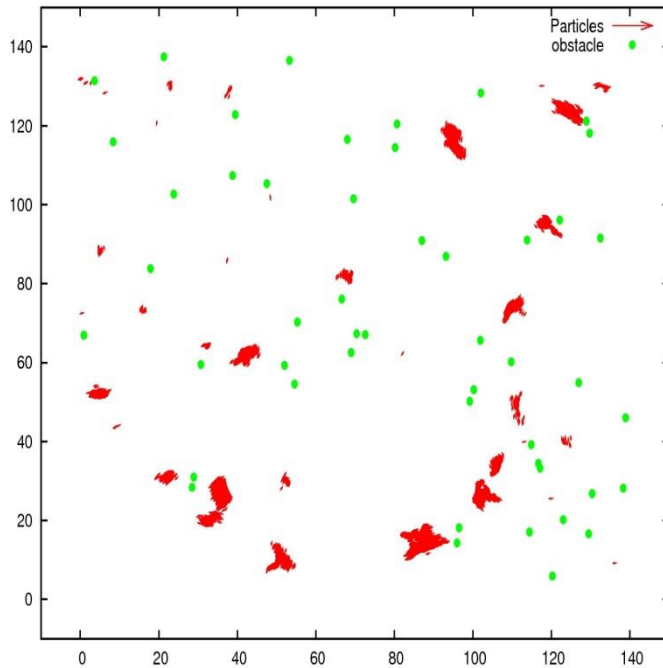
**Figure 6.10** Randomness in the direction of the particles at noise  $\eta = 0.6$

Figure 6.10 shows that the system is completely disordered and the self-propelled particles are completely scattered. This behaviour of the particles was due to the larger value of the noise ( $\eta = 0.6$ ). The particles took random directions with no group formation occurring in the system. The value of the order parameter was equal to 0.01, suggesting that there was disorder in the self-propelled particles model. The particles showed that the collective behaviour at each time step was approximately equal to zero. In this result, the order parameter has the lowest value compared to the other results shown in figures 6.4 to 6.9. The effect of noise was so high that the particles could not move or recognise the obstacles in the system. By providing further higher noise value, the particles showed similar behaviour of disorder and the motion of the particles froze.

### 6.4.2 Simulation results for 19600 particles

The simulation study results are described for 19600 particles and 49 obstacles in this section. The box length was equal to 140, the density of the particles was equal to 1, and the density of the obstacles was 0.0025. The number of the particles and obstacles were increased to test the model in larger system sizes using the same noise values as those in figures 6.4 to 6.10. In this section the results were also compared with the results in the study carried out in reference [115].

In the first case, the noise was  $\eta = 0.01$  and it was observed that at this lower noise level the particles formed groups with a strong coordination in the particles, as shown in the figure 6.11. The parameter values were: box length  $L = 140$ , time  $t = 10000$ , particles  $N_b = 19600$ , obstacles  $N_o = 49$ , interaction radius  $r = 1$ , avoidance radius  $R_o = 1$ , speed  $v_o = 1$ , particle's turning speed  $\gamma_o = 1$ , and time interval  $\Delta t = 0.1$ .



**Figure 6.11** Collective motion of the particles in groups at noise amplitude  $\eta = 0.01$

The particles exhibited a clustered phase as a result of the smaller noise value applied in this model. This result is shown in figure 6.11 and it can be clearly seen that most of the group formed by the particles occurred when they were distant from the obstacles. This type of behavior was also shown by the model when there were 10000 particles (figure 6.4). For closer obstacles, their collective motion was disturbed. The order parameter value at the 10000th time step was equal to 0.65, which was higher than for 10000 particles.

In figure 3.3 (left), Chepizhko *et al.* [115] used the same values for parameters and found that clusters were formed and the collective motion value was 0.58. In figure 6.11, the simulation result showed a similar behaviour of cluster formation. Furthermore, the value of the collective motion was  $w=0.65$ . This indicated that in the developed model (OAM), collective motion was higher.

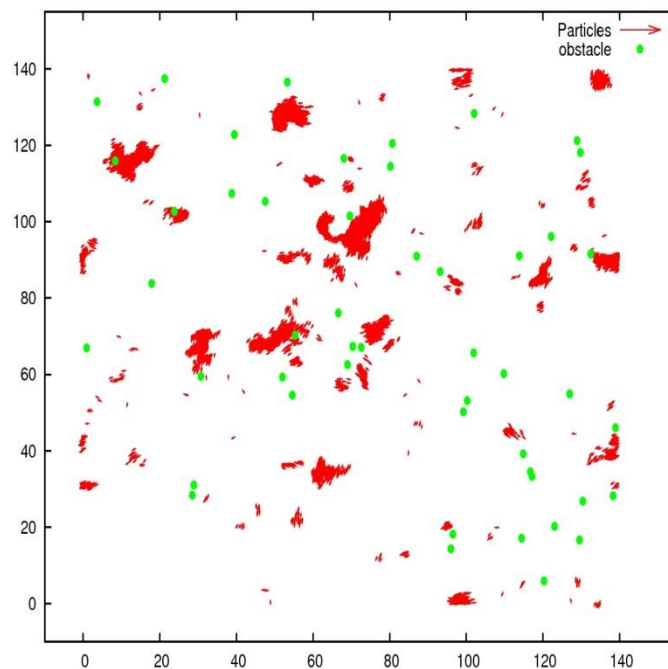


**Figure 6.12** Group for motion in the system by the particles at  $\eta = 0.03$

Figure 6.12 shows the impact of the noise at  $\eta = 0.03$  on the collective motion of self-propelled particles. There was evidently group formation in the system when the value

of the order parameter was equal to 0.84. It was also noticed that some smaller groups were formed by these particles which were greater than in the previous case where noise was 0.01 (figure 6.11). Comparing this result with the previous result at  $\eta = 0.01$  indicated a higher collective motion despite the increased noise. This result suggested optimality in the system. Furthermore, the order parameter was higher than that shown in figure 6.6 where it was equal to 0.45.

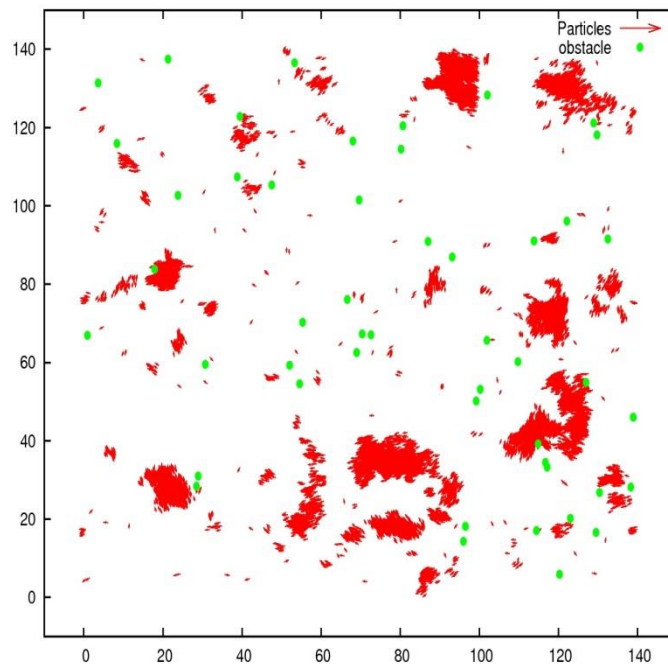


**Figure 6.13** Collective motion of the particles at  $\eta = 0.06$

The noise was further increased to 0.06 and the effect is demonstrated in figure 6.13 with the particles being more scattered. They showed greater disturbances in direction and lower alignment compared to those shown in the previous figure (6.12). However, the particles had more collective motion than in the result shown in figure 6.11 due to the value of the order parameter which was 0.66. Furthermore, the same noise value was applied for 10000 particles (figure 6.7). It was observed that the value of collective motion for 10000 particles was higher than in the case in which 19600 particles were used. This decline in the collective motion was due to the presence of 49 obstacles. This showed that

there was no consistency in the collective motion of the particles because of the random distribution of the obstacles.

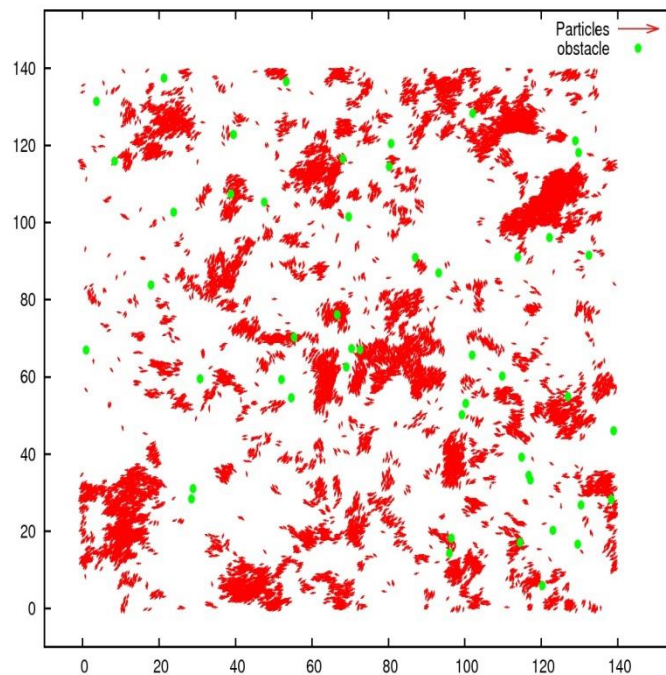


**Figure 6.14** Higher alignment in the direction of the particles at  $\eta = 0.1$

In figure 6.14 the effect for  $\eta = 0.1$  is demonstrated at the 10000<sup>th</sup> time step. It was observed from this result that the particles were scattered. The value of the order parameter was equal to 0.85 which suggested that there was alignment in the direction of the particles. From this result it was evident that due to the increased value of noise ( $\eta = 0.1$ ) there was a rise in the collective motion of the particles with the value of the order parameter being higher than in all the previous cases (figures 6.11 to 6.13). Hence, there existed an optimal noise value which maximised the collective motion.

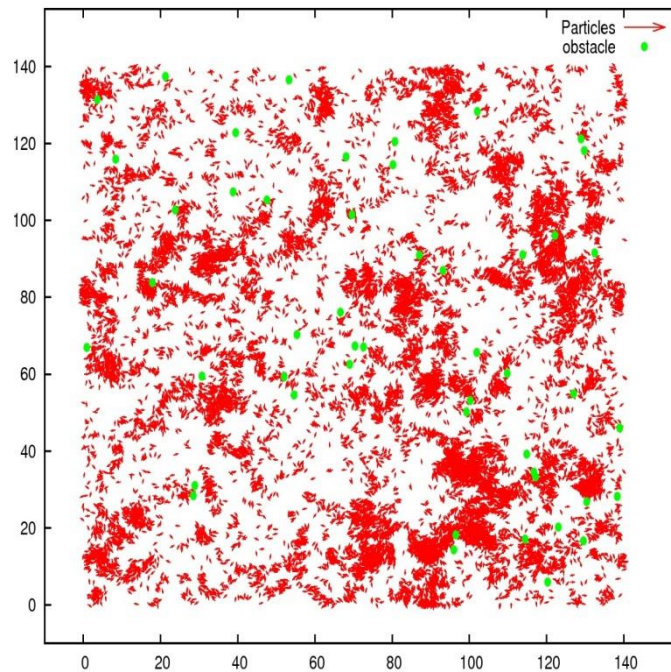


**Figure 6.15** Decline in the collective motion of the particles at  $\eta = 0.3$

There was a decline in the collective motion of the self-propelled particles due to a higher noise value  $\eta = 0.3$ . Figure 6.15 shows the particles had more disturbance in their directions. The value of the order parameter at the 10000<sup>th</sup> time step was equal to 0.25. This suggested a decline in the collective motion of the particles. This was the lowest value of the order parameter (figures 6.11 to 6.14). Furthermore, by comparing this result with the result given in figure 6.9, where same value for noise was used but there were 10000 particles, it showed that the particles have similar behaviour.

In figure 3.3 (centre), Chepizhko *et al.* [115] demonstrated the effect of the same noise value ( $\eta = 0.3$ ) when keeping the other parameters the same as in figure 6.15. Despite a higher noise level, there was very little impact on the value of the order parameter. The value of the order parameter was equal to 0.97, which suggested higher collective motion. This value was much higher, whereas in our case, the value of the order parameter was 0.25 which was very low. There is a known fact that there should be a decrease in the

collective motion of the particles when there is strong noise in the system; this happened in the developed model (OAM) because here, the order parameter had a lower value than in the previous case.

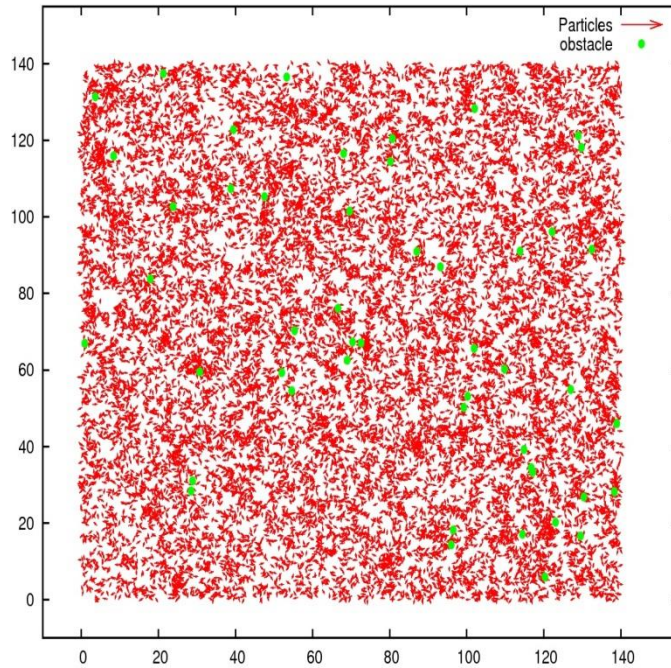


**Figure 6.16** Disordered motion of the particles at  $\eta = 0.6$

There was a further increase in the value of the noise amplitude,  $\eta = 0.6$ , and its impact on the system can be seen in figure 6.16. The value of the order parameter was equal to 0.02 which suggested that the system was completely disordered and there was no collective motion. The particles could not move properly and their directions were highly disturbed; they did not align in similar directions. If we compare this result with other results shown in figures 6.11 - 6.15, it can be observed that the system had no collective motion. The behaviour of the system for each time step can be seen in the figure 6.22, where the order parameter was plotted against each time step. Furthermore, if the higher noise ( $\eta > 0.6$ ) was applied to the system, it would show similar behaviour.

In figure 3.3 (right), Chepizhko *et al.*[115] showed results for  $\eta = 0.6$ . The system exhibited band phase. The particles moved in different directions. The value of the order

parameter was 0.73, whereas in the developed model order the parameter had a value 0.02. This shows that the proposed model (OAM) had less collective motion for  $\eta = 0.6$ . In the model developed, it was observed that the particles had a loss of cohesion where there was higher noise ( $\eta = 0.6$ ).

### **6.4.3 Comparison of 1000 and 10000 particles**

Figures 6.3-6.10 show simulation results for 10000 particles with 26 obstacles, whereas in figures 6.11-6.16, the simulation results were given for 19600 particles with 49 obstacles. A similar kind of behaviour was observed up to a noise value of 0.1. With lower noise in the system, the particles formed bands and moved in a group, whereas in the case of higher noise they had a disordered motion. This can be seen in the cases of  $\eta = 0.01$  and  $\eta = 0.6$ , where the collective motion of the particles was increased when  $\eta$  varied from 0.01 to 0.1. This behaviour suggested that there was an optimal noise level which maximised the collective motion. In the case of 10000 particles, optimal noise was at  $\eta = 0.06$ , whereas for 19600 particles, optimal noise was at  $\eta = 0.1$ , since the order parameter had a higher value at these noise values. This behaviour was due to the random distribution of the obstacles in the system. At  $\eta = 0.3$  the particles showed less collective motion in both cases, whereas at  $\eta = 0.6$  the system was in a state of complete disorder. This suggested that a higher noise system results in a state of disorder.

#### 6.4.4 Collective motion as a function of time

The collective motion was plotted as a function of time for different noise values, such as  $\eta = 0.01, 0.03, 0.06, 0.1, 0.3,$  and  $0.6$ . The simulation ranged from zero time steps to 10000 time steps. Time played an important role in the collective motion of the self-propelled particles. With increasing time, their coordination with each other started increasing and the particles reacted in a better way to the situations than when lower noise was applied to the system.

The parameters values used were: box length  $L = 140$ , time  $t = 10000$ , particles  $N_b = 19600$ , obstacles  $N_o = 49$ , interaction radius  $r = 1$ , avoidance radius  $R_o = 1$ , speed  $v_o = 1$ , particle's turning speed  $\gamma_o = 1$  and the time interval was  $\Delta t = 0.1$ .

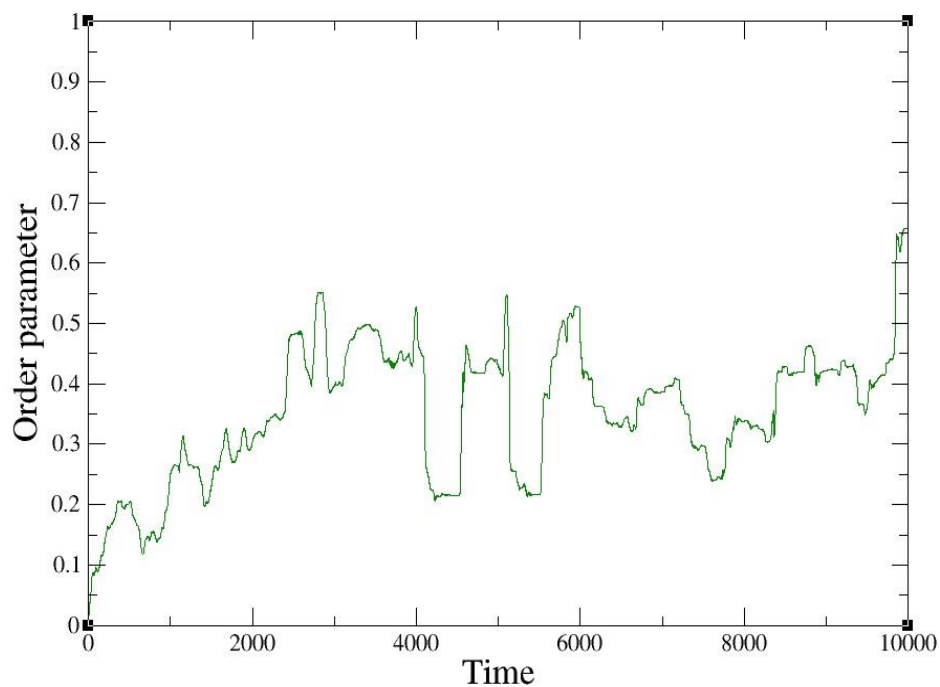


**Figure 6.17** Collective motion as a function of time at  $\eta = 0.01$

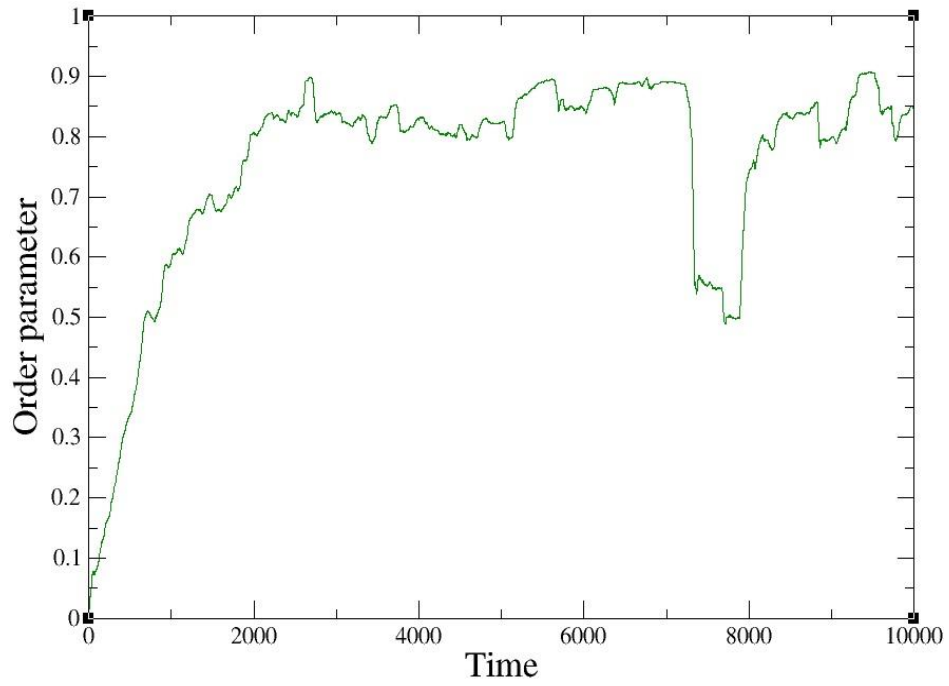


**Figure 6.18** Collective motion as a function of time at  $\eta = 0.03$

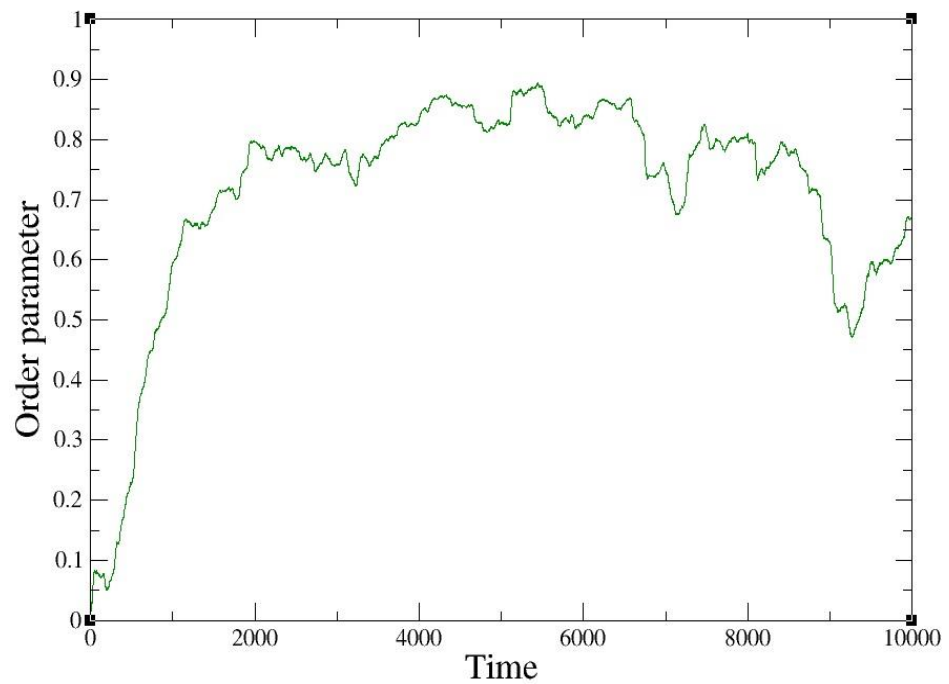


**Figure 6.19** Collective motion as a function of time at  $\eta = 0.06$

In figures 6.17 to 6.19, the impact of the lower noise is demonstrated. It can be seen that for  $\eta=0.01$  at the initial time the value of the order parameter was 0.009, which suggested that the particles were in a state of disorder since there was no collective motion. With increasing time, the collective motion also increased. This growth in the

value of collective motion continued up to  $t = 521$  where the order parameter had a value of 0.20. Subsequently, there appeared to be a decline in the order parameter but it again rose at  $t = 2855$  since the order parameter value at this point was 0.55. After this time step, the collective motion again decreased and then increased. This fluctuating behaviour continued up to the final time step ( $t = 10000$ ), at this point the order parameter was equal to 0.65.

Due to the random distribution of the particles, fluctuations appeared in the system. For  $\eta = 0.03$  the result was different to that in the previous case of noise (figure 6.18), since most of the time the collective motion of the particles remained higher. There appeared to be a decline in the collective motion which started from  $t = 7102$ , where the order parameter was 0.89 and went to  $t = 7711$  where the order parameter was 0.49. Subsequently, the collective motion again grew but with smaller fluctuations. This fluctuating behaviour continued to the final time step of  $t = 10000$ , with the value of the order parameter was 0.84, which suggested that there was alignment in the direction of the particles. For  $\eta = 0.06$ , the curve also showed fluctuations (figure 6.19). With the increasing time there was an increase in the value of the order parameter and most of the time the collective motion of the particles remained higher in the system. At  $t = 2000$ , the order parameter had a higher value than the result in figure 6.17. Furthermore, at  $t = 10000$ , the value of the order parameter was equal to 0.66, which was higher than the results for  $\eta = 0.01$  and lower than in the case of  $\eta = 0.03$ .

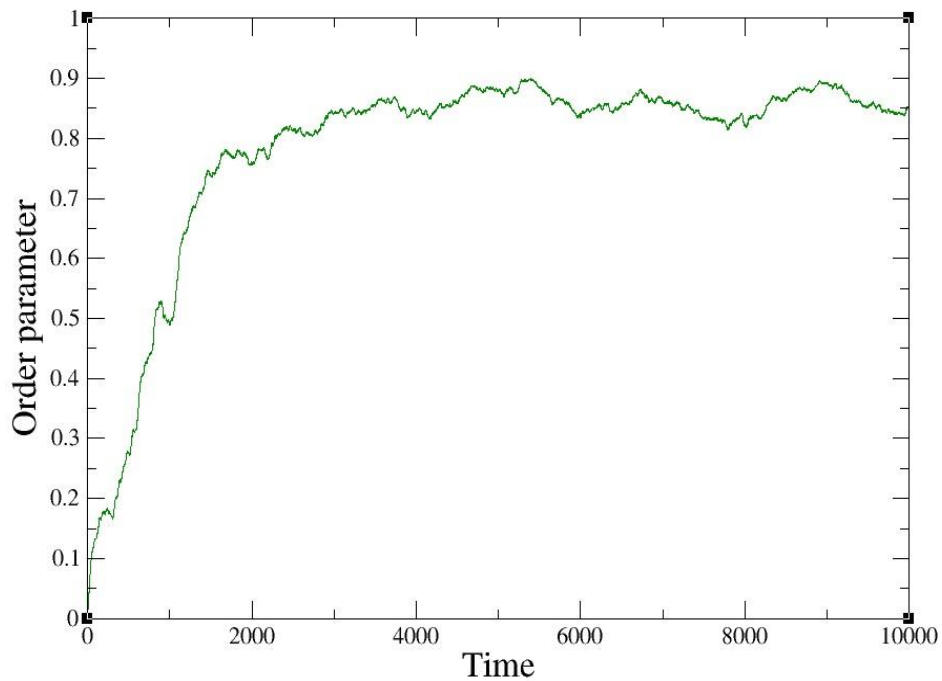


**Figure 6.20** Collective motion as a function of time at  $\eta = 0.1$

Figure 6.20 plots the order parameter at each time step for  $\eta = 0.1$ . At the initial time step the order parameter had the smallest value, which was equal to 0.008. Subsequently, the value of the order parameter increased with some fluctuations. These fluctuations were smaller than in the three previous noise cases (figures 6.17-6.19). Most of the time value of the order parameter remained higher in the system suggesting that there was higher alignment in the direction of the particles. At the final time step the value of the order parameter was 0.85. This value was greater than in all the other cases of noise.

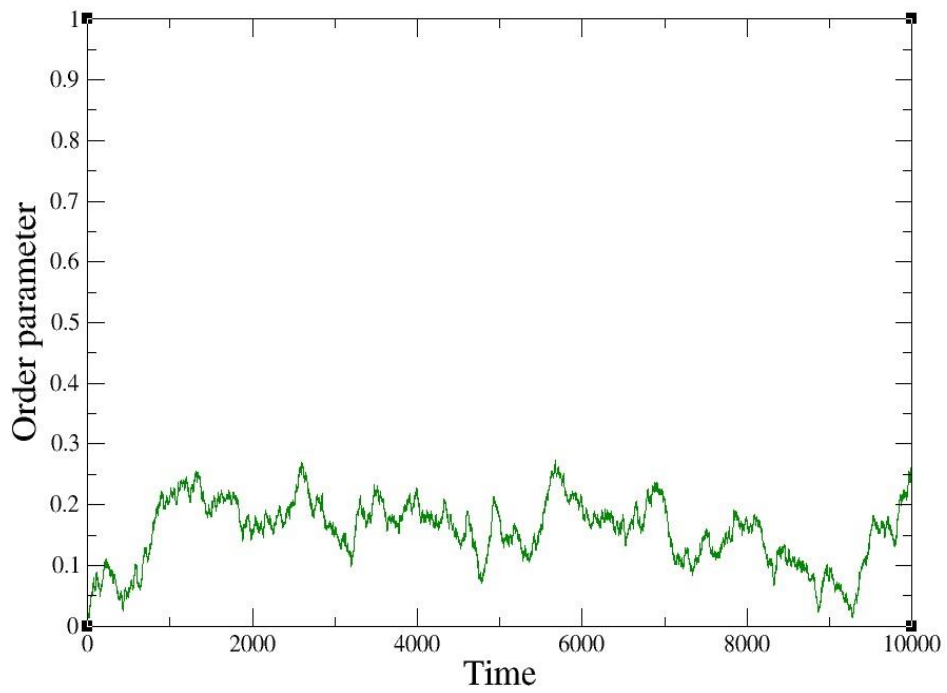


**Figure 6.21** Collective motion as a function of time at  $\eta = 0.3$

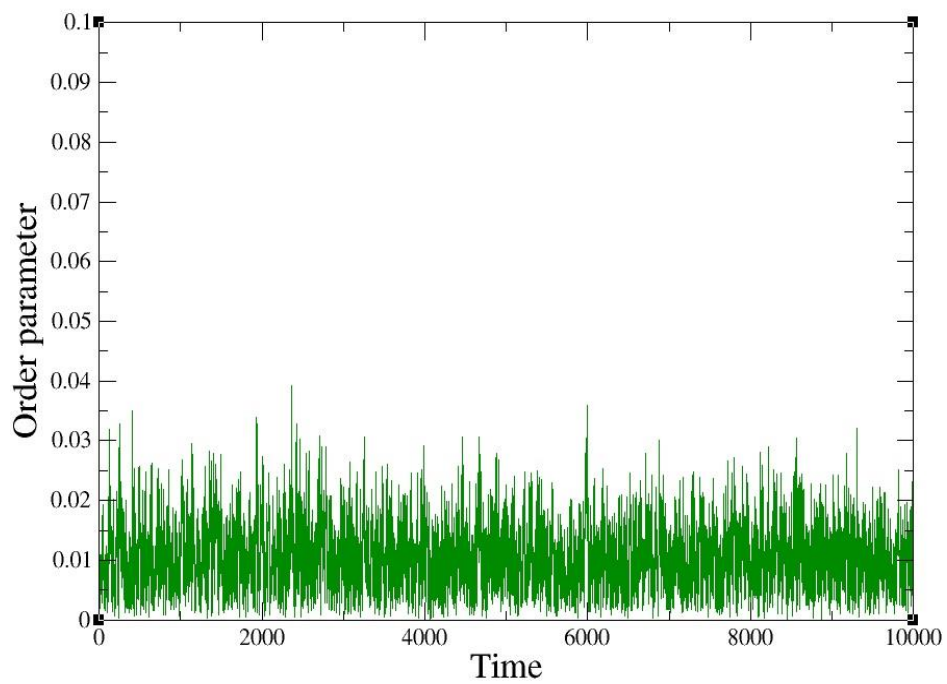


**Figure 6.22** Collective motion as a function of time at  $\eta = 0.6$

The effect of higher noise is exhibited in figures 6.21 to 6.22. It can be clearly seen that for  $\eta = 0.3$  the system showed a decline in the collective motion compared to the case in which  $\eta = 0.1$ . In figure 6.21, it was shown that most of the time collective motion did

not rise to a higher level as in the previous cases of noise, since the value of the collective motion remained lower than 0.3. At the final time step the value of the order parameter was equal to 0.25. This indicated that collective motion existed, but it did not exist at a high level in the system.

The impact of higher noise ( $\eta = 0.6$ ) is demonstrated in figure 6.22. Due to this noise value there was a lot of disturbance in the motion of the particles. The value of the order parameter was approximately zero at all time steps. The effect of this noise value was so high that the particles could not move properly in the system. This result showed that if stronger noise value was used then there would be similar behaviour, and the particles would show a state of disorder in the system. The value of the order parameter at the final time step was 0.01. This value was the smallest value compared to in the previous cases of noise.

#### **6.4.5 Effect of the interaction radius**

The interaction radius is the distance at which particles contact each other. Each particle had the same interaction radius and the effect of the interaction radius was investigated for  $N_b = 1000$  and  $10000$ . The main reason for doing this was to see how the particles behaved when they were in large numbers. Figure 6.23 shows collective motion as a function of the interaction radius with the obstacle density,  $\rho_o = 0$  (circles) and  $\rho_o = 0.0125$  (triangles).

The parameters used were: box length  $L = 40$ , time  $t = 2000$ , obstacles  $N_o = 20$ , interaction radius  $r = 1$ , avoidance radius  $R_o = 1$ , speed  $v_o = 1$ , particle's turning speed  $\gamma_o = 10$ , time interval  $\Delta t = 0.1$ , noise  $\eta = 0.0$ .

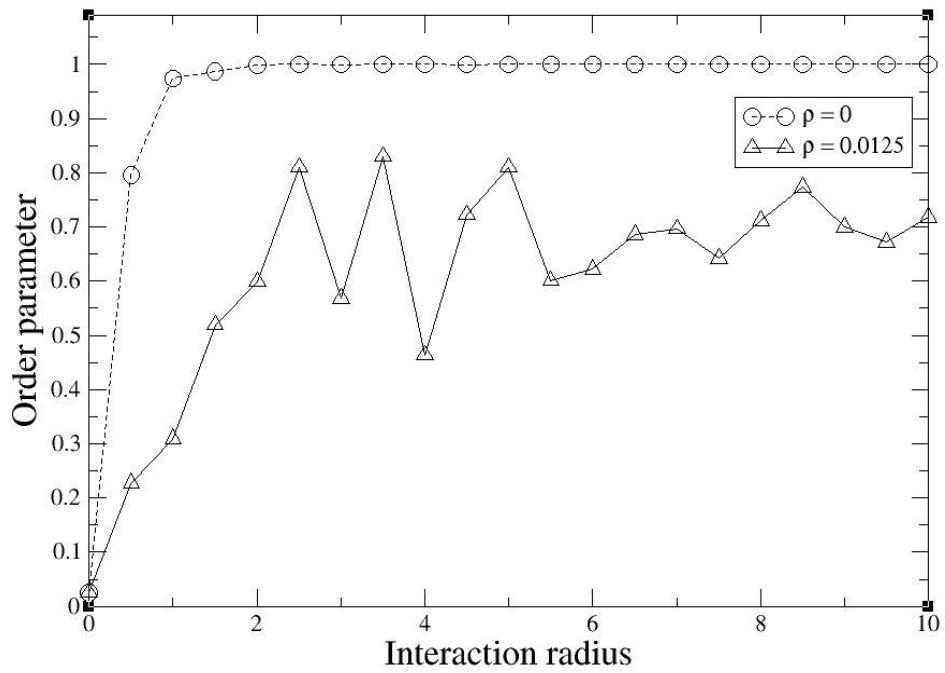


**Figure 6.23** Collective motion as a function of the interaction radius  $r$  for  $N_b = 1000$

The interaction radius was varied from 0 to 10 at an interval of 0.5. It was observed that the particles showed higher coordination with each other when the radius increased. The coordination among the particles made the system stable. For  $\rho_o = 0$ , at the value of  $r$  equal to zero, the system was in a completely disordered state; there was no emergence of the collective motion of the particles in the system. Increasing the radius of the particles made the system more consistent because the particles moved collectively with proper coordination without any hindrance. From  $r = 2$ , the order parameter gained a very consistent value which was equal to 0.99; this value is the evidence of the stable system. In the presence of obstacles, at  $\rho_o = 0.0125$ , the collective motion was smaller than in the previous case of  $\rho_o = 0$ . Despite the obstacle's existence, the particles showed collective motion and it never dropped to zero. The fluctuation of the collective motion as a function of the interaction radius was due to the number of the particles used in the calculation being not so large. In the following results, a large number of particles was used for the purpose of investigating the effect on the system.

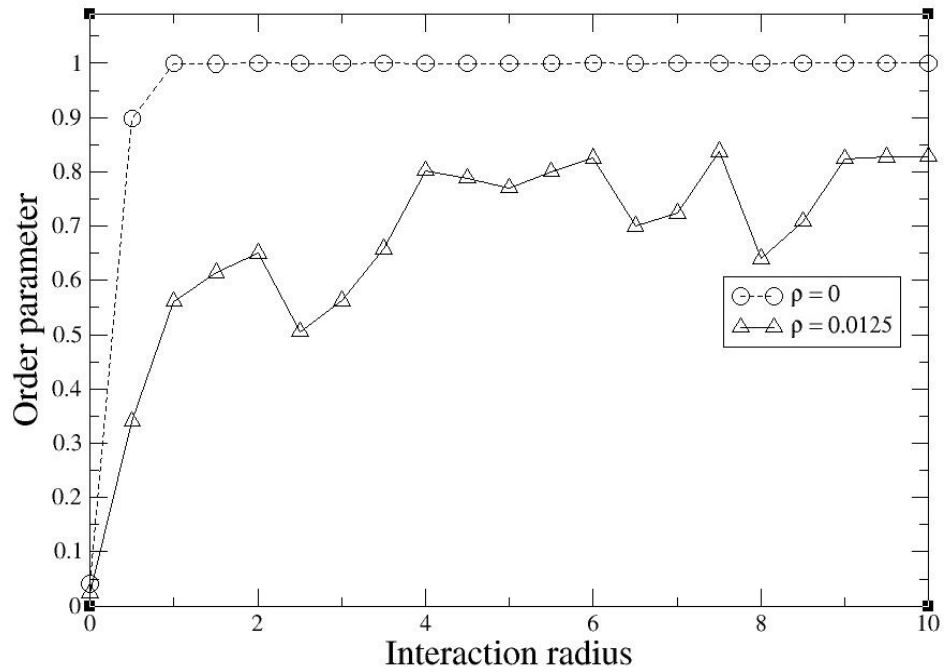


**Figure 6.24** Collective motion as function of  $r$  for  $N_b = 10000$

In figure 6.24, the effect of the interaction radius is demonstrated for 10000 particles. For  $\rho_o = 0$ , there was consistency in the collective motion of the self-propelled particles. The smooth curve showed that there was higher alignment in the direction of the particles, which exhibited similar behaviour as they showed for  $\rho_o = 0$  in figure 6.23. At  $\rho_o = 0.0125$ , it can be observed that there was no consistency in the collective motion of the particles. There appeared to be fluctuations in the curve. This was due to the random distribution of the obstacles in the system. It can be clearly seen that, at the same obstacle density in the case of 1000 particles, the system showed fluctuations (see figure 6.23). So it can be said that if we use more particles in the system then there will be similar behaviour by the particles.

### 6.4.6 Effect of noise

Noise effect was investigated for both homogeneous and heterogeneous systems. The order parameter ( $w$ ) was plotted against noise values in the homogeneous medium where the obstacle density was  $\rho_o = 0$  and in the heterogeneous medium where the obstacle density was  $\rho_o = 0.0125$ . The noise value was chosen from the range  $[-\pi, \pi]$  by using uniform probability distribution.

The parameter values used were: box length  $L = 40$ , time  $t = 2000$ , particles  $N_b = 1000$ , obstacles  $N_o = 20$ , interaction radius  $r = 1$ , avoidance radius  $R_o = 1$ , speed  $v_o = 1$ , particle's turning speed  $\gamma_o = 10$ , and time interval  $\Delta t = 0.1$ .

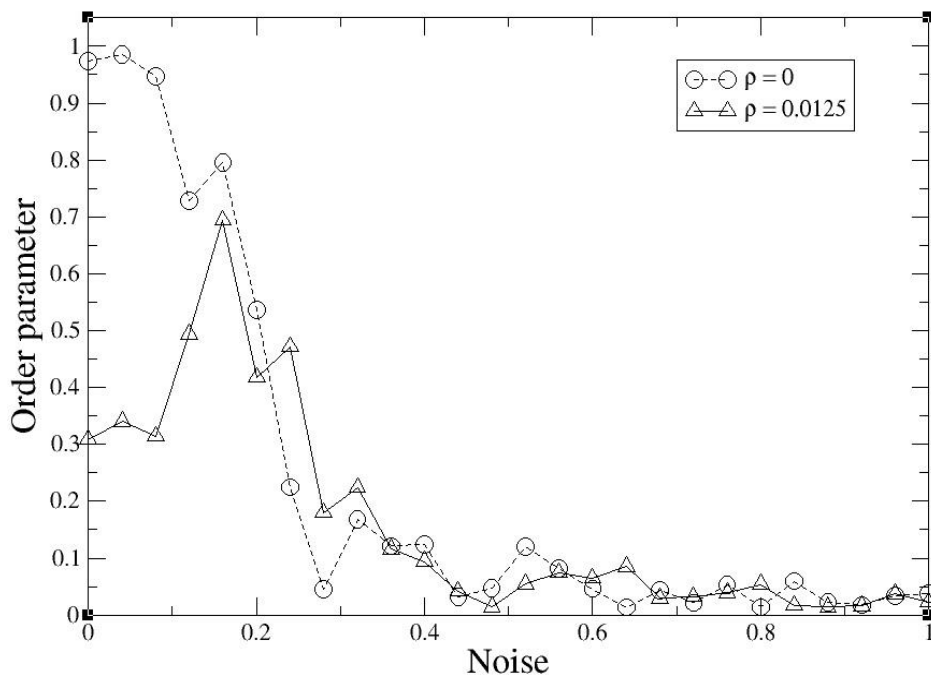


**Figure 6.25** Collective motion as a function of the noise for two values of obstacle density,  $\rho_o = 0$  and  $\rho_o = 0.0125$

Figure 6.25 shows the effect of noise on the collective motion of the self-propelled particles. Noise was varied from 0 to 1 with an interval length of 0.04. In the first case, where  $\rho_o = 0$  (circles line), there appeared to be randomness in the system with the higher

values of the noise order parameter  $w$  reaching zero. At lower noise values the system was in a state of order because the collective motion had a value near to 1. With the increasing noise, the system showed a disordered phase. At a noise level of 0.48, collective motion approached zero.

For  $\rho_o = 0.0125$  (triangle line), at noise value 0.16, the order parameter reached a maximum. At a starting value of noise such as  $\eta = 0$  the collective motion had a smaller value than at  $\eta = 0.16$ . Due to the random distribution of the obstacles, there existed an optimal noise level which maximised the collective motion of the self-propelled particles. Such type of behaviour did not exist in the homogeneous medium. It was also observed that with the increase in the noise, there was a decrease in the order parameter. The system was in a complete state of disorder when the noise was larger than 0.4.

#### **6.4.7. Effect of the speed**

In the model each particle carried a constant speed ( $v_o$ ). The speed parameter had a significant effect on the collective behaviour of the particles. Figure 6.26 demonstrates the collective motion as a function of speed for obstacle density,  $\rho_o = 0$  (circles) and  $\rho_o = 0.0125$  (triangles).

The parameter values used were: box length  $L = 40$ , time  $t = 2000$ , particles  $N_b = 1000$ , obstacles  $N_o = 20$ , interaction radius  $r = 1$ , avoidance radius  $R_o = 1$ , noise amplitude  $\eta = 0.0$ , particle's turning speed  $\gamma_o = 10$ , and time interval  $\Delta t = 0.1$ .

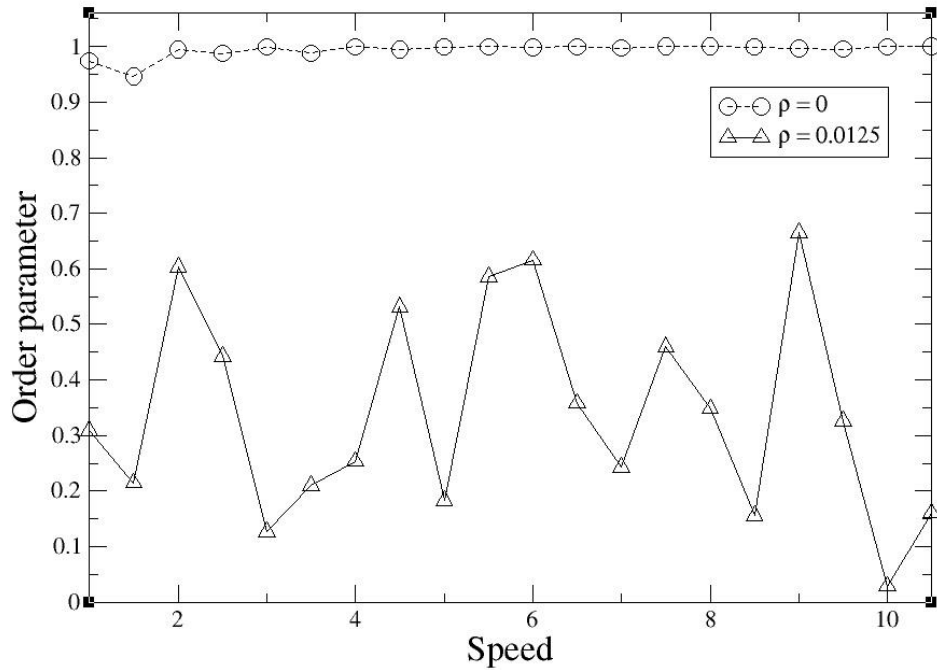


**Figure 6.26** Collective motion as a function of the speed for obstacle density, for  $\rho_o = 0$  and  $\rho_o = 0.0125$  (20 obstacles)

Figure 6.26 shows a smooth curve for zero obstacle density  $\rho_o = 0$  (circles). At the initial value of  $v_o$ , the system showed some fluctuations; from  $v_o = 3$  the collective motion had a consistent value which remained near to 1. By increasing the speed, the system showed the long range order and particles gained more coordination quickly and as a result the system became stable. There was no hindrance to the movement of the particles because there was no obstacle present in the system. In the absence of both noise and obstacles, the particles moved freely and they showed an ordered phase. In the case of  $\rho_o = 0.0125$ , the order parameter showed a non-monotonic behaviour because large fluctuations appeared due to the obstacles being randomly distributed. The collective motion of the self-propelled particles was widely distributed and the system was in a completely disordered state.

As the system consists of self-propelled particles where each particle assumes the average direction of the neighbouring particles along with some random perturbation, due to the self-propelling nature of the particles, alignment in the system takes place. Increasing the speed of the particles does not affect the stability of the system because of the self-propelling nature of the particles where the system can be only disturbed when higher noise is applied. The increasing velocity of the particles makes the system more stable by making the higher number of particles come closer to the interaction radius of each other. There is no repelling force provided to the particles; they can only be aligned and pursue the same direction when they are within the interaction range of each other; therefore, increasing velocity makes the system more stable. The particles gained coordination more quickly. There is also an absence of obstacles which also helps the particles in their free movement in the system

Peruani and Morelli [126] studied self-propelled particles in the context of fluctuating speed and the direction of the particles. They studied the case in which fluctuations in the speed are not correlated to the direction of the particles.

#### **6.4.8 Order of phase transition**

In this section the order of phase transition is investigated. The probability density function was plotted against the order parameter ( $w$ ) for different noise values with a higher number of particles used. If the curve has one hump then it is known as the second order phase transition; if the curve has more than one hump then it is known as the first order phase transition [5]. Here, the time for simulation started from 0 to 10000 particles. The noise parameter was varied while all other parameters were kept constant. These are defined as:

Box length  $L=140$ , time  $t=10000$ , particles  $N_b=19600$ , obstacles  $N_o=49$ , interaction radius  $r=1$ , avoidance radius  $R_o=1$ , speed  $v_o=1$ , particle's turning speed  $\gamma_o=1$ , time interval  $\Delta t=0.1$ .

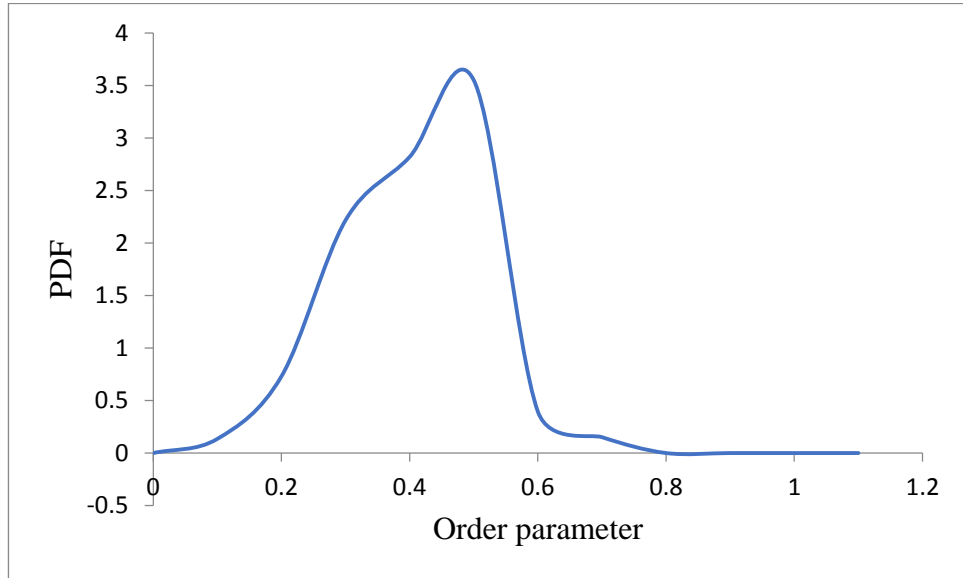


**Figure 6.27** Second order phase transition at  $\eta=0.01$

In Figure 6.27, the second order phase transition was demonstrated for  $\eta=0.01$ . The curve showed one big hump and the lower noise created a group formation. Due to the obstacles there was disturbance in the direction of the particles. At  $w=0.1$ , the PDF had a value of 0.135, which gradually increased and it rose to a maximum of  $w=0.5$ . At this point, the PDF was equal to 3.551. At a value of order parameter 0.5, the curve reached its highest value. On the left side of this there is a decline in the PDF, whereas on the right side there is a continuous decrease in the value of the PDF. This behaviour suggests continuous phase transition in the system.

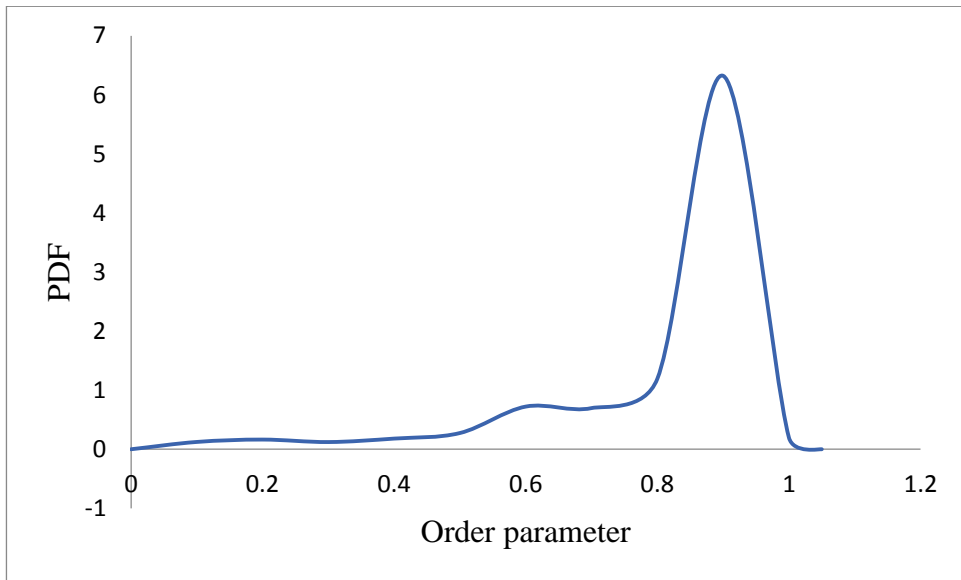


**Figure 6.28** First order phase transition at  $\eta = 0.03$

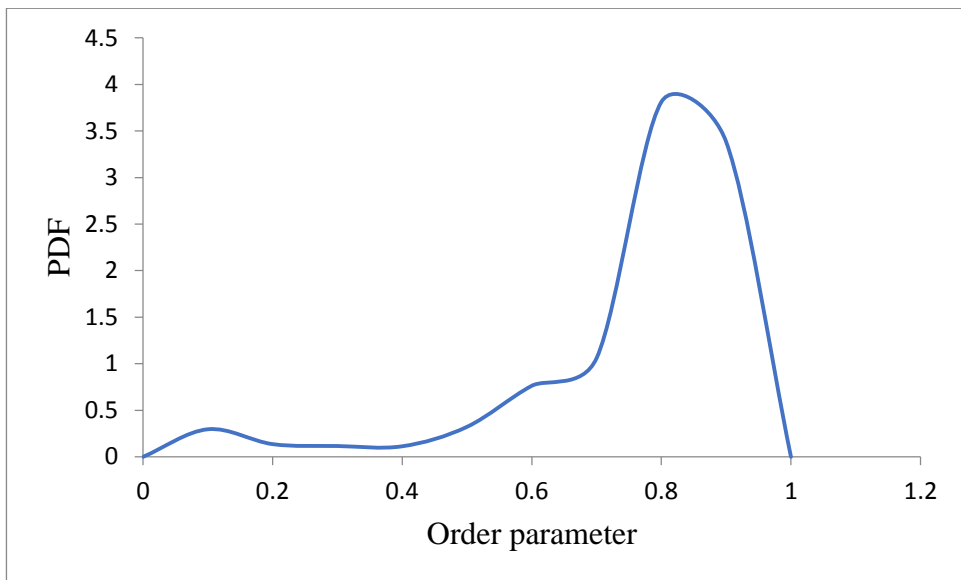


**Figure 6.29** First order phase transition at  $\eta = 0.06$

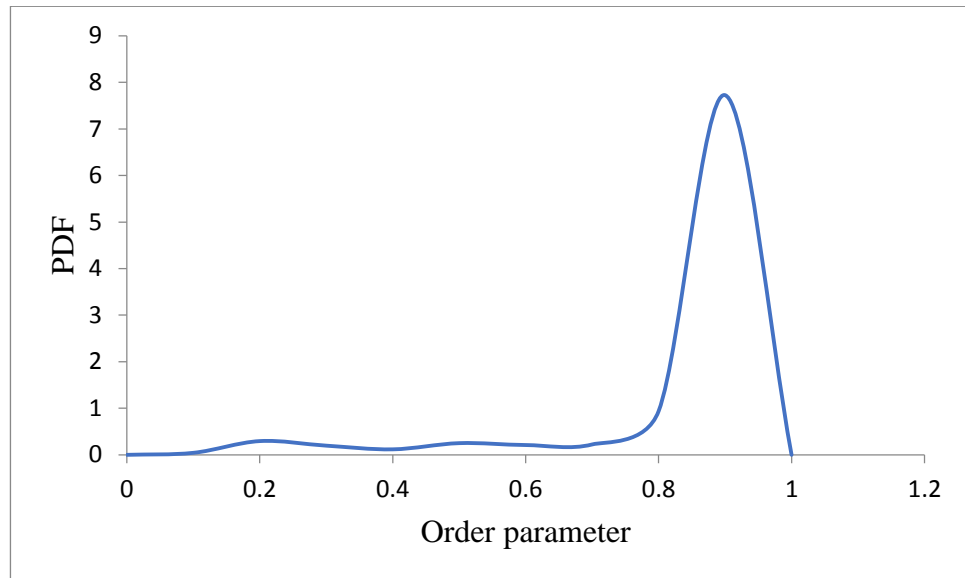


**Figure 6.30** First order phase transition at  $\eta = 0.1$

Figures 6.28-6.30 show a first order phase transition. At a noise level of  $\eta = 0.03$ , the order parameter showed variations because of the random distribution of the obstacles. The curve exhibited two humps, which suggested its first order phase transition nature. From 0.1 the value of the PDF was increasing which was equal to 0.124, but at 0.3 the value of the PDF was equal to 0.122 which showed a decline in the value. Subsequently, the PDF again started increasing but at 0.7 there was again a decline. This behaviour showed that there was no continuity. Similar behaviour was also observed in the case of  $\eta = 0.06$  and 0.1. Figure 6.29 shows that at  $w = 0.1$ , the PDF had a value equal to 0.296. This value decreased continuously and then started increasing from 0.5 and at  $w = 1.0$  it dropped to zero. Figure 6.30 demonstrates the result for the noise at  $\eta = 0.1$ , showing a first order phase transition.

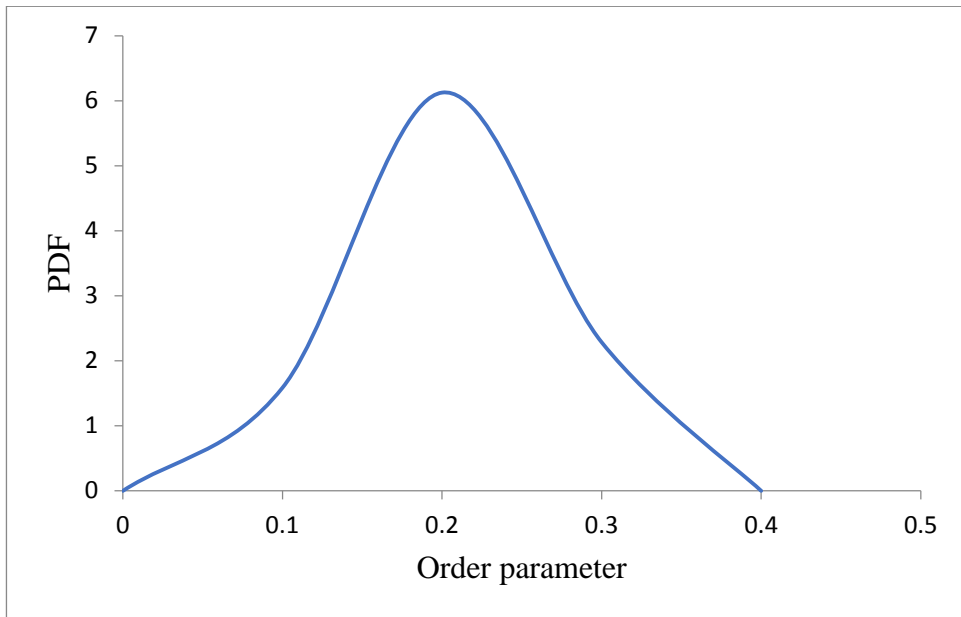


**Figure 6.31** Second order phase transition at  $\eta = 0.3$

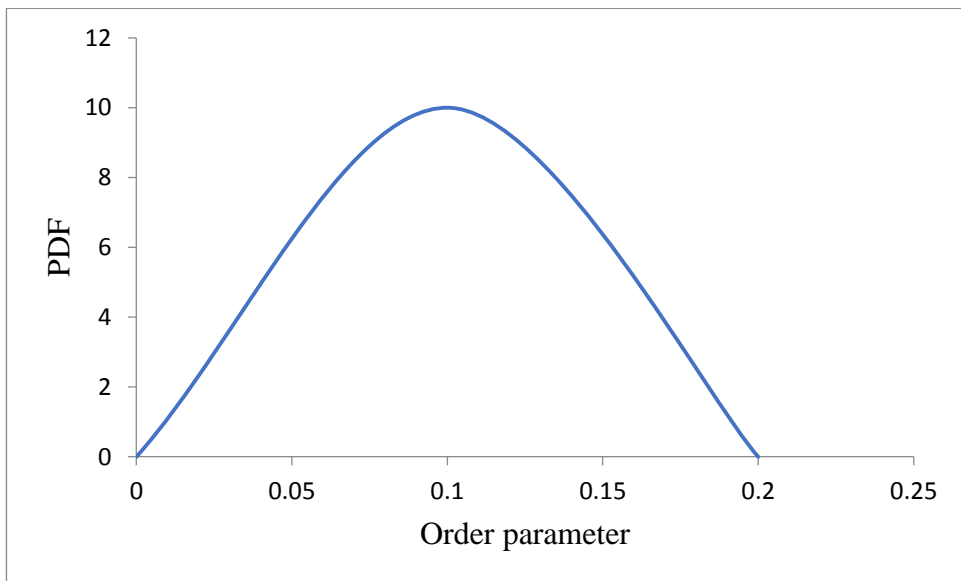


**Figure 6.32** Second order phase transition at  $\eta = 0.6$

The effect of higher noise on the system is demonstrated in figures 6.31-6.32. At noise level  $\eta = 0.3$ , the curve showed only one big hump which suggested a second order phase transition. The curve had the highest value at 0.3 which was equal to 6.127. At  $\eta = 0.6$ , the system had also shown first order phase transition. At this value of noise, the particles

took random directions and they could not move properly. Due to this behaviour the value of the order parameter remained between 0 and 0.1.

## 6.5 Conclusions

The collective behaviour of the self-propelled particles was investigated in both heterogeneous and homogeneous media. Six noise amplitudes were applied to the system. These noise values were used for  $N_b = 10000$ , and  $N_b = 19600$ . The particles exhibited a similar behaviour up to a noise value equal to 0.1. For lower noise  $\eta = 0.01$ , the particles formed bands and they moved in the group. In case of higher noise  $\eta = 0.6$ , the particles showed disordered motion and for  $\eta = 0.01$  to  $\eta = 0.1$  the collective motion of the particles increased despite the increase in the noise. This behaviour suggested that there was an optimal noise level which maximised the collective motion. In the case of 10000 particles, optimal noise was at  $\eta = 0.06$ , whereas in the case of 19600 particles, optimal noise was at  $\eta = 0.1$ . At  $\eta = 0.3$  the particles showed less collective motion in both cases, whereas at  $\eta = 0.6$  the system was completely disordered. This suggested that with higher noise the system achieves a state of disorder. Furthermore, the results were compared with the results of Chepizhko *et al.*[115]. It observed that in this project, for  $\eta = 0.01$ , collective motion was higher than it had been in their work. For  $\eta = 0.3$  and 0.6, collective motion was smaller than in their work. The collective motion of the particles was also plotted against each time step. From the results, fluctuations were observed. There was no consistency in the value of the order parameter. Collective motion was also plotted as a function with three parameters. These parameters were: interaction radius, noise and speed. It was shown that in the homogeneous medium, the order parameter gained a larger value when the values of the interaction radius and speed were increased, whereas in the case of noise there was a decline in the value of the order parameter. In the case of the

heterogeneous medium, large fluctuations took place, even in the case of the interaction radius of the particles. When we increased the number of particles, the system showed similar behaviour in which inconsistency was observed in the value of the order parameter. The fluctuations in the system were due to the random distributions of the obstacles. The order of phase transition was also investigated. For lower noise levels, there existed first order phase transition; for higher noise levels, there was second order phase transition.

## CHAPTER 7

### **Collective Behaviour of Self-Propelled Particles in the Presence of Moving Obstacles**

#### **7.1 Introduction**

The collective behaviour of particles is presented in the presence of moving obstacles in this chapter. Self-propelled particles show important non-equilibrium behaviour and interaction with moving obstacles that has remained the subject of academic debate [126]. The presence of the moving obstacles has a significant impact on the collective motion of the self-propelled particles.

The obstacles were moved in a two-dimensional coordinate system having a square-shaped box  $L \times L$ . Each particle followed the average direction of the particles present in its neighbourhood. There was random perturbation added to their direction. When the particles came close to the obstacles, their collective motion was disturbed and when the obstacles were further away, they again tried to move together. The simulation results are presented for different numbers of particles to investigate their behaviour in the presence of diffusive obstacles.

The effects of noise, avoidance radius and obstacle density on the collective motion of the particles was investigated. The order parameter was plotted against time to see the movement of the particles at each time step. The order of phase transition was also investigated.

**Table 7.1** – Symbols are defined which are used in figure captions

<i>Symbol</i>	<i>Description</i>
$L$	Length of box
$N_b$	Number of particles
$N_o$	Number of obstacles
$t$	Time step
$\eta$	Noise
$R_o$	Interaction radius between the particle and the obstacles (avoidance radius)
$r$	Interaction radius between the particles
$v_o$	Speed for particles
$\gamma_o$	Particle's turning speed when it interacts with obstacle
$\Delta t$	Time interval
$v_y$	Speed for moving obstacles
$w$	Order parameter for measuring collective motion.

## 7.2 Simulation results

First of all, the simulation results are shown for zero time steps to show their movement at the initial stage; later time steps extend to 10000 time steps.

The effect of noise on the system was investigated. The position of the obstacle is defined by Equation 3.15 in chapter 3. The obstacle had a random direction and moved from one point to another point with a time interval of 0.0021.

The parameters used in the results shown in figures 7.1 to 7.8 have the following values: box length  $L = 100$ , particles  $N_b = 10000$ , obstacles  $N_o = 26$ , interaction radius  $r = 1$ ,

avoidance radius  $R_o = 1$ , speed  $v_o = 1$ , particle's turning speed  $\gamma_o = 1$ , time interval  $\Delta t = 0.1$ , speed of obstacle  $v_y = 1$ . The value for time  $t$  and noise amplitude  $\eta$  are defined in the captions of the figures.

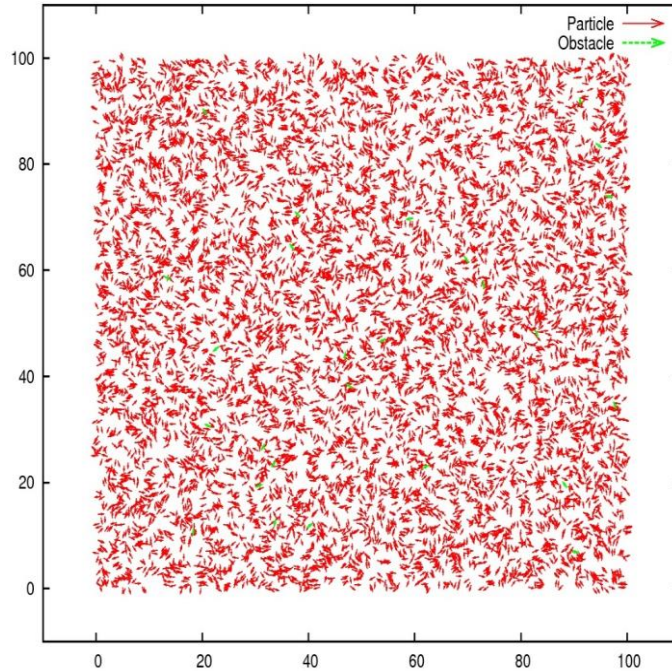


**Figure 7.1** Randomness in the motion of the particles at initial time  $t = 0$  for  $\eta = 0.01$

Figure 7.1 shows the results at the first time step. The red arrows represent the particles and the green arrows represent the obstacles. Particles were scattered across the whole box with each particle having a random direction. The order parameter was approximately equal to zero. There were 26 obstacles introduced into the system with random motion. At the first time step, the particles showed their self-propelling nature. At the second time step, the particles adopted the average direction of their neighbours. Furthermore, they started their interaction with the obstacles. The particles tried to escape from the obstacles when they were within the interaction range of the obstacles. The noise factor also disturbed the collective motion. In weaker noise, the particles exhibited cohesive motion, whereas in stronger noise a loss of cohesion occurred.

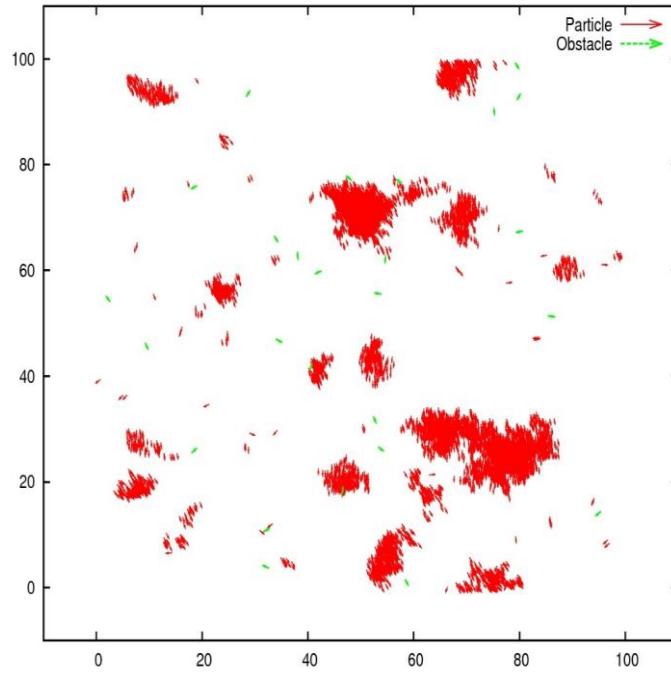


**Figure 7.2** Cluster formation by particles in presence of moving obstacles at  $t = 4000$  for  $\eta = 0.01$

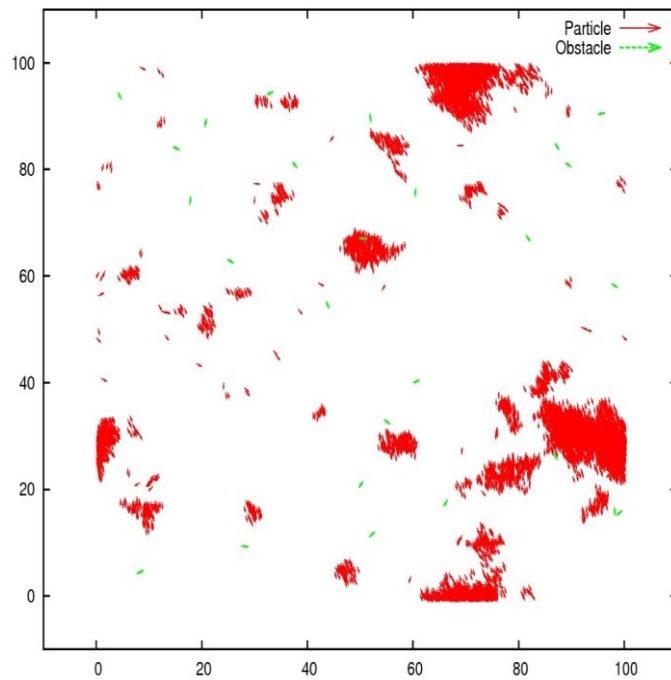


**Figure 7.3** Group formation by the particles at  $t = 7000$  for  $\eta = 0.01$

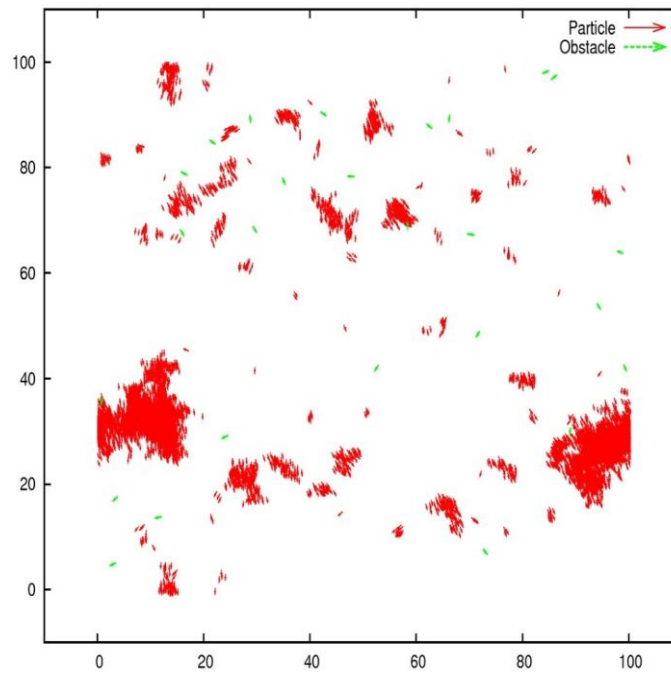


**Figure 7.4** Cohesive behaviour of the particles at  $t = 10000$  for  $\eta = 0.01$

The impact of lower noise is shown in figures 7.2 to 7.4 at various time steps. It can be clearly seen that due to the lower value of noise  $\eta = 0.01$ , there appeared to be cluster formation. Figure 7.2 demonstrates the results for  $t = 4000$ , with movement of the particles becoming groups. Few particles moved individually due to the noise and the random movement, with the order parameter being 0.97. Figure 7.3 shows the results for  $t = 7000$ . There was group formation and also alignment in the direction of the particles. The order parameter had a value of 0.98. Figure 7.4 exhibits the results at  $t = 10000$  showing two large groups being formed, while other groups were smaller and contained fewer particles. In this result, the particles were more scattered than in the previous cases due to the random movement of the obstacles. The order parameter was equal to 0.98, suggesting that the collective motion of the particles was higher. From these results it was observed that the particles exhibited similar behaviour at  $\eta = 0.01$  for higher time steps.

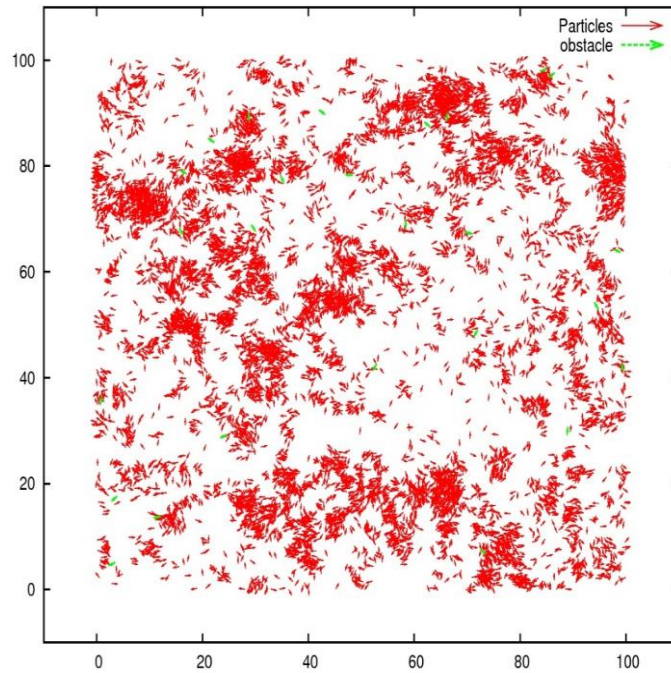


**Figure 7.5** Decline in the collective motion of the particles at  $t = 10000$  and  $\eta = 0.3$

The effect of the increased noise value is shown in figure 7.5 at  $\eta = 0.3$ . Due to this noise value, the motion of the particles was disturbed because there was random motion. The collective motion of the self-propelled particles was 0.27, whereas in the results in figure 7.4, it was equal to 0.98. In figure 7.5, the particles were more scattered than in the result in figure 7.4. These values suggest that noise had a huge impact on the system. The noise parameter had become more dominant than the other parameters; for example the interaction radius was introduced, which was equal to 1. Despite this value, the particles were unable to follow the direction of their neighbours properly, facing difficulty in dealing with the obstacles. This behaviour of the particles remained for all the time steps in the system (figure 7.12).

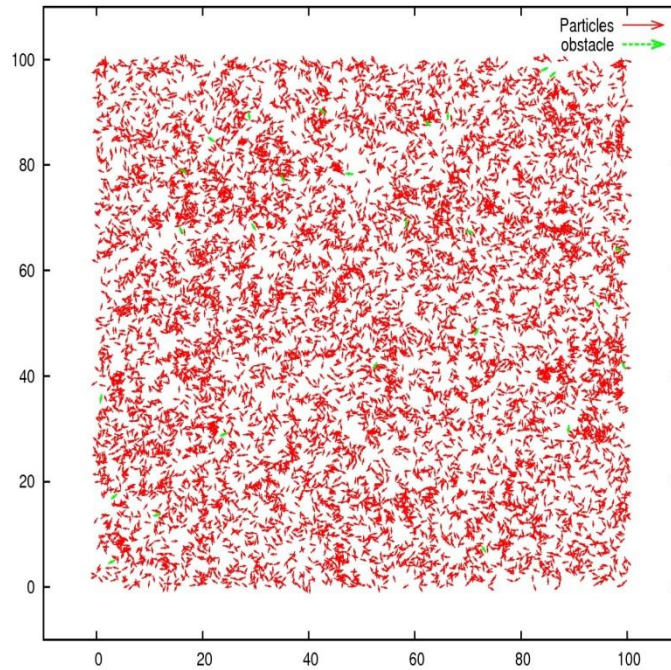


**Figure 7.6** Randomness in the direction of the particles due to  $\eta = 0.6$  at  $t = 10000$

The system seemed to be in a state of disorder because at  $\eta = 0.6$  there was a great deal of randomness, as shown in figure 7.6, with particles being scattered. There was no cluster formation and there was a loss of cohesion. Compared to the previous results, collective motion did not exist. This was evident from the order parameter that was equal to 0.017, which was a very small value. This value indicated no alignment with the particles, which did not follow the direction of their neighbouring particles.

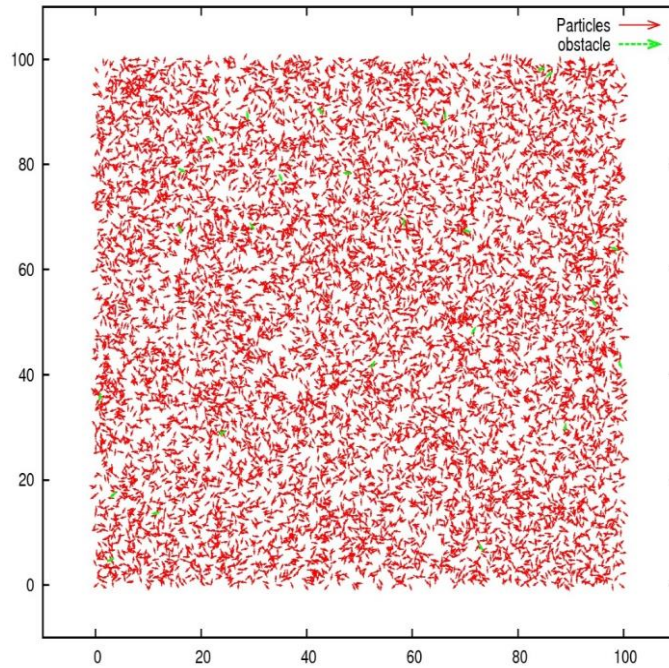


**Figure 7.7** Loss of cohesion in the system at  $t = 10000$  for  $\eta = 1.0$

The noise level changed from 0.6 to 1.0 (figure 7.7). It can be clearly seen that there was major randomness and the particles were scattered across the whole box. The order parameter had a value of 0.013, suggesting a complete loss of cohesion and zero alignment with the particles. From the first time step to the 1000th step there was completely disordered motion. The particles did not move properly and did not make contact with each other due to the noise chosen from the interval  $[\pi, -\pi]$ . It was anticipated that the particles would show similar behaviour if more time steps were used.

The model involving moving obstacles is similar to the predator model because of the escaping behaviour of the self-propelled particles in response to the interaction of the obstacles with the particles. There is alignment in the direction of the particles when there is no interaction between the particles and the obstacles. The obstacles have random motion and they cannot detect the particles; the obstacles have no contact among themselves. It is the duty of the particles to detect the obstacles and to avoid the obstacles. So here the particles can be considered to be the clever prey and the obstacles as the

predators which are not clever enough because they cannot see the particles. For this purpose we can see Lee's model, which investigated the escaping behaviour of the prey flock in response to the predator's attack [118]. In Lee's model, the behaviour of individuals in a school without a predator involved regions of repulsions, orientation and attraction. The predator's behaviour aligned its velocity to the centre of the prey. The Zheng model involved collective evasion from predation in schools of fish. This model also included zones, but in this case the prey behaved in a manner to confuse the predator as it made a strike. Individual prey components focus on the behavioural rules depending on the three zones: a selfish zone where prey orient to repulse the predator; a zone of decision to behave selfishly; and a no detection zone, where schooling motion takes place. In this model the predator selects its prey at random at every time step [128].

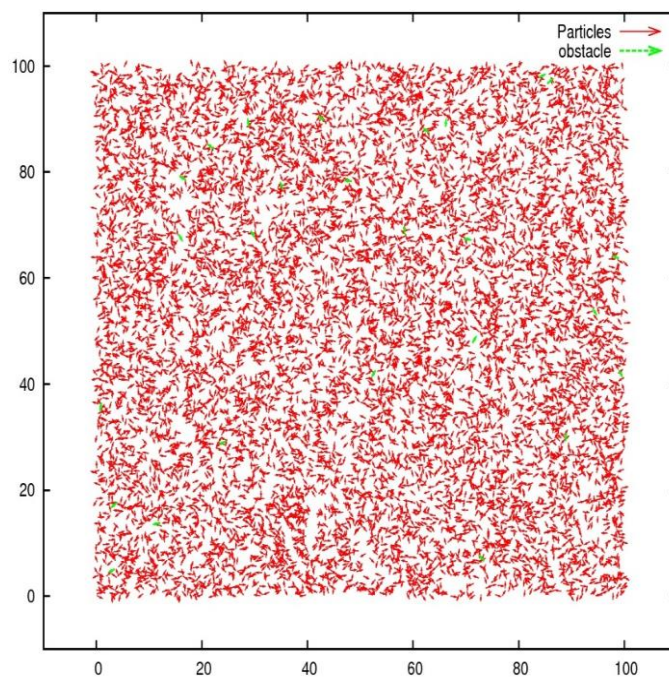


**Figure 7.8** System in state of disorder for noise  $\eta = 1.5$ ,  $t = 10000$

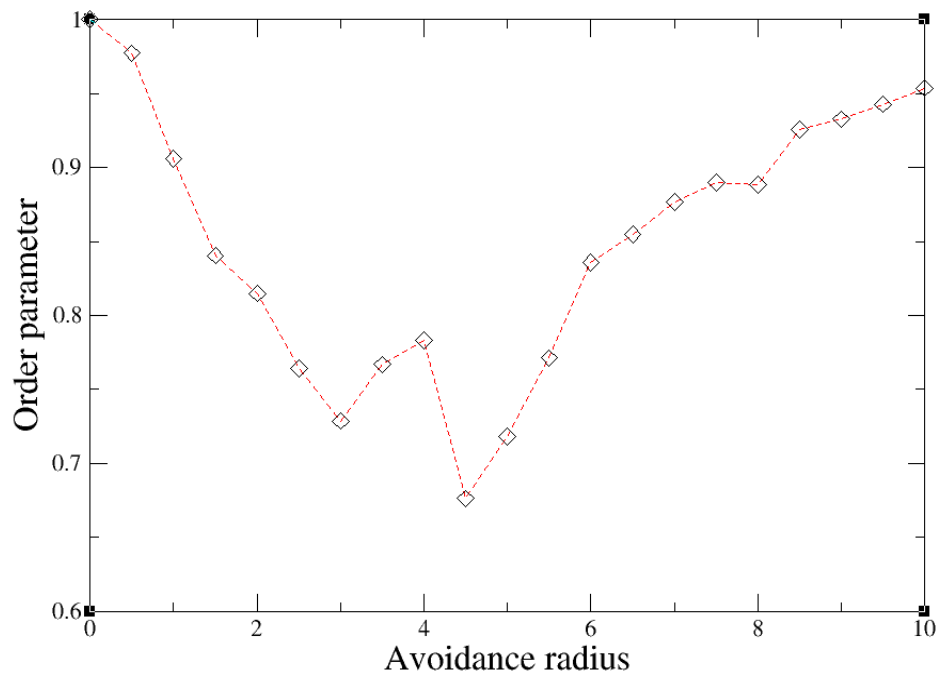
The noise level in the system was changed from 1 to 1.5 and, as can be seen from figure 7.8, the movement of the particles at the 10000<sup>th</sup> time step was almost similar to that in the previous case. The system was completely disordered. The impact of  $\eta = 1.5$  was so

high that the particles could not move and had no alignment; they did not interact properly with the obstacles. This behaviour was exhibited by the particles at each time step (figure 7.15). It is believed that for  $\eta > 1.5$ , particles would show a similar kind of behaviour in which there is a complete loss of cohesion. This was confirmed by the order parameter being zero.

### **7.2.1. Effect of avoidance radius**

The effect of the avoidance radius ( $R_o$ ) was investigated. The avoidance radius is a distance at which the particles sense the obstacles. The value of  $R_o$  was varied from 0 to 10 with an interval length of 0.5. The only variation was in the avoidance radius, while the rest of the parameters were kept constant.

The parameters used in the result, as shown in figure 7.9 have following values, box length  $L = 20$ , particles  $N_b = 3000$ , obstacles  $N_o = 15$ , interaction radius  $r = 1$ , speed of particle  $v_o = 1$ , particle's turning speed  $\gamma_o = 1$ , time interval  $\Delta t = 0.1$ , speed of obstacle  $v_y = 1$ , time  $t = 3000$ , and noise amplitude  $\eta = 0.0$ .



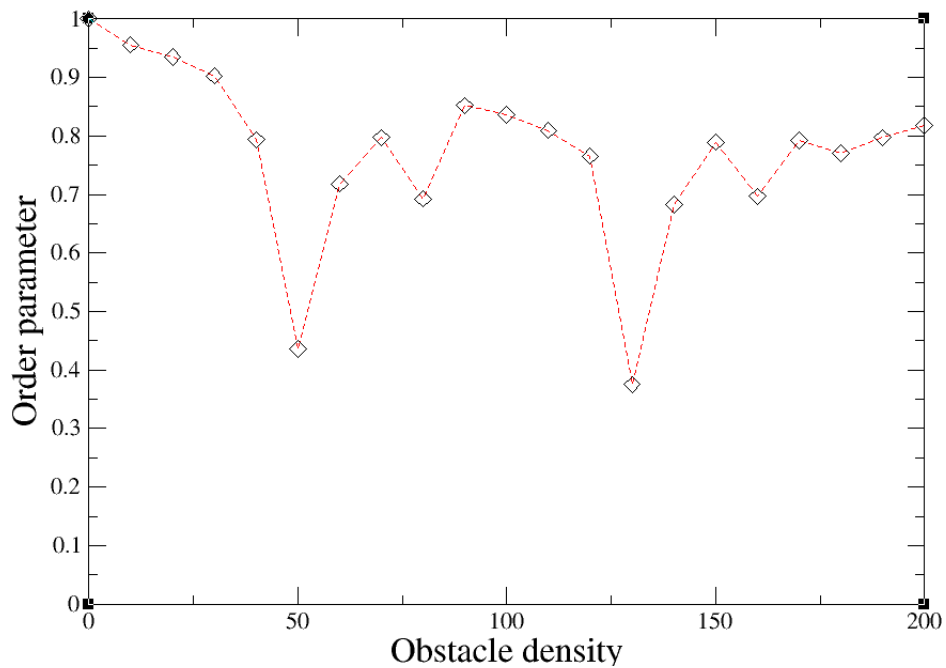
**Figure 7.9** Collective motion as a function of the avoidance radius

Figure 7.9 shows the collective motion of the self-propelled particles plotted against the avoidance radius. When the avoidance radius was zero, collective motion took place on a larger scale since the particles had no interaction with the obstacles. In essence they moved freely and did not contact any obstacle. When  $R_o > 0$ , fluctuations occurred in the order parameter; there was disturbance in the motion of the particles due to the obstacles. With the increase in the avoidance radius, there were more fluctuations in the collective motion and trapping of the particles occurred.

### 7.2.2. Effect of obstacle density

The effect of obstacle density was investigated with the other parameters being kept constant with only the number of obstacles being varied from 0 to 200 with an interval length of 10. The obstacles were randomly distributed and the movement of the obstacles was slower than the particles. The time taken by the obstacle to move from one point to another was 0.0021.

The parameters that were used in the result shown in figure 7.10 had the following values: box length  $L=20$ , particles  $N_b = 3000$ , interaction radius  $r = 1$ , avoidance radius  $R_o = 1$ , speed of particle  $v_o = 1$ , particle's turning speed  $\gamma_o = 1$ , time interval  $\Delta t = 0.1$ , speed of obstacle  $v_y = 1$ , time  $t = 3000$  and noise amplitude  $\eta = 0.0$ .



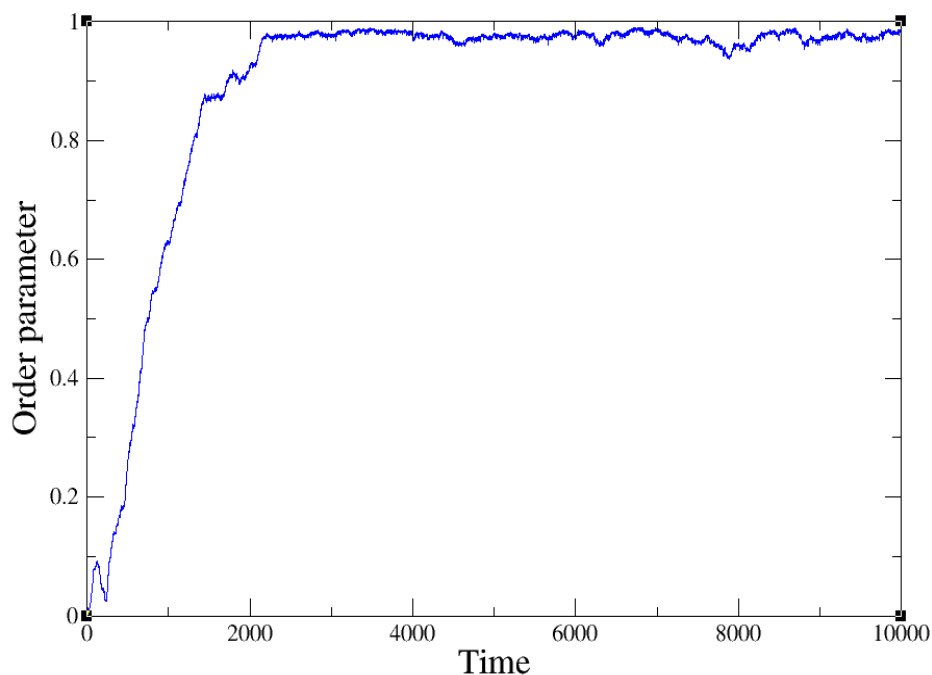
**Figure 7.10** Collective motion as a function of the obstacle density

Figure 7.10 demonstrates the results of increasing the obstacle density. There was non-monotonic behaviour when the obstacle density was greater than zero and the order parameter had a maximum value of zero obstacle density. This value of order was equal to 0.99, which suggested a higher alignment in the direction of the particles; whereas for 130 obstacles the order parameter had a minimum value of 0.37. The next minimum value was at 50 obstacles where the value was 0.43. For 200 obstacles the order parameter was 0.81. These values suggest that there were larger fluctuations. There was a rise and fall in the collective motion due to the continuous movement of the obstacles.

### 7.2.3 Collective motion as a function of time

The collective motion was plotted against each time step for different noise values. Time started from the zero time step to the 10000<sup>th</sup> time step. The order parameter ( $w$ ) was actually average normalized velocity of the particles by which the magnitude of the collective motion was measured. The parameter values used in the simulation were:

$$L = 100, N_b = 10000, N_o = 26, r = 1, R_o = 1, t = 10000, v_o = 1, \gamma_o = 1, \Delta t = 0.1, v_y = 1.$$



**Figure 7.11** Collective motion as a function of time at  $\eta = 0.01$

At  $\eta = 0.01$ , the particles showed fascinating behaviour, as seen in figure 7.11. At the initial time, the order parameter was approximately zero. After some time steps the value of the order parameter was approximately equal to 1. This value remained up to the final time steps. At  $t = 10000$  the value was 0.98. From this behaviour it was observed that there was higher alignment with the particles; they had higher coordination with each other. This result suggested that in the presence of moving obstacles, the particles showed more collective motion than in the cases where fixed obstacles existed.

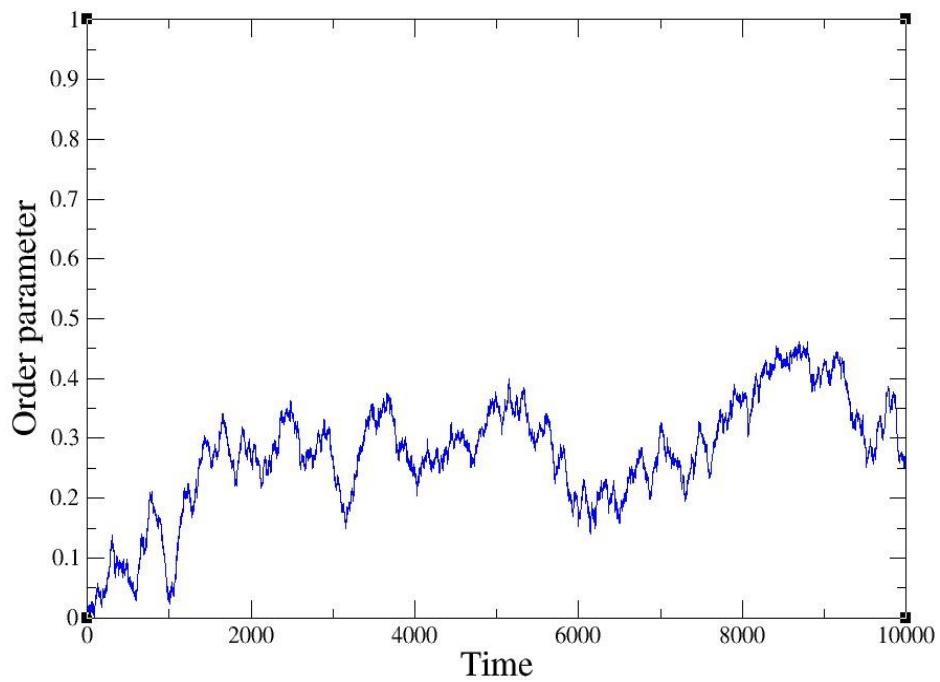


**Figure 7.12** Collective motion as a function of the time at  $\eta = 0.3$

The collective motion of the self-propelled particles decreased when the value of  $\eta$  varied from 0.01 to 0.03 with a greater impact on the system (figure 7.12). It was observed that the particles showed different behaviour than in the previous result since the system had shown more fluctuations. It can be clearly seen that the order parameter had a lower value than previously in the case of noise ( $\eta = 0.01$ ). The particles had a loss of cohesion and there was little alignment with the particles. The value of the order parameter at the final time step was 0.27, which was greater than the fixed obstacles where the same parameters were applied (figure 6.15).

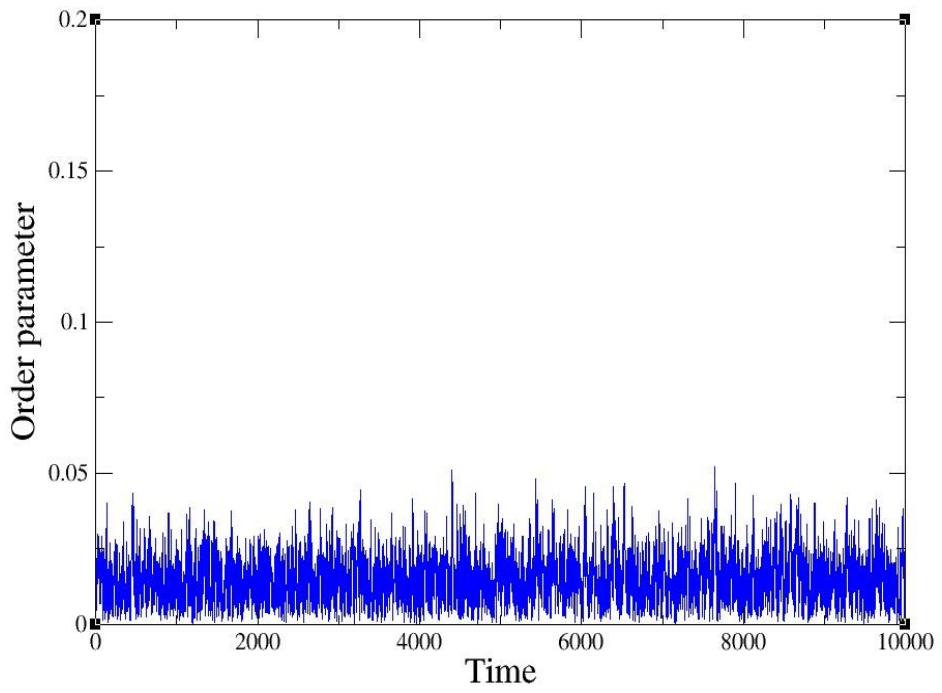


**Figure 7.13** Collective motion as a function of time at  $\eta = 0.6$

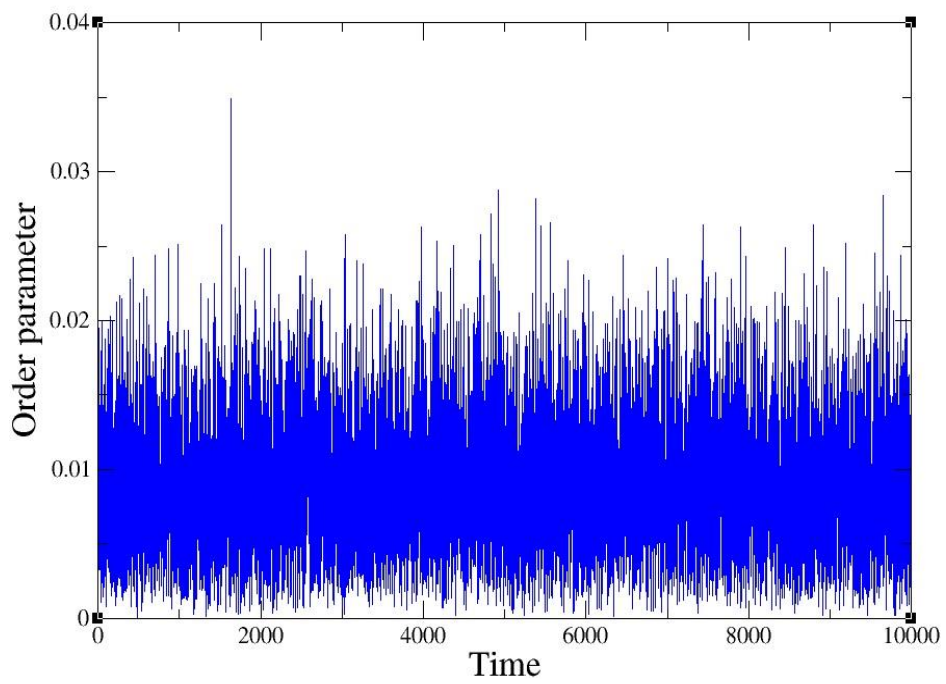


**Figure 7.14** Collective motion as a function of time; here  $\eta = 1.0$

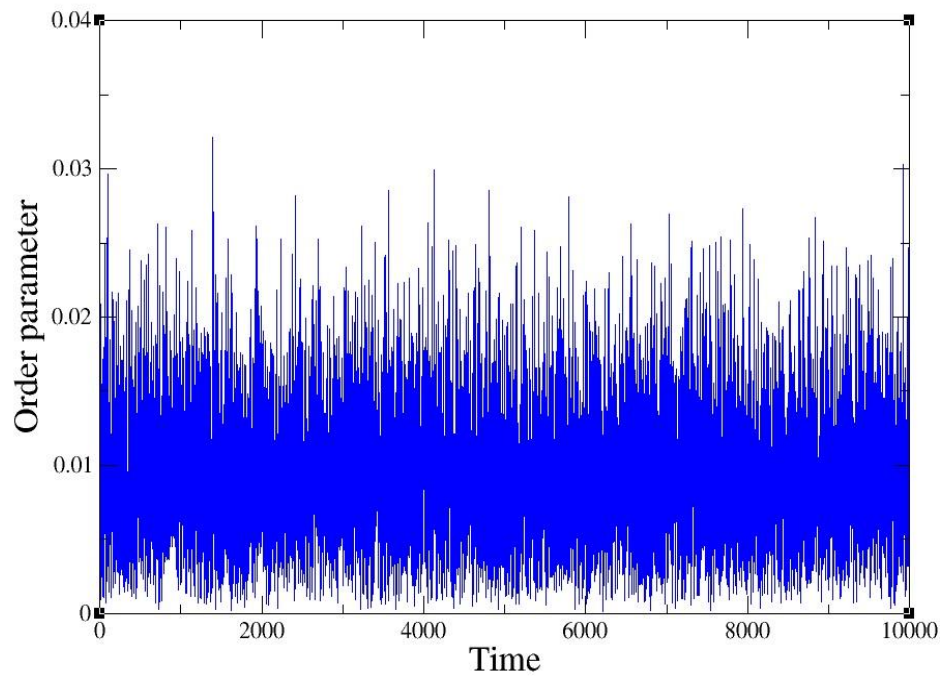
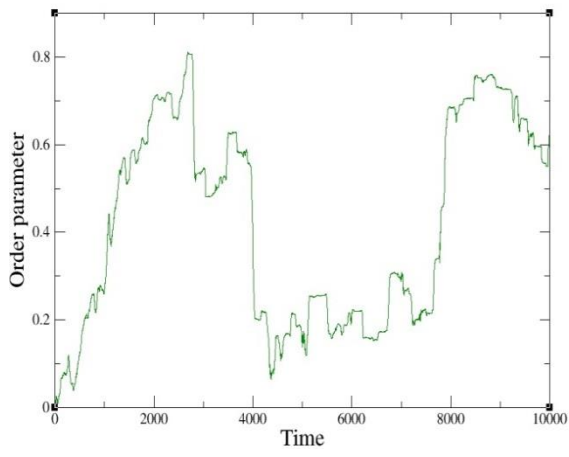
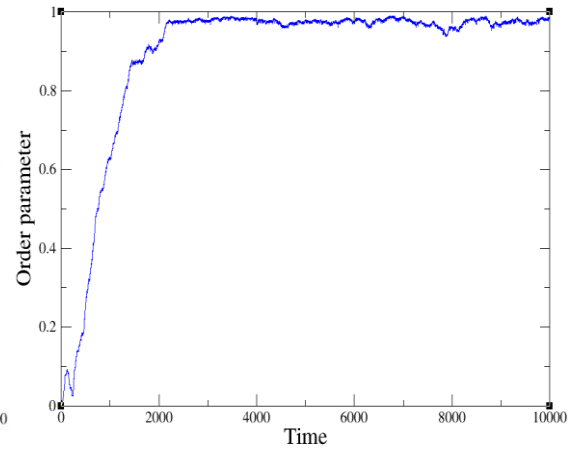


**Figure 7.15** Collective motion as a function of time at  $\eta = 1.5$

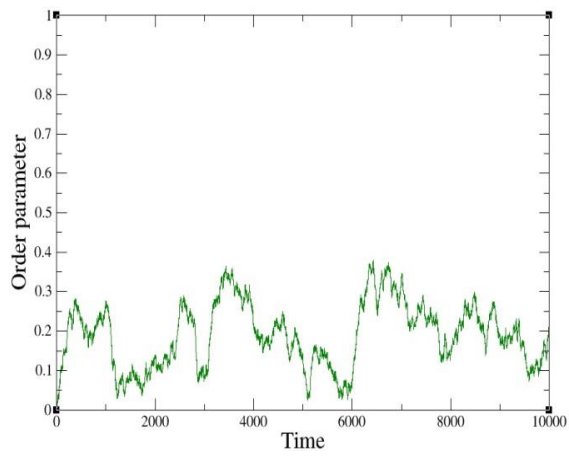
A higher noise level ( $\eta \geq 0.6$ ) had a major impact on the system. It was observed that the particles had a loss of cohesion in the presence of moving obstacles. The order parameter was near zero at all the time steps (see figures 7.13 to 7.15). The effect of noise was so high that the particles could not move properly and could not escape from the interaction zone of the obstacles. There was no alignment in their direction. For  $\eta = 0.6$ , in the case of the fixed obstacles, the particles showed a similar b



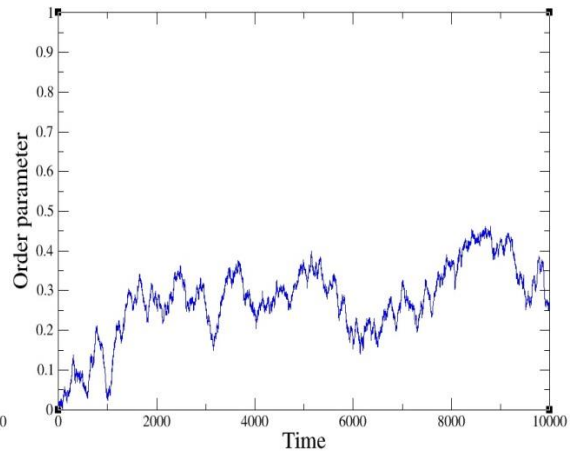
(a) Fixed obstacles at  $\eta = 0.01$



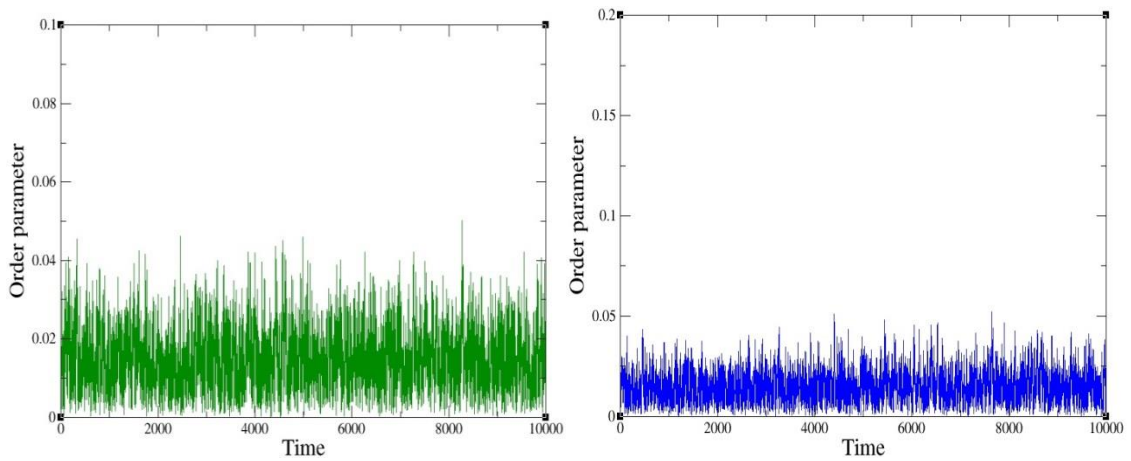
(d) Moving obstacles at  $\eta = 0.01$



(b) Fixed obstacles at  $\eta = 0.3$



(e) Moving obstacles at  $\eta = 0.3$



(c) Fixed obstacles at  $\eta = 0.6$

(f) Moving obstacles at  $\eta = 0.6$

**Figure 7.16** Comparison of collective motion for fixed and moving obstacles at different noise values

Collective motion as a function of time was plotted at different noise values for the fixed obstacles and the moving obstacles with the same parameters applied in both cases. It can be clearly seen from figure 7.16 that at  $\eta = 0.01$ , for moving obstacles the curve was smoother than for the fixed obstacles. At  $\eta = 0.3$ , fluctuations were observed in both cases. Collective motion did not exist at the larger scale. At  $\eta = 0.6$ , the particles showed similar behaviour in the case of both static and moving obstacles. The system was completely disordered with the order parameter being approximately zero.

The results in figures 7.16(a) and 7.16(d) have no similarity except that the same noise value was applied. It can be clearly seen in figure 7.16(a) that more disturbance existed in the system throughout the simulation time, whereas in figure 7.16(b) we see that a smooth curve is observed, which means there was a higher alignment in the direction of the particles because of the moving obstacles. The obstacles moved inside the system and provided less disturbance to the particles; when they came near to the particles, the particles started avoiding the obstacles and as a result they could not be fully trapped and

disturbed. It can be clearly seen that from  $t = 2000$ , the curve is more smooth because the value of the order parameter remained approximately 1 up to the 10000<sup>th</sup> time step.

In the static obstacles model, the system demonstrated more disturbances because it was only the particle that decided the avoidance force; but in the case of the moving obstacles model, not only the particles avoided the obstacles, but also the obstacles provided movement which was helpful in aligning the particles.

Some similarity appeared in figures 7.16(b) and 7.16(e). This similarity appeared in terms of the value of the order parameter. In both cases, the value of the order parameter remained less than 0.5; it is not much higher because the value of the noise was 0.3. Due to this noise value, the system was not in a full state of order position. Less collective motion was exhibited by the particles. Figure (b) demonstrates that a higher value of order parameter was 0.37 at the time  $t = 6422$ , whereas the figure (d) showed the highest value of the order parameter was 0.46 at time  $t = 8697$ . This behaviour of similarity in the graphs is due to the noise. The impact of noise was so high that the particles could not move properly and detected obstacles.

Figures 7.16 (c) and (f) demonstrate the impact of higher noise in the system. This noise value is equal to  $\eta = 0.6$ . These two figures tell us that the system is completely in a state of disorder. Furthermore, the impact of the noise is so high that the particles cannot move properly. Particles lost the capability of avoiding from the obstacles. There is no alignment in the direction of the particles.

We read the above graphs (figure 7.16 (c) and 7.16(f)) in the context of the value of the order parameter with respect to time. It was observed from these graphs that at each time step the value of the order parameter was near to zero which suggested that there was no collective motion exist in the system throughout the simulation time.

#### 7.2.4. Order of phase transition

The noise level was varied to investigate the order of phase transition. If the curve showed one hump then it was second order phase transition; if there was more than one hump then it was first order phase transition. The probability density function (PDF) was plotted against the order parameter ( $w$ ). This technique of finding the order of phase transition had been undertaken previously [5].

The parameter values used in the simulations were:  $L = 100$ ,  $N_b = 10000$ ,  $N_o = 26$ ,  $r = 1$ ,  $R_o = 1$ ,  $t = 10000$ ,  $v_o = 1$ ,  $\gamma_o = 1$ ,  $\Delta t = 0.1$ ,  $v_y = 1$ .

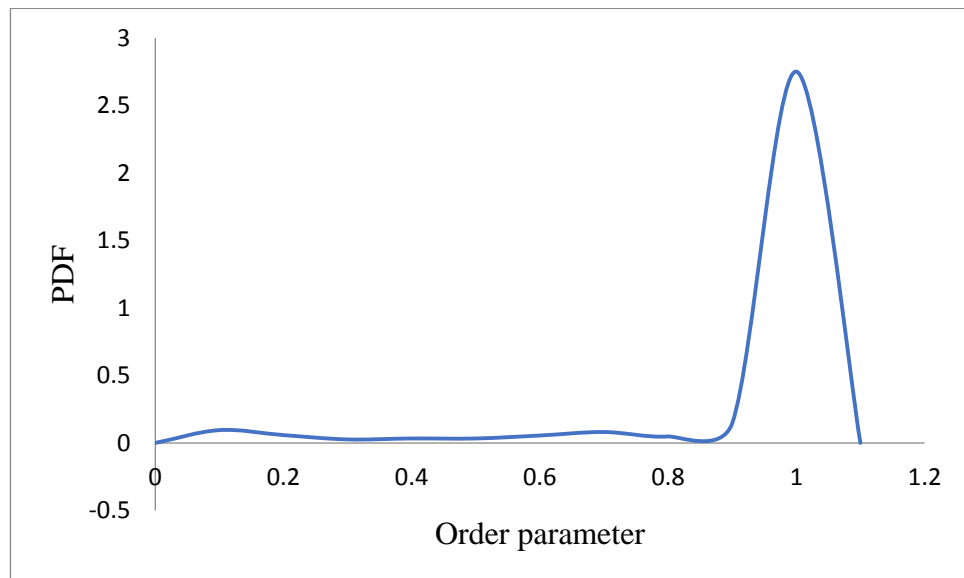


**Figure 7.17** First order phase transition at  $\eta = 0.01$

For weaker noise, the system showed discontinuity in the collective motion of the particles which moved in groups. When the particles interacted with the obstacles their collective movement broke up, hence discontinuity took place. Figure 7.17 demonstrates a first order phase transition with the curve having more than one hump. At  $w = 0.1$ , the value of the PDF was 0.095; this value decreased to 0.026 at  $w = 0.3$ . Subsequently there

was growth in the PDF. The shape of the curve suggested that there was discontinuity in the system when less noise was applied to the system.

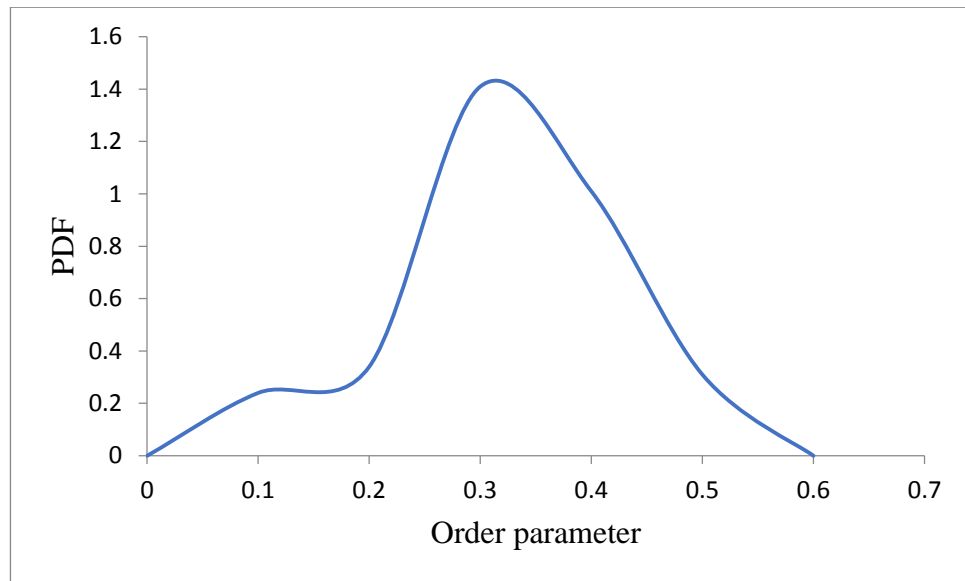


**Figure 7.18** Second order phase transition at  $\eta = 0.3$

The effect of  $\eta = 0.3$  on the system can be seen in figure 7.18, showing a second order phase transition nature. This is also called a continuous phase transition. At  $w = 0.1$ , the PDF had a value equal to 0.24 showing a continuous growth in the PDF. The value went to a maximum at  $w = 0.3$  and then there was a continuous decline in the PDF, reaching zero at  $w = 0.6$ .

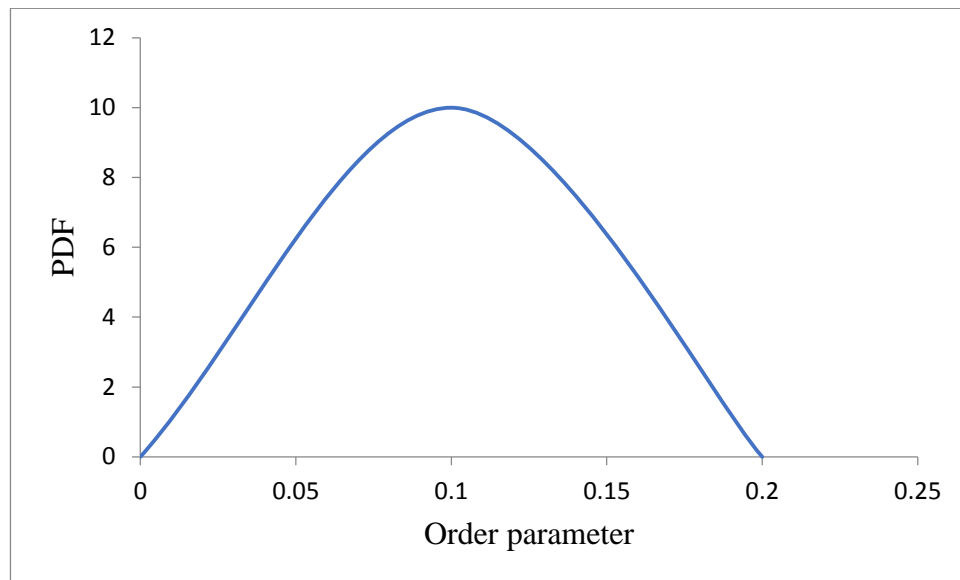


**Figure 7.19** Second order phase transition at  $\eta = 0.6$

When the noise value was changed from 0.3 to 0.6, the results showed second order phase transitions with the curve showing one big hump. At  $w = 0.1$ , the value of the PDF was 10. The order parameter remained approximately equally to zero (figure 7.19). At  $\eta = 0.6$ , the particles had a loss of cohesion with no alignment in the direction of the particles. It is believed that if higher values of noise were applied, there would be continuous phase transitions in the system.

### **7.3. Comparison between obstacle avoidance model and the physical system from the literature**

Carrer *et al.* [12] worked on the heterogeneous medium, where they investigated the variation in the flocking behaviour of starlings under a different predation risk; they tested the hypothesis that variation in aerial flocking was linked to predation risk. They described and quantified the flocking patterns of the starlings, approaching two urban roosts which had a different predation pressure. It was predicted that higher predation pressure in a roost would produce larger and more compact flocks, as it was thought that

larger flocks were less vulnerable to predation than small flocks. Observation was undertaken for 53 days for incoming flocks which were not under direct attack from predators. There were 12 flocking shapes observed, and it was seen that larger and compact flocks took place frequently at the roost when there was higher predation pressure. Furthermore, small flocks and singletons were observed at the roost when there was lower predation pressure. Similar patterns were witnessed when other flocks showed antipredator behaviour, even when flocks were far away and not in the existence of the predator at the focal roost. This may show that social information shared between the flocks affects flocking decisions. Success of predation was high at the roost with low predation pressure. These results propose that predation risk affects aerial flocking patterns. Furthermore, these flocking patterns can also be affected by the behaviour of other flocks in response to direct attack.

A new model that is introduced in this thesis is termed the ‘obstacle avoidance model’ (OAM). This model investigates the collective behaviour of self-propelled particles in the presence of fixed and moving obstacles. The OAM and the study undertaken by Carrer *et al.* [120] have similarity, because work done by them was studied in the context of a heterogeneous medium where particles have to face obstacles. In their work, obstacles were considered to be the predators (peregrine falcons) which disturbed the flocking behaviours. They carried out a qualitative and quantitative study of the flocking patterns.

As in the OAM, it was observed that when particles came close to the obstacles they turned away from the obstacles and also split into groups, and they again aligned when the obstacles were not close to them. An example of this can be seen in figures 6.4, 6.6, and 6.7. In figure 6.7 it can be clearly seen that when the particles are near to the obstacles they are more disturbed, but they are more aligned when they are bit far from the obstacles. The collective motion observed was equal to 0.82, which suggested higher

alignment in the direction of the particles. Furthermore, in figure 6.11 we can see group formation in the presence of 49 obstacles; this number of obstacles was higher than the number of obstacles used in the results in figures 6.4-6.7, so this indicates that even in higher obstacle densities, particles exhibited collective motion because of the occurrence of the group formation in the system due to the obstacles. There was also flock formation which occurred in the presence of moving obstacles, where particles collectively moved in the presence of diffusive obstacles. The moving obstacle case is more close to the predator prey model, where obstacles can be considered to be the predators and the particles can be considered to be the prey. From figures 7.2 to 7.4, it can be clearly seen that particles form groups because of the obstacles and these groups are considered to be the flocks of birds which are formed in response to avoid the obstacles. When these groups come close to the obstacles they split and again merge when the obstacles go away from the particles. The value of the order parameter in the results in figures 7.2 to 7.4 is approximately equal to 1, which suggests higher alignment in the direction of the particles. The same kind of behaviour was observed by Carrer *et al.* [120] in their study, they found that when there was higher predation pressure at the roost, larger flock formation took place and also two kinds of behaviour appeared: (1) splitting displays, and (2) agitation waves. ‘Splitting displays’ took place when the flocks under the predator attack split into two or more parts and these parts merged again. ‘Agitation waves’ took place when there were changes in the density; these waves propagated from one side of the flocks of thousands of birds to the other. They also found that wind intensity became a source affecting flocking patterns. In our model OAM, noise created the disturbance in the formation of groups, and the direction of the particles was totally disturbed. Noise can be also considered as the wind because it provides disturbance to the flocking patterns, so this is another similarity between the OAM and the work of Carrer *et al.* [120].

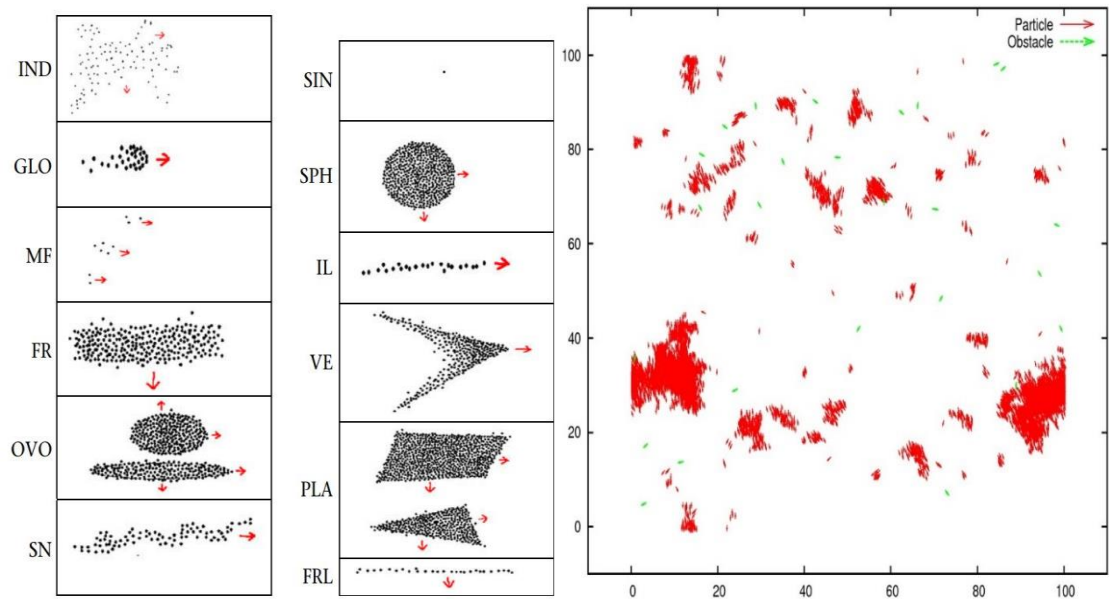


**Figure 7.20** Flock formation in starlings [120] **Figure 7.21** Group formation in particles

It can be clearly seen in figure 7.20 that different types of flocks were formed. This flock formation took place due to the predation pressure at the roost. Figure 7.21 demonstrates the result of the obstacle avoidance model. This figure also shows flock formation in the self-propelled particles, where the particles formed groups in the presence of the moving obstacles. The particles had a tendency to align with each other when the obstacles were away from them and these particles split into smaller groups or showed individual movement when the obstacles were near to them. In figure 7.20, IND shows an indefinite, disorganized shape; this behaviour is also shown in figure 7.21 on the top left hand side.

In figure 7.20 there are some other shapes demonstrated which are also found in the results of OAM.

- GLO: globular shape, this shape contains 6-50 birds;
- ML: mini flocks of two to five birds;
- OVO: Ovoidal or eclipse-like shape, this contains hundreds to thousands of birds;
- SIN: singletons;
- SPH: spherical shape.

Some of these shapes can be seen in figure 7.21 and others can be seen in figures 6.4 to 6.7 and figures 7.2 to 7.4. In figure 2, a singleton movement can also be seen on the top right side where a few particles showed individual movement. On the bottom left side of figure 7.21, a large and compact flock formed. Furthermore, similar kinds of flock also formed on the bottom right side of figure 7.21. These results show that the same kinds of particles form groups in a heterogeneous environment in response to the presence of obstacles in their way.

## 7.4. Conclusions

It was observed that at lower noise values the particles showed a higher collective motion. At higher noise values the motion of the particles was very small. The effect of the avoidance radius was also investigated. The results showed no consistency in the order parameter, which suggested that due to the movement of the obstacles there was disturbance in the collective motion of the particles. The obstacle density parameter was also varied and the results showed similar fluctuating behaviour. The curve of the collective motion became non-monotonic. In the presence of moving obstacles, the particles had first order phase transition when  $\eta = 0.01$ . The particles showed second order phase transition when  $\eta \geq 0.3$ .

Differences appeared in the results between static and moving obstacles. In the case of moving obstacles, the particles showed more collective motion than the results in which static obstacles were involved. For a noise value  $\eta = 0.01$  and  $0.3$ , the system showed more alignment in the direction of the particles in the case of the moving obstacles, whereas in the case of fixed obstacles, randomness was observed. For a higher noise value, such as  $\eta \geq 0.6$ , the system exhibited behaviour of higher randomness in both cases (static and moving obstacles). In the presence of moving obstacles, the particles exhibited first order phase transition for  $\eta = 0.01$ , whereas in the case of static obstacles, it was second order phase transition. In the context of the time graph, the curve of the order parameter was smoother for moving obstacles than for fixed obstacles. Furthermore, the model for the moving obstacles is more close to nature and it can be extended to the predator and prey model, where particles can be considered to be the prey and the obstacles can be considered to be the predators. So we can say that the moving obstacle model is much better than the fixed obstacle model.

# CHAPTER 8

## Conclusions and Future work

### 8.1 Summary

Collective behaviour of self-propelled particles was studied computationally in homogeneous and heterogeneous systems. The exciting collective behaviour of particles is analogous to real applications, such as in the movement of crowds, the flight of birds, the movement of bacteria and the migration of wildebeest. In the homogeneous medium, the collective behaviour of self-propelled particles was investigated using Vicsek 2D and 3D models.

In homogeneous systems using the Vicsek 2D model there was good alignment in the directions of the particles when high particle density ( $\rho = 12$ ) and small noise ( $\eta = 0.1$ ) were applied. In the case of smaller density ( $\rho = 0.48$ ) and smaller noise ( $\eta = 0.1$ ), group formation was observed in the system. There was a good correlation when smaller noise ( $\eta = 0.1$ ) and the particle density ( $\rho = 0.48$ ) were used between the model and theory. For larger system sizes, the particles also showed similar behaviour in terms of alignment, group formation and correlation. By varying the particle density at constant noise there was an increase in the value of the order parameter; this was attributed to higher collective motion with increasing particle density. There were fluctuations in the collective motion at a smaller time step when the speed was varied, whereas at higher time steps there was consistency in the collective motion. Higher collective motion was observed with increasing interaction between the particles; the first order phase transition appeared at lower noise ( $\eta \leq 0.198$ ), whereas for larger noise ( $\eta \geq 2.0$ ), a second order phase transition was exhibited.

In the Vicsek 3D model, the particles exhibited similar behaviour to that of the 2D model. There was alignment in the direction of the particles when smaller noise and higher density was used. The particles required more time steps to follow the directions of the neighbouring particles and cluster formation was evident in the system. With a higher interaction radius, speed and particle density, there was higher collective motion, which was approximately 1. There was a decline in the collective motion due to increasing noise and at higher noise the system was completely disordered.

In heterogeneous mediums the collective motion of the self-propelled particles in the presence of fixed obstacles showed inconsistency due to the random distribution of the obstacles in the system. The particles showed a disordered phase at the initial time step, whereas at higher time steps, along with smaller noise, the particles formed groups. At higher noise ( $\eta = 0.6$ ), cohesion was lost and no group formation occurred. Collective motion was compared in homogeneous and heterogeneous systems by varying the interaction radius, speed and noise. A smooth curve was obtained for collective motion for homogeneous mediums, whereas in the case of a heterogeneous medium, non-monotonic behaviour was observed. Collective motion of the particles was increased when  $\eta$  varied from 0.01 to 0.1; this behaviour suggested that due to the random distribution of obstacles there existed an optimal noise which maximised the collective motion.

The particles exhibited fluctuating behaviour in the presence of moving obstacles. At weaker noise there was higher collective motion and at stronger noise there was smaller collective motion. At  $\eta = 0.01$ , for moving obstacles the curve of the order parameter was smoother than for fixed obstacles. This suggested that particles behave more efficiently in the case of moving obstacles.

Work done by Carrer *et al.* [120] has a similarity with the obstacle avoidance model (OAM) because they studied the flocking behaviour in the heterogeneous medium where particles have to face the obstacles. In their work, obstacles were considered to be the predators (peregrine falcons) which disturbed the flocking behaviour. In OAM it was found that when particles came near the obstacles, they turned away from the obstacles and also the particles split into groups and they again aligned when there were no obstacles in the interaction range of the particles. This split and alignment behaviour was also found in the study of Carrer *et al.* [120]. In the results of OAM, it was also found that large and compact group formation occurred in the presence of obstacles; similar behaviour was also observed in their work. In OAM there was group formation by the particles, even in the case of increased obstacle density, and these groups were more compact. In their work, the starlings formed compact flocks when there was a higher predation risk, and they found that wind energy could also affect the flocking patterns. In OAM, noise also created disturbance in the direction of the self-propelled particles.

## **8.2 Findings and main contributions**

The major contribution in the field is the development of a new model which is termed the obstacle avoidance model, which investigates the collective behaviour of self-propelled particles in the presence of static and moving obstacles. This model will be helpful in developing navigation strategies, understanding the pedestrian flow in large crowded places, and investigation of the motion of flocks of birds when they face obstacles. The model shows better collective motion than the previously developed model, and has a capability of extension to a three-dimensional coordinate system. This model possesses optimal noise value in the presence of the static obstacle. At this noise value, collective motion of the particles is maximum. This model is easy to simulate and contains fewer terms; it is closer to nature; it can be extended to the predator prey model;

and it can be applied to biological systems to understand their collective motion, such as bacteria, cells, algae and other micro-organisms. Furthermore, there is possible application of this model to artificial systems such as robots, swimming janus colloids, nanomotors, walking gains and others.

The conclusion drawn from the simulation results of the homogeneous medium suggests that higher particle density along with smaller noise gives rise to alignment behaviour in the direction of particles, whereas in the case of smaller particle densities, group formation in the system will take place. Noise has a very significant impact on the system because smaller noise is proof of fewer disturbances to the motion of the particles, whereas higher noise becomes a source of the total chaos in the system because particles do not have the ability to move properly. The simulation time plays an important role in the system of self-propelled particles. A large number of time steps provides an opportunity to the particles to come close to each other and to make the system more stable by showing a higher alignment in the direction of the particles. The effect of larger time steps can be seen in the case of the variation in speed parameter; when time was smaller, such as  $t = 200$ , there was fluctuation in the system, and when time steps were higher, such as  $t = 500$ , consistency was observed.

In the heterogeneous medium, the collective motion of self-propelled particles does not remain consistent because of the random distribution of the obstacles. Due to this heterogeneity there is always non-monotonic behaviour exhibited by the curve of collective motion. Furthermore, optimal noise always exists in the system, which maximises collective motion. The conclusion drawn from the comparison of static and moving obstacles suggests that in the case of static obstacles, collective motion is more disturbed than moving obstacles. Self-propelled particles behave more efficiently in the presence of moving obstacles.

### **8.3 How objects were met?**

A detailed literature review was undertaken for the purpose of finding the research problem and understanding the current state of research.

FORTRAN programming language was used for simulation purposes. FORTRAN codes were developed and simulated through linux operating system. For the visualization of the simulation results, GNUPLOT and opendx were used.

The collective motion of self-propelled particles was investigated in a homogeneous medium using 2D and 3D Vicsek models. An order parameter was used to characterise the collective motion of the particles. The effect of different parameters was investigated by varying their values. These parameters were noise, interaction radius, speed, and particle density. A probability density function was used to investigate the order parameter.

In order to investigate the collective behaviour of self-propelled particles in the heterogeneous medium, obstacles were introduced into the system. This heterogeneity was introduced by using an obstacle interaction function. The collective behaviour of the particles was characterised through the order parameter. The effect of different parameters was investigated to check the impact of static and diffusive obstacles on the collective motion of the particles. These parameters were noise, speed, particle density, obstacle density and avoidance radius.

## 8.4 Future work

This study opens avenues for an exciting set of studies that can be performed in the future by researchers study collective motion of particles.

- The obstacle avoidance model can be extended to the three dimensional coordinate system providing new insights into collective behaviour.
- The behaviour of the moving obstacles will be investigated can be extended in 3D revealing further details information about particle behaviour in heterogeneous systems.
- In this study the collective motion of spherical particles was investigated in homogeneous and heterogeneous systems in both 2D and 3D. However, in reality the shape of the particles will have a significant impact on the collective motion. Hence, a study of the influence of particle shape on the collective motion will be highly informative and applied to greater number of real applications.
- The current study investigated static and dynamic obstacles reveal some useful insights. In real systems both static and dynamic obstacles coexist in a system. Therefore, a study of the static and moving obstacles combined in the box will prove to be highly interesting and would mimic real systems more closely. It will no doubt be more complex and challenging, nevertheless very exciting for researchers in this field of endeavour.

## References

- [1] F. Peruani, F. Ginelli, M. Bär and H. Chaté, "Polar vs. apolar alignment in systems of polar self-propelled particles," in *Journal of Physics: Conference Series*, 2011, pp. 012014.
- [2] C. Stokes, "Collective behaviour of self-propelling particles in the presence of a group of predators", *Masters thesis*, Computational Physics Group, University of Central Lancashire, June, 2011.
- [3] T. Vicsek, A. Zafeiris, "Collective motion" *Physics Reports*, vol. 51, 72012, pp. 71-140.
- [4] Hagan group. *Active matter* [online]. Available: <https://www.brandeis.edu/departments/physics/hagan/research/activematter.html> [Accessed on 6th 2014]
- [5] M. Nagy, I. Daruka and T. Vicsek, "New aspects of the continuous phase transition in the scalar noise model (SNM) of collective motion," *Physica A: Statistical Mechanics and its Applications*, vol. 373, pp. 445-454, 2007.
- [6] L. A. Cameron, J. R. Robbins, M. J. Footer and J. A. Theriot, "Biophysical parameters influence action-based movement, trajectory, and initiation in a cell-free system," *Mol. Biol. Cell*, vol. 15, pp. 2312-2323, May, 2004.
- [7] D. Selmeçzi, S. Mosler, P. H. Hagedorn, N. B. Larsen and H. Flyvbjerg, "Cell motility as persistent random motion: theories from experiments," *Biophys. J.*, vol. 89, pp. 912-931, 2005.
- [8] N. Kumar, M. H. Zaman, H. Kim and D. A. Lauffenburger, "A high-throughput migration assay reveals HER2-mediated cell migration arising from increased directional persistence," *Biophys. J.*, vol. 91, pp. L32-L34, 2006.
- [9] X. Wu and A. Libchaber, "Particle diffusion in a quasi-two-dimensional bacterial bath," *Phys. Rev. Lett.*, vol. 84, pp. 3017, 2000.
- [10] F. Schweitzer, W. Ebeling and B. Tilch, "Complex motion of Brownian particles with energy depots," *Phys. Rev. Lett.*, vol. 80, pp. 5044, 1998.
- [11] F. Schweitzer, W. Ebeling and B. Tilch, "Statistical mechanics of canonical-dissipative systems and applications to swarm dynamics," *Physical Review E*, vol. 64, pp. 021110, 2001.
- [12] F. Schweitzer, "Brownian agents and active particles. On the emergence of complex behaviour in the natural and social sciences," *Springer Series in Synergetics. Berlin, Germany, Springer*, 2003.
- [13] G. Sibona, "Evolution of microorganism locomotion induced by starvation," *Physical Review E*, vol. 76, pp. 011919, 2007.

- [14] B. Lindner, "The diffusion coefficient of nonlinear Brownian motion," *New Journal of Physics*, vol. 9, pp. 136, 2007.
- [15] G. E. Uhlenbeck and L. S. Ornstein, "On the theory of the Brownian motion," *Physical Review*, vol. 36, pp. 823, 1930.
- [16] O. Bénichou, C. Loverdo, M. Moreau and R. Voituriez, "Two-dimensional intermittent search processes: An alternative to Lévy flight strategies," *Physical Review E*, vol. 74, pp. 020102, 2006.
- [17] N. Komin, U. Erdmann and L. Schimansky-Geier, "Random walk theory applied to daphnia motion," *Fluctuation and Noise Letters*, vol. 4, pp. L151-L159, 2004.
- [18] U. Erdmann, W. Ebeling, L. Schimansky-Geier, A. Ordemann and F. Moss, "Active Brownian particle and random walk theories of the motions of zooplankton: application to experiments with swarms of daphnia," *ArXiv Preprint q-bio/0404018*, 2004.
- [19] G. M. Viswanathan, V. Afanasyev, S. Buldyrev, E. Murphy, P. Prince and H. E. Stanley, "Lévy flight search patterns of wandering albatrosses," *Nature*, vol. 381, pp. 413-415, 1996.
- [20] M. J. Krieger, J. Billeter and L. Keller, "Ant-like task allocation and recruitment in cooperative robots," *Nature*, vol. 406, pp. 992-995, 2000.
- [21] A. Jadbabaie and J. Lin, "Coordination of groups of mobile autonomous agents using nearest neighbour rules," *Automatic Control, IEEE Transactions*, vol. 48, pp. 988-1001, 2003.
- [22] D. Helbing, "Traffic and related self-driven many-particle systems," *Reviews of Modern Physics*, vol. 73, pp. 1067, 2001.
- [23] D. Helbing, I. Farkas and T. Vicsek, "Simulating dynamical features of escape panic," *Nature*, vol. 407, pp. 487-490, 2000.
- [24] J. K. Parrish and W. M. Hamner, *Animal Groups in Three Dimensions: How Species Aggregate*. Cambridge University Press, 1997.
- [25] L. Jelsbak and L. Sogaard-Andersen, "Pattern formation by a cell surface-associated morphogen in *Myxococcus xanthus*," *Proc. Natl. Acad. Sci. U. S. A.*, vol. 99, pp. 2032-2037, Feb 19, 2002.
- [26] R. Welch and D. Kaiser, "Cell behaviour in travelling wave patterns of myxobacteria," *Proc. Natl. Acad. Sci. U.S.A.*, vol. 98, pp. 14907-14912, Dec 18, 2001.
- [27] F. Peruani, *From Individual to Collective Motion of Self-Propelled Particles: The Role of Particle Shape, Orientational Ordering and Clustering*, 2008.

- [28] T. Vicsek, A. Czirok, E. Ben-Jacob, I. Cohen and O. Shochet, "Novel type of phase transitions in a system of self-driven particles" *Physical Review Letters*, vol. 75, pp. 1226-1229, 1995.
- [29] J. A. Drocco, C. O. Reichhardt and C. Reichhardt, "Bidirectional sorting of flocking particles in the presence of asymmetric barriers," *Physical Review E*, vol. 85, pp. 056102, 2012.
- [30] I. D. Couzin, "Collective cognition in animal groups," *Trends Cogn. Sci. (Regul. Ed.)*, vol. 13, pp. 36-43, 2009.
- [31] T. S. Deisboeck and I. D. Couzin, "Collective behaviour in cancer cell populations," *Bioessays*, vol. 31, pp. 190-197, 2009.
- [32] A. Czirók, E. Ben-Jacob, I. Cohen and T. Vicsek, "Formation of complex bacterial colonies via self-generated vortices," *Physical Review E*, vol. 54, pp. 1791, 1996.
- [33] I. Couzin, J. Krause, R. James, G. Ruxton, and N. R. Franks, "Collective memory and spatial sorting in animal groups", *Journal of Theoretical Biology*, vol. 218, pp. 1-11, 2002.
- [34] J. Park, "Collective Motion in 3D and Hysteresis," 2011.
- [35] J. Krause and G. D. Ruxton, *Living in Groups*. Oxford University Press, 2002.
- [36] I. Couzin, J. Krause, N. Franks and S. Levin, "Effective leadership and decision-making in animal groups on the move," *Nature*, vol. 433, pp. 513-516, Feb 3, 2005.
- [37] A. Simons, "Many wrongs: the advantage of group navigation," *Trends Ecol. Evol.*, vol. 19, pp. 453-455, Sep, 2004.
- [38] L. Conradt and T. Roper, "Consensus decision making in animals," *Trends Ecol. Evol.*, vol. 20, pp. 449-456, Aug, 2005.
- [39] D. J. Sumpter and S. C. Pratt, "Quorum responses and consensus decision making," *Philos. Trans. R. Soc. Lond. B. Biol. Sci.*, vol. 364, pp. 743-753, Mar 27, 2009.
- [40] I. R. Fischhoff, S. R. Sundaresan, J. Cordingley, H. M. Larkin, M. Sellier and D. I. Rubenstein, "Social relationships and reproductive state influence leadership roles in movements of plains zebra, *Equus burchellii*," *Anim. Behav.*, vol. 73, pp. 825-831, May, 2007.
- [41] A. J. King and C. Sueur, "Where Next? Group Coordination and Collective Decision Making by Primates," *Int. J. Primatol.*, vol. 32, pp. 1245-1267, Dec, 2011.
- [42] R. Freeman, R. Mann, T. Guilford and D. Biro, "Group decisions and individual differences: route fidelity predicts flight leadership in homing pigeons (*Columba livia*)," *Biol. Lett.*, vol. 7, pp. 63-66, Feb 23, 2011.

- [43] A. Flack, B. Pettit, R. Freeman, T. Guilford and D. Biro, "What are leaders made of? The role of individual experience in determining leader-follower relations in homing pigeons," *Anim. Behav.*, vol. 83, pp. 703-709, Mar, 2012.
- [44] M. Nagy, Z. Akos, D. Biro and T. Vicsek, "Hierarchical group dynamics in pigeon flocks," *Nature*, vol. 464, pp. 890-U99, Apr 8, 2010.
- [45] D. Biro, D. J. T. Sumpter, J. Meade and T. Guilford, "From compromise to leadership in pigeon homing," *Curr. Biol.*, vol. 16, pp. 2123-2128, Nov 7, 2006.
- [46] A. L. Burns, J. E. Herbert-Read, L. J. Morrell and A. J. Ward, "Consistency of leadership in shoals of mosquitofish (*Gambusia holbrooki*) in novel and in familiar environments," *PLoS One*, vol. 7, pp. e36567, 2012.
- [47] L. Conradt, J. Krause, I. D. Couzin and T. J. Roper, "'Leading According to Need' in Self-Organizing Groups," *Am. Nat.*, vol. 173, pp. 304-312, Mar, 2009.
- [48] W. Hamilton, "Geometry for Selfish Herd," *J. Theor. Biol.*, vol. 31, pp. 295-&, 1971.
- [49] C. C. Ioannou, V. Guttal and I. D. Couzin, "Predatory fish select for coordinated collective motion in virtual prey," *Science*, vol. 337, pp. 1212-1215, Sep 7, 2012.
- [50] A. Berdahl, C. J. Torney, C. C. Ioannou, J. J. Faria and I. D. Couzin, "Emergent sensing of complex environments by mobile animal groups," *Science*, vol. 339, pp. 574-576, Feb 1, 2013.
- [51] B. Pettit, A. Perna, D. Biro and D. J. Sumpter, "Interaction rules underlying group decisions in homing pigeons," *J. R. Soc. Interface*, vol. 10, pp. 20130529, Sep 25, 2013.
- [52] A. Kudrolli, G. Lumay, D. Volfson and L. S. Tsimring, "Swarming and swirling in self-propelled polar granular rods," *Phys. Rev. Lett.*, vol. 100, pp. 058001, 2008.
- [53] J. Deseigne, O. Dauchot and H. Chaté, "Collective motion of vibrated polar disks," *Phys. Rev. Lett.*, vol. 105, pp. 098001, 2010.
- [54] C. A. Weber, T. Hanke, J. Deseigne, S. Léonard, O. Dauchot, E. Frey and H. Chaté, "Long-range ordering of vibrated polar disks," *Phys. Rev. Lett.*, vol. 110, pp. 208001, 2013.
- [55] H. Jiang, N. Yoshinaga and M. Sano, "Active motion of a Janus particle by self-thermophoresis in a defocused laser beam," *Phys. Rev. Lett.*, vol. 105, pp. 268302, 2010.
- [56] R. Golestanian, "Collective behaviour of thermally active colloids," *Phys. Rev. Lett.*, vol. 108, pp. 038303, 2012.
- [57] I. Theurkauff, C. Cottin-Bizonne, J. Palacci, C. Ybert and L. Bocquet, "Dynamic clustering in active colloidal suspensions with chemical signalling," *Phys. Rev. Lett.*, vol. 108, pp. 268303, 2012.

- [58] J. Palacci, S. Sacanna, A. P. Steinberg, D. J. Pine and P. M. Chaikin, "Living crystals of light-activated colloidal surfers," *Science*, vol. 339, pp. 936-940, Feb 22, 2013.
- [59] R. Golestanian, "Anomalous diffusion of symmetric and asymmetric active colloids," *Phys. Rev. Lett.*, vol. 102, pp. 188305, 2009.
- [60] W. F. Paxton, K. C. Kistler, C. C. Olmeda, A. Sen, S. K. St. Angelo, Y. Cao, T. E. Mallouk, P. E. Lammert and V. H. Crespi, "Catalytic nanomotors: autonomous movement of striped nanorods," *J. Am. Chem. Soc.*, vol. 126, pp. 13424-13431, (n.d.).
- [61] N. Mano and A. Heller, "Bioelectrochemical propulsion," *J. Am. Chem. Soc.*, vol. 127, pp. 11574-11575, 2005.
- [62] J. R. Howse, R. A. Jones, A. J. Ryan, T. Gough, R. Vafabakhsh and R. Golestanian, "Self-motile colloidal particles: from directed propulsion to random walk," *Phys. Rev. Lett.*, vol. 99, pp. 048102, 2007.
- [63] J. M. Boyd, S. Malstrom, T. Subramanian, L. Venkatesh, U. Schaeper, B. Elangovan, C. D'Sa-Eipper and G. Chinnadurai, "Adenovirus E1B 19 kDa and Bcl-2 proteins interact with a common set of cellular proteins," *Cell*, vol. 79, pp. 341-351, 1994.
- [64] O. Chepizhko and F. Peruani, "Diffusion, subdiffusion, and trapping of active particles in heterogeneous media," *Phys. Rev. Lett.*, vol. 111, pp. 160604, 2013.
- [65] J. Bouchaud and A. Georges, "Anomalous diffusion in disordered media: statistical mechanisms, models and physical applications," *Physics Reports*, vol. 195, pp. 127-293, 1990.
- [66] H. Berry and H. Chaté, "Anomalous subdiffusion due to obstacles: A critical survey," *ArXiv Preprint arXiv: 1103.2206*, pp. 1-33, 2011.
- [67] M. Hauser and L. Schimansky-Geier, "Statistical physics of self-propelled particles," *The European Physical Journal Special Topics*, vol. 224, pp. 1147-1150, 2015.
- [68] S. You, D. Kwon, Y. Parks, S. Kim, M.H. Chung and C. Kim, "Collective behaviours of two-component swarms", *Journal of Theoretical Biology*, vol. 261, pp. 494-500, 2009.
- [69] A. Czirók and T. Vicsek, "Collective behaviour of interacting self-propelled particles," *Physica A: Statistical Mechanics and its Applications*, vol. 281, pp. 17-29, 2000.
- [70] H. P. Zhang, A. Be'er, E. L. Florin and H. L. Swinney, "Collective motion and density fluctuations in bacterial colonies," *Proc. Natl. Acad. Sci. U.S.A.*, vol. 107, pp. 13626-13630, Aug 3, 2010.
- [71] P. Romanczuk, I. D. Couzin and L. Schimansky-Geier, "Collective motion due to individual escape and pursuit response," *Phys. Rev. Lett.*, vol. 102, pp. 010602, 2009.

- [72] V. Schaller, C. Weber, C. Semmrich, E. Frey and A. R. Bausch, "Polar patterns of driven filaments," *Nature*, vol. 467, pp. 73-77, 2010.
- [73] C. W. Reynolds, "Flocks, herds and schools: A distributed behavioural model," in *ACM SIGGRAPH Computer Graphics*, pp. 25-34, 1987.
- [74] F. Peruani, A. Deutsch and M. Bär, "A mean-field theory for self-propelled particles interacting by velocity alignment mechanisms," *The European Physical Journal Special Topics*, vol. 157, pp. 111-122, 2008.
- [75] R. Lukeman, Y. Li and L. Edelstein-Keshet, "Inferring individual rules from collective behaviour," *Proceedings of the National Academy of Sciences*, vol. 107, pp. 12576-12580, 2010.
- [76] E. Forgoston and I. B. Schwartz, "Delay-induced instabilities in self-propelling swarms," *Physical Review E*, vol. 77, pp. 035203, 2008.
- [77] M. R. D'Orsogna, Y. Chuang, A. L. Bertozzi and L. S. Chayes, "Self-propelled particles with soft-core interactions: patterns, stability, and collapse," *Phys. Rev. Lett.*, vol. 96, pp. 104302, 2006.
- [78] H. Chen and K. Leung, "Rotating states of self-propelling particles in two dimensions," *Physical Review E*, vol. 73, pp. 056107, 2006.
- [79] K. Leung and H. Chen, "Rotating states of self-propelling particles in free space", *International Journal of Modern Physics B*, vol. 21, pp. 3954-3959, 2007.
- [80] I. Couzin, J. Krause, R. James, G. Ruxton, and N.R. Franks, "Collective memory and spatial sorting in animal groups", *Journal of Theoretical Biology*, vol. 218, pp. 1-11, 2002.
- [81] M. Ballerini, N. Cabibbo, R. Candelier, A. Cavagna, E. Cisbani, I. Giardina, V. Lecomte, A. Orlandi, G. Parisi and A. Procaccini, "Interaction ruling animal collective behaviour depends on topological rather than metric distance: Evidence from a field study," *Proceedings of the National Academy of Sciences*, vol. 105, pp. 1232-1237, 2008.
- [82] M. Camperi, A. Cavagna, I. Giardina, G. Parisi and E. Silvestri, "Spatially balanced topological interaction grants optimal cohesion in flocking models," *Interface Focus*, vol. 2, pp. 715-725, 2012.
- [83] V. Kulinskii, V. Ratushnaya, A. Zvelindovsky and D. Bedeaux, "Hydrodynamic model for a system of self-propelling particles with conservative kinematic constraints," *EPL (Europhysics Letters)*, vol. 71, pp. 207, 2005.
- [84] B. Lemasson, J. Anderson and R. Goodwin, "Collective motion in animal groups from a neurobiological perspective: the adaptive benefits of dynamic sensory loads and selective attention," *J. Theor. Biol.*, vol. 261, pp. 501-510, 2009.
- [85] E. Yong. (2013, March 19). *The power of swarms can help us fight cancer, understand the brain, and predict the future.*[online]. Available: <http://redefineschool.com/swarms/>

- [86] A. Bricard, J. Caussin, N. Desreumaux, O. Dauchot and D. Bartolo, "Emergence of macroscopic directed motion in populations of motile colloids," *Nature*, vol. 503, pp. 95-98, 2013.
- [87] A. M. Menzel, "Unidirectional laning and migrating cluster crystals in confined self-propelled particle systems," *Journal of Physics: Condensed Matter*, vol. 25, pp. 505103, 2013.
- [88] G. Grégoire and H. Chaté, "Onset of collective and cohesive motion," *Phys. Rev. Lett.*, vol. 92, pp. 025702, 2004.
- [89] B. Gönci, M. Nagy and T. Vicsek, "Phase transition in the scalar noise model of collective motion in three dimensions," *The European Physical Journal Special Topics*, vol. 157, pp. 53-59, 2008.
- [90] M. Aldana and C. Huepe, "Phase transitions in self-driven many-particle systems and related non-equilibrium models: a network approach," *Journal of Statistical Physics*, vol. 112, pp. 135-153, 2003.
- [91] M. Aldana, V. Dossetti, C. Huepe, V. Kenkre and H. Larralde, "Phase transitions in systems of self-propelled agents and related network models," *Phys. Rev. Lett.*, vol. 98, pp. 095702, 2007.
- [92] V. Dossetti, F. Sevilla and V. Kenkre, "Phase transitions induced by complex nonlinear noise in a system of self-propelled agents," *Physical Review E*, vol. 79, pp. 051115, 2009.
- [93] G. Baglietto and E. V. Albano, "Finite-size scaling analysis and dynamic study of the critical behaviour of a model for the collective displacement of self-driven individuals," *Physical Review E*, vol. 78, pp. 021125, 2008.
- [94] G. Baglietto and E. V. Albano, "Computer simulations of the collective displacement of self-propelled agents," *Comput. Phys. Commun.*, vol. 180, pp. 527-531, 2009.
- [95] H. Chaté, F. Ginelli, G. Grégoire and F. Raynaud, "Collective motion of self-propelled particles interacting without cohesion," *Physical Review E*, vol. 77, pp. 046113, 2008.
- [96] H. Chaté, F. Ginelli, G. Grégoire, F. Peruani and F. Raynaud, "Modelling collective motion: variations on the Vicsek model," *The European Physical Journal B*, vol. 64, pp. 451-456, 2008.
- [97] E. Bertin, M. Droz and G. Grégoire, "Boltzmann and hydrodynamic description for self-propelled particles," *Physical Review E*, vol. 74, pp. 022101, 2006.
- [98] C. L. Vestergaard, J. N. Pedersen, K. I. Mortensen and H. Flyvbjerg, "Estimation of motility parameters from trajectory data," *The European Physical Journal Special Topics*, vol. 224, pp. 1151-1168, 2015.

- [99] M. Götz, K. Hodeck, P. Witzel, A. Nandi, B. Lindner and D. Heinrich, "Probing cytoskeleton dynamics by intracellular particle transport analysis," *The European Physical Journal Special Topics*, vol. 224, pp. 1169-1183, 2015.
- [100] M. Raatz, M. Hintsche, M. Bahrs, M. Theves and C. Beta, "Swimming patterns of a polarly flagellated bacterium in environments of increasing complexity," *The European Physical Journal Special Topics*, vol. 224, pp. 1185-1198, 2015.
- [101] B. Rodiek and M. Hauser, "Migratory behaviour of *Physarum polycephalum* microplasmidia," *The European Physical Journal Special Topics*, vol. 224, pp. 1199-1214, 2015.
- [102] P. Romanczuk, M. Romensky, D. Scholz, V. Lobaskin and L. Schimansky-Geier, "Motion of *Euglena gracilis*: Active fluctuations and velocity distribution," *The European Physical Journal Special Topics*, vol. 224, pp. 1215-1229, 2015.
- [103] A. Solon, M. Cates and J. Tailleur, "Active Brownian particles and run-and-tumble particles: A comparative study," *The European Physical Journal Special Topics*, vol. 224, pp. 1231-1262, 2015.
- [104] S. Hernández-Navarro, P. Tierno, J. Ignés-Mullol and F. Sagués, "Liquid-crystal enabled electrophoresis: Scenarios for driving and reconfigurable assembling of colloids," *The European Physical Journal Special Topics*, vol. 224, pp. 1263-1273, 2015.
- [105] A. Kaiser, A. Sokolov, I. S. Aranson and H. Löwen, "Motion of two micro-wedges in a turbulent bacterial bath," *The European Physical Journal Special Topics*, vol. 224, pp. 1275-1286, 2015.
- [106] T. Ihle, "Large density expansion of a hydrodynamic theory for self-propelled particles," *The European Physical Journal Special Topics*, vol. 224, pp. 1303-1324, 2015.
- [107] R. Großmann, P. Romanczuk, M. Bär and L. Schimansky-Geier, "Pattern formation in active particle systems due to competing alignment interactions," *The European Physical Journal Special Topics*, vol. 224, pp. 1325-1347, 2015.
- [108] J. Ślómka and J. Dunkel, "Generalized Navier-Stokes equations for active suspensions," *The European Physical Journal Special Topics*, vol. 224, pp. 1349-1358, 2015.
- [109] D. S. Cambui, A. S. de Arruda and M. Godoy, "Critical exponents of a self-propelled particles system," *Physica A: Statistical Mechanics and its Applications*, vol. 444, pp. 582-588, 2016.
- [110] W. Simoes, V. Delucena, "Blind User Wearable Audio Assistance for Indoor Navigation Based on Visual Markers and Ultrasonic Obstacle Detection", *2016 IEEE International Conference on Consumer Electronics (ICCE)*, pp. 60-63, 2016.

- [111] B. R. Fajen, "Guiding locomotion in complex, dynamic environments," *Front. Behav. Neurosci.*, vol. 7, pp. 85, Jul 19, 2013.
- [112] T. Frank, T. Gifford and S. Chiangga, "Minimalistic model for navigation of mobile robots around obstacles based on complex-number calculus and inspired by human navigation behaviour," *Math. Comput. Simul.*, vol. 97, pp. 108-122, 2014.
- [113] C. Kuo, H. Chou, S. Chi and Y. Lien, "Vision-based obstacle avoidance navigation with autonomous humanoid robots for structured competition problems," *International Journal of Humanoid Robotics*, vol. 10, 2013.
- [114] G. Csaba and Z. Vamosy, "Fuzzy based obstacle avoidance for mobil robots with kinect sensor," in *Logistics and Industrial Informatics (LINDI), 2012 4th IEEE International Symposium*, pp. 135-144, 2012.
- [115] O. Chepizhko, E. G. Altmann and F. Peruani, "Optimal noise maximizes collective motion in heterogeneous media," *Phys. Rev. Lett.*, vol. 110, pp. 238101, 2013.
- [116] S. Croft, R. Budgey, J. W. Pitchford and A. J. Wood, "The influence of group size and social interactions on collision risk with obstacles," *Ecological Complexity*, vol. 16, pp. 77-82, 2013.
- [117] Y. Inada and K. Kawachi, "Order and flexibility in the motion of fish schools," *J. Theor. Biol.*, vol. 214, pp. 371-387, 2002.
- [118] S. Lee, H. Pak and T. Chon, "Dynamics of prey-flock escaping behaviour in response to predator's attack," *J. Theor. Biol.*, vol. 240, pp. 250-259, 2006.
- [119] S. I. Nishimura and T. Ikegami, "Emergence of collective strategies in a prey-predator game model," *Artif. Life*, vol. 3, pp. 243-260, 1997.
- [120] C. Carere, S. Montanino, F. Moreschini, F. Zoratto, F. Chiarotti, D. Santucci and E. Alleva, "Aerial flocking patterns of wintering starlings, *Sturnus vulgaris*, under different predation risk," *Anim. Behav.*, vol. 77, pp. 101-107, 2009.
- [121] L. Angelani, "Collective Predation and Escape Strategies," *Phys. Rev. Lett.*, vol. 109, pp. 118104, 2012.
- [122] A. Czirók, M. Vicsek and T. Vicsek, "Collective motion of organisms in three dimensions," *Physica A: Statistical Mechanics and its Applications*, vol. 264, pp. 299-304, 1999.
- [123] Y. Li, S. Wang, Z. Han, B. Tian, Z. Xi and B. Wang, "Optimal view angle in the three-dimensional self-propelled particle model," *EPL (Europhysics Letters)*, vol. 93, pp. 68003, 2011.
- [124] S. Ramaswamy, "The mechanics and statistics of active matter," *Annu.Rev.Condens.Matter Phys.*, vol. 1, 2010.
- [125] J. Bergdahl. (2014, May 21). *Quantitative analysis of physical and statistical properties of flocks* [online]. Available: <http://www.diva-portal.se/smash/get/diva2:721440/fulltext01.pdf>.

[126] F. Peruani and L. G. Morelli, "Self-propelled particles with fluctuating speed and direction of motion in two dimensions," *Phys. Rev. Lett.*, vol. 99, pp. 010602, 2007.

[127] D. Takagi, J. Palacci, A. B. Braunschweig, M. J. Shelley and J. Zhang, "Hydrodynamic capture of microswimmers into sphere-bound orbits," *Soft Matter*, vol. 10, pp. 1784-1789, 2014.

[128] M. Zheng, Y. Kashimori, O. Hoshino, K. Fujita and T. Kambara, "Behavior pattern (innate action) of individuals in fish schools generating efficient collective evasion from predation," *J. Theor. Biol.*, vol. 235, pp. 153-167, 2005.

## Appendix

### Collective motion of self-propelled particles in homogeneous and heterogeneous medium

Israr Ahmed<sup>1</sup>, Waqar Ahmed<sup>2</sup>, Dung Q. Ly\*<sup>1,3</sup>

<sup>1</sup>School of Physical Sciences and Computing, University of Central Lancashire, Preston, United Kingdom.

<sup>2</sup>School of Medicine and Dentistry, University of Central Lancashire, Preston, United Kingdom.

<sup>3</sup>School of Engineering and Design, Brunel University London, London, United Kingdom.

**Abstract:** The concept of self-propelled particles is used to study the collective motion of different organisms such as flocking of birds, swimming of schools of fish or migrating of bacteria. The collective motion of self-propelled particles is investigated in the presence of obstacles and without obstacles. A comparison of the effects of interaction radius, speed and noise on the collective motion of self-propelled particles is conducted. It is found that in the presence of obstacles, mean square displacement of the particles shows large fluctuation, whereas without obstacles fluctuation is less. It is also shown that in the presence of the obstacles, an optimal noise, which maximises the collective motion of the particles, exists.

**Key words:** Self-propelled particles, Collective motion, Obstacles.

---

\*Corresponding author: dly@uclan.ac.uk

## 1. Introduction

Movements in dynamic and complex environments are an integral part of the daily life activities; this includes walking in crowded spaces, playing sports, etc. Many of these tasks that human performs in such environments involve interactions with stationary or moving obstacles. There is always a need to coordinate the information with other individuals to deal with the obstacles [1]. This movement is also applied to other living things such as flocks of birds which are facing obstacles while moving collectively. Understanding the detection and avoidance from the obstacles when there is noise in the system is of extreme importance. Many works have focused on interaction of individuals with obstacles from different perspectives. For example, in computer science field lots of works have been carried out where robots interact with obstacles [2-4]. However there are limited works done where natural systems involving with obstacles. There are many examples available in the environment where dynamics of the particles is given in the presence of obstacles. Bacteria show complex collective behaviours, for example swarming in heterogeneous environment such as soil or highly complex tissues in a gastrointestinal tract. Herds of mammal travel long distances crossing rivers and forests [5]. Despite these facts, so far there have been little works both on experimental and theoretical levels about the impacts of heterogeneous medium on the collective motion [6]. Croft *et al* [7] have simulated particle's avoidance behaviour. In their work individual based modelling approach was investigated which defined group interactions with obstacles. Moreover effect was measured on group size when there is probability of single particle colliding with fixed obstacle. They proved that when huge model suppositions and large values of parameters occur, social interactions have high chances of colliding with obstacles. Furthermore, the motion created due to social interactions can have important effects on the metrics used to inform management and policy decisions. Mecholsky *et al* [8] considered a continuum model which involved flocks. Linearized interaction of flocks to an obstacle was studied. Flock behaviour after interacting with obstacles was shown by density disturbances. This disturbance is like Mach cones, in which the order is expressed by anisotropic spread of waves of flocking. Chepizkho *et al* [9] studied the movement of self-propelled particles in the heterogeneous environment where obstacles were randomly placed in the two dimensional spaces. In their model particles avoid the obstacles, and particle's avoidance was determined by the turning speed,  $\gamma$ . The mean square displacement of individuals gives two regimes as a function of the obstacle density  $\rho_o$  and  $\gamma$ . In the first regime it was observed that when there is a smaller value of  $\gamma$ , movement of particles is diffusive and defined by diffusion coefficient which shows a minimum at an intermediate densities of obstacles  $\rho_o$ . In the second regime it was observed that for high obstacle densities  $\rho_o$  and for large values of  $\gamma$ , spontaneous trapping of particles takes place. They also showed that the existence of obstacles, which could be static or mobile, can change the dynamics of collective motion. Furthermore optimal noise amplitude

maximizes the collective motion while in a homogeneous medium this type of optimal does not exist. When a small obstacles density exists in the system collective motion shows a unique critical point, below which the system shows long range order, similar in homogeneous media. When there exists a high obstacle density in the system, two critical points appear which make the system disordered at both low and large noise amplitudes and show only quasi long range order in between these critical points [5].

In this work we present the computer simulation of the self-propelled particles in heterogeneous and homogeneous medium. We study the collective motion of self-propelled particles in the presence of obstacles and without obstacles. We compare the effects of the interaction radius, speed and noise on the collective motion of self-propelled particles with and without obstacles. We have found that in the presence of obstacles, mean square displacement of the particle show large fluctuations in the system, whereas without obstacle density mean square displacement of the particle shows very less fluctuations. It is also shown that in the presence of the obstacles, optimal noise exists which maximises the collective motion of the particles. Optimal noise that increases the collective motion is helpful in developing and understanding migration and navigation strategies in moveable or non-moveable heterogeneous media, which help to understand evolution and adaptation of stochastic components in natural systems which show collective motion.

## 2. Methodology

A continuum time and two dimensional model is considered for  $N_b$  self-propelled particles (SPPs). This model investigates the effects of different parameters on collective motion of the self-propelled particles. The motion of  $N_b$  self-propelled particles confined in two-dimensional box  $L$  with a periodic boundary applied. Interaction of the particles among themselves is treated the same way as in Vicsek *et al* [10] where particle assumes the average direction of its neighbours that are in its interaction radius,  $r$ . Spatial heterogeneity is given by the presence of the  $N_o$  fixed obstacles. The new element in the equation of motion of self-propelled particles is introduced by the obstacle avoidance interaction as it is given in Ref. [5]. Obstacles are randomly distributed in the system. Noise parameter is also introduced in the system, which is randomly given and has values between  $[-\pi, \pi]$ . At the initial time-step each particle has a random position and a random direction. Particles update their positions as follows:

$$\mathbf{x}_i(t + \Delta t) = \mathbf{x}_i(t) + \mathbf{v}_i(t)\Delta t, \quad (1)$$

and direction of the particle is given by the following equation:

$$\theta_i(t + \Delta t) = \langle \theta(t) \rangle_r + h(\mathbf{x}_i) + \eta\Delta\theta. \quad (2)$$

In equation 1,  $\mathbf{x}_i$  represents the position of  $i^{\text{th}}$  particle,  $\mathbf{v}_i(t)$  is the velocity of the particle with absolute velocity  $v_o$ .  $\Delta t$  is the time interval that particles take to move from one point to another.

In equation 2,  $\theta_i$  represents the direction of the particle and  $\Delta\theta$  is the random fluctuation in the system, which is created by noise and has value in the range of  $[-\pi, \pi]$ .  $\eta$  is the noise amplitude.  $\langle\theta(t)\rangle_r$  represents the average direction of the particles which is within the interaction radius  $r$ , where  $r$  is the radius of interaction between the self-propelled particles.  $\langle\theta(t)\rangle_r$  is given in the following equation:

$$\langle\theta(t)\rangle_r = \arctan\left\{\frac{\langle\sin(\theta)\rangle_r}{\langle\cos(\theta)\rangle_r}\right\}. \quad (3)$$

The function  $h(\mathbf{x}_i)$  in equation 2 defines the interaction of particle with obstacles. Through this function particles avoid the obstacles that are located in its neighbourhood:

$$h(\mathbf{x}_i) = \begin{cases} \frac{\gamma_o}{n_o(\mathbf{x}_i)} \sum_{|\mathbf{x}_i - \mathbf{y}_k| < R_o} \sin(\alpha_{k,i} - \theta_i) & \text{if } n_o(\mathbf{x}_i) > 0 \\ 0 & \text{if } n_o(\mathbf{x}_i) = 0. \end{cases} \quad (4)$$

Here  $\mathbf{x}_i$  is the position of  $i^{\text{th}}$  particle, and  $\mathbf{y}_k$  is the position of  $k^{\text{th}}$  obstacle.  $R_o$  is known as the interaction radius between particle and obstacle.  $n_o(\mathbf{x}_i)$  represents the number of the obstacles located at the distance less than  $R_o$  from  $\mathbf{x}_i$ . In the above equation two conditions are given. Firstly, if  $n_o(\mathbf{x}_i)$  is greater than zero,  $h(\mathbf{x}_i)$  will show interaction with obstacles, secondly, if  $n_o(\mathbf{x}_i)$  is equal to zero,  $h(\mathbf{x}_i)$  will be zero. In equation 4, the term  $|\mathbf{x}_i - \mathbf{y}_k| < R_o$ , means that if the distance between the obstacle and particle is less than the interaction radius  $R_o$ , then the summation of sine  $\left(\sum \sin(\alpha_{k,i} - \theta_i)\right)$  will take place. Number of sine values that will be summed, depends on the number of obstacles  $n_o(\mathbf{x}_i)$  that are located in the interaction radius range of the particle  $\mathbf{x}_i$ . The term  $\alpha_{k,i}$  shows the angle in polar coordinates of the vector  $\mathbf{x}_i - \mathbf{y}_k$ . Also the parameter  $\gamma_o$  which is for interaction purpose, known as the particle's turning speed when it interacts with obstacle.

### 2.1. Order parameter

The order parameter,  $w$ , is used to characterise the macroscopic collective movement of the particles [5].

$$w = \langle w(t) \rangle_t = \left\langle \left| \frac{1}{N_b} \sum_{i=1}^{N_b} e^{i\theta_i(t)} \right| \right\rangle_t. \quad (5)$$

Here  $\langle \rangle$  represents temporal average. This term is represented by a complex number. This complex number is a particle whose direction is determined after interacting with obstacles. In this equation modulus of complex numbers is determined and then divided by total number of particles. Equation 5 determines the average collective motion of the particles.

The obstacle density  $\rho_o$  can be interpreted by using the following equation:

$$\rho_o = N_o / L^2, \quad (6)$$

here  $N_o$  is the number of obstacles, and  $L$  is the box length.

<i>Symbol</i>	<i>Description</i>
$L$	Length of box
$N_b$	Number of particles
$N_o$	Number of obstacles
$t$	Time step
$\eta$	Noise amplitude
$R_o$	Interaction radius between the particle and the obstacles
$r$	Interaction radius between the particles
$v_o$	Absolute velocity
$\gamma_o$	Particle's turning speed when it interact with obstacle
$\Delta t$	Time interval
$w$	Collective motion parameter

Table 1: Parameters used in the simulation.

### 3. Results and Discussion

Simulation is performed in a square box of length  $L$ . We first consider the case in which noise,  $\eta = 0.01$ . At initial time steps particles move randomly with constant speed. After that each particle adopts an average direction of the particles which is in its neighbourhood. Particles interact with the obstacles and they turn away from the obstacles when they come closer to obstacle. It was observed that at lower noise particles make groups. There is strong coordination in the particles as shown in the Figure 1. Strong coordination means particles have higher interaction with each other. Phase exhibited by the system is known as the clustered phase. At the same noise value, clustered phase was also observed in other work [5]. If we compare the order parameter in our model and in Ref [5] we found that our model exhibits more collective motion.

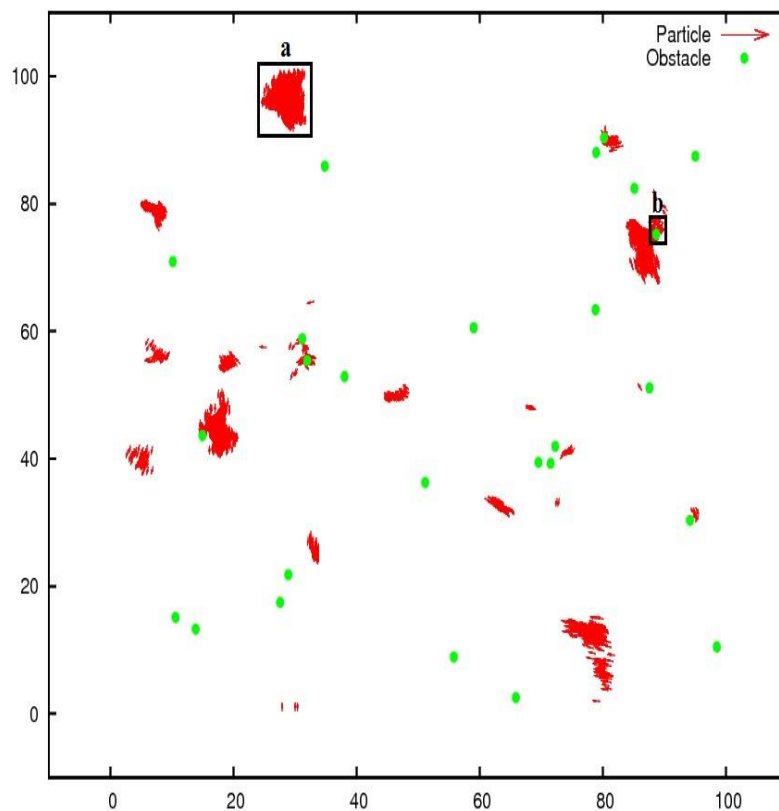


**Figure 1:** Collective motion of the particles in groups. Box length  $L = 100$ , noise amplitude  $\eta = 0.01$ , time  $t = 10000$ , particles  $N_b = 10000$ , obstacles  $N_o = 26$ , interaction radius  $r = 1$ , avoidance radius  $R_o = 1$ , speed  $v_o = 1$ , particle's turning speed  $\gamma_o = 1$ , time interval  $\Delta t = 0.1$ . The crops of areas “a” and “b” are shown in the Figure 2.

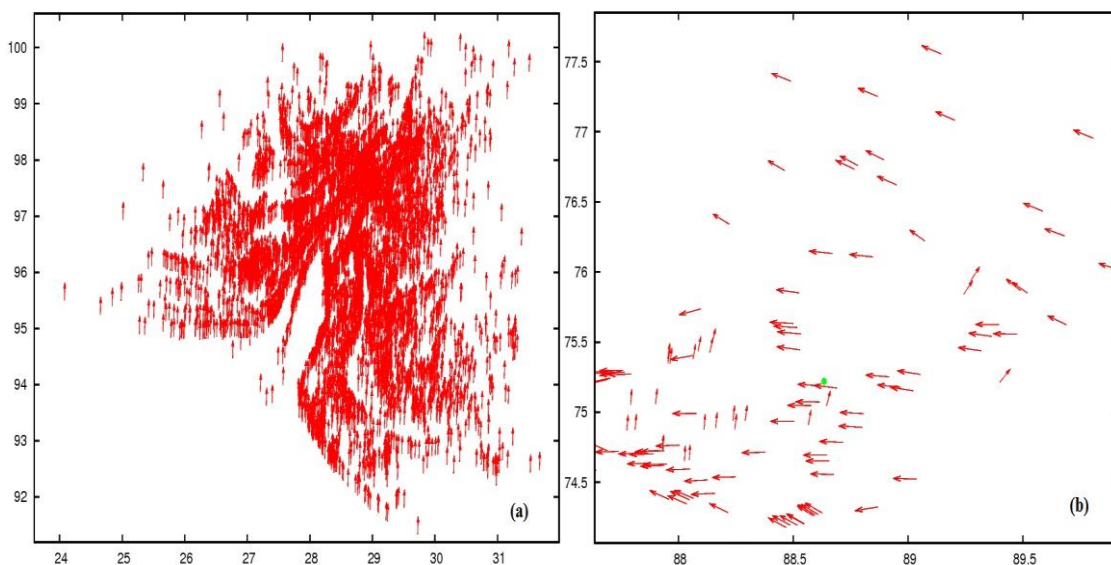


**Figure 2:** Close-up from areas “a” and “b” in the Figure 1.

In the Figure 1 green circles show obstacles, whereas red arrows represent particles. Collective motion exhibited by the particles is calculated to be 0.65. This figure shows the result of the movement of the particles at 10000<sup>th</sup> time step. In the system dense clusters are formed. We can see that when particles move closer to the obstacles they try to avoid from the obstacle. At initial time steps particles have random motion, after some time-steps they start developing coordination with each other. When particles collide or near to the obstacles they scatter and their collective motion is disturbed. After the scattering they again try to move together. Interaction between the particles follows the rule of interaction as shown in the Vicsek model [10] where velocities of the particles are summed when they are in the interaction radius.

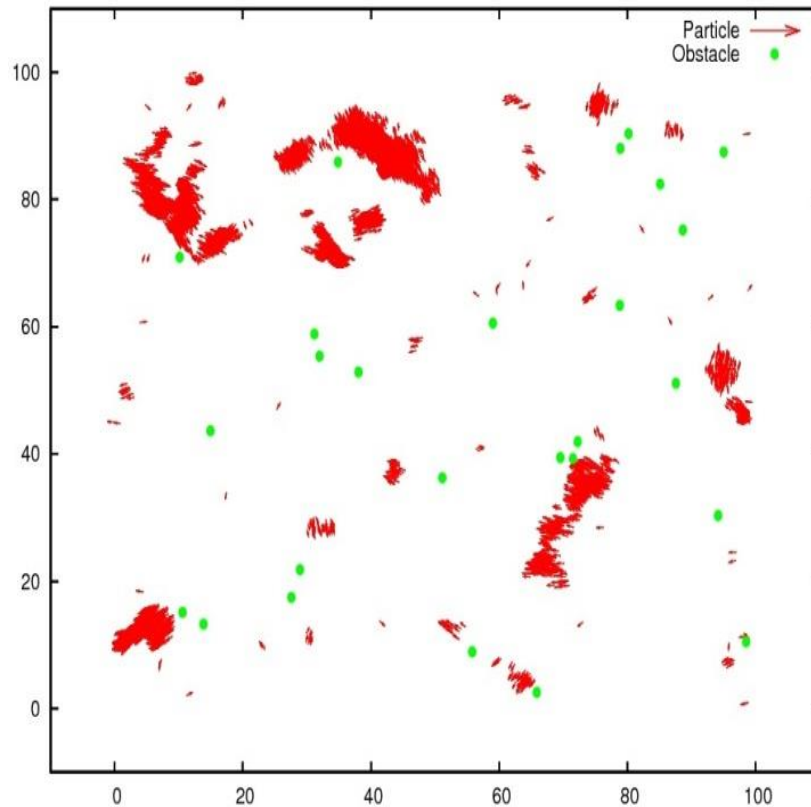


**Figure 3:** Increasing noise from 0.01 to 0.3.  $L = 100$ ,  
 $t = 10000$ ,  $N_b = 10000$ ,  $N_o = 26$ ,  $r = 1$ ,  $R_o = 1$ ,  $v_o = 1$ ,  $\gamma_o = 1$ ,  $\Delta t = 0.1$ .

The Figure 3 demonstrates the effect of noise when it is increased from 0.01 to 0.3. It is observed that there appears a slight randomness in the orientation. It can be clearly seen that particles have formed some smaller clusters which are the result of the increase in the noise. Here each cluster has different direction and the collective motion of the particles is decreased, which shows that there is an effect of the noise on the system. This can be easily seen by comparing the Figures 1 and 3. It was obtained that the value of average velocity is  $w = 0.65$  for  $\eta = 0.01$  while it is  $w = 0.22$  for  $\eta = 0.3$ .

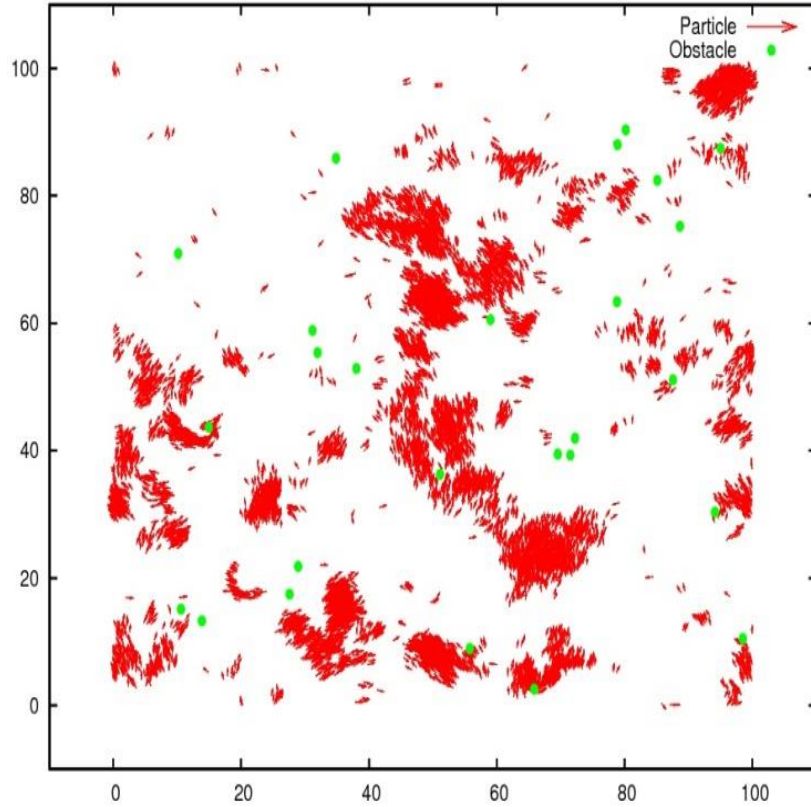


**Figure 4:** Segregation of the particles.  $\eta = 0.6, L = 100, t = 10000, r = 1,$   
 $N_b = 10000, N_o = 26, R_o = 1, v_o = 1, \gamma_o = 1, \Delta t = 0.1.$

By increasing the noise to 0.6, Figure 4, it shows that particles are scattered at larger scale. There are more cluster forming. By applying higher noise the system shows an interesting behaviour as the collective motion reaches to  $w = 0.77$ , which is higher than the result of the previous two noise values. This higher value is attributed to the random distribution of the obstacles. This is contradictory to the fact when particles move in the homogeneous medium where increasing in noise results in declining in collective motion of the particles [6]. It is in good agreement with the results obtained in Ref. [5].

### 3.1. Effect of parameters

Now we show results that demonstrate the effects of different parameters on the collective motion. These parameters represent the interaction radius  $r$ , speed of the particles  $v_o$  and noise  $\eta$ . These parameters are summarised as in the Table 2.

<i>Parameter</i>	<i>Value</i>
$L$	40
$N_b$	1000
$N_o$	20
$t$	2000
$\eta$	0
$R_o$	1
$r$	1
$v_o$	1
$\gamma_o$	10
$\Delta t$	0.1

Table 2: Parameters values used in the calculation.

### 3.1.1. Effect of the Interaction radius

The interaction radius is the distance at which particles contact with each other. Each particle in the system has the same interaction radius. The larger value of the interaction radius encourages the collective motion in the system. In Figure 5 the collective motion as a function of interaction radius is plotted for the system where obstacle density  $\rho_o = 0$  (circles) and  $\rho_o = 0.0125$  (triangles).

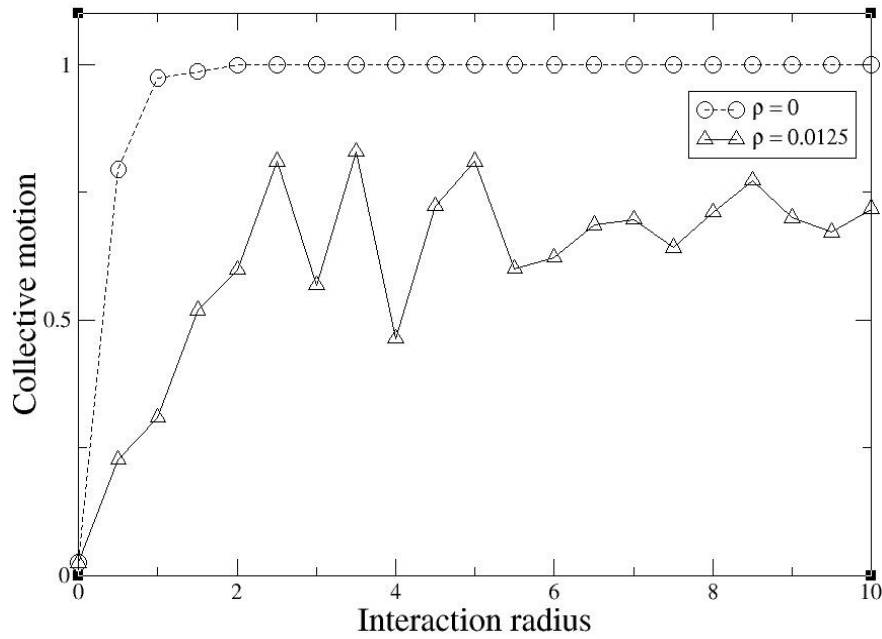


**Figure 5:** Collective motion as a function of the interaction radius  $r$ .

The interaction radius is varied from 0 to 10 with an interval of 0.5. It is observed that particles show higher coordination with each other when radius increases. This coordination among particles makes the system stable. For  $\rho_o = 0$ , it can be clearly seen that at the value of  $r$  equal to zero, the system is completely in disordered state, there is no emergence of the collective motion of the particles in the system. Increasing the radius of the particles makes the system more stable, because particles move collectively with proper coordination without any hindrance. From  $r = 2$ , order parameter has gained a very consistent value which is equal to 0.99. This value is the evidence of the stable system. When there is a presence of obstacles in the system, at  $\rho_o = 0.0125$ , the collective motion is smaller than the previous case of  $\rho_o = 0$ . Despite of the obstacle's existence, particles show collective motion and it never goes to zero. Fluctuation of the collective motion as a function of interaction radius is due to the number of the particles used in the calculation is not so large. We believe that if we increase the number of particles in the system, fluctuation will occur at smaller scale.

### 3.1.2. Effect of the speed

In the model each particle carries a constant speed. Speed parameter has a significant effect on the collective behaviour of the particles. The Figure 6 demonstrates the collective motion as a function of speed for obstacle density  $\rho_o = 0$  (circles) and  $\rho_o = 0.0125$  (triangles).

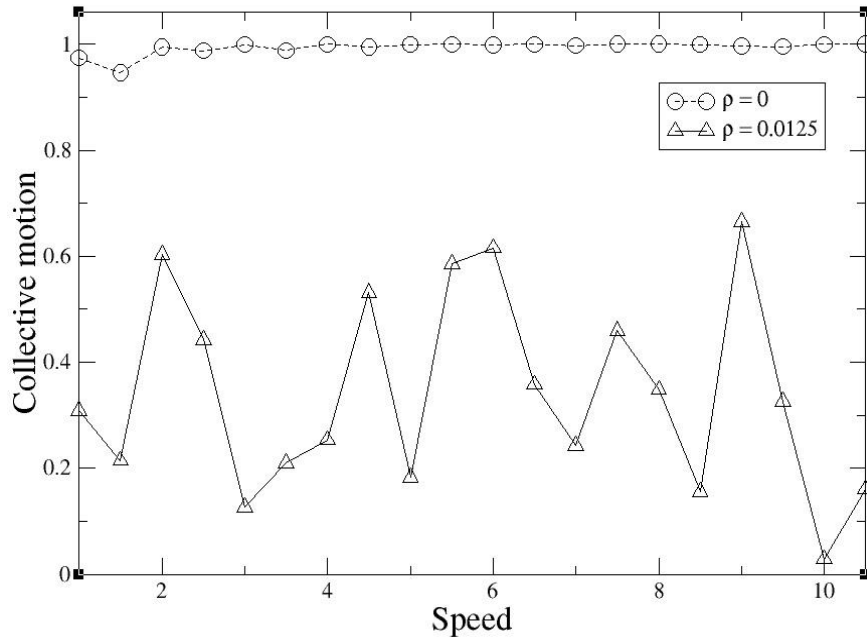


**Figure 6:** Collective motion as a function of the speed for obstacle density, for  $\rho_o = 0$  and  $\rho_o = 0.0125$  (20 obstacles).

In the Figure 6 for  $\rho_o = 0$  (circles) line which demonstrates the results for zero obstacle density. With the higher value of the speed parameter particles move faster. At initial values of  $v_o$ , system shows some fluctuations, from  $v_o = 3$  collective motion has consistent value which remains near to 1. It can be clearly seen that by increasing the speed parameter the system show long range order, particles gain more coordination quickly in time, as a result the system becomes stable. There is no any hindrance in the movement of the particles because there is no any obstacle present in the system. In the absence of noise and obstacles, particles move freely and they show ordered phase. In the case of  $\rho_o = 0.0125$  order parameter,  $w$ , shows a non-monotonic behaviour because there appears large fluctuations in the system. This happens because obstacles are randomly distributed in the system. Collective motion of the self-propelled particles is hugely distributed and the system is completely in a disordered state.

### 3.1.3. Effect of noise

Noise effect is investigated for both homogeneous and heterogeneous systems. Order parameter,  $w$  is plotted against noise values in the homogeneous medium where obstacle density is  $\rho_o = 0$  and in heterogeneous medium where obstacle density is  $\rho_o = 0.0125$ . Noise value is chosen from the range  $[-\pi, \pi]$ , by using uniform probability distribution.

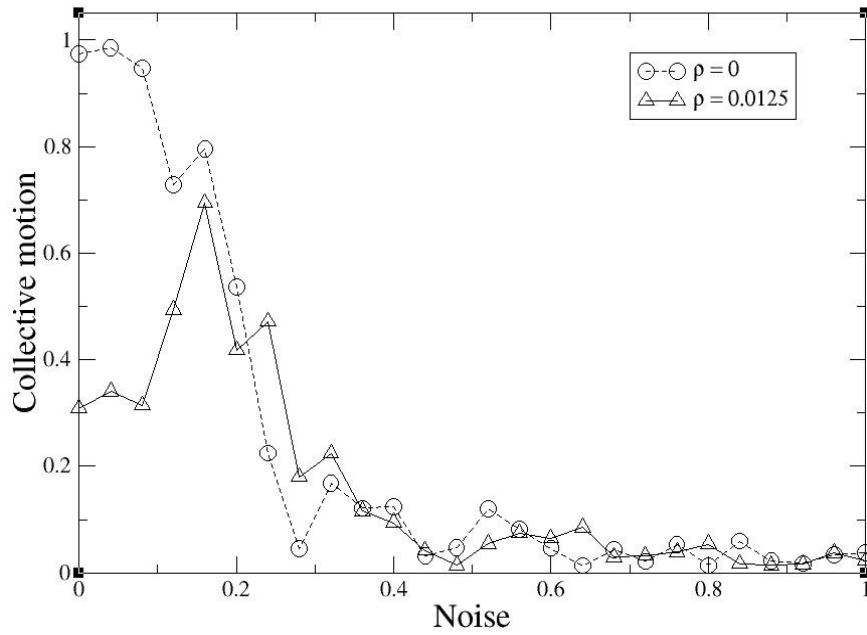


**Figure 7:** Collective motion as a function of the noise for two values of obstacle density,  $\rho_o = 0$  and  $\rho_o = 0.0125$ .

The Figure 7 demonstrates the effect of the noise on the collective motion of the self-propelled particles. Noise amplitude has been varied from the 0 to 1 with an interval length of 0.04. In the first case where  $\rho_o = 0$  (circles line) we see there appears huge randomness in the system. With higher values of the noise order parameter  $w$  reaches to zero. From the above result we see that at lower noise values system is in a state of order because collective motion has value near to 1. When the noise is increasing, the system starts to show disordered phase. It can be clearly seen that when the noise is from 0.48, system shows collective motion approaches to zero.

In the case of  $\rho_o = 0.0125$  (triangle line), it can be clearly seen that at the noise value 0.16, order parameter  $w$  has reached to the maximum. At the starting value of the noise such as  $\eta = 0$  collective motion has smaller value than at  $\eta = 0.16$ . Due to the random distribution of the obstacles, there exists an optimal noise which maximises the collective motion of the self-propelled particles. Such type of behaviour does not exist in the homogeneous medium. It is also observed that with the increase of the noise, there is decrease in order parameter. System is completely in the state of disorder when noise is larger than 0.4.

## 4. Conclusions

Collective behaviour of self-propelled particles was investigated for both heterogeneous and homogeneous medium. We investigated the effects of the interaction radius, speed and noise on the collective motion of the self-propelled particles. It was shown that in the homogeneous medium the order parameter gains larger values when the interaction radius and speed are increased, whereas in the case of noise we found that noise has caused fluctuations in the order parameter. In the case of heterogeneous medium large fluctuations take place when the interaction radius of the particles is small. By increasing the interaction radius the fluctuation is getting smaller. Furthermore, in heterogeneous medium, the variation of noise causes the collective motion to behave in a non-monotonic manner. This is because of the randomly distribution of the obstacles in the system. It is observed that the collective motion is always less in the case of the presence of obstacles. It is also observed that there exists an optimal noise which maximises the collective motion of the self-propelled particles. At noise = 0.16, the order parameter has reached its maximum value.

## References

- [1]. B. R. Fajen, "Guiding locomotion in complex, dynamic environments," *Front. Behav. Neurosci.*, vol. 7, pp. 85, 2013.
- [2]. T. Frank, T. Gifford and S. Chianga, "Minimalistic model for navigation of mobile robots around obstacles based on complex-number calculus and inspired by human navigation behavior," *Math. Comput. Simul.*, vol. 97, pp. 108-122, 2014.
- [3]. C. Kuo, H. Chou, S. Chi and Y. Lien, "Vision-based obstacle navigation with autonomous humanoid robots for structured competition problems" *International Journal of Humanoid Robotics*, vol. 10, 2013.
- [4]. G. Csaba and Z. Vamossy, "Fuzzy based obstacle avoidance for mobil robots with kinect sensor," in *Logistics and Industrial Informatics (LINDI), 2012 4th IEEE International Symposium on*, 2012, pp. 135-144.
- [5]. O. Chepizhko, E. G. Altmann and F. Peruani, "Optimal noise maximizes collective motion in heterogeneous media," *Phys. Rev. Lett.*, vol. 110, pp. 238101, 2013.
- [6]. T. Vicsek and A. Zafeiris, "Collective motion," *Physics Reports*, vol. 517, pp. 71-140, 2012.
- [7]. S. Croft, R. Budgey, J. W. Pitchford and A. J. Wood, "The influence of group size and social interactions on collision risk with obstacles," *Ecological Complexity*, vol. 16, pp. 77-82, 2013.
- [8]. N. A. Mecholsky, E. Ott and T. M. Antonsen Jr, "Obstacle and predator avoidance in a model for flocking," *Physica D*, vol. 239, pp. 988-996, 2010.
- [9]. O. Chepizhko and F. Peruani, "Diffusion, subdiffusion, and trapping of active particles in heterogeneous media," *Phys. Rev. Lett.*, vol. 111, pp. 160604, 2013.
- [10]. T. Vicsek, A. Czirók, E. Ben-Jacob, I. Cohen and O. Shochet, "Novel type of phase transition in a system of self-driven particles," *Phys. Rev. Lett.*, vol. 75, pp. 1226, 1995.